University of Alberta

The Regulation of Lysophosphatidate-induced Fibroblast Migration by Lipid Phosphate Phosphatase-1

by

Carlos Salvador Pilquil 

A thesis submitted to the Faculty of Graduate Studies and Research
in partial fulfillment of the requirements for the degree of

Doctor of Philosophy

Department of Biochemistry

Edmonton, Alberta
Fall 2007

Your file Votre référence
ISBN: 978-0-494-33046-3
Our file Notre référence
ISBN: 978-0-494-33046-3

Abstract

Lysophosphatidate (LPA) is among the most investigated signaling lipid, and is linked to roles that promote wound healing, development, and angiogenesis. LPA signaling is also linked to disease states such as tumor growth, metastasis, atherosclerosis, and inflammatory diseases. Therefore, regulation of the metabolism of LPA is critical in controlling its accumulation and signaling effects. Lipid phosphate phosphatases (LPP) are transmembrane enzymes that can dephosphorylate various signaling lipid phosphates including LPA, and phosphatidate (PA). There are three isoforms of LPP, and each has specific functions *in vivo.* This thesis will focus on LPP1 that acts partly in the plasma membrane as an ecto-enzyme that can degrade external LPA. LPA stimulates pertussis toxin-sensitive migration of fibroblasts through cell surface receptors. We found that LPP1 over-expression can attenuate LPA-, but not platelet-derived growth factor (PDGF)- or endothelin-induced fibroblast migration. Conversely, knockdown of endogenous LPP1 activity increased LPA-, but not PDGF-induced migration. LPP1 also attenuated migration induced by a non-hydrolysable LPA receptor agonist. This demonstrates that inhibition of LPA-induced migration was not dependent on external LPA dephosphorylation, and that LPP1 controls signaling downstream of LPA receptors. This is consistent with work that shows LPP1 can regulate intracellular accumulation of lipid phosphates. Indeed we found that LPP1 can decrease PA accumulation by attenuating LPA-induced phospholipase D (PLD) activation, and that PLD2 activity was necessary for LPA-, but not PDGF-induced fibroblast migration. Increased LPP1 activity also decreased LPA-, but not PDGF-stimulated ERK and Rho activities, and the basal activities of Rac and Cdc42. These signaling proteins are

important in fibroblast migration. LPP1 affected the phosphorylation of cellular proteins stimulated with various signaling agonists, such as PDGF, which also had its PLD activation inhibited by LPP1. In addition, over-expression of LPP1 decreased LPA-induced migration of neighboring wild-type cells, as did the conditioned media from the former cells. The affect by the conditioned media could be due to the alteration of secretion of extracellular matrix remodeling proteins, matrix metalloproteinases and their regulators. This thesis increases our knowledge of how LPP1 regulates intracellular signaling by bioactive lipids.

Acknowledgements

This work would not be possible without the support of the Alberta Heritage Foundation for Medical Research, and the Canadian Institute of Health Research.

I have special gratitude for my supervisor and mentor Dr. David N. Brindley. We persevered through very difficult times, and by following his example of hard work, honesty and optimism, helped me through those times.

Many thanks to Dr. Luc Berthiaume and Dr. Charles Holmes whose guidance helped shape this thesis. I would also like to acknowledge Dr. Denis English for getting me started on cell migration, and Dr. Kevin Lynch for providing the crucial reagents for my work.

Cheers to all my 'lab mates' past and present, and my friends 'on the outside' who made these grueling years a pleasure.

My mother and sister, Ida and Fresia, have always been a touchstone of support and I appreciate their encouragement.

Above all, I thank my wife, Rania, who has helped me through this long journey with patience, understanding and love, and gave me the opportunity to meet my beautiful daughter, Madeleine, yet another source of inspiration.

Table of Contents

List of Tables

List of Figures

List of Abbreviations

ABC	ATP-binding cassette
ADP	adenosine diphosphate
AGK	acylglycerol kinase
Akt	serine-threonine protein kinase B
ARF	ADP ribosylation factor
Arg	arginine
Asn	asparagine
Asp	aspartic acid
ATP	adenosine triphosphate
ATX	autotaxin
bFGF	basic fibroblast growth factor
BCA	bicinchoninic acid
BSA	bovine serum albumin
cAMP	cyclic adenosine monophosphate
CDase	ceramidase
Cdc42	cell division cycle 42/GTP-binding protein
cDNA	complementary deoxyribonucleic acid
C1P	ceramide-1-phosphate
CERK	ceramide kinase
CFTR	cystic fibrosis transmembrane regulator
CMV	cytomegalovirus
COX-2	cyclo-oxygenase-2
$cPLA_2\alpha$	cytosolic phospholipase $A_2\alpha$
CPO	fungal vanadium chloroperoxidase
CSS2	type 2 candidate sphingomyelin synthase
Cys	cysteine
DAG	diacylglycerol
DGPP	diacylglycerol pyrophosphate
DMEM	Dulbecco's modified eagle medium

DPP1	diacylglycerol pyrophosphate phosphatase
ECM	extracellular matrix
EGF	epidermal growth factor
EGFR	epidermal growth factor receptor
ER	endoplasmic reticulum
ERK	extracellular signal-regulated kinase
EST	expressed sequence tag
FAK	focal adhesion kinase
FBS	fetal bovine serum
FBS-c	charcoal-stripped fetal bovine serum
GAG	glycosaminoglycan
GFP	green fluorescent protein
Gly	glycine
Glu	glutamic acid
G6P	glucose 6-phosphatase
GPCR	G-protein coupled receptor
Grb	growth factor receptor-bound protein
GTP	guanosine triphosphate
GTPase	guanosine triphosphatase
HBS	Hepes buffered saline
HEK 293	human embryonic kidney cells
HIRcB	human insulin receptor rat1 fibroblasts
His	histidine
IgG	Immunoglobulin G
IP_3	inositol trisphosphate
IL-1β	Interleukin-1β
IL-8	interleukin-8
LCAT	lecithin cholesterol acyl transferase
LPA	lysophosphatidate
LPA_{1-5}	lysophosphatidic acid receptors
LPAAT	lysophosphatidate acyltransferase

LPC	lysphosphatidylcholine
LPE	lysophosphatidylethanolamine
LPL	lysophospholipid
LPP	lipid phosphate phosphatase
LPS	lysophosphatidylserine
LPT family	lipid phosphatase/phosphotransferase family
LRP	lipid phosphatase-related protein
Lys	lysine
lysoPLD	lysophospholipase D
MAG	monoacylglycerol
MDCK	Madin Darby canine kidney cell
MEF	mouse embryonic fibroblast
MEK	mitogen activated protein kinase/ERK kinase
MMP	matrix metalloproteinase
mPA-PLA$_1\alpha/\beta$	membrane-associated PA-selective PLA$_1\alpha/\beta$
mRNA	messenger ribonucleic acid
MT1-MMP	membrane-type-1 matrix metalloproteinase
mTOR	mammalian target of rapamycin
Myc	v-myc myelocytomatosis viral oncogenic homolog
NADPH	reduced nicotinamide adenine dinucleotide phosphate
NEM	N-ethylmaleimide
NGF	nerve growth factor
PA	phosphatidate
PAP	phosphatidate phosphohydrolase
PB	phosphatidylbutanol
pBP	pBabepuro
PBS	phosphate buffered saline
PBS-CM	PBS supplemented with calcium and magnesium
PC	phosphatidylcholine
PCPE	procollagen C-proteinase enhancer
PCR	polymerase chain reaction

PDGF	platelet-derived growth factor
PDGFR	platelet-derived growth factor receptor
PDZ	PSD95/Dig/Z0-1 domain
PE	phosphatidylethanolamine
Pfu	plaque-forming units
PI	phosphatidylinositol
P_i	inorganic phosphate
PI3K	phosphatidylinositol 3-kinase
PIP_2	phosphatidylinositol 4,5-bisphosphate
PIP_3	phosphatidylinositol 3,4,5-trisphosphate
PKC	protein kinase C
PLA_1	phospholipase A_1
PLA_2	phospholipase A_2
PLC	phospholipase C
PLD	phospholipase D
PP1	protein phosphatase 1
PP2A	protein phosphatase 2A
PPARγ	peroxisome proliferator-activated receptor-gamma
PRG	plasticity-related genes
PS	phosphatidylserine
PS-PLA_1	phosphatidylserine-specific PLA_1
Rac	ras-related C3 botulinum toxin substrate
Raf-1	v-raf-1 murine leukemia viral oncogene homolog 1
Rap1	Ras-related protein 1
Ras	rat sarcoma viral oncogene
RECK	reversion-inducing–cysteine-rich protein with Kazal motifs
Rho	Ras homolog
RISK	RNA-induced silencing complex
ROCK	Rho-associated coiled-coil forming protein kinase
RT	room temperature
RTK	receptor tyrosine kinase

RT-PCR	reverse transcription polymerase chain reaction
S1P	sphingosine-1-phosphate
$S1P_{1-5}$	sphingosine-1-phosphate receptors
S.D.	standard deviation
SDS	sodium dodecyl sulfate
SDS-PAGE	sodium dodecyl sulfate polyacrylamide gel electrophoresis
Ser	serine
SH2	Src homology 2
SH3	Src homology 3
siRNA	small interfering ribonucleic acid
SK	sphingosine kinase
SM	sphingomyelin
SMase	sphingomyelinase
SMS	sphingomyelin synthase
Sos	son of sevenless
SPC	sphingosylphosphorylcholine
S-phase	synthesis phase
$sPLA_2$-IIA	type IIA secretory PLA_2
SPP	sphingosine 1-phosphate phosphatase
Src	avian sarcoma viral oncogene
TGFβ	transforming growth factor beta
Thr	threonine
TIMP	tissue inhibitor of metalloproteinase
TLC	thin layer chromatography
TNF-α	tumor necrosis factor-α
tPA	tissue-type plasminogen activator
Trk A	tropomyosin receptor kinase A
Trp	tryptophan
Tyr	tyrosine
VEGF	vascular endothelial growth factor
Wnt	wingless type murine mammary tumor virus integration site

CHAPTER 1

INTRODUCTION

1.1 Wound healing

1.1.1 *Role of fibroblasts in wound healing* - The main function of the skin is to shield the internal environment from mechanical, chemical, and irradiation damage from the outside world [1, 2]. It also serves as an immunological barrier protecting the body from pathogens. The skin is separated into the epidermis consisting mostly of keratinocytes, and the dermis, composed of the collagen-depositing fibroblasts and macrophages (Fig. 1.1A) [2]. The outer-most layer of the skin is the *stratum corneum,* composed of dead, enucleated terminally differentiated keratinocytes filled with densely packed keratin protein. Beneath this layer in the epidermis are differentiated keratinocytes bound to their neighbors by desmosome junctions. These cells form the prickle cell layer. Still beneath this layer are polarized basal keratinocytes that are attached to the basement membrane through hemidesmosomes. At this level keratinocytes proliferate, detach from the basement membrane as they differentiate and become part of the prickle cell layer. These keratinocytes will eventually replace the dead keratinocytes that shed at the skin surface [1, 2]. The basement membrane, composed mainly of a meshwork of collagen-IV, laminin-V, and proteoglycans, separate and bind the epidermis and the dermis, where the fibroblasts reside. Fibroblasts are largely responsible for the production and remodeling of the extracellular matrix (ECM) of the dermis, also known as connective tissue (Fig. 1.1A) [1]. The two main classes of macromolecules in connective tissue that are secreted by fibroblasts are polysaccharide chains known as glycosaminoglycans (GAGs), which are covalently linked to proteoglycans, and fibrous proteins such as collagen, elastin, and fibronectin. The GAGs and proteoglycans form a porous hydrated-gel, where the fibrous proteins are embedded.

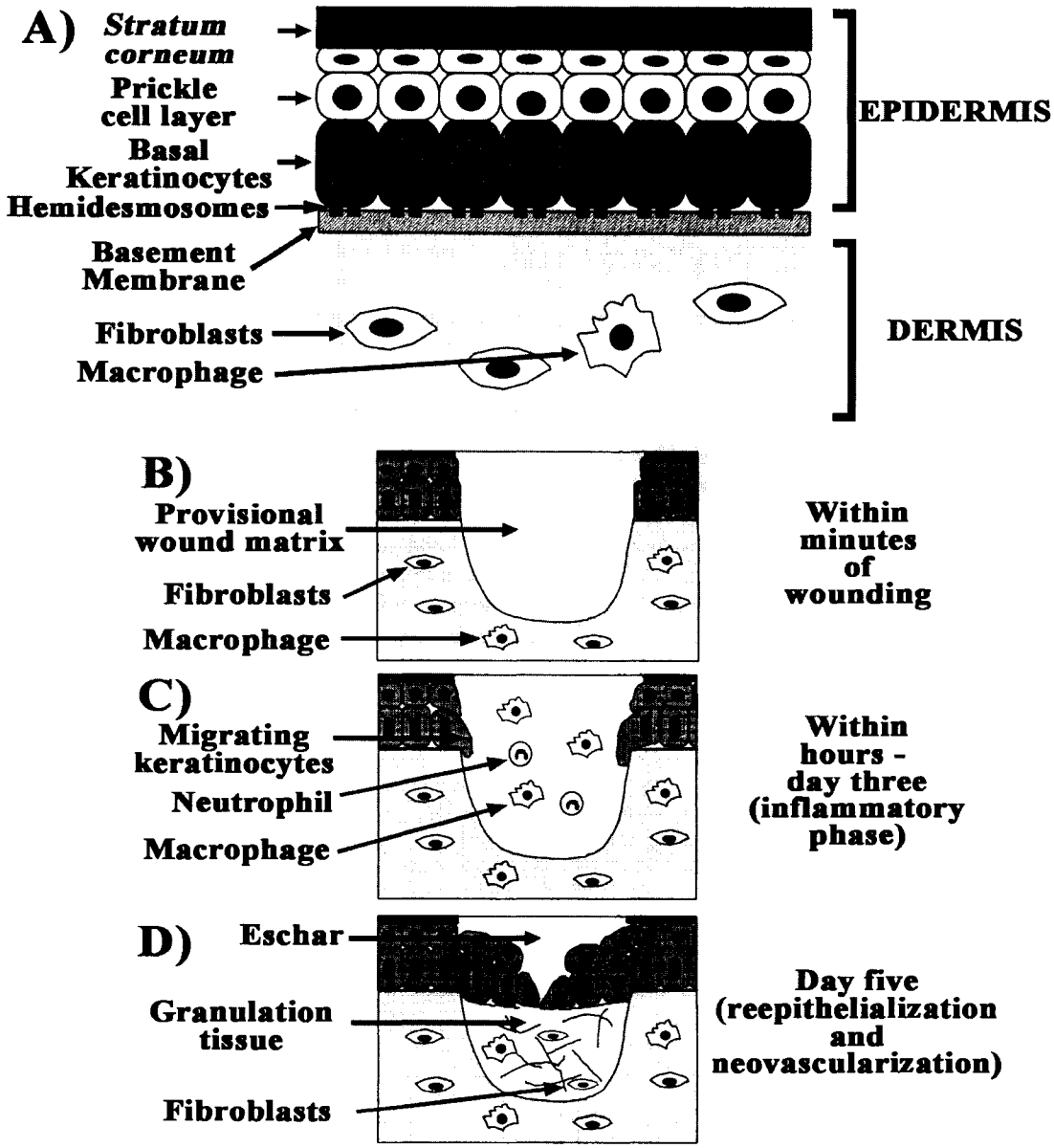

Figure 1.1 Cutaneous wound healing. *Panel A* shows a schematic drawing of the epidermis comprised mostly of keratinocytes. Polarized basal keratinocytes attach to the basement membrane (composed of a meshwork of collagen-IV, laminin-V, and proteoglycans) mediated by specialized junctions called hemidesmosomes. At this level keratinocytes proliferate, move to the prickle cell layer and eventually replace dead keratinocytes shed from the *stratum corneum*. Below the basement membrane lies the dermis, a mesenchymal connective tissue with fibroblasts, macrophages, and collagen fibrils. *Panels B-D* shows a schematic presentation of cutaneous wound healing. (*Panel B*) A blood clot consisting of platelets and fibrin seals the wound providing a provisional wound matrix. The platelets are induced to degranulate and release cytokines and growth factors that attract neutrophils and macrophages from blood, which begin the inflammation phase (*Panel C*). Within hours keratinocytes start migrating down the wound edge along the dermis. Local fibroblasts are activated to divide and by day three start to migrate to the provisional wound matrix where they produce large amounts of collagen and fibronectin to form the granulation tissue (*Panel D*). Blood vessels are produced to provide oxygen and nutrients to the new tissue. Keratinocytes migrate on top of the granulation tissue to reepithelialize the wound. The dead eschar is eventually sloughed off. Diagram is adapted from Brakebusch [2].

The aqueous portion allows nutrients, metabolites, and hormones to diffuse between the blood and the tissue cells. Collagens, and elastins function structurally to give the connective tissue some organization, strength, and resilience. Fibronectin functions as an adhesive glycoprotein that promotes cell attachment, migration, and proliferation [1, 3].

When the cutaneous layer is wounded, there is a disruption of blood vessels and extravasation of blood content. A blood clot is quickly formed to provide a provisional matrix through which cells can migrate and start the healing process (Fig. 1.1B) [4, 5]. The clot is composed of a meshwork of fibrin with embedded platelets. The platelets are induced to degranulate and release cytokines and growth factors, including platelet-derived growth factor (PDGF), epithelial growth factor (EGF), and transforming growth factors (TGF)-β1 and -β2 [5]. Platelets also secrete and synthesize extracellular phospholipid growth factors such as sphingosine 1-phosphate (S1P), and lysophosphatidate (LPA) [6-8]. The activation of platelets provides the chemotactic signals to recruit circulating inflammatory cells, such as neutrophils, and monocytes, to the wound site (Fig. 1.1C) that starts the inflammatory phase [5]. Angiogenesis is also stimulated early in the process so that oxygen and nutrients can be provided during wound healing. In addition, the recruitment of neutrophils, and monocytes, together with platelets provide the early signals to activate reepithelialization by keratinocytes, and activation of connective tissue fibroblasts, and macrophages [2]. Reepithelialization of the wound commences within hours of the injury. This involves the dissolution of hemidesmosomes that anchors the basal keratinocytes to the basement membrane at the edge of the wound, and stimulates their proliferation and migration into the provisional matrix [2]. Local dermal fibroblasts start proliferating early, but are activated to migrate

into the provisional matrix three to four days after injury. This lag phase can be due to the time for the fibroblasts to emerge from quiescence, and express the proper integrins that bind and facilitate migration to fibrin and fibronectin in the clot [4]. Cytokines and growth factors secreted by platelets, epidermal cells, and macrophages also induce migration. Once the fibroblasts arrive to the site of the wound, TGF-β1 induces the fibroblasts to quickly lay down a collagen-rich matrix, and replace the provisional matrix with granulation tissue (Fig. 1.1D) [5]. New capillaries that sustain the development of the granulation tissue with nutrients and oxygen, give it the granular appearance. A week after wounding, the clot has been generally replaced by activated fibroblasts and the freshly deposited collagen matrix. TGF-β1 transforms a population of fibroblasts into myofibroblasts [4]. They resemble smooth muscle cells in their ability to generate contractile forces. They are also responsible for the contraction of the wound in the connective tissue, and help to bring the wound margins closer together to facilitate reepithelialization. Fibroblasts stop making collagen after reepithelialization is complete and abundant collagen matrix is deposited. Most of the myofibroblasts involved in the synthesis of the newly formed scar die by apoptosis [1, 4, 5].

1.1.2 *Fibrotic disorders* - In some cases the deposition of collagen is excessive, such as in scleroderma patients [4, 5]. This can occur when fibroblasts do not die after wound closure and in some cases proliferate due to persistent production of growth factors and inflammation [9]. This can lead to vascular damage, and skin thickening. Most scleroderma patients also develop pulmonary fibrosis. Fibrotic diseases can occur in a variety of organs including lung, liver, intestine and kidneys. In these cases, mesenchymal cells (fibroblasts are classified as mesenchymal cells) excessively

proliferate and uncontrollably deposit collagen, leading to progressive scarring and loss of organ function [9].

There is currently no effective treatment for fibrotic diseases, except with some liver diseases. Corticosteroid and immunosuppressive therapy are not very effective in prevention and treatment of fibrosis [9]. Proliferation of myofibroblasts, the cells chiefly responsible for excessive collagen deposition, is not decreased by anti-inflammatory drugs, but in some cases it is increased by these drugs [10]. PDGF and LPA are important activators of fibroblasts, in that they promote proliferation and migration. Perhaps drugs that decrease the proliferation and migration of mesenchymal cells would be more effective for treatment. In fact many drugs that target PDGF receptor kinase activity are being developed to treat fibrotic diseases [11].

1.2 Extracellular signaling molecules: platelet-derived growth factor, lysophosphatidate, and sphingosine 1-phosphate

1.2.1 *Platelet-derived growth factor production and signaling* - Currently, there are four members of the PDGF family [12]. Each are encoded by their own gene that produces the classic PDGFs; PDGF-A, and -B, and the newly discovered PDGF-C, and -D [13, 14]. They assemble via disulphide bonds into homodimers and heterodimers. Five different dimers have been identified so far: PDGF-AA, PDGF-BB, PDGF-AB, PDGF-CC, and PDGF-DD [12]. Processed and biologically active PDGF-A, and -B are secreted from cells. PDGF-C, and -D are proteolytically cleaved outside of the cell by serum [13-15], and possibly by plasmin and tissue-type plasminogen activator (tPA) [13, 14, 16]. These proteases are also involved in the migration of cells, and the remodeling of the

ECM in wound healing [5]. The PDGF-dimers bind to dimers of PDGF receptors, PDGFRα and PDGFRβ. PDGF-AA, PDGF-AB, PDGF-BB and PDGF-CC can bind to and activate PDGFRα, while PDGF-BB and PDGF-DD can specifically bind to and activate PDGFRβ. PDGF-AB, PDGF-BB and PDGF-CC can also stimulate heterodimeric PDGFRα/β complexes [12]. The extracellular ligand-binding domain of the receptors has five immunoglobulin domains followed by a transmembrane domain, and then an intracellular tyrosine kinase domain (Fig. 1.2) [17]. Because they have tyrosine kinase activity, PDGFRs are classified as receptor tyrosine kinases (RTK).

Upon ligand binding, the receptors dimerize and the two-receptor molecules cross-phosphorylate each other on tyrosine amino acids. Auto-phosphorylation of Tyr^{857} (on human PDGFRβ) in the activation loop of the tyrosine kinase domain regulates phosphorylation of the other tyrosine residues (Fig. 1.2) [18]. The other auto-phosphorylation sites are binding sites for Src homology 2 (SH2)-containing signaling proteins, which bind phosphorylated tyrosine residues depending on amino acid sequence. The SH2-domains of phosphatidylinositol 3-kinase (PI3K), Src, and phospholipase C-γ1 (PLCγ1) binds to phospho-tyrosine residues at the receptor (Fig. 1.2) [17]. The recruitment of the SH2-containing Grb2, and the proline-rich-domain binding Src homology 3 (SH3) of Sos1, forms a complex and leads to the conversion of inactive GDP-bound Ras to active GTP-bound Ras. Within minutes all of these signaling molecules are activated to induce endpoints such as cell proliferation, migration, and cell survival (Fig. 1.2) [17]. PDGFR is also internalized after activation, and endosomal PDGFR signaling is sufficient to stimulate cell proliferation [19].

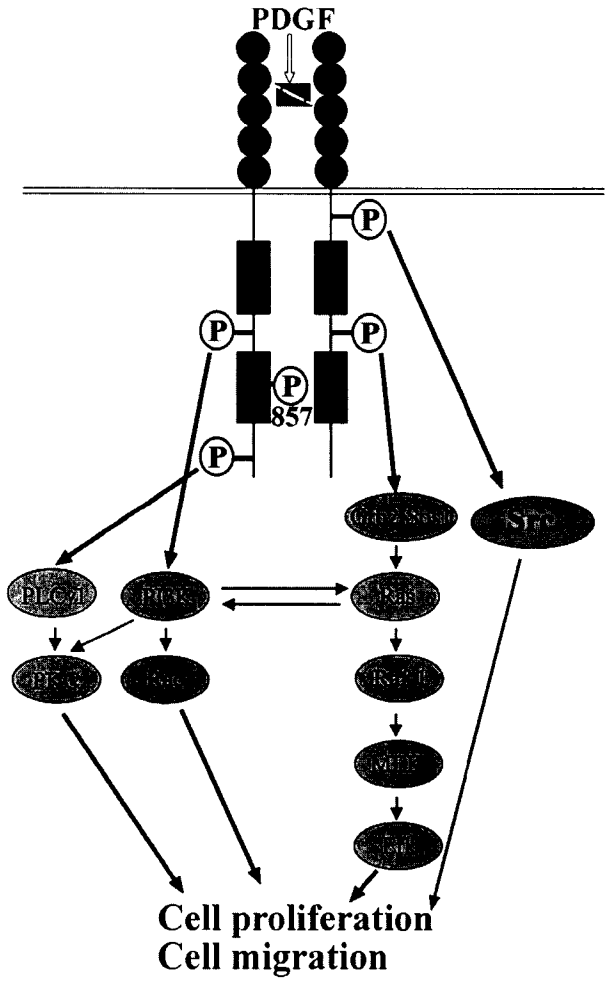

Figure 1.2 PDGFRβ-induced pathways. A ligand-bound human PDGFRβ induces the auto-phosphorylation of Tyr^{857} that regulates the auto-phosphorylation of other tyrosines. Signaling proteins bind the phospho-tyrosines through their SH2 domains and induce signaling pathways leading to cell proliferation and cell migration. *Arrows* originating from *circled-P's* to the first signaling protein in the indicated signaling pathways represent direct binding by SH2 domains to the phospho-tyrosines. This figure was adapted from a diagram published by Rönnstrand *et al.* [17].

PDGF-A, and-B are expressed in most organs. As mentioned in Section 1.1.1, platelets, macrophages, and epidermal cells can produce PDGF, which activates fibroblasts to proliferate and migrate to the wound site [4, 5]. In pulmonary fibrosis, alveolar macrophages have enhanced PDGF production [20]. Pulmonary fibroblasts also have increased PDGFR expression, which increases proliferation and migration [21]. In other organs with fibrotic damage, there is a consistent relationship with increased PDGF

and PDGFR so that fibroblast proliferation and migration is enhanced at the site of organ damage [9].

PDGF, and PDGFR are also required in development. Deletion of either PDGFR results in embryonic lethality. PDGF-A or PDGFRα null embryos have defects in the production of mesenchymal cells [22]. PDGF-B or PDGFRβ null embryos have a severe shortage of vascular smooth muscle cells and die from widespread microvascular bleedings [23]. PDGF also has a role in regulating tumor angiogenesis and tumor fibroblasts to maintain tumor stroma [24].

1.2.2 *Extracellular lysophosphatidate production* - Lysophosphatidate (LPA) is the most basic of the signaling lipid phosphates. It is composed of a glycerol backbone, a phosphate moiety and a single acyl-chain in either the *sn*-1 or *sn*-2 positions (Fig. 1.3). Despite its simple structure, LPA evokes a wide range of cellular effects, including cell proliferation, cell migration, prevention of apoptosis, cytokine and chemokine secretion, platelet aggregation, and neurite retraction [25, 26]. Topical application of LPA to a wound on a rat increased the immigration of macrophages to the wound site and promoted wound healing [27]. LPA also stimulates the contraction of a collagen matrix by myofibroblasts *in vitro* in a Rho/Rho kinase dependent manner [28]. These steps are important in the wound healing process, and the importance of LPA involved in these physiological situations is still growing. Among the important questions about LPA signaling, it is still uncertain how and where it is produced *in vivo*.

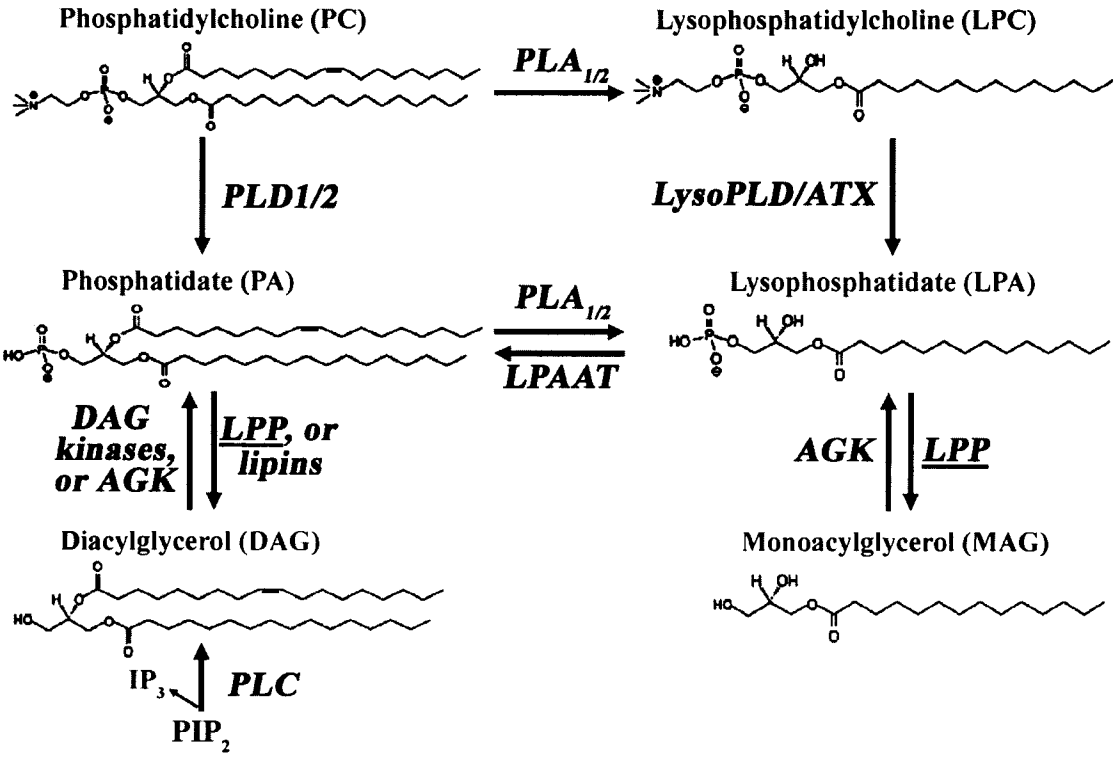

Figure 1.3 Metabolism of PA, LPA, and DAG. The major pathways for the synthesis, and degradation of signaling PA, LPA, DAG are shown. The enzymes are italicized. PLD1/2 are specific for PC. $PLA_{1/2}$, phospholipase A_1 or A_2; PLD1/2, phospholipase D1 or D2; LysoPLD, lysophospholipase D; ATX, autotaxin; AGK, acylglycerol kinase; LPP, lipid phosphate phosphatase; LPAAT, LPA acyltransferase; PLC, phospholipase C; PIP_2, phosphatidylinositol 4,5-bisphosphate; IP_3, inositol trisphosphate.

Significant concentrations of LPA ranging from 0.6 μM in plasma and 80 μM in the ascites of ovarian cancer patients have been detected in biological fluids [6, 29]. There is more LPA in serum than plasma because blood coagulation produces LPA *de novo*, in large part by platelets (Fig. 1.4) [30]. Upon activation of isolated platelets about 10% of the LPA produced is associated with the platelets [30]. In this pathway phospholipase-A_1 or -A_2 ($PLA_{1/2}$) remove the acyl-chain from position *sn*-1 and *sn*-2, respectively, of phosphatidate (PA) (Fig. 1.3 and pathway (3) in Fig. 1.4). Secreted $sPLA_2$-IIA has been implicated in the production of LPA from PA, among the many identified PLA_2 (pathway (3) in Fig. 1.4). Rat and human platelets secrete $sPLA_2$-IIA.

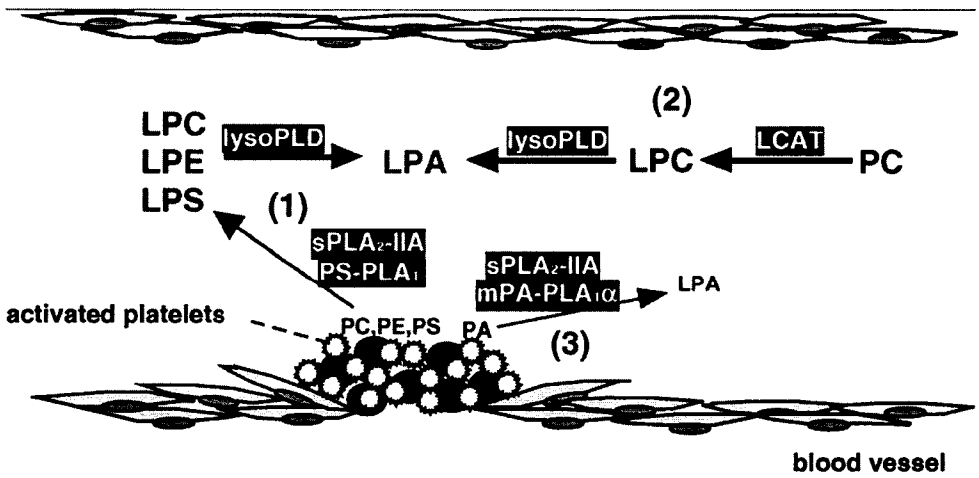

Figure 1.4 Synthetic pathways for serum LPA. Figure originally published by Aoki, J. [6]. This figure shows a schematic presentation of the lumen of a damaged blood vessel. The blood clot is the site of platelet aggregation and activation. Pathway (1) demonstrates how the majority of serum LPA is formed trough the generation of lysophospholipid species (LPC, lysophosphatidylcholine; LPE, lysophosphatidylethanolamine; LPS, lysophosphatidylserine) from membrane phospholipids (PC, phosphatidylcholine; PE, phosphatidylethanolamine; PS, phosphatidylserine) of activated platelets by $sPLA_2$-IIA or PS-PLA_1. The lysophospholipids are then converted to LPA by plasma lysoPLD/ATX. (2) During blood clotting LPA can also be derived from the sequential actions of lecithin cholesterol acyl transferase (LCAT) then lysoPLD/ATX from PC in high-density lipoproteins, or from plasma LPC associated with albumin. (3) PA generated by platelets or PA from microvesicles shed by erythrocytes or platelets can be deacylated to LPA by $sPLA_2$-IIA or membrane-associated PA-selective PLA_1 (mPA-PLA_1). The LPA levels produced by pathway (3) are less than that by pathway (1). However, pathway (3) generates LPA rapidly and is highly inducible.

Fourcade *et al.* [31] showed that LPA is produced when $sPLA_2$-IIA was added to microvesicles shed by activated inflammatory cells including erythrocytes, platelets and white blood cells (pathway (3) in Fig. 1.4). The disrupted asymmetry of these membranes exposes PA that had been accumulated by these activated cells. However, LPA with an unsaturated fatty acid acyl-chain is generally produced by PLA_1 and is biologically more potent than LPA with saturated fatty acid acyl-chain, which is produced by PLA_2 [6, 29]. Two secreted and membrane-associated PA-selective PLA_1s (mPA-$PLA_1\alpha$ and -β) have been identified that could increase biologically potent extracellular LPA with an unsaturated fatty acid acyl-chain (pathway (3) in Fig. 1.4) [6].

PA is generated by phospholipase D 1 or 2 (PLD1/2), which produces PA from phosphatidylcholine (PC) (Fig. 1.3). PA can also be generated by phospholipase C (PLC) activity that generates diacylglycerol (DAG) from phosphatidylinositides (PI), and then PA is formed by DAG kinases (Fig. 1.3). An advantage of these pathways is that they are inducible by external stimuli and are highly regulated sources of LPA [6]. Most of these enzymes are found inside the cell, with the exception of secreted $PLA_{1/2}$. How PA is transported from the inner-leaflet to the outer-leaflet of the plasma membrane to be metabolized by secreted $PLA_{1/2}$ is unknown. As mentioned above, the coagulation of platelets is usually at a site of injury that produces cell debris, and where inflammation disrupts plasma membrane asymmetry so that PA is exposed to extracellular enzymes. Secreted PLD from bacteria can degrade PC to PA on the outer-leaflet of the plasma membrane, where secreted PLA_1 produces external LPA [32]. This could be a relevant source of LPA since bacteria can be introduced through the exposure of a wound to the environment.

The synthesis of LPA by the deacylation of exposed PA is not unique to activated platelets, and have been proposed to occur in ovarian cancer cells [33-35], and prostate cancer cells [36] in the production of extracellular LPA. Recently, a novel intracellular acylglycerol kinase (AGK), an enzyme that phosphorylates monoacylglycerol (MAG) and DAG, was found to enhance the formation of LPA and PA, respectively, and increase the production of bioactive extracellular LPA by prostate cancer cells and fibroblasts [37].

As mentioned above, the production of LPA from PA by isolated platelets accounted for 10% of total LPA in serum. When plasma was added to these platelets,

there was an enhanced accumulation of LPA produced *de novo* [30], which accounted for most of the LPA produced by activated platelets. Most of this LPA was derived from the action of plasma lyso-phospholipase D (lysoPLD) that degrades lysophospholipids (LPL) to LPA (Fig. 1.3 and pathway (1) in Fig. 1.4). The most abundant LPL in plasma is lysophosphatidylcholine (LPC), which can be found at concentrations as high as several hundred μM [38, 39]. LPC is usually associated with albumin and lipoproteins in plasma (pathway (2) in Fig. 1.4). Plasma LPC with unsaturated fatty acid acyl-chains is secreted by hepatocytes [38, 39]. LPC with saturated fatty acid acyl-chains is generated by lecithin cholesterol acyl transferase (LCAT) on lipoproteins (pathway (2) in Fig. 1.4) [39, 40]. Activated platelets generate other LPLs including lysophosphatidylserine (LPS), and lysophosphatidylethanolamine (LPE). Plasma lysoPLD are also known to degrade these LPLs (Fig. 1.3 and pathway (1) in Fig. 1.4) [39]. The LPLs are generated by the actions of secreted $PLA_{1/2}$, such as $sPLA_2$-IIA, which can deacylate PA, phosphatidylserine (PS), and phosphatidylethanolamine (PE), and PS-PLA_1, which prefers PS (Fig. 1.3 and pathway (1) in Fig. 1.4) [39]. PS and PE are usually found in the inner-leaflet of the plasma membrane, but disruption of phospholipid asymmetry in activated platelets, apoptotic cells, and cells stimulated by inflammatory cytokines can result in the exposure of PS and PE. These states are associated with wound healing, and fibrosis. In the case of cancer cells, there is high secretion of microvesicles and apoptotic cells where $sPLA_2$-IIA and lysoPLD can produce a high amount of LPA [41].

A lysoPLD from plasma and serum that generated LPA from circulating LPC was identified as autotaxin (ATX) [42, 43]. ATX was originally identified as an autocrine motility factor for melanoma cells, and is implicated in tumor progression [41, 44]. It is a

ubiquitously expressed transmembrane enzyme that can be proteolytically cleaved to produce a soluble form found in plasma. Many biological functions attributed to LPA are also attributed to ATX. For example, ATX, like LPA induces neurite retraction [45], and fibroblast migration [46]. ATX heterozygous knockout mice appear healthy but show half-normal plasma LPA levels [47, 48], therefore ATX maintains plasma LPA concentrations. ATX null mice die as embryos with profound vascular defects, which supports a role for ATX and LPA in the stabilization of preformed blood vessels [47, 48]. LPA and ATX are also found in blister fluid, and are proposed to be involved in the migration of basal keratinocytes for reepithelialization after blister rupture [49]. LPA secreted by adipocytes stimulate preadipocyte proliferation in a paracrine manner [50]. In parallel, ATX mRNA expression is highly up-regulated during differentiation of preadipocytes. This up-regulation is paralleled by the ability of newly differentiated adipocytes to release ATX, produce LPA and stimulate preadipocyte proliferation [51]. There is also an increase of ATX mRNA in an obese mouse model [51]. ATX mRNA is also up-regulated in many cancers such as renal cell carcinoma, glioma, melanoma, and in ovarian cancer cell lines [29]. These cancers are associated with elevated LPA levels that facilitates angiogenesis, tumor progression and resistance to drug treatment [29].

1.2.3 *Extracellular sphingosine 1-phosphate production* - Sphingosine 1-phosphate (S1P) is structurally similar to LPA (Fig. 1.5), and it also has diverse biological functions dependent on extracellular signaling. External S1P is a potent stimulator of angiogenensis [7, 52], and it is important in the vascular stabilization of developing blood vessels by recruiting vascular smooth muscle cells [53]. S1P accounts for the major chemotactic activity of clotted blood for vascular endothelial cells and for

stimulating angiogenesis *in vivo* [54]. S1P is involved in the recirculation of lymphocytes from the thymus and lymph nodes [55]. Recently, a biospecific monoclonal antibody to S1P reduced tumor progression and in some cases eliminated measurable tumors in murine xenograft and allograft models. Tumor growth inhibition was attributed to antiangiogenic and antitumorigenic effects of the antibody [56].

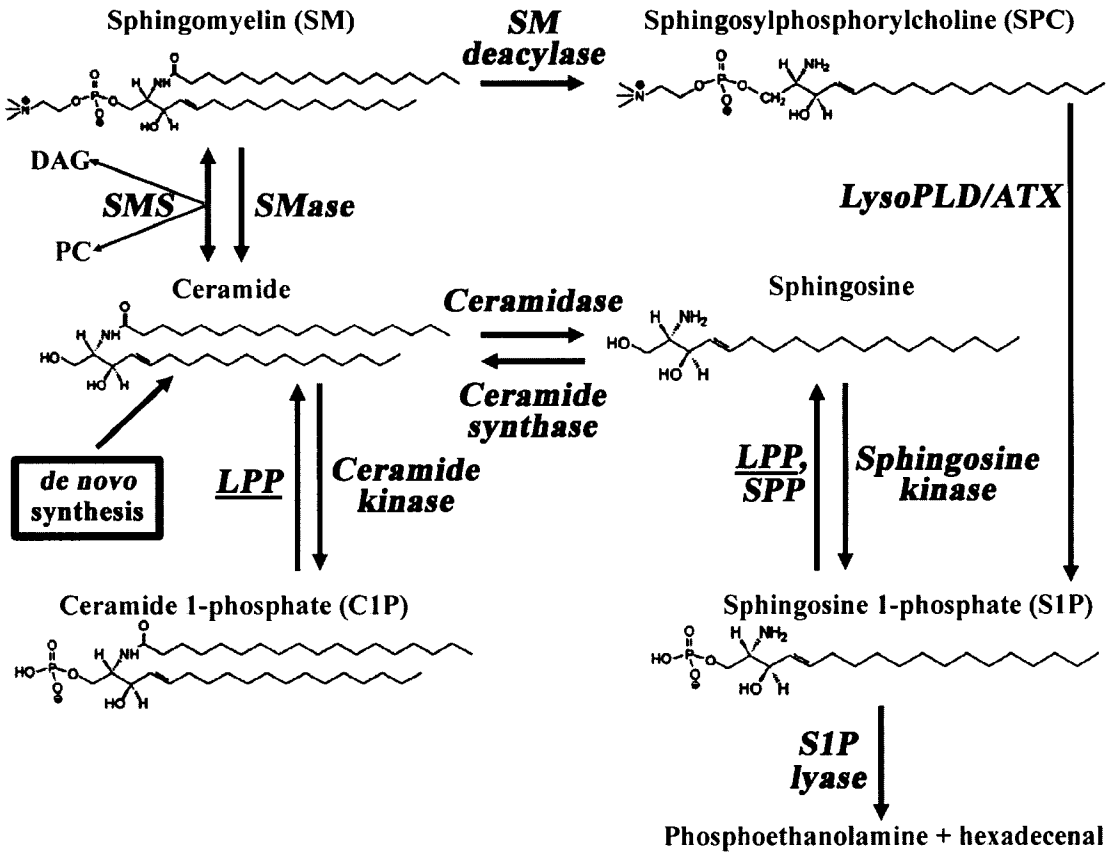

Figure 1.5 Metabolism of signaling sphingolipids. The major pathways for the synthesis and degradation of signaling sphingolipids are shown. *De novo* synthesis of ceramide is initiated by the condensation of serine and palmitoyl-CoA by serine palmitoyl-CoA transferase. The SMS phosphotransferase reaction reversibility is shown as a double-ended arrow. The enzymes are italicized. SMase, sphingomyelinase; SMS, sphingomyelin synthase; SPP, sphingosine 1-phosphate phosphatase; lysoPLD, lysophospholipase; ATX, autotaxin; LPP, lipid phosphate phosphatase; DAG, diacylglycerol; PC, phosphatidylcholine.

Significant concentrations of S1P are found in plasma (190 nM), and in serum (484 nM) [57]. One source of S1P could come from the actions of sphingomeylin (SM) deacylase to produce sphingosylphosphorylcholine (SPC) from SM (Fig. 1.5). ATX can then degrade SPC to S1P (Fig. 1.5) [58]. However, this source of S1P needs to be confirmed since the levels of plasma SPC are very low (nanomolar) compared to that of plasma LPC (several hundred micromolar) of which ATX readily metabolize. Moreover, heterozygous ATX knockout mice have a 50% decrease of circulating LPA, but no change in circulating S1P levels [48]. Currently, two paths are known that can produce physiologically relevant extracellular S1P: phosphorylation of extracellular sphingosine by sphingosine kinase 1 (SK1) released by vascular endothelial cells [59], and release of intracellular S1P from cells [8].

The first pathway requires that sphingosine and adenosine triphosphate (ATP) are present in the extracellular space for extracellular SK1. There are secreted and membrane associated enzymes with ecto-activity that can produce exogenous sphingosine. For example, sphingomyelinases (SMase) are ubiquitous and constitutively secreted enzymes that remove the phospho-choline group from abundantly available SM to generate ceramide (Fig. 1.5) [8]. Ceramide is then deacylated by neutral ceramidase (CDase) (Fig. 1.5), a transmembrane enzyme with ecto-activity. A soluble form of neutral CDase also exists. CDase action produces sphingosine, which can be immediately transported into the cell or quickly phosphorylated by extracellular SK1. As for extracellular ATP, activated platelets, endothelial cells, and smooth muscle cells [60] can secrete ATP. Extracellular ATP can also be generated by a cell surface H^+-ATP synthase found on vascular endothelial cells [61].

The second source of S1P comes from the secretion of S1P stores that activate cells in an autocrine and paracrine manner. External stimuli from PDGF, vascular endothelial growth factor (VEGF), and tumor necrosis factor-α (TNF-α) can stimulate internal SK1 to produce S1P (Fig. 1.5), which is then released from the cell and activates neighboring cells [62]. The amount of S1P released from blood cells such as erythrocytes, neutrophils, and platelets is much higher then other cells [30, 63]. This mechanism of release is unclear since S1P is polar compound and will not readily traverse the lipid bilayer of the plasma membrane [64, 65]. Therefore, export into the extracellular space requires secretory organelles or specific transporters. An ATP-binding cassette (ABC) transporter, ABCC1, but not ABCB1, exports S1P from mast cells [64].

Both of the pathways that form S1P depend on SK activity. Knockout of both SK isoforms resulted in embryonic death, and embryos with extreme deficiency of S1P levels [66]. This provides further evidence that the actions of sphingomyelin deacylase, which converts SM to SPC, and subsequent actions of ATX to generate extracellular S1P (Fig. 1.5), cannot substitute for the SK pathway in the production of extracellular S1P *in vivo*.

1.2.4 *Signaling by extracellular lysophosphatidate and sphingosine 1-phosphate* - Exogenous LPA, and S1P are known to elicit a response in most mammalian cells tested. About a decade ago the identification of G-protein coupled receptors (GPCRs) for LPA and S1P provided a mechanism for the extracellular effects [67, 68]. Currently there are five known receptors for LPA and S1P (LPA_{1-5} and $S1P_{1-5}$) [69, 70]. The LPA and S1P receptors are differentially expressed, depending on the cell type and physiological or pathophysiological situation. They can transduce a variety of signals depending on what

heterotrimeric G-proteins they couple with, and the balance of their relative expression (Fig. 1.6) [69, 71].

Activation of $G_{i/o}$ decreases cAMP concentrations and induces Ras-dependent signaling leading to the activation of extracellular signal-regulated kinase (ERK) (Fig. 1.6). These signals are associated with cell proliferation. $G_{i/o}$ also activates phosphatidylinositol 3-kinase (PI3K), which is an effector for cell migration, and

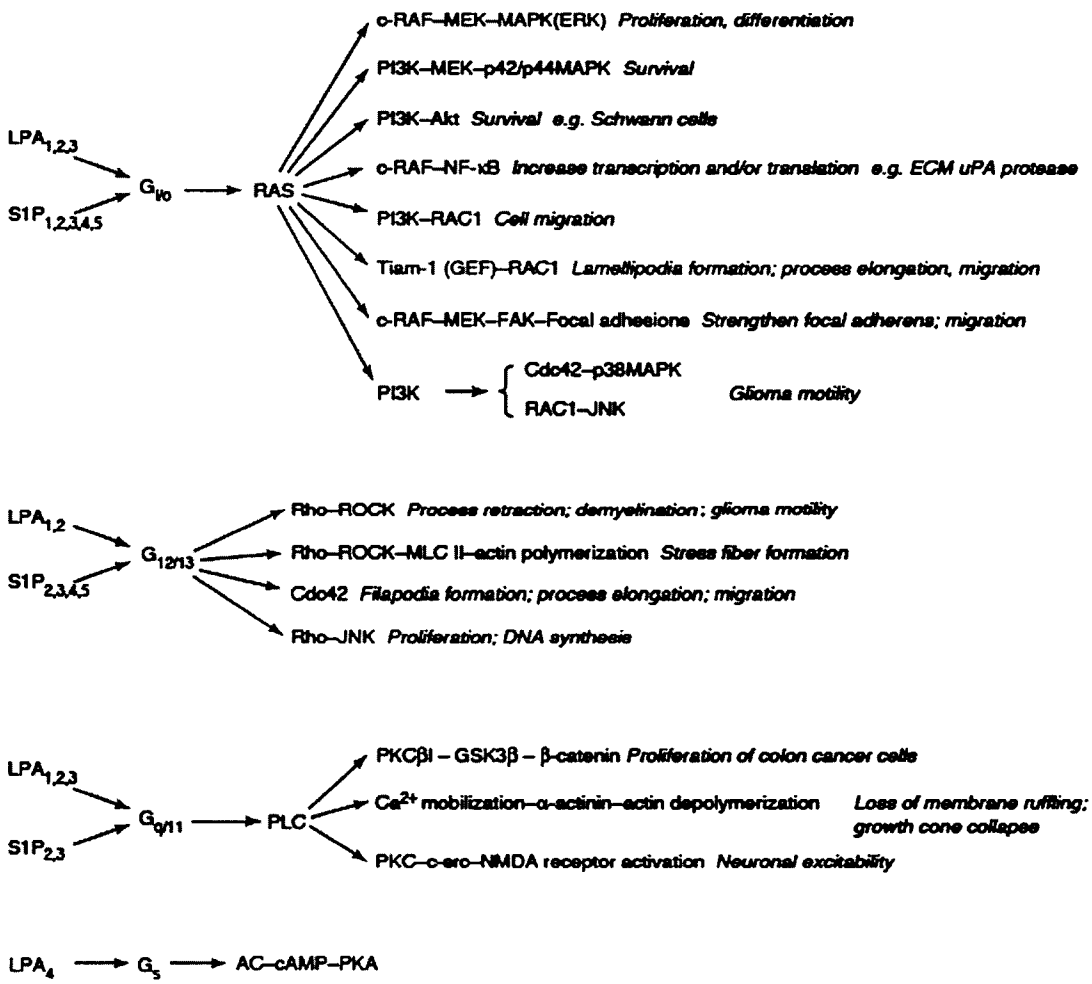

Figure 1.6 LPA and S1P receptor signaling. This figure was first published by Gardell *et al* [69]. LPA and S1P receptors (LPA_{1-4} and $S1P_{1-5}$) activate diverse second messenger pathways through the coupling of heterotrimeric G-proteins. This figure shows examples of the signaling proteins and the pathways they mediate to produce an effect on cell function, which are shown in italics. Since the publication of this figure another LPA receptor (GPR92/LPA_5) was identified. It couples to $G_{12/13}$ and G_q and increases cAMP levels [70].

survival. The $G_{i/o}$-dependent activation of Rac is also an important signal for cell migration. Migration of mouse embryonic fibroblasts induced by LPA is mediated by LPA_1-G_i-Rac1, with some contribution from LPA_2 [46]. The knockout of $S1P_1$, which is solely coupled to $G_{i/o}$ results in embryo death and severe hemorrhaging [53]. This is because the new blood vessels are not reinforced by vascular smooth muscle cell recruitment.

$G_{12/13}$ is associated with the activation of Rho and Cdc42 (Fig. 1.6) and involves cytoskeletal responses, such as stress fiber formation, cell rounding, and neurite retraction and wound contraction. Rho also stimulates cell proliferation [71]. The C-termini of LPA_1 and LPA_2 also have classical PDZ domain interaction motifs that interact with signaling molecules such as PDZ-containing RhoGEF's [72]. This interaction provides a mechanism for LPA to activate Rho by $G_{12/13}$. $LPA_{1,2,3}$ are coupled to $G_{i/o}$ and $G_{q/11}$, and both $LPA_{1,2}$ is coupled to $G_{12/13}$, which can activate Rac and Rho, respectively (Fig. 1.6). This is important because Rac and Rho activities regulate the cytoskeletal responses that control cell shape changes required for cell migration [73]. Rac activation leads to membrane ruffling and production of lamellipodial protusions at the leading edge of migrating cells. Rho activation induces cell rounding, dissolution of old cell adhesions and regulates the contraction and retraction forces observed at the trailing edge. This suggests that the activation of $G_{i/o}$ and $G_{12/13}$ by LPA_1, LPA_2 and/or LPA_3 is coordinated such that cell migration can occur [71]. Coordination can be regulated at many levels, for example, the relative concentrations of the LPA receptors, and the ratio of LPA receptor subtype coupled to $G_{i/o}$ versus $G_{12/13}$. Also the location of receptors and G-proteins is important. Perhaps the receptor and/or the G-proteins that control Rac activity are

concentrated at the front of the migrating cell, and those that regulate Rho activity are concentrated in the rear of the migrating cell. These conditions can determine the relative extent of Rac and Rho activation and dictate the nature of the cytoskeletal response [71]. The modulation of Rac and Rho activation is facilitated by the ability of these proteins to negatively regulate each other [73]. Therefore, cross talk between the receptors and the activated heterotrimeric G-proteins is important in the final cell response, and this is dictated by cell type and physiological condition.

Activation of G_q binds to and activates phospholipase C (PLC) β (Fig. 1.6). PLC catalyzes the conversion of phosphatidylinositol 4,5-bisphosphate (PIP_2) to DAG and inositol trisphosphate (IP_3). DAG can activate classical and novel PKC isoforms, and IP_3 binds to receptors on the endoplasmic reticulum (ER) resulting in the mobilization of stored Ca^{2+}. Ca^{2+} can also activate classical PKCs and other signaling molecules such as myosin light chain kinase, and Ca^{2+}/calmodulin-dependent kinase [71]. The activation of PKCs by G_q action and the activation of Rho by $G_{12/13}$ can increase the activation of phospholipase D1 (PLD1) to generate PA [74], which is another example of cross talk between two receptor subtypes with the same ligand.

There is a wide variety of signaling that is transduced by LPA and S1P receptors (Fig. 1.6). The response from the cell depends on the expression and concentration levels of the receptor subtypes and the heterotrimeric G-proteins that couple to them. LPA receptors also have differential affinities for the type of fatty acid acyl-chain on the LPA. For example, $LPA_{1/2}$ demonstrate selectivity towards saturated LPA as ligands, whereas $LPA_{3/4}$ preferentially bind unsaturated LPA [29]. Therefore, the species of LPA that is present can determine how the cell responds. There is also preferential coupling to

heterotrimeric G-proteins, for example $S1P_3$ activation of PLC through G_q is almost abolished in $S1P_3$ null mouse embryonic fibroblasts (MEFs), but not in $S1P_2$ null fibroblasts even though $S1P_2$ can couple to G_q [75]. Additionally, in cells that express more than one receptor subtype responses are affected by cross talk from other signals generated by the other lipid phosphate specific receptors. The PDZ-interacting domains of LPA_1 or LPA_2 provides another layer of complexity as they bind to several signaling regulators of Rho [72], and the chloride channel, cystic fibrosis transmembrane regulator [76]. Other PDZ-dependent interactions with LPA_1 or LPA_2 could reveal more mechanisms of LPA function. Finally, not only are there signals from the activated GPCRs themselves, there is transactivation and augmentation of receptor tyrosine kinases (RTKs) signaling by LPA and S1P receptors [77, 78]. For example, activated LPA receptor $G_{\beta\gamma}$ subunits mediate Src-dependent phosphorylation of the EGF receptor to activate the Ras pathway [79]. PLD2 is required to mediate LPA-induced transactivation of PDGFRβ in bronchial epithelial cells [80]. Transactivation of the EGF receptors by LPA and S1P can also be mediated by metalloproteinase-dependent shedding of membrane bound EGF to a soluble form capable of binding and activating the EGF receptor [81]. It was also found that $S1P_1$ is tethered to PDGFRβ, and LPA_1 is tethered to the nerve growth factor (NGF) receptor, tropomyosin receptor kinase A (Trk A) [78]. These complexes are proposed to provide a platform to share associated signaling molecules so that there is more efficient cell stimulation.

1.3 Production and signaling of intracellular lipid phosphates

1.3.1 *Metabolism of bioactive glycerolipids: phosphatidate, and lysophosphatidate* - The metabolism of PA and LPA was discussed in Section 1.2.2 in terms of the production of external PA and LPA. The extracellular enzymes lysoPLD/ATX, and the secreted isoforms of PLA_1, and PLA_2 produced local LPA. However, some of the other enzymes are found inside of the cell, including PLC (converts PIP_2 to DAG), PLD (converts PC to PA), and cytosolic PLA_1 and PLA_2. These enzymes are capable of forming intracellular PA and LPA (Fig. 1.3). Again, cytosolic PLA_1 or PLA_2 can convert PA to LPA. LPA can be converted to PA by the LPA acyltransferase (LPAAT) family of enzymes (Fig. 1.3). PA and LPA levels can be regulated by lipid phosphate phosphatases (LPPs) by their dephosphorylation to DAG and MAG, respectively. Conversely, DAG kinase, and acylglycerol kinase (AGK) can convert DAG and MAG back to their phosphorylated forms [37] (Fig. 1.3). Internal PA can also be dephosphorylated by phosphatidate phosphohydrolase-1 (PAP1) activity, which has been recently attributed to the actions of lipin-1, -2, and -3 [82]. These pathways are depicted in a schematic diagram in figure 1.3.

Another interesting source of intracellular LPA could be from externally generated LPA. The cystic fibrosis transmembrane regulator (CFTR) is a member of the ATP binding cassette family, and was recently postulated to function as a flippase for S1P and LPA [83]. The LPA_2 receptor also interacts with CFTR mediated by its PDZ-interaction domain [76], therefore CFTR may regulate LPA_2 signaling and control the entry of LPA into the cell. The LPPs could also help transport external LPA, in that its lipid phosphatase catalytic site is facing the outside of the cell where it can degrade

membrane impermeable LPA to cell permeable MAG. MAG can be internalized and intracellular acylglycerol kinases can convert it back to LPA [84, 85].

1.3.2 *Intracellular actions of phosphatidate, and lysophosphatidate* - Not only is PA an important metabolite in the synthesis of external LPA, PA is an important signaling second messenger inside of the cell. PA generated by PLD stimulates NADPH oxidase to induce degranulation of neutrophils [86]. PA can also bind and activate protein kinase C-ζ [87], and phospholipase C-γ [88]. PA increases Ras-GTP concentrations by inhibiting its GTPase activating protein [89]. PA can bind to sphingosine kinase-1 and increase its activity when recruited to membranes [90]. PA binds and inhibits the γ isoform of protein phosphatase-1 catalytic subunit (PP1cγ) [91]. PA formation in MDCK [92] and HIRcB cells [93] directly binds to and recruits Raf-1 to membranes so that it can activate the ERK pathway. PA also increases cell division and promotes cell survival through binding and activation of mammalian target of rapamycin (mTOR) [94-96]. PA stimulates stress fiber formation [97, 98] by activating phosphatidylinositol 4-phosphate 5-kinase [99, 100]. The relative concentrations of LPA and PA in membranes control their curvature and vesicle budding [101, 102]. PLD1 and its activator, ARF, are involved in vesicle movement through PA production [103, 104].

Degradation of PLD generated PA to DAG by the LPPs can also produce potential signaling molecules. For instance DAG can stimulate classical and novel PKC isoforms. However, Pettitt *et al.* [105] observed that the acyl-chain composition of PA produced by PLD is mostly monounsaturated and/or saturated, in contrast to DAG produced by PI-specific PLC, which produces DAG with polyunsaturated acyl-chains. They found that DAG derived from PLD activities did not activate PKCs *in vivo*, whereas

DAG with polyunsaturated acyl-chains from PLC activities did activate PKCs *in vivo.* Therefore, it appears the degradation of PLD-derived PA may ultimately be a way to attenuate the PA signal [74].

Intracellular signaling by LPA is less defined, but recent studies show that LPA can directly affect the activation of nuclear receptors. It was reported that LPA_1 was localized to the nucleus in unstimulated porcine cerebral microvascular endothelial cells and PC12 cells [106, 107]. Stimulation of highly purified isolated nuclei with LPA induced increases of Ca^{2+} transients, and the expression of genes involved in inflammation [106]. Additionally, McIntyre *et al.* [108] showed that LPA, and synthetic LPA analogs directly bind to and activate the nuclear transcription factor, peroxisome-proliferator-activated receptor γ (PPARγ). It was also shown that LPA induced neointima formation through the activation of PPARγ [109] that can lead to atherosclerotic diseases. Conversely, a report found that LPA is not a PPARγ agonist in adipocytes [110]. LPA activation of LPA_1 decreased PPARγ expression that led to decreased adipocyte differentiation.

1.3.3 *Metabolism of bioactive sphingolipids: ceramide 1-phosphate, and sphingosine 1-phosphate* - The metabolism of sphingolipids was discussed in Section 1.2.3 in the context of extracellular S1P production (Fig. 1.5). Ceramide is the central core lipid in the metabolism of spingolipids. It is produced *de novo* in the ER with the initial step by serine palmitoyl-CoA transferase that condenses serine and palmitoyl-CoA [8, 111, 112]. In the Golgi apparatus, ceramide is converted to SM by SM synthase-1 (SMS1). SM could also be formed on the outer-leaflet of the plasma membrane by SMS2, since its active site is directed to the extracellular space [113]. The second main source of

ceramide is the metabolism of sphingomyelin by SMases (SMases are found inside and outside of the cell depending on the isoform), and by the reverse reaction of the SMSs. Ceramide can be phosphorylated by ceramide kinase (CERK) to ceramide 1-phosphate (C1P), and dephosphorylated back to ceramide by the LPPs. Ceramide is also degraded to sphingosine by ceramidase, and the reverse reaction is catalyzed by ceramide synthase. Sphingosine can be phosphorylated by sphingosine kinases (SKs) to produce S1P. Three types of enzyme action can degrade S1P: the three LPPs, two specific sphingosine phosphate phosphatases (SPPs), and S1P lyase that cleave S1P irreversibly to phosphoethanolamine and hexadecenal. As mentioned in Section 1.2.3, SM can be converted to SPC by SM deacylase, which can then be converted to S1P by ATX. These pathways are depicted in a schematic diagram in figure 1.5.

1.3.4 *Intracellular actions of ceramide 1-phosphate, and sphingosine 1-phosphate* - A vast accumulation of studies on sphingolipid signaling has shed light on the importance of these lipids in controlling cell fate [114]. Generally, it has been observed that sphingosine and ceramide promote apoptosis and cell-cycle arrest, and their phosphorylated forms, S1P and C1P, respectively, promote cell proliferation, cell survival, and cell motility. It is hypothesized that because these metabolites are interconvertible, the relative amounts of these opposing signals determine the fate of the cell (Fig. 1.7) [114]. The kinases involved in the proposed 'sphingolipid rheostat' are sphingosine kinases (SK) and ceramide kinase (CERK). The lipid phosphatases are the LPPs and S1P specific, SPPs. Because these metabolites can be interconverted by one enzymatic step, the actions of a single enzyme can affect the fate of the cell (Fig. 1.7).

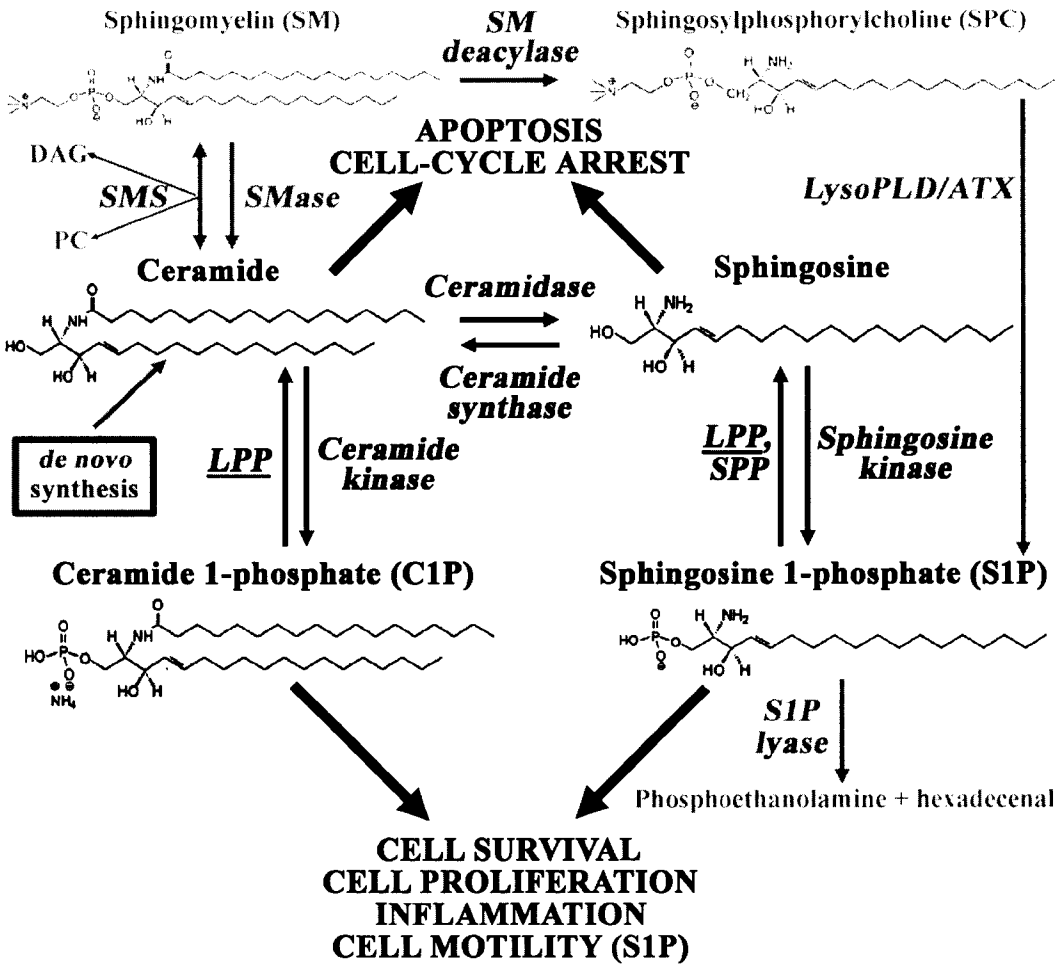

Figure 1.7 The sphingolipid rheostat. The schematic shows the opposing signaling roles of sphingosine, S1P, ceramide, and C1P. Because of the interconvertibility of these molecules, the activity of a single enzyme in the depicted pathways may affect the fate of the cell.

As mentioned in Section 1.2.3, S1P produced intracellularly can be secreted to activate cell surface GPCRs in an autocrine and paracrine manner. This can stimulate cell growth, cell migration, and cell survival, angiogenesis, and inflammation [69, 114]. S1P can also function inside the cell independently of S1P receptors. For example activation of Ras and ERK signaling pathways by VEGF required SK1, and is independent of S1P receptor action [115]. S1P inhibits apoptosis of male germ cells independently of receptors by inhibiting NF-κB and phosphorylating Akt [116]. S1P can induce Ca^{2+}-mobilization independently of GPCRs and IP_3 production [117, 118]. The location of S1P

production also determines cellular outcome. Upon serum starvation active SK2 is translocated to the ER and induces apoptosis [119]. Targeting SK1 to the ER is sufficient to induce apoptosis. Therefore, the location of sphingolipid production is important. An important aspect of intracellular S1P signaling that is lacking is that no direct intracellular targets for S1P have been identified in mammalian cells as they have been for ceramide, C1P, LPA, and PA.

C1P is synthesized by a Ca^{2+}-dependent ceramide kinase. C1P added to the outside of the cell stimulates cell division, however, unlike S1P and LPA, it did not increase PLD, or ERK activities, nor did it decrease cAMP levels [120, 121]. A specific cell surface receptor for C1P has not been identified [111, 122]. C1P is also a potent inhibitor of both protein phosphatase 1 (PP1) and protein phosphatase 2A (PP2A) *in vitro* [111]. Inhibition of PP1 and PP2A is linked to cell proliferation and survival [123, 124], unlike ceramide, which binds and activates PP1 and PP2A. This activation is linked to ceramide-induced apoptosis [125]. C1P was also shown to bind and activate cytosolic phospholipase $A_2\alpha$ ($cPLA_2\alpha$) to generate arachidonic acid and increase eicosanoid production in inflammation [126]. C1P is also involved in mast cell degranulation in a calcium-dependent manner [127], and is formed during phagocytosis by neutrophils [128].

1.4 Lipid phosphate phosphatases

1.4.1 *Introduction* - The precise effect that a signaling lipid can cause is determined by many factors, including if its production is outside of the cell or inside of the cell. In some cases, the lipid produced inside of the cell is secreted and affects

biological functions in an autocrine and paracrine manner. The explanation of the biological function of signaling lipids is made more complex with the knowledge that there are different pools of lipids. Many signaling lipids are present in different organelles, and micro-domains found on membranes. The presence and location of these lipid pools affects signaling, and are dependent on the expression of enzymes and metabolites that generate them. Lipid signaling is also dependent on the expression of receptors and target proteins to transduce their effects on cellular response. These responses are modulated by the myriad of other signals that can occur simultaneously.

Just as important as the enzymes that produce these lipids are the enzymes that can metabolize them, and thus regulate their functions. Generally, the phosphorylated forms of these lipids induce signals that favor cell proliferation, prevent apoptosis, and induce cell motility. In the case of signaling sphingolipids S1P and C1P, their dephosphorylated forms, sphingosine and ceramide, are known to induce cell-cycle arrest and apoptosis. Therefore enzymes that can dephosphorylate C1P and S1P have the ability to attenuate these signals, and in one metabolic step produce other signals that result in opposing responses. The lipid phosphate phosphatases (LPP), have been shown to effectively dephosphorylate lipid phosphates, including the glycerophospholipids, LPA, PA, and diacylglycerolpyrophosphate (DGPP); sphingophospholipids, S1P, and C1P, and also isoprenyl-based lipid phosphates. Knowledge of their function in regulating lipid phosphate signaling is growing steadily and proving to be important.

1.4.2 *Characterization of lipid phosphate phosphatase activity* - Before the purification and cloning of lipid phosphate phosphatases, they were described as members of a class of phosphatidate phosphohydrolases (PAPs), of which there are PAP-

1 and PAP-2 activities. PAP-1 activity was identified in being involved in the conversion of PA to DAG for triacylglycerol, PC and PE synthesis [129]. This enzyme was called PAP-1 for its dependency on Mg^{2+} and being inhibited by the alkylating agent, N-ethylmaleimide [130]. PAP-1 is found in the cytosol of cells and is able to translocate to the ER or mitochondria when glycerolipid synthesis is stimulated [131]. PAP-1 activity is selective for PA [82, 132], therefore the presence of PA on the cytosolic leaflet of membranes is susceptible to its actions [131]. PAP-1 is also able to affect signaling. PAP-1 activity is required for the increased expression of cyclo-oxygenase-2 (COX-2) expression and eicosanoid formation when human amnionic WISH cells are activated by PKC [133], and macrophages are stimulated by lipopolysaccharide [134]. PAP-1 activity is co-immunoprecipitated with EGF receptor [135]. This association is decreased upon EGF receptor activation and occurs concomitant with an increase of PAP-1 activity associated with PKC-ε. Until recently, the gene product responsible for PAP-1 activity was not known. *PAH1* in *Saccharomyces cerevisiae* has PAP-1 activity, and shows homology to the mammalian protein, lipin-1, a protein known for regulating obesity [132]. Expression of recombinant lipin-1 in *E. coli* demonstrated that it has PAP-1 activity. Recent work from our group also showed that lipins-2, and -3 also have PAP-1 activity [82]. The discovery of this enzyme provides a promising opportunity to study the role of PAP-1 activity in lipid metabolism and cell signaling specifically by PA.

PAP-2 activity is not dependent on Mg^{2+}, insensitive to N-ethlymaleimide, and restricted to membranes, particularly the plasma membrane [131]. Purification of PAP-2 demonstrated that is has broad substrate specificity and that it dephosphorylates a variety of lipid phosphates including PA, LPA, S1P, C1P, and DGPP [136, 137]. The reaction

catalyzed by PAP-2 obeys a surface dilution kinetic model, which confirms that it is a lipid phosphate phosphohydrolase [137]. Kai *et al.* [138] were the first to describe the cDNA encoding PAP-2A, which was then followed by the identification of more cDNAs for other PAP-2 isoforms [122]. The newly identified PAP-2 isoforms showed the same broad substrate specificity as purified PAP-2. Consequently, to reflect this broader substrate specificity the enzymes were renamed the lipid phosphate phosphatases (LPP1, 2, and 3) [139]. Furthermore, the name is appropriate because the true physiological substrates for the LPPs are not firmly established.

Data on the substrate specificity of the LPP isoforms are varied. Kai *et al.* [138] claim that human LPP1 hydrolyzes PA and LPA and had relatively little activity towards C1P or S1P. LPP3 preferred S1P and PA [138]. Roberts *et al.* [140] performed a thorough kinetic analysis on all three of the LPP isoforms and found that LPP1 and LPP3 have higher substrate selectivity for the glycerophospholipids, and that LPP2 showed no obvious selectivity for either glycerophospholipids or sphingophospholipids.

1.4.3 *Structural characteristics of the lipid phosphate phosphatases* - The LPPs belong to the phosphatase super-family that includes enzymes with a variety of substrates and functions, such as fungal haloperoxidase, mammalian glucose 6-phosphatase, DGPPase, and the wunens, which are *Drosophila* LPPs involved in embryonic development [139, 141]. Three highly conserved domains that constitute the active site of the enzyme define the phosphatase super-family (Fig. 1.8A). The reaction mechanism of the phosphatase super-family was inferred thorough studies on the related fungal vanadate-dependent chloroperoxidase (Fig. 1.8B) [142-147].

A)

Phosphatase Consensus	C1 KXXXXXXRP	C2 SGH	C3 SRXXXXXHXXXD
Fungal CPO	(353) KWEFEFWRP	(402) SGH	(489) SRIFLGVHWRFD
Yeast DPP1	(118) KNWIGRLRP	(167) SGH	(216) SRTQDYRHHFVD
Human G6P	(76) KWILFGQRP	(117) SGH	(169) SRIYLAAHFPHQ
Human SPP1	(178) KDIIRWPRP	(206) STH	(249) SRIYMGMHSILD
Human SPP2	(136) KDVLKWPRP	(164) STH	(206) SRLYTGMHTVLD
Human LPP1	(125) KYSIGRLRP	(174) SGH	(221) SRVSDYKHHWSD
Human LPP2	(117) KYMIGRLRP	(166) SGH	(213) TRVSDYKHHWSD
Human LPP3	(148) KVSIGRLRP	(197) SGH	(244) SRVSDHKHHPSD
Human LPR1/PRG3	(146) PYFLTVCKP	(198) SKH	(245) NRVSEYRNHCSD
Human LPR2/PRG4	(148) PHFLSVCRP	(207) CKD	(154) VRVAEYRNHWSD
Human LPR3/PRG1	(197) QLSTGYQAP	(250) SQH	(296) TRITQYKNHPVD
Human LPR4/PRG2	(152) QLATGYHTP	(205) SQH	(279) TQITQYRSHPVD
Human CSS2α	(184) KGLVRRRRP	(212) SGH	(249) SRVMLGRHNVTD
Human CSS2β	(163) QKLIKRRGP	(191) AGH	(228) SRVMIGRHHVTD
Human SMS1	Not Present	(283) SGH	(321) CILLAHDHYTVD
Human SMS2	Not Present	(227) SGH	(265) CILVAHEHYTID

B)

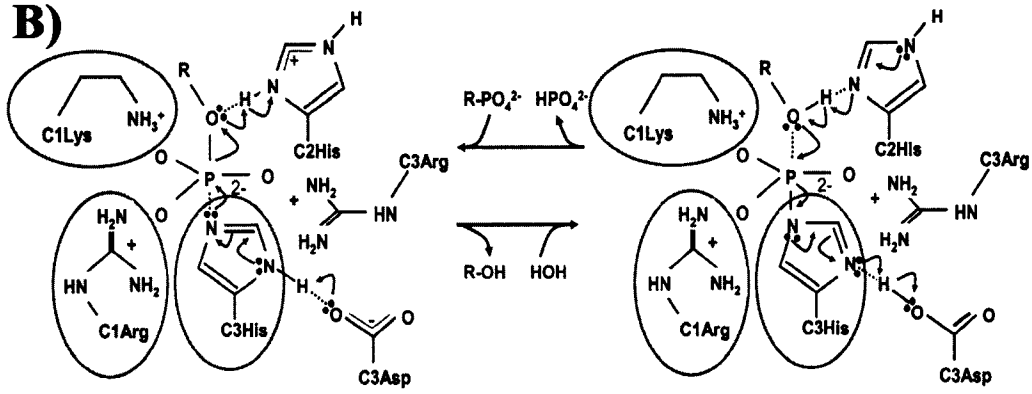

Figure 1.8 The phosphatase consensus sequence and the phosphatase reaction mechanism. *Panel A* shows the alignment of catalytic domain sequences of members of the human lipid phosphatase/phosphotransferase (LPT) family and sequences found in the phosphatase super-family including fungal vanadium chloroperoxidase (CPO), yeast diacylglycerol pyrophosphate phosphatase-1 (DPP1), and human glucose 6-phosphophatase (G6P). Other abbreviations are: SPP, sphingosine 1-phosphatase; LPP, lipid phosphate phosphatase; lipid phosphate phosphatase related proteins, LPR; plasticity related genes, PRG; CSS, candidate sphingomyelin synthase; SMS, sphingomyelin synthase. *Panel B* is a representation of the predicted catalytic mechanism used by the LPPs. The first step involves the C3 histidine, and aspartic acid residues (*in pink*) promoting the formation of the phospho-histidine intermediate. The C2 histidine residue promotes the removal of the phosphate group from the lipid phosphate. The second step is the C2 histidine residue promoting the hydrolysis of the phospho-histidine intermediate that frees the active site for another round of catalysis. The lysine and arginine residues (*in blue*) stabilize the phospho-histidine intermediate through hydrogen bonds with the oxygen atoms of the phosphate moiety. The C3 arginine residue depicted (*in blue*) was mutated to lysine (R217K) in mouse LPP1 cDNA for use in our experiments. This mutation abolishes LPP1 catalytic activity. These figures were adapted from Sigal *et al.* [113].

According to the model the histidine and aspartic acid residues in the third conserved domain (C3) operate as a charge-relay system in which the histidine residue acts a nucleophile that forms a phospho-histidine intermediate. The C2 histidine residue cleaves the phosphate bond followed by hydrolysis of the phospho-histidine intermediate, which frees the active site for another round of catalysis. The invariant lysine, arginine, serine and glycine residues of the C1, C2, and C3 domains form hydrogen bonds with the phosphate-oxygen molecules and stabilize the transition state of the reaction (Fig. 1.8B) [113]. Mutagenesis analysis performed on LPP1 [148], LPP2 [149, 150] and LPP3 [151] confirmed that the two critical histidine residues, and the arginine, lysine and serine residues are essential for enzymatic activity on lipid phosphates.

Amino acid sequence for mouse LPP1 shares 87% and 84% identity with rat and human LPP1, respectively (Fig. 1.9A) [139, 141]. hLPP2 has 56% amino acid identity with hLPP1 [139, 141], and hLPP1 has 47% amino acid identity with hLPP3 (Fig. 1.9A) [152]. Human LPP1, its splice variant hLPP1a [153], and LPP2 have relatively short N-termini compared to LPP3. Transcripts from adult rat lung and type II cells encoded two novel isoforms of LPP1, designated as LPP1b and LPP1c [154]. These latter isoforms contain frameshifts that would result in premature termination and the loss of catalytic activity. The significance of these splice variants are at present not understood.

Sigal *et al.* [113] further classified the LPPs into the mammalian lipid phosphate/phosphotransferase (LPT) family. Some members of this family were mentioned in Section 1.3.3 in their involvement in the metabolism of sphingolipids. They include the S1P-specific sphingosine phosphate phosphatases (SPP1 and 2), and sphingomyelin synthase (SMS1 and 2), that catalyzes the interconversion of PC and

ceramide to DAG and SM (Fig. 1.4). Additionally, lipid phosphatase-related proteins/plasticity-related genes (LPR1/PRG3, LPR2/PRG4, LPR3/PRG1, LPR4/PRG2) are involved in brain development, the hippocampal injury response, and cytoskeletal arrangements [155-157], and type 2 candidate sphingomyelin synthases (CSS2α and β) whose functions are unknown [113]. All members of the LPT family share limited homology to the phosphatase super-family [113]. The LPPs, SPPs, and CSS2α have a consensus phosphatase catalytic domain with a minor substitution in the C2 sequence of the SPPs (Fig. 1.8A). CSS2β, and the LPRs/PRGs lack critical amino acids for catalysis (Fig. 1.8A). The SMSs contain C2 and C3 catalytic domains but lack the C1 domain (Fig. 1.8A). Another fundamental similarity of the LPTs is that they are transmembrane proteins. Hydropathy analyses identify at least six transmembrane α-helices, five extramembrane loops, and cytosolic N- and C- termini (Fig 1.9A shows the alignment of mammalian LPP amino acid sequences, and Fig 1.9B shows the predicted topology of mouse LPP1, which is predicted to be similar to the other LPT family members). Indirect immunofluorescence of a C-terminal tagged LPP1 showed fixed cells that were not permeabilized before probing with an antibody for the C-terminal tag had negative fluorescent signal (Fig. 1.9B) [158]. This is in contrast to the cells that were permeabilized and had a positive fluorescent signal confirming that the C-terminus was cytosolic. The transmembrane topology was thoroughly confirmed experimentally for LPP3 by *in vitro* insertion of various truncated forms of LPP3-reporter fusion proteins into microsomes [159]. SPPs are proposed to have two more C-terminal transmembrane α-helices [160]. The arrangement of LPT transmembrane domains, make it that the three conserved catalytic domains are luminal if the enzyme is expressed in cellular organelles,

or exposed to the cell surface if expressed on the plasma membrane (Fig. 1.9B). C1 and C2 domains would then be part of the middle luminal loop, and the C3 domain would be on the third luminal loop. Mutagenesis work by Dr. Zhang [148] in our group determined that there is an N-glycosylated asparagine residue between the C1 and C2 domains (Fig. 1.9B). This implies that this loop has access to the lumen of the ER and Golgi complex as it traverses the secretory pathway, and that when expressed at the plasma membrane, they would be extracellular. To have catalytic activity the extramembrane loop containing the C3 domain would also have to be luminal.

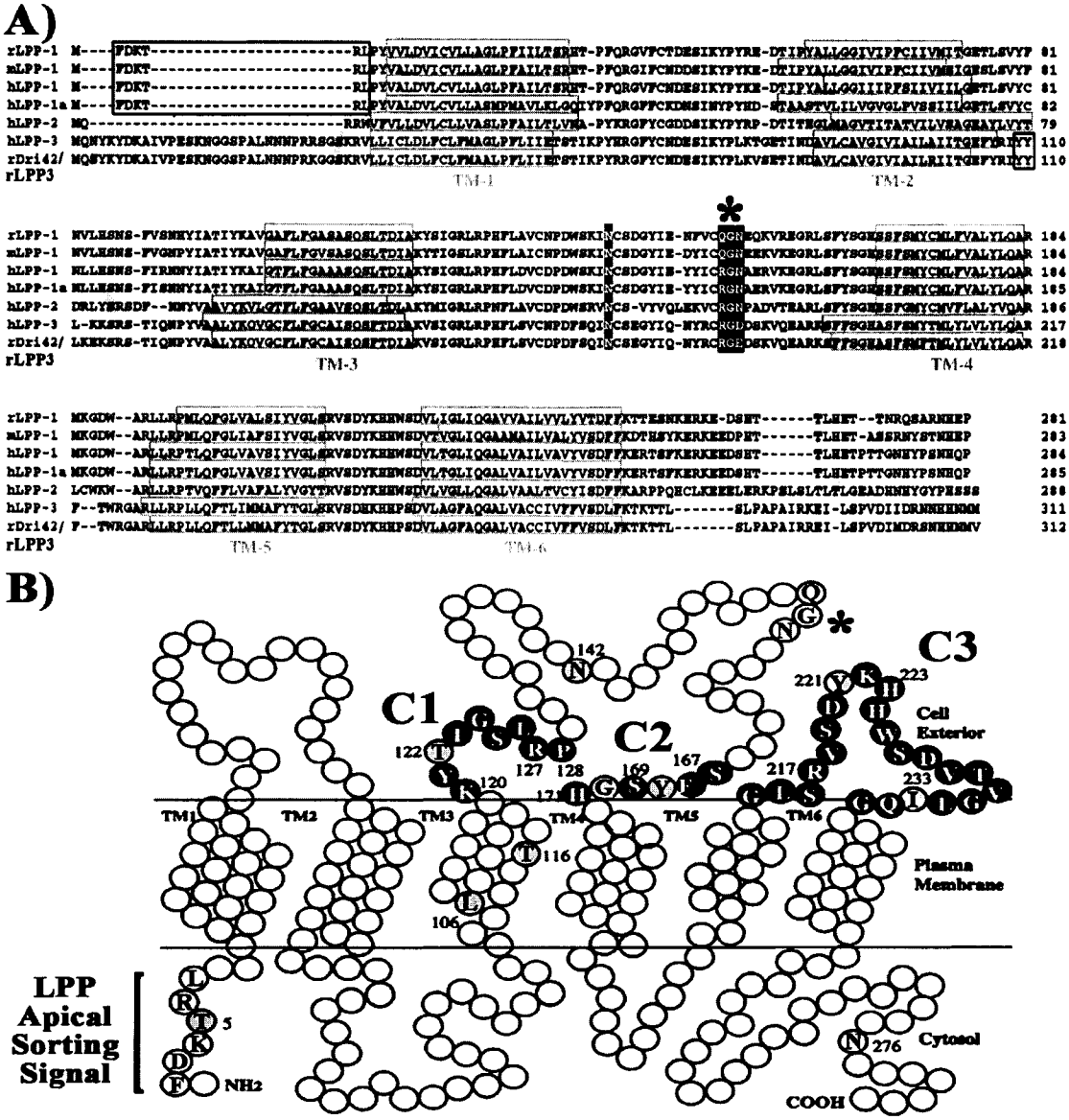

Figure 1.9 Amino acid alignment of mammalian LPPs, and predicted topology of mouse LPP1. The *green boxed areas* (*TM 1-6*) represent transmembrane domains. The conserved phosphatase domains (C1, 2,and 3) are highlighted in *yellow*. The *red-colored* amino acids are essential for catalytic activity. The *pink-colored* asparagine residues are part of a consensus sequence for N-glycosylation. The *boxed* sequences in the LPP1, and LPP3 sequences are sorting signals for apical, and basolateral membranes, respectively. The * represent potential integrin binding sequences, particularly for LPP3. *Turquoise-colored* amino acids indicate potential protein kinase C, casein kinase II, and cAMP-dependent protein kinase phosphorylation sites. This figure was adapted from Brindley *et al.* [139]. *Panel B* shows a schematic representation of the structural organization of mouse LPP1 in the plasma membrane. The conserved phosphatase domains (C1, 2, and 3) are shown in *blue*. Mutagenesis analysis showed that the amino acids in *red* are essential for catalysis, and amino acids in *green* are not essential for catalysis. The asparagine residue in *turquoise* (amino acid 142 between C1 and C2) is N-glycosylated. The * indicates where the corresponding human LPP3 RGD sequence would be. QGN of mouse LPP1 is not expected to bind integrins. The novel apical sorting signal is located at the N-terminus. This figure is adapted from Zhang *et al.* [148].

1.4.4 *Localization of the lipid phosphate phosphatases* - The subcellular localization of the LPPs has been examined in a number of cell lines. All of the LPPs are partly localized to the plasma membrane [150, 158, 161-165]. Increases of lipid phosphatase activity against exogenous LPA, S1P, PA, and C1P on intact cells over-expressing each LPP isoform are consistent with plasma membrane localization, and consistent with an extracellular active site (Fig. 1.9B) [85, 158, 161, 162, 166]. However, the involvement of LPP2 in the degradation of extracellular LPA or S1P is minimal, since Dr. Morris [150] from our group measured no detectable increase of extracellular LPA or S1P degradation on intact fibroblasts over-expressing LPP2.

There is also localization of the LPPs to the ER, and possibly the Golgi complex, endosomes, and unidentified cytoplasmic vesicles [84, 159, 167]. LPP2 is partly located on early endosomes [150]. On the cell surface of polarized MDCK cells Kanoh's group found that LPP1 was predominantly expressed in the apical surface membrane, and LPP3 was expressed in the basolateral membrane [163]. They found a novel apical sorting signal in the N-terminus of LPP1, which consisted of FDKTRL (Fig. 1.9). This signal is found in rat, mouse, and human LPP1 and LPP1a. A dityrosine motif in the second cytoplasmic loop of LPP3 is responsible for targeting to the basolateral membrane (Fig. 1.9A). Furthermore, biochemical fractionation experiments indicate that LPP1 and LPP3 exhibit localization to detergent-resistant membrane domains or lipid rafts [165, 168, 169]. Kai *et al.* [168] found that unlike LPP3, LPP1 is soluble in Triton X-100 at 4°C, but LPP1 and LPP3 are insoluble in the non-ionic detergent, CHAPS. LPP1 colocalized with the raft marker cholera toxin B subunit, but existed in rafts distinct from

LPP3. LPP2 is also colocalized with caveolin-1 at the plasma membrane and intracellular membranes [150]. Recruitment of the LPPs to these membrane domains may be a way to compartmentalize them with LPA or S1P receptors [170, 171] along with other lipid signaling molecules such as the PLDs which are also found in caveolin enriched detergent-resistant membrane domains [165, 172, 173].

1.4.5 *Functions of lipid phosphate phosphatase ecto-activity* - The LPPs exhibit "ecto"-phosphatase activity against exogenous PA, LPA, S1P, and C1P [85, 158, 161, 162, 166]. It is by virtue of this ecto-activity that indicated the LPPs could control exogenous LPA and S1P concentrations. This would then decrease LPA and S1P interactions with their specific cell surface receptors. It was originally proposed that this ecto-activity explained how LPP1 over-expression attenuated the effects of exogenous LPA in activating cell division, ERK, and Ca^{2+} transients [158, 174]. Gonadotropin releasing hormone increases LPP expression in the plasma membranes of ovarian cancer cells [175]. The increase of LPP ecto-activity on extracellular LPA explains the anti-proliferative effects of gonadotropin releasing hormone on ovarian carcinomas. Subsequently, it was found that LPP3 translocation to the plasma membrane of ovarian cancer cells increased upon treatment with gonadotropin releasing hormone [176]. Over-expression of LPP3 increases apoptosis, decreases cell-colony formation, and the colony formation of neighboring cells not over-expressing LPP3. Sub-cutaneous injection of ovarian cancer cells into mice developed tumors, however injected cancer cells stably producing LPP3 had a decreased tumor growth. It is concluded that this occurred through the increase in exogenous LPA degradation [177]. Ovarian cancer cells express decreased levels of LPP1, which could contribute to increases in extracellular LPA and the

promotion of transformation [178]. Consistent with this view, over-expressing LPP1 in these cells decreased LPA-induced migration, and decreased the colony formation of neighboring cells not over-expressing LPP1 [178]. Exogenous LPA increased the expression of LPP1 to the platelet surface and increased LPP ecto-activity, thus decreasing net LPA production and LPA-induced shape changes and aggregation [179]. The use of a receptor-inactive PA analogue that is a potent competitive inhibitor of LPP1 activity enhances platelet aggregation and shape change responses to LPA and amplifies LPA production by activated platelets. Therefore, external LPA-degradation by LPP1 ecto-activity regulates LPA-signaling and LPA production during blood clotting [179]. Hooks *et al.* [180] synthesized non-hydrolysable LPA analogues that were able to induce HEK 293 cell proliferation. LPP1 over-expression decreased cell proliferation induced by exogenous LPA, but not to the non-hydrolysable LPA analogues. It was concluded that LPP1-mediated degradation of external LPA decreased cell proliferation. Ecto-LPP activities were also concluded to regulate extracellular LPA accumulation that results in the differentiation of pre-adipocytes [181]. The explanation for these combined results is that the ecto-LPP activities control extracellular LPA concentrations, thereby regulating LPA receptor activation. These studies also describe an important function by the LPPs in regulating production and accumulation of extracellular LPA in cancers, obesity and blood clotting. In addition to regulating signaling by LPA receptors, the ecto-activity of the LPPs could be involved in promoting uptake of bioactive lipids. LPA, PA, S1P, and C1P are polar lipids and cannot readily enter the cell. However, their dephosphorylated products can be taken up into the cell more readily, and then these products could either induce intracellular signaling themselves, or they can be metabolized to induce signaling

as mentioned in Sections 1.3.2 and 1.3.4 [85, 182].

1.4.6 *Intracellular functions of lipid phosphate phosphatases* - Although the ecto-activities of the LPPs can regulate external LPA accumulation and cell signaling, there are also many studies that indicate an intracellular role for the LPPs. In our groups experiments on fibroblasts we limited the degradation of exogenous LPA to <10% of the total added LPA, and LPP expression still attenuated the LPA-induced stimulation of cell division, ERK, PLD and Ca^{2+} transients [158, 174]. Alderton et al. [161] showed that LPP3 can degrade exogenous LPA, PA and S1P, but it was unable to decrease activation of ERK by these lipid phosphates. Additionally, cells that over-express LPP1, -1a, and -2 attenuated ERK activation by LPA, PA, S1P, even though LPP1a does not significantly degrade external LPA or S1P, and LPP2 does not significantly degrade external S1P. Furthermore, LPP1, -1a, and -2 decreases the activation of ERK induced by thrombin. The effect on thrombin signaling, and the disparity of external lipid phosphate degradation and decreased ERK signaling among the LPP isoforms indicates that ecto-LPP activity is not responsible for attenuating ERK activation. The decrease of ERK activation is attributed to a decrease of intracellular PA concentrations [161]. Human LPP1-transfected endothelial cells correlated with a >50% decrease in the steady-state PA level [153]. Over-expression of lazaro, a *Drosophila* LPP homolog, decreased retinal PA levels, whereas light-induced PA production is enhanced in flies lacking catalytically functional lazaro [183]. Over-expression of LPP2 and LPP3 increased apoptosis in serum-deprived HEK 293 cells and this correlated with decreased concentrations of PA and S1P in the cells, respectively [167]. It was proposed that LPP2 decreases the accumulation of PA generated by PLD. PA was shown to activate SK1 activity to

produce S1P [90], and that LPP3 regulates cellular S1P levels [167].

Dr. Morris in our group [150] found that LPP2 over-expression of catalytically active, but not an inactive LPP2 mutant caused pre-mature entry of fibroblasts into S-phase of the cell cycle. Conversely, LPP2 knockdown delayed cyclin A accumulation and entry into S-phase. At high passage, LPP2 over-expressed cells arrested, and accumulated ceramide, but had a decrease of cellular LPA levels.

HEK 293 cells that over-express LPP3 exhibited greater DAG formation subsequent to PLD stimulation by PMA. PLD2 and LPP3 are both present in caveolin-1-enriched micro-domains in this study [165]. Zhao *et al.* [184] also concluded that the effects of LPP1 in inhibiting Ca^{2+}-transients and the secretion of the inflammatory cytokine, IL-8, did not depend on the degradation of extracellular LPA, and that it was downstream of LPA receptor activation. Furthermore, *in vivo* studies with LPP1 over-expressing transgenic mice failed to detect alterations in circulating LPA levels [185]. It remains to be seen if there will be changes in LPA accumulation in the transgenic mice during conditions of stress, such as blood clotting. However, immortalized fibroblasts from the LPP1 transgenic mice revealed decreased steady-state levels of PA and a rise in DAG [185]. Work by Long *et al.* [186] found there is a decrease of ERK activation by LPA, S1P, and PDGF in immortalized fibroblasts from the transgenic mice that expressed 20 gene copies for *Lpp1*. These cells also had a decrease of LPA- and PDGF-induced migration measured in an *in vitro* "wound healing" assay. It is postulated that due to long-term increases of DAG in these cells, PKC levels are down-regulated, thus PKCs are not available to mediate cell signaling required for migration [186].

1.4.7 *Non-catalytic functions of lipid phosphate phosphatases* - In addition to the LPPs catalytic effects on cellular function, there is evidence that the LPPs have non-catalytic functions. Homozygous inactivation of the mouse *Lpp3* gene caused early embryonic lethality partly due to an increased Wnt signaling that resulted in duplication of axis symmetry of the developing embryo [151]. Expression of wild-type or mutant LPP3 that does not have phosphatase activity decreased Wnt signaling in LPP3 null cells. Furthermore, expression of inactive LPP3 in *Xenopus* embryos suppressed axis duplication induced by Wnts, although not as effectively as active LPP3. Therefore, it was postulated that LPP3 has a novel role as a negative regulator of Wnt signaling, and that it does not depend on phosphatase activity. Homozygous inactivation of the *Lpp3* gene did result in increases of PA and LPA levels, and a decrease of DAG levels with a concurrent decrease of PKC activation. Therefore the development defects of the LPP3 null mouse embryos could result from lack of both enzymatic and non-enzymatic properties of LPP3.

LPP3 null mouse embryos also have defects in vasculogenesis in the chorio-allantoic placenta and yolk sac (Fig 1.10A-C) [151]. Work from another group revealed non-catalytic functions of LPP3 in the development of blood vessels that could be related to the vascular defects of LPP3 null mouse embryos. Humtsoe *et al.* [187] found that during capillary morphogenesis or treatment of vascular endothelial cells with VEGF, basic fibroblast growth factor (bFGF), TNFα, IL-1β, and PMA increased the expression of LPP3. Retroviral over-expression of LPP3 in endothelial cells promotes cell-cell interactions. LPP3 contains a Arg-Gly-Asp (RGD see Fig. 1.9) cell adhesion sequence on the third loop exposed to the cell surface that interacts with neighboring cells through

their $\alpha_v\beta_3$-, and $\alpha_5\beta_1$-integrins. LPP3 induced integrin responses including increased cell adhesion, cell spreading and phosphorylation of focal adhesion kinase (FAK) and paxillin. There is also an increased expression and a colocalization of VEGF, $\alpha_v\beta_3$-integrin and LPP3 in tumor endothelium [187, 188]. Furthermore, an antibody for LPP3-RGD specifically and significantly blocks bFGF- and VEGF-induced capillary morphogenesis of endothelial cells [188]. The RGD motif in human LPP3 is not conserved in mouse LPP3 that has an Arg-Gly-Glu (RGE) motif (Fig. 1.9) [139, 141]. Site-directed mutagenesis of human LPP3 RGD to RGE did not increase cell-cell interactions when expressed in endothelial cells [187]. However, the same group recently reported that indeed intact mouse LPP3 could functionally engage with $\alpha_v\beta_3$-, and $\alpha_5\beta_1$-integrins on neighboring cells [189]. As mentioned in Section 1.4.4 LPP3 is translocated to the basolateral membrane of polarized epithelial cells adjacent to neighboring polarized cells [163]. Perhaps LPP3 function includes interaction with neighboring endothelial, smooth muscle or epithelial cells through its integrin-binding site.

The potential role of LPP3 in vasculogenesis is intriguing in that the LPP3 null mice studies that observed defective Wnt signaling, also observed defects in vasculogenesis (Fig 1.10A-C) [151]. The link between LPP3-mediated cell-cell interactions in the formation of capillaries and the Wnt signaling pathway is interesting, because retroviral expression of LPP3 induces the expression p120-catenin in endothelial cells [187]. p120-catenin plays a role in regulating adherens junctions with neighboring cells, and can increase Wnt-mediated transcription of target genes [190, 191]. How the non-catalytic functions of LPP3 affect vasculogenesis and Wnt signaling in the developing mouse embryo is not known. However, the LPP3 function in promoting

endothelial cell-cell interactions through it extracellular integrin-binding sequence is a promising cue. It is also of significant interest to establish a relationship between the non-catalytic and catalytic functions of LPP3 in vasculogenesis and Wnt signaling.

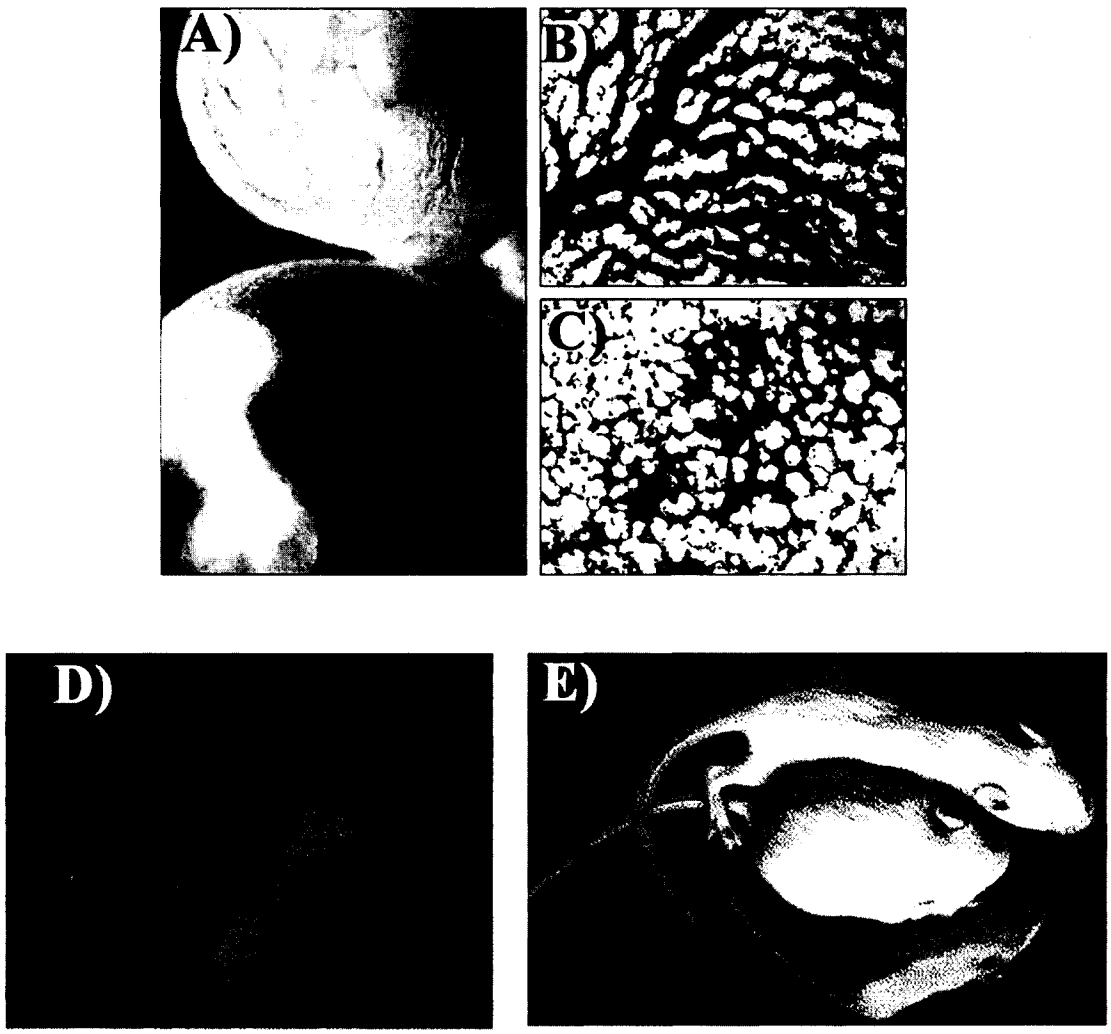

Figure 1.10 Mouse models for investigating LPP3 and LPP1 function. *Panel A* shows the external appearance of the yolk sac in normal (*top*) and homozygous LPP3 mutant (*bottom*) conceptuses recovered at E10.5. The yolk sac from the LPP3 null embryo is pale and translucent, and lack noticeable blood vessels. Mutant embryo development is also delayed. *Panel B* shows the formation of large blood vessels and a robust vascular network in wild-type yolk sac, whereas mutant yolk sac had no large blood vessels and a limited vascular network (*Panel C*). These figures were first published by Escalante-Alcalde *et al.* [151]. *Panel D* shows a reduced birth size in LPP1 over-expressing transgenic pups (*left*) compared to wild-type pups (*right*). Reduced size is sustained, and differences in the abundance and length of body hair are noticeable at one month (*Panel E*). Upper and middle mice are wild-type, and the lower mouse is transgenic. These figures were first published by Yue *et al.* [185] in collaboration with our group.

1.4.8 *Animal models for determining lipid phosphate phosphatase function* - Other functions for the LPPs have been explored using animal models. There are no LPP1 knockout mice as yet, but transgenic mice that over-express LPP1 have been produced. The LPP1 transgenic mice have smaller body size and decreased birth weight compared to their wild-type counterparts (Fig. 1.10 D and E above) [185]. There are also abnormalities in fur growth and disrupted hair structure with decreased numbers of hair follicles. The males showed decreased fertility and defects in spermatogenesis. Female transgenic mice also have fertility defects. Implantation of LPP1 transgenic and wild-type embryos into pseudopregnant LPP1 transgenic mothers yielded decreases in litter size [185]. There was also no change in circulating LPA levels in plasma, however these mice were not investigated under conditions of stress. It would be of interest to explore the production of LPA during platelet activation, and determine if LPP1 over-expression affects wound healing or tumorigenesis in these mice.

LPP2 null mice are viable and are reported to exhibit no overt phenotype [192]. Work by Dr. Morris in our group showed that LPP2 regulates the timing of S-phase progression in the cell cycle of cultured fibroblasts [150]. Other knockouts in mice of genes that regulate S-phase entry, such as cyclins D and E and cyclin dependent kinase-2, also did not show obvious defects [193]. This indicates the mouse has evolved mechanisms to compensate for the lack of important cell cycle regulators, which is not surprising since they regulate a fundamental process for life. Therefore, LPP2 may still have a viable role in regulating the progression of the cell cycle *in vivo.* Homozygous inactivation of the mouse LPP3 gene results in early embryonic lethality and defects of both vasculogenesis, and patterning during embryo development (Fig 1.10A-C) [151].

These studies were described in detail in Section 1.4.7.

Studies in *Drosophila* have identified roles for two LPP homologues, wunen, and wunen2, in regulation of embryonic germ cell migration and survival. Wunen, and wunen2 act redundantly as repellent factors to guide migrating germ cells into the mesoderm of the *Drosophila* embryo where they mature [194]. These proteins are normally expressed in somatic tissues that the germ cells avoid. When both genes are disrupted, the germ cells scatter, and die. Over-expression of these proteins in somatic tissue, and the mesoderm that normally attracts germ cells, also result in germ cell repulsion and death [194, 195]. The repulsive effect of these LPPs on the migrating germ cells are dependent on catalytic activity, and are suggested to be a result of their ability to degrade an unidentified lipid phosphate that guides the cells to the mesoderm. Over-expression of mammalian LPP3, but not mammalian LPP1, in somatic tissue, and the mesoderm also causes aberrant migration and germ cell death [196, 197]. Therefore, LPP1 and LPP3 have distinct functions *in vivo*. Surprisingly, germ cells express wunen2, which is required for proper migration and germ cell survival [197]. Mammalian LPP3, but not mammalian LPP1 can substitute for wunen2 in the germ cell. Furthermore, germ cell death induced by wunen2 over-expression in somatic cells can be suppressed by over-expression of wunen2 or LPP3 in germ cells. Germ cell death resulting from decreased expression of wunen2 in germ cells can be rescued by decreasing wunen2 expression in somatic cells. Under normal developmental conditions wunen and wunen2 activities of the somatic tissues properly guide the germ cells. Wunen2 activities in the germ cells keep them alive by preventing death that can be caused by wunen and wunen2 activities of the somatic tissues. These results suggest a model in which wunen and

wunen2 expressed in the somatic tissues compete with germ cell wunen2 for the same lipid phosphate substrate. Degradation of this lipid phosphate by wunen and wunen2 in somatic cells results in germ cell repulsion and death, whereas germ cell degradation of the lipid phosphate by wunen2 results in germ cell survival. The uptake of the dephosphorylated lipid by the germ cell could increase its survival. Treatment of insect cells over-expressing wunen2 with a PA analogue that is fluorescently labeled on its lipid moiety, results in an increased accumulation of fluorescence in the cytoplasm. Uptake is dependent on the intact phosphatase activity of wunen2 [197]. This was also observed in insect cells that over-expressed LPP1, and results in the increase of fluorescently labeled DAG and free fatty-acids in the cell [85]. Therefore, wunen2 ecto-activity provides a mechanism that can internalize functional lipids by dephosphorylating polar lipid phosphates that otherwise do not readily enter the cell.

1.4.9 *Regulation of lipid phosphate phosphatases* - The LPPs can be regulated transcriptionally in many cases. LPP1 and LPP3 transcripts are widely expressed in human tissues, whereas the levels of LPP2 transcripts are lower in most tissues and expression is more restricted (Table 1.1) [113]. Expression of LPP1 transcripts is decreased in many types of cancers including ovarian, breast, colon, pancreas, gastric and lung [42]. The decrease of LPP1 expression in ovarian cancer is associated with the increase of LPA accumulation and pathophysiological consequences [178]. LPP3 transcripts are also lower in breast, colon, and gastric cancers [29]. In most of these cancers the decrease of the LPPs that can degrade external LPA is concurrent with a marked increase of ATX, which can produce external LPA from lysophospholipids [29]. Therefore, these cancers are in a metabolic state that heightens the production and

Table 1.1 Expression of LPPs in adult human tissues. The abundance of EST transcripts corresponding to each gene in human adult tissue is given as transcripts per million. Expression profiles were compiled from data online at http://www.ncbi.nlm.nih.gov/UniGene/. This table was adapted from Sigal *et al.* [113].

	LPP1	LPP2	LPP3
Bladder	191	0	47
Bone	35	17	143
Bone marrow	27	0	136
Brain	107	30	166
Cervix	72	48	24
Colon	64	347	58
Eye	80	43	222
Heart	161	0	287
Kidney	172	44	202
Larynx	41	0	292
Liver	22	7	197
Lung	67	56	106
Lymph node	39	0	724
Mammary gland	132	24	490
Muscle	119	0	82
Ovary	63	116	21
Pancreas	74	211	161
Peripheral nervous system	318	0	238
Placenta	108	4	535
Pituitary	–	–	–
Prostate	483	38	576
Skin	30	12	6
Soft tissue	102	0	153
Spleen	0	0	0
Stomach	77	58	48
Tongue	36	0	36
Testis	60	7	68
Thymus	0	0	0
Uterus	196	156	214
Vascular system	154	0	656
Whole blood	105	0	39

accumulation of the protumorigenic LPA molecule, which can possibly lead to metastasis. LPP1 mRNA can also be increased in human prostatic adenocarcinoma cells by androgen [198]. LPP1 mRNA is decreased in keratinocytes and endothelium from wounded rabbit cornea [199], and therefore could promote an enhanced healing signal by

LPA. Differentiation of preadipocytes into adipocytes leads to decreased mRNA expression for LPP1, LPP2, and LPP3, and a significant decrease of ecto-LPP [181]. Ectopic expression of the p53-related protein, p73, increased LPP1 expression, by directly binding to a p53-like responsive element in the LPP1 promoter [200]. Capillary morphogenesis or treatment of vascular endothelial cells with VEGF, bFGF, TNFα, IL-1β, and PMA increased the expression of LPP3 [187]. In HeLa cells, the transcription of LPP3 is induced by epidermal growth factor (EGF) [152].

The LPPs have potential phosphorylation sites predicted by software analysis of their primary sequence [139, 149]. However, there is no direct evidence of LPP phosphorylation under basal or stimulatory conditions. The LPPs may respond acutely to stimuli. LPP3 constitutively colocalizes with SK1 in cytoplasmic vesicles, and upon PLD1 stimulation LPP3 translocates to a perinuclear compartment [167]. LPP3 translocation parallels SK1 translocation to the perinuclear compartment, and is suggested to regulate levels of S1P generated by SK1 [201]. LPP activity in caveolin-enriched domains is increased upon PMA treatment of rat lung epithelial cells [164], thus LPPs could be induced to translocate or have their activities enhanced in lipid rafts or caveolae.

The LPPs are also known to associate with each other. LPP1, LPP3, wunen and wunen2 proteins from *Drosophila* can homodimerize, but do not heterodimerize [202]. Dimer formation of wunen is dependent on the last 35 amino acids of the C-terminus and an intact catalytic site. The authors of this study concluded that wunen dimerization is not essential for catalytic and biological activity, but perhaps confer structural or functional stability [202]. The oligomerization of the LPPs had been suspected since LPP activity

that was purified and detected by Western blot analysis demonstrated molecular weights larger than the 32-35 kDa predicted by cloned LPP cDNA [150, 203-205]. The physiological importance of these associations is unknown.

1.5 Matrix metalloproteinases

1.5.1 *General functions of matrix metalloproteinases* - Wound healing, like development and tumor metastasis, involves the migration of cells through the extracellular matrix (ECM). The ECM is constantly undergoing changes. Cells such as fibroblasts remodel the ECM by degradation, synthesis and deposition of new ECM proteins [3]. ECM remodeling requires the activities of endoproteinases called matrix metalloproteinases (MMP) that together can degrade almost all the ECM proteins [206]. MMPs belong to the matrixin family, a sub-group of the metzincin super-family of proteases. The association of a zinc atom in a conserved catalytic site defines the metzincins. Currently there are over 20 known MMPs grouped according to substrate specificity: the collagenases, gelatinases, stromelysins and matrilysins [206]. The grouping of MMPs is misleading in that there are large overlaps of ECM substrates within the MMPs.

Generally, MMPs are regarded as ECM proteases that permit the remodeling of the ECM for wound healing, development, contribute to pathological tissue destruction (or lack-there-of in the cases of fibrotic disease), and provides a mechanism for tumor cell invasion [206-208]. However, evidence is growing that shows MMPs have additional roles other than degrading ECM proteins. Indeed, the degradation of the ECM by MMPs, leads to changes in the interaction of the cell to the extracellular environment, which also

includes the exposure of cryptic cell receptor recognition sites and release of ECM-sequestered cytokines [206]. MMPs have additional substrates that regulate cell signaling, such as growth factor and cytokine precursors, growth factor receptors, cytokine receptors, cell surface adhesion receptors, integrins, and cadherins [206, 207].

1.5.2 *Regulation of matrix metalloproteinases* - Most MMPs are expressed at low levels in normal resting-state tissues, but are highly inducible when exposed to stimuli during tissue repair, inflammation, and development. MMPs can also be constitutively expressed by oncogenes, and chronic conditions such as some fibrotic diseases or chronic wounds [4, 206, 208]. MMPs are produced by a variety of cells including fibroblasts, myofiboblasts, endothelial cells, epithelial cells, chondrocytes, osteocytes and leukocytes [4, 206]. They are also constitutively produced by a variety of malignant cells [208].

The minimal domains that constitute the MMPs include the zinc-binding active site, a secretory signal sequence, and a propeptide domain (Fig. 1.11A) [206]. Therefore, most MMPs are secreted as inactive zymogens that require extracellular cleavage for full activation. The majority of MMPs have a hemopexin-like domain that plays an important role in the interaction of substrates or negative-regulators. A sub-type of MMPs contains a transmembrane, and are referred to as membrane-type (MT)-MMPs.

MMP activation is controlled by a mechanism known as the cysteine switch. In the propeptide there is a conserved cysteine whose sulphydryl group forms a non-covalent bond with the zinc ion in the active site. Proteolytic cleavage of the propeptide disrupts the association of the cysteine residue from its complex with the catalytic zinc ion. Proteolytic cleavage can be performed by plasminogen, trypsin, and other MMPs [209]. Therefore, the activation of MMPs can be subject to control by the

availability of proteases that themselves are controlled by stimuli or conditions that require ECM remodeling. Under the conditions of oxidative stress, the critical cysteine can also be subject to S-glutathiolation, which activates the MMP without the removal of the propeptide [209].

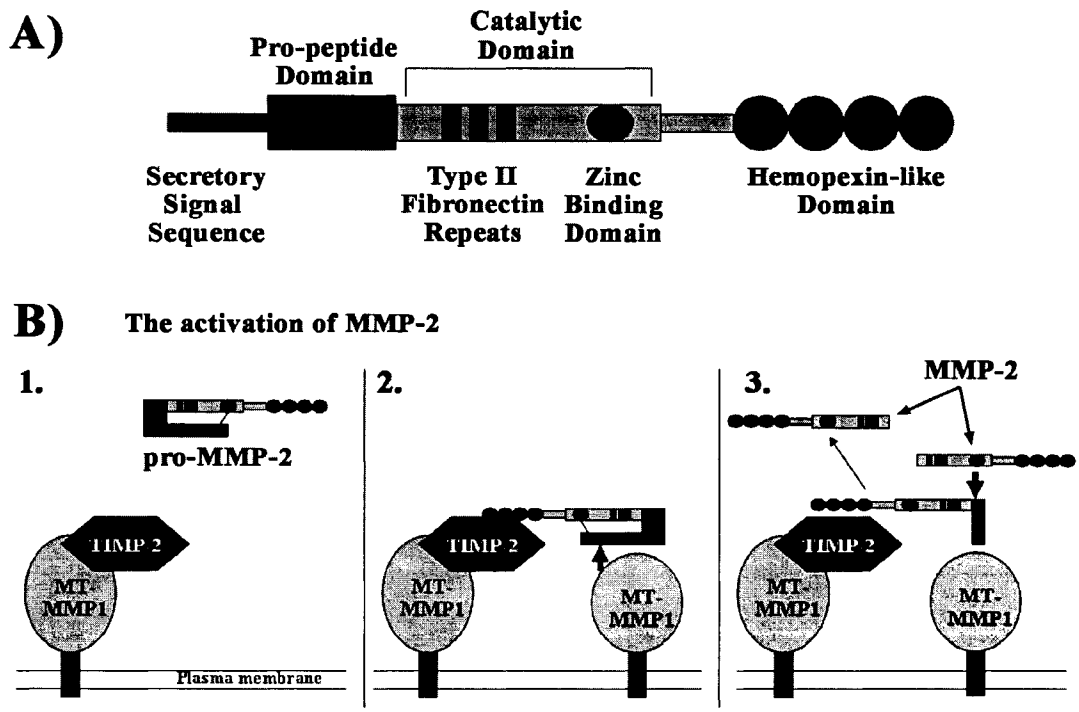

Figure 1.11 The domains of MMP-2, and MMP-9, and the activation of MMP-2. *Panel A* is a diagram of the domains of MMP-2 and MMP-9. *Panel B* is a schematic diagram of the mechanism of MMP-2 activation. See the text for details. This figure is adapted from the thesis of Katherine Morris [149].

Natural inhibitors secreted by cells can also inhibit the MMPs. These include low-affinity binding by α-macroglobulins that mediate rapid MMP clearance and degradation [210]. Highly specific inhibitors known as tissue inhibitor of metalloproteinases (TIMPs) bind MMPs in a 1:1 ratio. There are four TIMPs with low molecular weights between 20-28 kDa that have been characterized, and each has specificities for various MMPs

[206]. The only known cell surface inhibitor of MMPs is the reversion-inducing–cysteine-rich protein with Kazal motifs (RECK), that can selectively bind and inhibit MMP-2, -9, and MT1-MMP [211].

1.5.3 *Regulation and functions of matrix metalloproteinases-2 and -9* - Proteolytic cleavage of fibrillar collagens by the collagenases, MMP-1, -8, and -13, result in a collagen cleavage product that is susceptible to denaturation to gelatin at body temperature [208]. The gelatinases, MMP-2 and -9 can then cleave gelatin. However the name, gelatinase, is a misnomer because MMP-2 and -9 can also degrade other ECM proteins including collagen I, V, X, and the basement membrane proteins collagen IV, and laminin V [212]. The ability of MMP-2 and -9 to degrade the basement membrane proteins is important in light of their roles in cell invasion during tissue repair and metastasis [206, 213]. Furthermore, MMP-2 and -9 can cleave non-ECM proteins, such as pro-TGF-β, proTNF-α, and pro-IL-1β, producing active forms of these growth factors and cytokines so that they can activate their respective receptors [206, 207]. MMP-2 can also attenuate fibroblast growth factor (FGF) signaling by cleaving its receptor [214].

In addition to the minimal MMP domains, MMP-2 and -9 have a hemopexin-like domain that confers bindings to substrate and TIMP inhibitors, and type II fibronectin-like repeats that facilitates binding to ECM substrates (Fig. 1.11A) [209]. MMP-2 and -9 are 72, and 92 kDa in size as pro-enzymes, respectively, however the "pro-enzyme" label is misleading because they have activity in both pro-enzyme form and mature form. As mentioned in Section 1.5.2, S-glutathiolation of the critical cysteine residue in the propeptide domain can activate MMPs without propeptide cleavage. The significance of their dual active forms is not known. Generally, transcriptional expression of MMP-9 is

highly inducible and the propeptide can be cleaved by MMP-13 [215] to an 82 kDa "activated" enzyme.

MMP-2 is constitutively produced, and in situations such as wound healing or tumor malignancy, expression can be further increased [216-218]. A novel mechanism for the activation of MMP-2 has been elucidated involving MMP-14 (also known as MT1-MMP) and TIMP-2 (Fig. 1.11B) [219-222]. A complex between the N-terminus of TIMP-2 and the membrane-anchored MMP, MT1-MMP, is formed, which inhibits MT1-MMP activity (Fig. 1.11B). The C-terminus of TIMP-2 recruits a 72 kDa pro-MMP-2 via the hemopexin-like domain of pro-MMP-2. A second MT1-MMP, free of bound TIMP-2, then partially cleaves the propeptide domain of the bound pro-MMP-2, which partially activates pro-MMP-2 (Fig. 1.11B). Another unbound and fully processed MMP-2 then completes the propeptide cleavage of the bound pro-MMP-2, which is then released by the TIMP-2/MT1-MMP complex as a fully activated MMP-2 (Fig. 1.11B). Paradoxically, TIMP-2 is a potent inhibitor and activator of MMP-2. Therefore the relative concentrations of MMP-2, MT1-MMP and TIMP-2 are important in the activation of MMP-2. If there are over-whelming levels of TIMP-2, free MMP-2 and MT-MMP that are required for MMP-2 activation will be bound and inhibited.

MMP-2 is also known to interact with integrins through its hemopexin-like domain on invasive cells [223]. MMP-9 association with the cell surface that is mediated by cell surface receptors, and integrins is also important for its actions [206]. Cell surface association of theses MMPs provides a mechanism for cells to remodel proximal ECM, and locally release both latent and ECM-sequestered growth factors and cytokines.

1.6 Thesis objectives

Lipid phosphate phosphatases (LPPs) are important regulators of signaling. The LPPs ability to dephosphorylate lipid phosphates, such as lysophosphatidate (LPA), phosphatidate (PA), sphingosine 1-phosphate (S1P), and ceramide 1-phosphate (C1P) has focused attention on their regulation of lipid phosphate signaling. The discovery that LPA and S1P have specific cell surface receptors that mediate vital cell signaling functions, and that the ecto-activity of the LPPs can degrade external LPA and S1P led to studies that established a role for the LPPs as a negative regulator of cell surface lipid phosphate signaling. In addition to their role of degrading extracellular lipid phosphates, there is mounting evidence demonstrating that LPPs can regulate intracellular signaling lipid phosphates. It is the objective of this thesis to investigate the role of the LPP isoform, LPP1, in the migration of fibroblasts induced by extracellular LPA. The main reason to study the LPP1 isoform is that it appears to be the major contributor of LPP activity in fibroblasts, since increasing or decreasing its expression significantly altered total LPP activity compared to changing LPP2 of LPP3 [150]. A key focal point of this study is to determine whether LPP1 affects LPA-induced migration by degrading external LPA, or by regulating migration downstream of the activated LPA receptor. The effect of LPP1 on the activation of internal signaling proteins was measured along with the levels of internal PA and diacylglycerol (DAG). Comparison of LPA signaling to other external signaling molecules such as platelet-derived growth factor (PDGF), and endothelin enabled us to determine if LPP1 affects LPA signaling specifically or if it has a broader influence. Another aim of this thesis was to determine if LPP1 could affect proteins that

regulate remodeling of the extracellular matrix (ECM), which is important for fibroblast function. We employed Rat2 fibroblasts that stably expressed LPP1, or that could be efficiently infected with adenovirus to produce either wild-type or catalytically inactive LPP1. Conversely, we used siRNAs to specifically reduce endogenous LPP1 expression. The elucidation of how LPP1 can control fibroblast migration induced by LPA and other signaling molecules is physiologically relevant in wound healing, fibrosis, and cancer.

CHAPTER 2

MATERIALS AND METHODS

2.1 Reagents

Reagents used were of the highest grade available. Dulbecco's minimum essential medium (DMEM), and trypsin-EDTA were purchased from Invitrogen Life Tecnologies, Inc. (Carlsbad, CA). Fetal bovine serum, and human recombinant PDGF-BB were from Medicorp, Inc. (Montréal, PQ, Canada). Fatty-acid free bovine serum albumin, soybean trypsin inhibitor, LPA, and human endothelin-1 were from Sigma Chemical Co. (St. Louis, MO). Other reagents and their sources are mentioned within the text.

2.2 Modifying lipid phosphate phosphatase-1 and phospholipase D production

2.2.1 *Stable over-expression of lipid phosphate phosphatase-1 in Rat2 fibroblasts* – Preparation of mouse LPP1 cDNA, and its various modifications were produced by Dr. Qiu-Xia Zhang, of the University of Alberta. cDNA for mouse LPP1 was sub-cloned into the pBABEPURO (pBP) ecotropic retroviral expression vector. We engineered mixed populations of Rat2 fibroblasts that stably over-express LPP1 by using puromycin selection [158]. They were maintained in DMEM containing 10% FBS, 1% penicillin and streptomycin and incubated at 37°C in an atmosphere of 5% CO_2. The overlap-extension PCR method fused a GFP tag to the C-terminus of LPP1, and introduced conservative point mutations at Lys^{127} and Lys^{217} to arginine residues in the first and second conserved phosphatase domains, respectively (Figures 1.8 and 1.9). These mutations produced catalytically inactive LPP1[R127K]-GFP, and LPP1[R217K]-GFP. We also modified cDNA to express LPP1[N142Q]-GFP, an LPP1 that could not be glycosylated in the external loop between the first and second conserved catalytic domains (Fig. 1.9). This

mutation did not affect LPP activity [148]. These mutated LPP1s were stably over-expressed in Rat2 fibroblasts.

2.2.2 *Fibroblasts from transgenic mice over-expressing lipid phosphate phosphatase-1* - Fibroblasts obtained from transgenic mice that over-expressed 2-, 8-, and 20-copies of the mouse LPP1 cDNA were a kind gift from Dr. Gabor Tigyi (University of Tennessee). These fibroblasts were obtained from the tails of transgenic newborn pups and were immortalized by transfection of SV40 large T antigen. They were maintained in DMEM containing 10% FBS in the presence of penicillin and streptomycin and incubated at 37°C in an atmosphere of 5% CO_2 [185].

2.2.3 *Green fluorescent protein and c-myc tagged lipid phosphate phosphatase-1 were sub-cloned to pCMV5 plasmid vectors* - Catalytically active LPP1 and the inactive R217K mutant had a c-myc-tag fused to the C-terminus using overlap-extension PCR. Various mouse LPP1-GFP cDNA constructs produced by Dr. Qiu-Xia Zhang, and the c-myc-tagged constructs were sub-cloned into pCMV5 expression plasmids for transient transfection.

2.2.4 *Transient transfection of Cos7 cells* - To express these constructs in Cos7 cells, 1 x 10^6 cells were plated in 10-cm dishes with DMEM containing 10% FBS and no antibiotics, and were incubated overnight so that the cells were 50-60% confluent at the time of transfection. The medium was replaced with fresh medium 3 h before transfection. In a 1.5-ml centrifuge tube, 20 μg of plasmid DNA and then 62 μl of 2M $CaCl_2$ were mixed with sterile, deionized water to a final volume of 500 μl. The DNA solution was added drop-wise to another 1.5-ml centrifuge tube containing 500 μl of 2X BES transfection solution (50 mM, N,N-bis[2-hydroxyethyl]-2-aminoethanesulfonic

acid, 274 mM NaCl, and 1.9 mM Na_2HPO_4) while gently vortexing in a tissue culture hood. The slightly opaque solution was incubated at room temperature for 30 min. This transfection solution was added drop-wise and the plates were swirled to distribute the precipitate evenly over the cells. The plates were incubated at 37°C for 14 h, at which point the medium was replaced with fresh DMEM containing 10% FBS and no antibiotics for an additional 34 h. Lysates were collected for subsequent Western blot, or enzymatic analysis.

2.2.5 *Preparation of adenovirus, and infection of Rat2 fibroblasts to express various lipid phosphate phosphatase-1, phospholipase D-1 and -2 constructs* - Adenovirus that expressed c-myc-tagged wild-type mouse LPP1, and the catalytically inactive c-myc-tagged LPP1[R217K] mutant were prepared by the University of Iowa Gene Transfer Vector Core. Purified preparations contained about 10^{10} plaque-forming units/ml. Adenovirus used for expressing wild type and dominant-negative PLD1 and PLD2 were a kind gift from Dr. Natarajan. The following is a brief description of how the adenovirus was produced: cDNAs were sub-cloned to the pShuttle-CMV vector (Stratagene, La Jolla, CA). This shuttle vector was recombined with pAdEasy-1 in BJ5183 bacteria and the recombined adenovirus plasmid was amplified in XL10-Gold bacteria (Stratagene). The recombinant adenovirus plasmids were linearized and used to transfect HEK 293 cells where deleted viral assembly genes were complemented.

To quantitatively transfect Rat2 fibroblasts with adenovirus without causing significant death to the cells we used a transfection adenovirus concentration between 40 and 60 MOI (multiplicity of infection, or average number of plaque forming units per cell). Cells were incubated with adenovirus at 37°C in DMEM containing 10% FBS and

no antibiotics, for at least 24 h when significant expression of the recombinant protein was detected.

2.2.6 *Knockdown of rat lipid phosphate phosphatase-1 expression using siRNA* - Knockdown of rat LPP1 activity was achieved by using *SMARTpool* ® siRNAs Dharmacon Inc. (Lafayette, CO). *SMARTpool* ® siRNAs consists of four duplex siRNAs designed to decrease mRNA levels by targeting four separate sequences on rat LPP1 transcript. About 500,000 Rat2 fibroblasts were plated on 10 cm plates with 10 ml DMEM containing 10% FBS and no antibiotics, and allowed to double in number over 24 h. Shortly before transfection, the medium was replaced with 4 ml of fresh DMEM containing 10% FBS and no antibiotics. Ten μl of 100 μM siRNA stock was diluted in 0.5 ml Opti-MEM Reduced Serum Medium (Invitrogen Life Technologies, Carlsbad, CA). In another tube, 7 μg of Lipofectamine 2000 (Invitrogen) was gently mixed with 0.5 ml Opti-MEM Reduced Serum Medium, and incubated at room temperature for 15 min. The diluted siRNA and the diluted Lipofectamine 2000 were combined and incubated for a further 15 min at room temperature. One ml of the siRNA-Lipofectamine 2000 complexes was added drop wise to a plate of cells that was swirled, and achieved a final siRNA concentration of 200 nM. After 4.5 h of incubation at 37°C, the transfection media was replaced by DMEM containing 10% FBS and no antibiotics. The cells to be used for migration were starved 24 h after transfection with DMEM containing 0.4% BSA for 18 h. Samples were taken for LPP-activity assays, and mRNA quantitation by real time RT-PCR (see Section 2.3.1 and 2.3.4, respectively).

For each experiment, controls for the LPP1 knockdown were performed with functional non-targeting siCONTROL (Dharmacon) siRNAs, which can silence firefly

luciferase, and with Lipofectamine 2000 alone as a mock transfection. A siGLO RISC-FREE (Dharmacon) siRNA control was also employed as a non-functional negative control as this RNA duplex is chemically modified to not bind to the RNA-induced silencing complex (RISC, the RNA interference machinery in the mammalian cell). Furthermore, the siGLO modification is a fluorescent label for detection using fluorescence microscopy, and is found in the nuclear and perinuclear regions of the cell. Thus, it is also a transfection marker of uptake (Fig. 2.1).

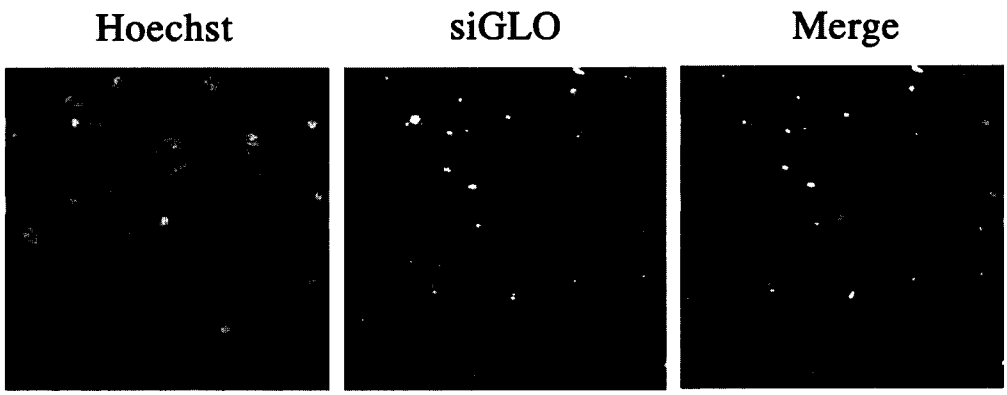

Figure 2.1 Transfection efficiency of siRNAs in Rat2 fibroblasts is approximately 90%. Rat2 fibroblasts were transfected with siRNA controls: 200 nM of the functional non-targeting siCONTROL siRNA, together with 100 nM of the non-functional, non-targeting fluorescent labeled siGLO RISC-FREE siRNA. The cells were fixed then stained with Hoechst 33258 dye (*blue*) and visualized using fluorescence microscopy. The left panel shows the nuclei of cells that have migrated through a microporous membrane (see Section 2.4.2) induced by 20 ng/ml of PDGF. The center panel shows the fluorescence from siGLO (*red*) detected at 570 nm of the same field of the left panel. The two images were *merged* (right) and the percent transfection was calculated by dividing the number of nuclei with perinuclear staining from siGLO siRNA by the number of total nuclei. Panels depict typical cells from 1 of 6 fields. Results are from one experiment.

2.3 Detection of lipid phosphate phosphatase-1 and phospholipase D expression

2.3.1 *Measuring lipid phosphate phosphatase activity using the Triton-micelle assay* - LPP activity of cell lysate was measured *in vitro* using ^{3}H-labeled phosphatidate (PA) in Triton X-100 micelles. The reaction was performed in 100 mM Tris maleate (pH 6.5), 2 mg/ml BSA, 5 mM N-ethylmaleimide, and 1 mM EDTA/EGTA. Protein

concentration in lysate was determined using the Bio-Rad Detergent Compatible protein assay kit (Bio-Rad Laboratories, Hercules, CA). This protein assay can determine accurate protein concentration in the presence of high detergent concentration, particularly in the LPP solubilization lysis buffer (50 mM Hepes, 137 mM NaCl, 1 mM MgCl, 1 mM CaCl, 10% glycerol, 0.1% SDS, 1% Triton X-100, 0.5% deoxycholate, 2.5 mM EDTA, and 1% Sigma protease inhibitor cocktail). Orthovanadate and NaF were excluded from the lysis buffer as these inhibit LPP activity. The amount of protein used and the time of incubation for the assay were such that no more than 15% of the substrate was hydrolyzed. The LPP assay was performed using three different protein concentrations in order to ensure that the assay was proportional to the amount of protein used, thereby validating the assay. The range of protein used was typically 1 μg to 10 μg, however, to avoid excess enzyme on a limited amount of substrate, as in the case of high LPP expression, less protein was used. Since the reaction is performed in the presence of Triton X-100 micelles, the extra Triton X-100 in the lysis buffer (1%) would decrease PA mol % in the reaction by as much as half as more protein from lysates are added. The PA mol % was kept constant by adding more lysis buffer to compensate for each reaction with less protein, and for the background control with no protein. The reaction was started by adding ^{3}H-labeled PA (0.83 Ci/mol) with Triton X-100 to a final concentration of 0.6 mM and 8 mM, respectively, to a final volume of 100 μl. Incubations were performed at 37°C, for 30 minutes.

The reaction was stopped by adding 2.2 ml of chloroform/methanol (95:5, by vol), to extract [^{3}H]diacylglycerol (DAG), and 0.8 g basic alumina to bind, and sequester anionic-PA, and any released palmitate. After vortexing and centrifugation of the

samples, the organic phase (1 ml) was removed and dried down for liquid scintillation counting of [^{3}H]DAG.

LPP activity was also measured after immunoprecipitation of the tagged LPP1 from protein lysates. This allowed us to measure activity from target recombinant LPP, and removes background from endogenous LPP activity. Briefly, cell lysates containing 250, 150, and 50 μg of protein in 100 μl of LPP solubilization lysis buffer, were pre-cleared with 15 μl of 1:1 protein A-Sepharose (GE Healthcare Life Sciences, Chalfont St. Gilles, UK)/PBS slurry for 1h at 4°C. To immunoprecipitate tagged LPP1 we used mouse monoclonal anti-c-myc (9E10 diluted 1:50) or rabbit polyclonal anti-GFP (1:100), and added this to the pre-cleared lysates from cells expressing LPP1-myc, or LPP1-GFP fusion proteins respectively. The mixtures were gently rocked at 4°C overnight. Twenty μl of 1:1 protein A-Sepharose/PBS slurry was added and gently rocked for 3 h at 4°C. The samples were then gently centrifuged and the beads were washed three times with immunoprecipitation washing buffer (50 mM Tris base, pH7.5, 1% Triton X-100, 100 mM NaCl, 5 mM EDTA and 1% Sigma protease inhibitor cocktail). The LPP activities of the immunoprecipitates were measured using the same method for the whole lysates described above, but with more rigorous shaking to keep the beads in suspension. The assay was performed at room temperature for 90 min. The beads from the pre-clearances, and the supernatant of the immunoprecipitations were also analyzed for use as controls.

2.3.2 *The measurements of external lysophosphatidate-dephosphorylation on 35-mm plates, and in Transwell chambers* - Rat2 fibroblasts were plated at 50,000 cells per 35-mm dish and incubated for 2 days to reach 80-90% of confluence. Cells were

rinsed twice with HBS to remove any serum, which could contain LPA, and other growth factors or enzymes that could interfere with the ecto-LPP assay. Cells were then incubated with DMEM containing 0.4% fatty acid-free BSA for 2 h. This medium was replaced with 0.8 ml of the same medium containing 10 μM ^{32}P-labelled LPA at about 6 Ci/mol (roughly equivalent to 100,000 dpm per plate). The bulk LPA, from a 25 mM stock prepared in water, was dispersed with ^{32}P-labeled LPA by probe sonication. One mM of glycerol 3-phosphate was added to the medium to limit the possible degradation by ecto-alkaline phosphatase of glycerol 3-[^{32}P]phosphate formed by phospholipase A-type activities on ^{32}P-labelled LPA [129]. After 20 min 0.6 ml of the media was collected and added to 0.6 ml of 1M $HClO_4$ to precipitate the protein and the majority of ^{32}P-labeled LPA. After centrifugation, 1 ml of the supernatant was added to 1 ml of water-saturated butan-1-ol, and mixed. After another centrifugation, the top butanol phase was aspirated and another volume of water-saturated butan-1-ol was added to extract remaining lipid. A sample (0.8 ml) of the aqueous phase was recovered and 80 μl of 125 mM ammonium molybdate was added to react with any inorganic phosphate. The phosphomolybdate complex was then quantitatively extracted by adding 0.9 ml *iso*-butanol/benzene (1:1) leaving any other water-soluble organic phosphates in the aqueous phase. $^{32}P_i$ was measured by scintillation counting. Medium from plates that did not have cells were assayed for background $^{32}P_i$, which never exceeded 0.5% of the total dpm added. The cells on the 35-mm plate were harvested and homogenized for protein determination by a bicinchoninic acid assay (Pierce Biotechnology, Inc. Rockford, IL). Ecto-LPP activity was expressed as LPA dephosphoryated/ min per mg of protein.

The percentage (w/v) of BSA in DMEM used for all the experiments involving Rat2 fibroblasts was based on the highest % LPA degraded when ecto-activity was measured at various concentrations of BSA (Fig. 2.2).

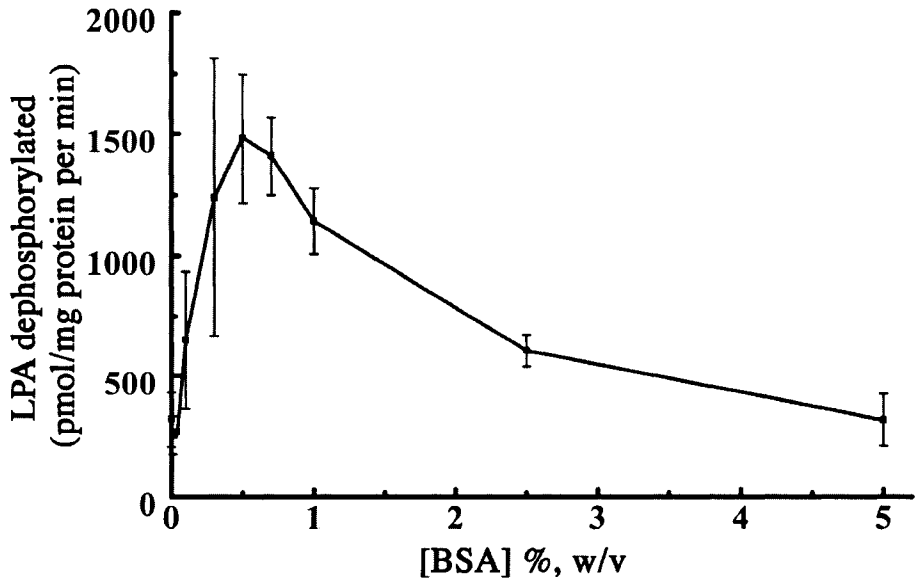

Figure 2.2 The rate of external LPA dephosphorylation is dependent on BSA concentration in DMEM medium. The graph shows the rate of dephosphorylation of exogenous LPA (50 μM) after 20 min. The peak of LPA dephosphorylation was between 0.3 and 0.7% BSA, w/v, in DMEM, which gives a molar ratio of LPA:BSA of 1:1 and 0.5:1, respectively. Results are means ± S.D. for three independent experiments on wild-type Rat2 fibroblasts.

The dephosphorylation of ^{32}P-labelled LPA by fibroblasts in Transwell chambers was also measured (see Section 2.4.2 about Transwells and Fig. 2.3A). The ^{32}P-labelled LPA was added to the bottom chamber, and therefore was mostly exposed to cells that have migrated from the upper chamber through the 8-μm pores in the membrane separating the two compartments. After 6 h of migration, medium from both the upper and the lower chambers were combined to a total of 0.4 ml, and added to an equal volume of 1M $HClO_4$. The rest of the procedure to extract $^{32}P_i$ was identical to that described above adjusting for volumes proportionally.

2.3.3 *Western blot analysis of lipid phosphate phosphatase-1 and phospholipase D* - Cell lysates were collected in LPP solubilization lysis buffer (see Section 2.3.1) supplemented with 2 mM orthovanadate and 100 mM of NaF. Fifty µl of lysate with 75 µg of protein was diluted in 10 µl of 6 X sample buffer (1 X sample buffer concentrations: 62.7 mM Tris base, pH 6.8, 10% glycerol, 1% SDS, 0.0005% bromophenol blue, and 1% 2-mercaptoethanol added fresh). It was important to boil the samples for 5 minutes, but samples to be probed for PLD were not boiled since this promotes aggregation of PLD. The samples were loaded on stacking gels composed of 0.375 M Tris-HCl, pH 8.8, 0.1% SDS, 3.9 % acrylamide, and 0.1% bisacrylamide. Separating gels were composed of 0.125 M Tris-HCl, pH 6.8, 0.1% SDS, and 7.5% acrylamide/ 0.2% bisacrylamide to resolve PLD and 10% acrylamide/ 0.27% bisacrylamide to resolve LPP1. Proteins were separated at 100 mV for 3 h using a Mini-Protean II protein electrophoresis apparatus (Bio-Rad) in Laemmli electrophoresis buffer. Five µl of Precision Plus Protein standards from Bio-Rad were also loaded as molecular weight standards (Molecular weights: 250, 150, 100, 75, 50, 37, 25, 20, 15, and 10-kiloDaltons). After separation the proteins were transferred to 0.45 µm Transblot nitrocellulose membranes (Bio-Rad) for 3 h at 400 mA in Tris-glycine buffer containing 20% ethanol. The membranes were blocked in Odyssey Blocking Buffer (LI-COR, Lincoln, NB) overnight. Rabbit polyclonal antibodies for mouse LPP1 [158], PLD1 (BioSource International Inc., Camarillo, CA) and PLD2 (a gift from Dr. S Bourgoin, University of Laval, Québec, PQ, Canada) were diluted 1 to 1000 in the Odyssey Blocking Buffer supplemented with 0.1% Tween-20 and the membranes were incubated for 2 h. The membranes were washed 4 times with PBS containing 0.1% Tween-20 for

5 min per wash with constant agitation. Goat anti-rabbit IgG conjugated to an IR Dye800 (Rockland Immunochemica, Gilbertsville, PA) was diluted 1 to 10,000 in Odyssey Blocking Buffer supplemented with 0.1% Tween-20 and incubated with the membrane for 1 h. Once again the membranes were washed 4 times with PBS-0.1% Tween-20 for 5 min per wash with constant agitation. Fluorescence on the Western blot was scanned with the Odyssey Infrared Imaging System (LI-COR) using the 800 nm channel.

To detect LPP1 from transgenic fibroblasts, 200 μg of protein was loaded on a 10%-SDS-PAGE gel, and run overnight at 20 mA at 4°C using a Protean II protein electrophoresis apparatus (Bio-Rad). Transfer of proteins onto nitrocellulose membrane was also performed overnight at 300 mA using a Transblot transfer chamber (Bio-Rad). The membrane was blocked in 2.5% milk, and 2.5% BSA in PBS for 2h at room temperature. The membrane was probed overnight using rabbit polyclonal anti-mouse LPP1 at a 1 to 1000 dilution in the same blocking solution. Anti-rabbit IgG conjugated to horseradish peroxidase (GE Healthcare Life Sciences) at a dilution of 1 to 5000 was incubated with the membrane at room temperature for 1 h. Detection of mouse LPP1 was achieved using ECL (GE Healthcare Life Sciences) and Kodak BioMax film according to manufacturer's directions.

2.3.4 *Measuring mRNA levels by real-time RT-PCR* - RNA was collected using the RNAaqueous kit (Ambion Inc. Austin TX) according to manufacturer's instructions. Contaminating DNA was removed using a DNA-free kit (Ambion) according to manufacturer's instructions. RNA was quantified spectrophotometrically at 260 nm, and the quality was determined by an absorbance ratio of 260 nm/280 nm, for which a ratio of higher than 1.8 was acceptable. No less than 1 μg of RNA was used for the reverse

transcription reaction performed with Superscript II (Invitrogen), random primers (Invitrogen), and RNaseOUT (Invitrogen) according to the manufacturer's instructions. Blank controls lacking RNA and controls with RNA but no reverse transcriptase enzyme added were also performed in parallel. Real time PCR was performed on a 7500 system (Applied Biosystems, Foster City,CA) with a built-in thermal cycler. Approximately 100 ng of cDNA from reverse transcription, 0.2 μM of each primer, and SYBER green PCR master mix (Applied Biosystems) were combined for the PCR reaction performed in triplicate. An annealing temperature of 57°C was used for all primer pairs. Standard curves for each primer pair was performed and the slopes and efficiency calculated from these relationships were used to determine the amount of target mRNA relative to the housekeeping gene cyclophilin A. Melting curves for each sample was performed to determine product specificity of the PCR reaction, and a single band on a 2% agarose gel from a PCR confirmed specificity. Primers used for PCR were as follows:

LPP1 forward - GGTCAAAAATCAACTGCAG

LPP1 reverse - TGGCTTGAAGATAAAGTGC

Cyclophilin A forward - CACCGTGTCTTCGACATCAC

Cyclophilin A reverse - CCAGTGCTCAGAGCTCGAAAG

Rat MMP2 forward - CTATTCTGTCAGCACTTTGG

Rat MMP2 reverse - CAGACTTTGGTTCTCCAACTT

Rat MMP9 forward - AAATGTGGGTGTACACAGGC

Rat MMP9 reverse - TTCACCCGGTTGTGGAAACT.

2.3.5 *Indirect immunofluorescence of lipid phosphate phosphatase-1 in Cos7 cells* - To visualize the expression and localization of LPP1 and various mutants of LPP1, Cos7 cells were transiently transfected with plasmid DNA containing cDNA for both myc-tagged LPP1 and myc-tagged LPP1 (R217K) for immunofluorescence analysis. Briefly, 30,000 cells were plated on sterile 12-mm circular cover slips (Fisher Scientific International Inc., Hampton, NH) that were placed in each well of a 24-well plate (Corning Inc., Corning, NY), and incubated overnight at 37°C at an atmosphere of 5% CO_2. Calcium phosphate transfection was carried out as described in Section 2.2.4, except that all the conditions were scaled down by a factor of 28, which includes the use of 0.714 μg of plasmid DNA. Many of these experiments involved co-transfecting Cos7 cells with two different plasmid DNAs that express two versions of LPP1. To avoid killing the cells in these experiments, 0.357 μg of each plasmid was used for transfection (0.357 μg plasmid DNA X 2 = 0.714 μg plasmid DNA). At 48 h post-transfection, the cells were carefully washed once with warm PBS, and fixed with -20°C methanol for 5 minutes. After washing the fixed cells twice with PBS, they were permeabilized with PBS containing 0.1% Triton X-100 (PBS-T) for 10 min. The cover slips were placed with the fixed cells facing down on 5μl of primary antibody (see Table 2.1) diluted in PBS-T and 4% FBS to block non-specific sites, and then incubated at room temperature for 1 h. The cover slips were dipped in PBS to wash away the primary antibody and stained with secondary antibody under similar conditions as the primary antibody. Many of the studies involved staining for two different targets; therefore the primary antibodies from two separate sources of animal were incubated together at their respective dilutions. Secondary antibodies recognizing IgG of the animals used to raise both of the primary

antibodies were also incubated together using 1 to 100 dilutions. To distinguish between the targets, the secondary antibodies were conjugated to either FITC or TRITC dyes (Jackson ImmunoResearch West Grove, PA), so that interchangeable filters can allow the visualization of the two targets from the same image-field. The stained cells were analyzed by conventional fluorescence microscopy and Zeiss (Thornwood, NY) oil immersion lens. Color photographs were taken with a digital camera by superimposing the monochrome graphs of the two channels. Controls minus primary antibodies were used for determining background staining by the secondary antibodies.

Table 2.1 Primary antibodies used for immunofluorescence in Cos7 cells.

Target	Host Species	Dilution	Supplier
EGFR	Sheep	1:100	Upstate
Giantin	Rabbit	1:100	Dr. P. Melançon, U of A
Calreticulin	Goat	1:50	Dr. M. Michalek, U of A
Green Fluorescent Protein	Rabbit	1:1000	Dr. L. Berthiaume
c-myc (9E10)	Mouse	1:50	Dr. T. Hobman, U of A

2.3.6 *Cell-surface biotinylation of lipid phosphate phosphatase-1* - LPP1 was predicted to be a cell surface protein because cells over-expressing LPP1 have an increased ecto-activity [158]. EZ-Link Sulfo-N-hydroxysuccinimide (NHS)-LC-Biotin (Pierce) was used as a cell impermeable labeling agent to biotinylate exposed proteins on intact cells [224]. Rat2 fibroblasts over-expressing GFP alone, wild-type LPP1-GFP,

catalytically inactive mutants LPP1[R127K]-GFP and LPP1[R217K]-GFP were grown to 80-90% of confluency in DMEM containing 10% FBS at 37°C and an atmosphere of 5% CO_2. The cells were then washed twice with warm HBS and incubated in DMEM containing 0.1% BSA starvation media. After 18 h the cells were washed three times with ice-cold PBS supplemented with 0.1 mM $CaCl_2$ and 1mM $MgCl_2$ (PBS-CM), and placed on ice. This step safely washes the monolayer of cells free of proteins that adhere nonspecifically and that potentially interfere with the efficiency of biotinylation of surface proteins. The cold essentially stalls cycling of LPP1 to-and-from the plasma membrane. Cells were then incubated with or without Sulfo-NHS-LC-Biotin freshly dissolved in PBS-CM, pH 7.0, at a concentration of 0.5 mg/ml, and cooled on ice for 30 min to allow the reaction to proceed. Cells were then rinsed twice with PBS-CM plus 100 mM glycine, and then washed in this buffer for 20 min with gentle motion to quench any unreacted biotin. Cells were then rinsed twice with PBS-CM to wash away the quenched biotin. Cells were then harvested with PBS with protease inhibitors, sonicated twice on ice, centrifuged in a tabletop centrifuge for 5 min to remove debris and nuclei, and the supernatant was then centrifuged in a Beckman Optima MAX Ultracentrifuge (Beckman Coulter, Inc., Fullerton, CA) at 99,000 rpm for 1 h at 4°C, using a T100.2 rotor (Beckman Coulter). This step separated the membranes from the cytosol. The membranes were resuspended in LPP solubilzation lysis buffer (see Section 2.3.1) supplemented with 2 mM orthovanadate and 100 mM of NaF. A Bio-Rad Dc protein assay was performed so that 300 µg of protein was immunoprecipitated using rabbit polyclonal anti-GFP antibodies as described in Section 2.3.1. The beads were resuspended in 100 µl of washing buffer and 20 µl of 6X sample buffer and boiled for

5 min. The beads were spun down and 100 µl of the supernatant was loaded on to a 7.5% SDS-PAGE gel that was exposed overnight to 20 mA in a Protean II protein electrophoresis apparatus (Bio-Rad) at 4°C. Proteins were then transferred onto nitrocellulose membranes overnight at 300 mA, and then blocked overnight in Odyssey blocking buffer. The membrane was probed with mouse monoclonal anti-GFP (Santa Cruz Biotechnology, Inc., Santa Cruz, CA) at a dilution of 1 to 1000 in Odyssey blocking buffer, in the presence of IRDye 800 conjugated streptavidin (Rockland), at a dilution of 1 to 2500 to detect the biotinylated proteins. Alexa 680 goat anti-mouse IgG (Molecular Probes, Eugene, OR) at a dilution of 1 to 10,000 was subsequently used to probe the membrane still in the presence of IRDye 800 conjugated streptavidin. The Odyssey Infrared Imaging System then detected emission from both the 700 nm and 800 nm range, and the software digitally superimposed the scans from the two channels.

2.3.7 *Detection of glycosylation of lipid phosphate phosphatase-1* - Rat2 cells over-expressing LPP1 and empty vector control cells were plated on 100-mm dish until confluent, at which time they were harvested in PBS supplemented with protease inhibitors. Cell membranes were collected as described in Section 2.3.6. The membranes were resuspended in 10 mM Tris-HCl, pH 7.4, 1 % Triton X-100, 1 mM o-phenanthroline as protease inhibitor, and 2.5 mM EDTA, and sonicated to homogeneity. Two hundred µg of membrane protein was heat inactivated at 95°C for 5 min and was then treated with 10 units of recombinant N-glycosidase F (Roche Diagnostics, Manheim, Germany) for 6 h at 37°C with occasional vortexing. Control incubations were performed in the absence of N-glycosidase F. Western blotting for the

mouse LPP1, using the rabbit polyclonal anti-mouse LPP1 was performed as previously described in Section 2.3.3.

2.3.8 *Measurement of phospholipase D activity by the production of phosphatidylbutanol* - For the measurement of PLD activity, 73,000 fibroblasts were plated in DMEM and 10% FBS on 3.5 cm dishes. After 48 h, the medium was changed to 1 ml DMEM that contained 0.4% BSA and 5 μCi of 57 Ci/mmol [9,10-^{3}H]palmitate (Perkin-Elmer Life Sciences, Boston, MA). The media was replaced 18 h later with unlabeled DMEM containing 0.4% BSA and the cells were incubated for 2 h more. The fibroblasts were then pre-treated with 30 mM butan-1-ol for 15 min and then treated with agonists for 6 min so that PLD activity could be measured through the formation of phosphatidylbutanol (PB). The reactions were stopped by washing twice with ice-cold HEPES buffered saline. The cells were then collected by scrapping twice in 0.5 ml methanol. One ml of chloroform and 0.9 ml of 1 M KCl containing 0.2 M HCl was added to the combined methanol fractions and the mixtures were vortexed and then centrifuged. The bottom organic phase was isolated and dried under N_2 and dissolved in 100 μl of chloroform/methanol (9:1). Samples of the lipids including 50 μg of 1,2-dioleoly-*sn*-glycero-3-phosphobutanol (Avanti Polar Lipids Inc. Alabaster, AL) internal standard were loaded on glass-supported silica gel 60 thin layer chromatography plates (Merck, Darmstadt, Germany) and the plates were developed using the upper organic phase obtained by mixing ethylacetate/iso-octane/acetic acid/ water (130:20:30:100, by vol). Lipids were detected by I_2 staining and PB and the total phospholipids lipids near the origin were collected by scrapping. ^{3}H-labeling was measured by liquid scintillation

counting. Relative PLD activity was calculated as the percentage of PB relative to the labeling of total phospholipids.

2.4 Fibroblast migration

2.4.1 *In vitro wound healing assay* - Rat2 fibroblasts were grown to confluence in twenty four-well plates (Corning) and starved with DMEM and 0.4% fatty-acid free BSA for 18 h. The monolayer was scratched from one wall of the well to the opposing wall of the well using the pointed end of a 200 µl pipette tip. The detached cells were removed by three washes with Hepes buffered saline (HBS). DMEM containing 0.4% fatty-acid free BSA with, or without agonists was added to each well as indicated. Images at 25X magnification were taken at different time intervals with a digital camera and a microscope (Leica DM IRB). The size of the image was quantitated by using the graduations on a hemocytometer. This enabled us to estimate the average distance (measured at seven different points) by which the walls of the wound had closed.

2.4.2 *Fibroblast migration in Transwell chambers* - About 500,000 Rat2 fibroblasts were plated on 10 cm dishes with DMEM containing 10% FBS and no antibiotics. After 24 h the fibroblasts were treated with adenovirus at 40 M.O.I for LPPs and 50 M.O.I. for the PLDs, or siRNA as indicated. After a further 24 h the cells were starved with DMEM containing 0.4% fatty-acid free BSA for 18 h. The 6.5 mm diameter Transwell inserts with 8.0 µm pore size polycarbonate filters (Corning Inc., Fig. 2.3A) were pre-coated with 6 µg of human plasma fibronectin (Sigma) dissolved in water and let to air dry overnight. The cells were collected using trypsin-EDTA and quickly neutralized with 0.1% soybean trypsin inhibitor (Sigma) in HBS. Cells (100,000) in

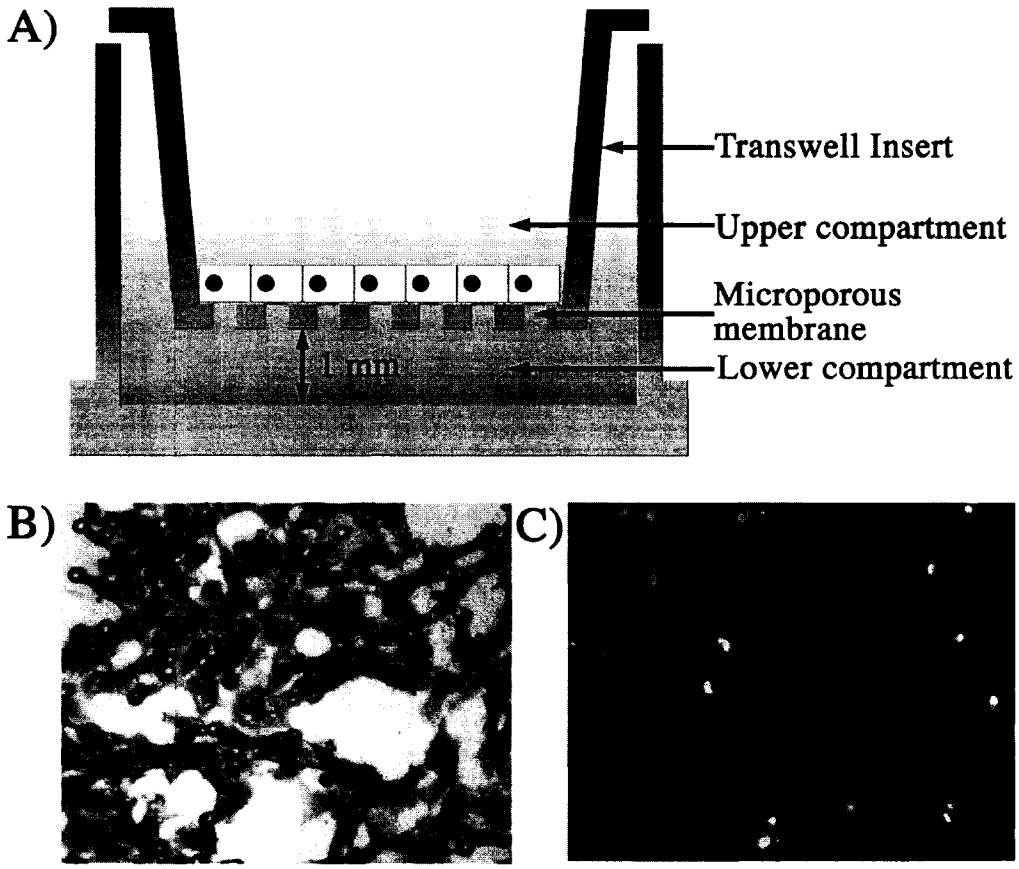

Figure 2.3 Fibroblast migration in Transwell chambers. *Panel A* shows a cross-section representation of a Transwell chamber. Fibroblasts (*yellow*) are shown plated on the upper compartment face of the microporous membrane. Agonists are added to the lower compartment to generate a gradient in the upper compartment. *Panel B* shows a bright-field image of hematoxylin/eosin combination stained Rat2 fibroblasts that have migrated through the pores to the underside of the membrane in response to 0.5 μM LPA after 6h. The 8 μm pores can be seen as *dark-outlined circles*. *Panel C* shows Hoechst 33258 dye stained nuclei of migrated fibroblasts from another experiment. Both images were magnified 100-fold.

DMEM containing 0.4% fatty-acid free BSA were plated inside the Transwell inserts for 2 h before they were placed in the bottom well. The bottom wells contained the agonists where indicated and DMEM containing 0.4% fatty-acid free BSA supplemented with 0.4% charcoal-treated FBS. The cells were incubated at 37°C in 5% CO_2 and allowed to migrate for 6 h at which time the top of the filters was cleared by using a wet cotton-tipped applicator followed by more clearing using a dry cotton-tipped applicator. The migrated cells were then fixed in 5% formaldehyde in HBS for 30 min. Visualization of

the fixed cells on the filters was achieved with a hematoxylin/eosin combination stain (Sigma), or the nuclei were stained with 1 μg/ml Hoechst 33258 dye (Sigma) for 2 h. Images of about 6 fields per filter were taken using a digital camera and a fluorescence microscope (Leica DM IRB) and these were magnified 100-fold so that the numbers of cells per field could be counted (Fig. 2.3 B and C).

2.4.3 *The addition of butanol and inhibitors in Transwell assays* - To measure the

Table 2.2 Inhibitors used in the migration of fibroblasts.

Inhibitor	Target	Final Concentration/ Vehicle	Preincubation Time	Supplier
Butan-1-ol	PLD-dependent PA formation	30 mM	30 min	Fischer Scientific
Butan-2-ol	Negative control for butan-1-ol	30 mM	30 min	Fischer Scientific
GW 9662	PPARγ	200 nM / DMSO	30 min	Sigma
PD 98059	MEK	40 μM / DMSO	30 min	EMD Biosciences
Pertussis Toxin	Gα subunit of heterotrimeric G-proteins: G_i, G_o, G_t	100 nM / water	18 h	Sigma
AG1296	PDGFR tyrosine kinase	10 μM / DMSO	30 min	EMD Biosciences
BAPTA-AM	Chelates intracellular Ca^{2+}	35 μM / DMSO	1 h	EMD Biosciences
Phenanthroline	Matrix metalloproteinases	0.4 mM / water	30 min	Sigma
Doxycycline	Matrix metalloproteinases	100 μM / water	30 min	Sigma
Batimastat	Matrix metalloproteinases	20 μM / DMSO	30 min	Kind gift from Servier
Marimastat	Matrix metalloproteinases	20 μM / DMSO	30 min	Kind gift from Servier
TAPI-1	Matrix metalloproteinases	100 μM / methanol	30 min	EMD Biosciences

effects of inhibitors on the migration of fibroblasts to agonists in Transwell chambers, the inhibitors or the vehicle control (Table 2.2) were added to the Transwell insert 30 min before migration started, 1.5 h after the fibroblasts were plated in the Transwell insert. The insert was then placed in the bottom well that contained the agonists, DMEM containing 0.4% fatty-acid free BSA supplemented with 0.4% charcoal-treated FBS plus inhibitors as indicated. The fibroblasts were then allowed to migrate for 6 h as described in Section 2.4.2.

2.4.4 *Determination of chemotaxis versus chemokinesis* - The *in vitro* wound healing assay mainly measures the non-directional, chemokinetic, movement of the fibroblasts since no diffusion gradient of the agonist is established. Therefore, we also employed the Transwell chamber assay to distinguish between chemotaxis (migration towards a gradient of chemo-attractant) and chemokinesis. The mode of the migration that was stimulated by agonists was determined by adding the same concentration of agonist to the top and bottom chambers and comparing the migration to the agonist when it was present only in the bottom chamber.

2.4.5 *Measuring fibroblast detachment from cell culture plates* – Confluent monolayers of various fibroblast cell lines on 35-mm dishes were incubated with 0.5 ml of trypsin/EDTA (Invitrogen), 2 mM EDTA, or HBS alone as a control at 37°C in an atmosphere of 5% CO_2. At various times the medium was collected and the detached cells were concentrated using a tabletop centrifuge spinning the samples at 2000 rpm for 5 min. The cells were resuspended in 1 ml HBS. Cells remaining on the plate were also colleted in 1 ml HBS by gently scrapping them off the plate using a cell lifter (Corning Inc.). Background controls using no cells were also processed as described above. Cells

were disrupted by quickly freezing at 80°C and thawing at RT twice. The lysed cells were vortexed and 100 µl of each sample were added into the wells of a black 96-well plate (Corning Inc.) in duplicate. One hundred µl of 0.1 µg/ml Hoechst 33258 (Sigma) solution was added to each sample in the well to stain DNA. Fluorescence was measured by a Fluoroskan Ascent FL (Labsystems Oy, Helsinki, Finland) fluorometer at 460 nm. A standard curve of calf thymus DNA (Sigma) from 10 ng to 1000 ng was used to quantify the amount of DNA.

2.4.6 *Differential labeling of fibroblasts* - A mixed population of fibroblasts expressing an empty vector or over-expressing LPP1 can be distinguished from each other by labeling each cell line with different PKH fluorescent cell linkers (Sigma). PKH26 emits maximally at 567 nm, and PKH67 emits maximamlly at 502 nm and can be detected by a fluorescent microscope using rhodamine and fluorescein filters, respectively. These fluorescent dyes have long aliphatic tails that embed into the lipid bilayer with very low cell-to-cell transfer. Labeling of the fibroblasts was done after trypsinizing and resuspending fibroblasts as directed by the manufacturer's protocol. Labeled fibroblasts (100,000) were then plated inside the Transwell inserts as described in Section 2.4.2. To study the effect of LPP1 over-expressing fibroblasts on the migration of neighboring wild type fibroblasts, 50,000 vector control fibroblasts labeled with PKH26 were mixed with 50,000 fibroblasts over-expressing LPP1 labeled with PKH67. The stained cells were analyzed by conventional fluorescence microscopy. A field of migrated fibroblasts was magnified 100-fold, and two images of the same field was taken with a digital camera using two sets of filters to detect vector control cells or LPP1 over-expressing cells.

2.4.7 *Preparation of conditioned media* - Fibroblasts were grown to confluency in DMEM containing 10% FBS and were incubated at 37^0C in 5% CO_2 on 100-mm dishes. To prepare conditioned media, the cells were washed three times with 5 ml of HBS. DMEM (3.5 ml) was added to each dish, which was then incubated for at least 18 h. This conditioned media was used for detecting gelatinase activity released by the cells, and for separating proteins in two dimensions described in Sections 2.7 and 2.9, respectively. To use conditioned media for migration assays 3.5 ml of DMEM with 0.4% fatty-acid free BSA supplemented with 0.4% charcoal-treated FBS was added to each dish for at least 18 h. All conditioned media was collected and centrifuged at 2500 rpm in a Beckman tabletop centrifuge TJ-6 for 20 min to remove detached cells and debris.

2.5 Detection of GTP bound G-proteins: Rho, Rac, and Cdc42

The relative concentrations of Rho-GTP were determined by affinity precipitation using mouse Rhotekin Rho binding domain (amino acids 7-89) fused to GST and bound to glutathione-agarose beads (Upstate, Charlottesville, VA). The assay was performed according to the manufacturer's directions. The relative concentrations of Rac-GTP and Cdc42-GTP were determined by using the GTPase binding domain of human p21-activated kinase 1 (PAK1, amino acids 67-150) fused to GST (a gift from Dr. G. Eitzen, University of Alberta) and bound to glutathione Sepharose 4B beads (GE Healthcare Life Sciences) following the procedure of Benard V. *et al* [225]. The affinity-precipitated proteins bound to the beads were then boiled in sample buffer and loaded on a 10% - SDS-PAGE gel where they were separated. The amounts of bound Rho, Rac and Cdc42 were then determined by Western blot analysis (Section 2.3.3) using mouse monoclonal

antibodies for Rho (Upstate) and Rac (Upstate) at 3 μg/ml and 1 to 2000 dilution, respectively, and polyclonal antibodies for Cdc42 (Santa Cruz) at 1 to 500 dilution. Goat anti-rabbit IgG conjugated to an IRDye800 and goat anti-mouse IgG conjugated to an Alexa Fluor 680 fluorescent markers were diluted 1 to 10 000 and incubated for 1 h at room temp. Fluorescence on the Western blots at 700 nm and 800 nm was scanned with the Odyssey Infrared Imaging System and quantified with Odyssey software. The results were normalized to the total amount of Rho, Rac, or Cdc42, from the same lysate that was used for the affinity precipitation.

2.6 Extracellular signal-regulated kinase activation

Extracellular signal-regulated kinase (ERK) is activated when specific threonine and tyrosine residues are phosphorylated by MEK [226, 227]. To determine the relative amount of activated ERK, 30 μg of protein was loaded on to a 7.5%-SDS-PAGE gel and subsequently separated as described in Section 2.3.3. The resolved proteins were transferred on to a nitrocellulose membrane, and were probed simultaneously with rabbit polyclonal anti-ERK1 (Santa Cruz) antibodies, and a mouse monoclonal antibody (both diluted 1 to 2000, Cell Signaling) that recognize the important phosphorylated threonine and tyrosine residues that cause activation of ERK1 and 2. Goat anti-rabbit IgG conjugated to an IRDye800 and goat anti-mouse IgG conjugated to an Alexa Fluor 680 fluorescent markers were diluted 1 to 10 000 and incubated for 1 h at room temp. Fluorescence on the Western blots at 700 nm and 800 nm was scanned with the Odyssey Infrared Imaging System and quantified with Odyssey software. The relative phosphorylation of ERK was expressed relative to total ERK.

2.7 Matrix metalloproteinase activity measured by zymography

To detect the gelatinase activities of matrix metalloproteinase (MMP) -2, and -9 by an in-gel assay, we analyzed samples from both conditioned media and lysates in non-reducing conditions in gels impregnated with gelatin. We used 3.5 µl of conditioned media collected as described in Section 2.4.7, or 10 µg of cell lysate protein both diluted to 10 µl with DMEM and MMP lysis buffer (120 mM Tris, pH8.7, 0.1% Triton X-100, 0.1% NaN_3, and 5% glycerol), respectively. Two µl of 6 X sample buffer (0.35 M Tris-HCl, pH 6.8, 3% glycerol, 1% SDS, 0.012% bromophenyl blue) was added to 10 µl of sample and loaded on to a 11% SDS-PAGE gel impregnated with 0.2% gelatin, w/v, from Sigma. The gels were developed using a Mini-Protean II protein electrophoresis apparatus. The gels were then washed 4 times with 2.5% Triton X-100, 15 min each wash, at room temperature with agitation. The gels were rinsed with MMP incubation buffer containing 50 mM Tris-HCl, pH 7.6, 150 mM NaCl, 5 mM $CaCl_2$, 0.05% NaN_3, and then 200 ml of MMP incubation buffer per gel at 37°C for 18 h with gentle agitation. The gels were then stained for 45 min with 0.25% Coomassie Brilliant Blue R250, w/v, dissolved in 40% methanol, 10% acetic acid. The gels were destained with 40% methanol, 10% acetic acid, until clear bands were seen in the blue background. The stained gels were scanned using the 700 nm channel of the Odyssey Infrared Imaging System that can detect Coomassie staining with high sensitivity. A control lane of conditioned media obtained from HT 1080 human fibrosarcoma cells treated with 100 nM PMA was run with the sample to identify the MMP isoform by the migration pattern on the gel.

2.8 Measurement of phosphatidate and diacylglycerol concentrations

2.8.1 *Phosphatidate mass assay* - Approximately 1 x 10^6 fibroblasts were plated on 100-mm dishes with DMEM containing 10% FBS for 48 h at 37°C in an atmosphere of 5% CO_2. The medium was replaced with DMEM containing 0.4% BSA and incubated at 37°C in 5% CO_2 for18 h to starve the cells. The starved cells were treated with various agonists or equivalent vehicle. The reaction was stopped by washing the cells three times with ice-cold HBS. The cells were collected by scrapping twice with 0.5 ml of ice-cold methanol. Chloroform (1 ml) was added to the combined methanol extracts followed by 0.9 ml of 1 M KCl containing 0.2M HCl, and the mixtures were vortexed and then centrifuged. The top layer was removed and 1.9 ml of synthetic top phase obtained by mixing chloroform/methanol/1 M KCl containing 0.2M HCl (1:1:0.9 by vol) was added to wash the organic bottom layer, and the mixtures were vortexed and then centrifuged. The top layer was removed and 0.9 ml of the bottom organic phase was collected to a new tube, where it was dried under N_2, and dissolved in 100 µl of chloroform/methanol (9:1). Twelve µl were immediately removed to measure total lipid-phosphate. Samples of the lipids were loaded in the middle of plastic-supported silica gel 60 thin layer chromatography plates (Merck). Plates were developed twice in chloroform/methanol/ammonium hydroxide (65:35:7.5, by vol), and the plates were cut 1 cm above the 1,2-diacyl-*sn*-glycero-3-phosphate standard (PA, Sigma). They were then turned upside down, and developed in the reverse direction with chloroform/methanol/acetic acid/acetone/water (50:10:12:20:5, by vol). The dried plates were then stained for 1h with 0.03% Coomassie Brilliant Blue R250 (BioRad) in 20%

methanol and containing 100 mM NaCl. The plates were destained in 20% methanol for 15 min, and this was repeated until the background was low enough. The plates were scanned using the 700 nm channel of the Odyssey Infrared Imaging System where Coomassie stained lipids can be detected with high sensitivity. A standard curve of PA from 0.1 μg to 8 μg was run with each plate of samples to identify and quantify the mass of PA (Fig. 2.4).

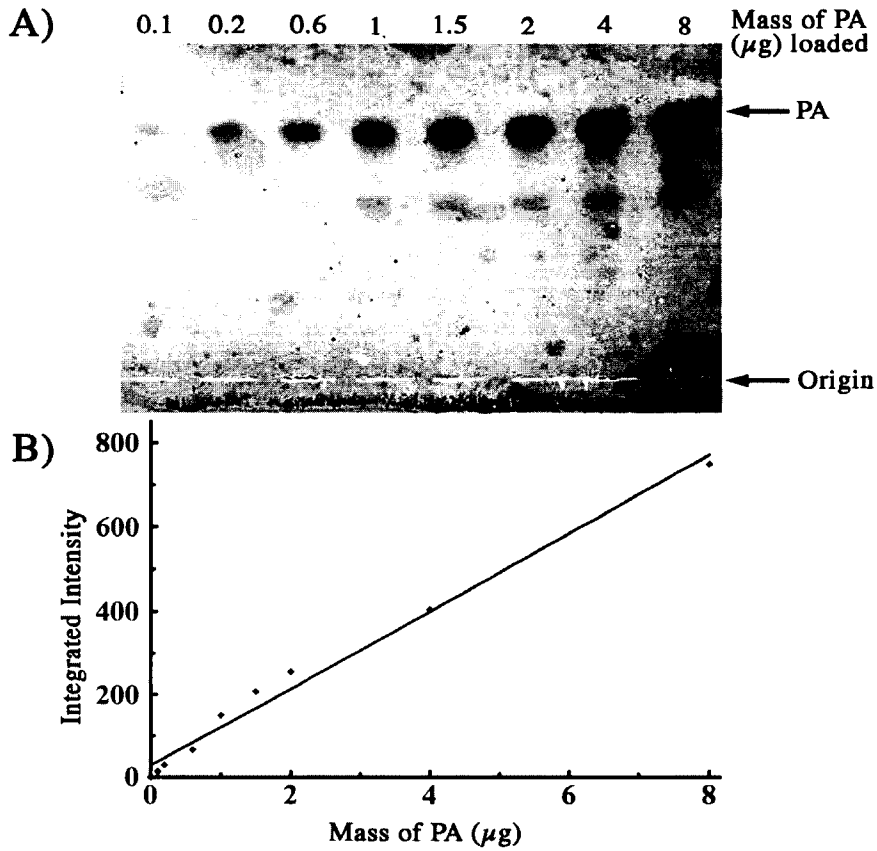

Figure 2.4 Standard curve of PA mass. *Panel A* shows the PA standards on the Coomassie stained thin layer chromatography plate scanned by the Odyssey infrared imaging system. Quantification of the PA standards shows a linear correlation with mass (*Panel B*). The line of best fit is shown and the slope was used to quantify the mass of PA in a sample. The r^2 value for this line is 0.986, which confirms linearity. Integrated intensities are in arbitrary units

2.8.2 *Phosphate assay* - PA concentration was expressed as a percentage of total phospholipid. Total phospholipid is determined from the 12 µl of the chloroform-extracted sample of cells described above. The samples and a standard curve of 1-100 nmol of glycerol-3-phosphate in water were evaporated. Fifty µl of perchloric acid was added and the samples were heated to 180°C for 30 min. This step allows the acid to digest the organic phosphate to inorganic phosphate. After cooling to room temperature, 278 µl of water was added followed by 55 µl of 2.5% ammonium molybdate and 55 µl of fresh 10% ascorbic acid. The samples were then placed in a 90°C water bath for 15 min. A portion (180 µl) of this mixture was added to duplicate wells of a 96 well plate and absorbance was measured using an Easy Reader EAR 340 AT (SLT-Labinstruments, Austria) set at 700 nm.

2.8.3 *Diacylglycerol mass assay* - Lipids were extracted from the cultured cells as described in Section 2.8.1 and lipid phosphate was measured (Section 2.8.2). Thirty nmol of total phospholipid was dried under N_2 for use in the DAG mass assay. DAG kinase reaction mixture containing 50 mM imidazole, 1 mM diethylenetriaminepentaacetic acid, 50 mM NaCl, 12.5 mM $MgCl_2$, 1 mM EGTA, 10 mM DTT, 1 mM ATP, 1.5% N-octyl-β-D-glucopyranoside, 1 mM cardiolipin, cold 1 mM ATP and 2 µg of recombinant DAG kinase (equivalent to 4 mU from Biomol) was incubated for 20 min at 37°C. This procedure phosphorylated contaminants in the reaction mixture before the addition of 1 µCi/assay of [γ-^{32}P]ATP at 10 Ci/mol (GE Healthcare Life Sciences). One hundred µl of this incubation mixture was then added to the dried down samples and standards of *sn*-1,2-dioleoylglycerol, DAG, (range of 100-1000 pmol DAG for standard curve, Avanti Polar Lipids).

Samples were vortexed before placing the tubes in a 37°C water bath for 5 min. The tubes were then moved to sonicating water bath (Brounsonic 1200) for 10 min. The tubes were moved back to the 37°C water bath for 5 min and returned to the sonicating water bath for 5 min, and finally back at 37°C for 20 min. One ml of methanol was added to stop the reaction followed by 1 ml chloroform, and 0.8 ml of 2 M KCl and 0.2 M H_3PO_4. This mixture was vigorously vortexed and then centrifuged to separate the phases. The top phase was aspirated and the bottom phase was washed twice with synthetic phase with vortexing and centrifugation between each wash. A sample of the bottom phase (0.8 ml) was dried under N_2 and dissolved in 100 µl of chloroform/methanol (9:1). Fifty µl was loaded on to glass-supported silica gel 60 thin layer chromatography plates and the plate was developed with chloroform/methanol/ammonium hydroxide (65:35:7.5, by vol.). The plates were dried and then developed with chloroform/methanol/acetic acid/acetone/water (50:10:10:20:5, by vol). The dried plates were then subjected to audioradiography for at least 6 h to overnight using Kodak Biomax film. The PA, produced from the DAG by DAG kinase, was identified by a PA standard (1,2-diacyl-*sn*-glycero-3-phosphate) and detected by I_2 staining. Bands were scraped and ^{32}P-labeling was measured by liquid scintillation counting (Fig. 2.5).

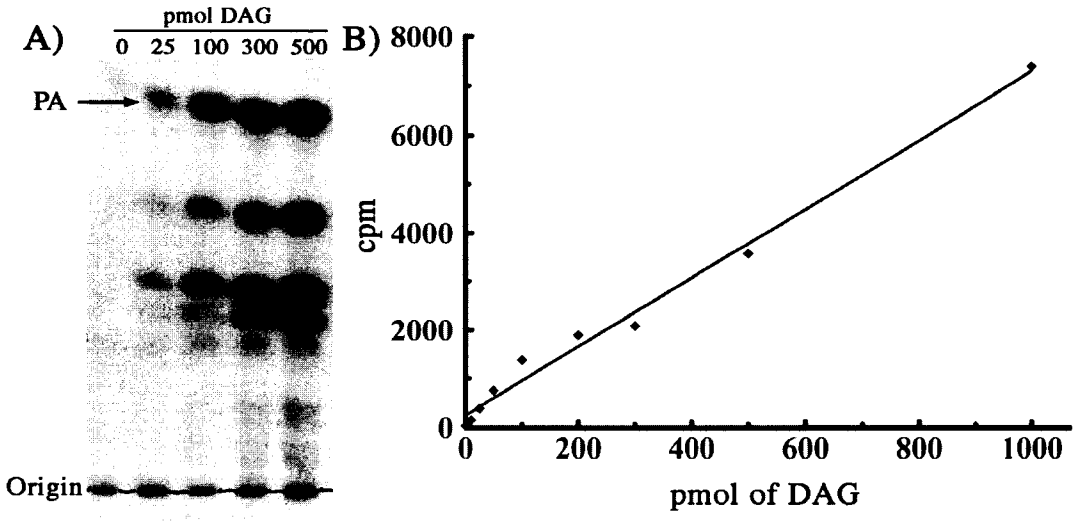

Figure 2.5 Standard curve for the DAG kinase assay. *Panel A* shows an autoradiograph of ^{32}P-labeled PA produced by the combination of DAG standards at the indicated amounts, [γ-^{32}P]ATP, and recombinant DAG kinase. *Panel B* shows the linearity (r^2=0.989) of the DAG kinase assay. This slope of the line of best fit (*shown*) was used to calculate the amount of DAG in a sample. The graph shows the combined data from one experiment that had points developed on more than one thin layer chromatography plate. *Panel A* is an example of one of the plates.

2.8.4 *Radiolabeling of phosphatidate and diacylglycerol* - PA concentrations can also be determined by labeling the fibroblasts with 57 Ci/mmol [9,10-^{3}H]palmitate. To do this 350,000 Rat2 fibroblasts, and fibroblasts over-expressing LPP1 or empty vector were plated on 10 cm dishes with DMEM containing 10% FBS. After 48 h the medium was changed to DMEM that contained 0.4% BSA and 20 μCi of 57 Ci/mmol [9,10-^{3}H]palmitate. The cells were incubated 18 h when the media was removed and unlabeled DMEM containing 0.4% BSA was added to the cells for 2 h more. The cells were then treated with agonists for 30 min, and the reactions were stopped by washing twice with ice-cold HEPES buffered saline. The harvesting and extraction of lipids into the organic phase is described in Section 2.3.8. After the organic phase was dried under N_2 and dissolved in 100 μl of chloroform/methanol (9:1), 50 μl samples were loaded in the

middle of plastic-backed silica gel 60 thin layer chromatography plates to resolve PA as described in Section 2.8.1 The PA and phosphatidylcholine (PC) bands on the plates were identified by comparison with standards (PA, 1,2-diacyl-*sn*-glycero-3-phosphate, and PC, 1,2-diacyl-*sn*-glycero-3-phosphorylcholine, Sigma) and ^{3}H-labeling was measured by scintillation counting. PA concentrations were expressed relative to the labeling in PC.

The other half of the recovered total lipids were loaded 2 cm from the bottom of glass-supported silica gel 60 thin layer chromatography plates, and the plates were developed in hexane/diethyl ether/acetic acid (60:40:1, by vol.). The bands containing *sn*-1,2-DAG and *sn*-1,3DAG were identified by comparison with DAG standards and ^{3}H-labeling was measured by scintillation counting. DAG concentrations were expressed relative to the labeling of lipids remaining at the origin where phospholipids are found.

2.9 Two-Dimensional electrophoresis

Three volumes of ice-cold acetone were added to precipitate 1 mg of cell lysate at -20°C for 2 h. The proteins were pelleted by centrifugation and the pellet was washed three times with acetone at -20°C. Residual acetone was removed by air-drying. The pellet was dissolved in rehydration buffer containing 7 M urea, 2 M thiourea, 40 mM DTT, 4% CHAPS, 0.004% bromophenol blue, 0.1 μM mycrocystin LR (a gift from Dr. C. Holmes, University of Alberta) as protein phosphatase inhibitor, and 0.2% carrier Bio-Lyte ampholyte for immobilized pH gradient (IPG, Bio-Rad) gels of pH range 3-10.

One hundred μl samples of conditioned media proteins that had been concentrated 10-fold using 10,000 Dalton cut-off, Millipore filters were also analyzed by 2-dimensional electrophoresis. These samples were washed with PlusOne 2-D clean-up

kit (GE Healthcare Life Sciences) according to manufacturer's instructions. This step quantitatively precipitates proteins while interfering contaminants in the concentrated conditioned media such as salts, lipids, and nucleic acids remain in solution and were subsequently washed from the pellet, thus improving the quality of the 2-D electrophoresis results. The pellet was dissolved with 8 M urea, 2% CHAPS, 50 mM DTT, 0.2% Bio-Lyte 3/10 ampholyte, and 0.001% Bromophenol Blue.

The protein mixture was centrifuged to remove any undissolved material, and 185 µl samples were loaded on a rehydration tray. An 11-cm ReadyStrip™ IPG strip of pH range of 3-10 (Bio-Rad) was allowed to passively rehydrate overnight at room temperature with mineral oil covering the rehydrating sample. The IPG strip was placed face down on an isoelectric focusing tray with the acidic end of the strip on the positive electrode. The IEF tray was positioned in the Bio-Rad PROTEAN IEF, and the strips were exposed for 35,000-volt hours with rapid ramping. To solubilize focused proteins with SDS for the second dimension we equilibrated the focused IPG strips in equilibration base buffer consisting of 6 M urea, 2% SDS, 50 mM of Tris-HCl, pH 8.8, 20% glycerol, first with 2% DTT present, and then with the same equilibration base buffer with 2.5% iodoacetamide for 10 min each. The strips were rinsed in SDS-PAGE Laemili running buffer and placed in Criterion™ 4-20% gradient SDS precast gels (Bio-Rad), and embedded in 0.5% agarose. The gels were developed in a Criterion Dodeca™ (Bio-Rad) electrophoresis apparatus at 200 mV until the lowest of the Bio-Rad broad range markers was approximately 0.5 cm from the bottom. The gels were stained with Bio-Safe™ Colloidal Coomassie Blue G-250 stain (Bio-Rad) and destained with ionized

water until desired contrast is achieved. Proteins in gels can also be transferred to nitrocellulose membranes as described in Section 2.3.3.

The stained gels were scanned with an Image Scanner (GE Healthcare Life Sciences) and protein spots were identified and compared between gels using Image Master 2D, version 2002.01 software (GE Healthcare Life Sciences). Selected spots were sent to the Institute for Biomolecular Design for identification of trypsin-digested peptides by a MALDI-ToF (Applied Biosystems) mass spectrometer.

2.10 Statistical analysis

Results were presented as representative experiments, or as mean ± SD from at least 3 independent experiments. Statistical differences were calculated by ANOVA followed by a Newman-Keuls post-hoc test. Paired T-tests were also performed between two samples. Statistical analyses and graphing were performed using GraphPad 4 software (Prism).

CHAPTER 3

EXPRESSION AND CHARACTERIZATION OF LIPID PHOSPHATE PHOSPHATASE-1 IN RAT2 FIBROBLASTS AND COS7 CELLS

A version of this chapter has been published. Pilquil, C., Dewald, J., Cherney, A., Gorshkova, I., Tigyi, G., English, D., Natarajan, V., Brindley, D. N. 2006. J Biol. Chem. 281: 38418-29.

3.1 Introduction

Fibroblasts are one of the key cell types involved in wound healing. When tissue is injured they migrate to the wound and reestablish the extracellular matrix. Their ability to thrive in the face of injury probably makes them one of the easiest mammalian cells to grow in culture. It is this physiological significance that makes fibroblasts an ideal tool for studies in migration under a controlled cell culture environment. In this thesis Rat2 fibroblasts were used to modify the expression of lipid phosphate phosphatase-1 (LPP1), and to examine this effect on migration. Rat2 fibroblasts express relatively high endogenous LPP activity compared to Cos7, and endothelial cells. Additionally all three LPP isoforms are expressed in Rat2 fibroblasts making them physiologically relevant to characterize LPP1's role in migration. Signaling in Rat2 fibroblasts involving lysophosphatidate (LPA), phosphatidate (PA), sphingosine 1-phosphate (S1P), sphingosine, ceramides, platelet-derived growth factor (PDGF), and tumor necrosis factor-α (TNF-α) has also been well characterized.

To distinguish the role of LPP1 in migration, Rat2 fibroblasts were transduced with cDNA of mouse LPP1 using a retroviral expression system. This system allowed us to select a population of fibroblasts that stably over-express LPP1. To avoid the risk of compensatory mutants, or artifacts that clones could have, a mixed population was maintained. To avoid any cell drift, or damage that can come with older populations the number of times a population of fibroblasts were detached and re-plated for experiments never exceeded 25. Rat2 fibroblasts transduced with empty vector were also selected and used as an additional control to wild-type Rat2 fibroblasts. Wild-type LPP1, two catalytically inactive LPP1 mutants, and an LPP1 that cannot be glycosylated were all

tagged with green fluorescent protein (GFP) on the C-termini, and were also stably expressed in Rat2 fibroblasts using the same retroviral expression system. The GFP tag was useful because there was not an antibody available that could efficiently immunoprecipitate LPP1.

To complement the studies using stable over-expression, immortalized fibroblasts from transgenic mice with 2-, 8-, and 20-gene copies of mouse *Lpp1* were used. In addition an adenovirus transfection system was used to transiently over-express c-myc tagged mouse LPP1 with high transfection efficiency. A conservative point mutation of an arginine residue to a lysine residue at position 217 rendered LPP1-myc catalytically inactive, and this was also over-expressed using adenovirus. The over-expression of this catalytically inactive LPP1 allowed us to distinguish between catalytic and possible non-catalytic functions of LPP1.

The knockdown of endogenous rat LPP1 expression with siRNA was used as an opposite complement to over-expression of mouse LPP1. This was a powerful tool to directly evaluate the endogenous function of LPP1 in fibroblasts.

Cos7 cells were an additional mammalian cell line used because they are relatively easy to transfect with plasmid DNA, and their large size, and flat morphology on cover slips make them an ideal cell to analyze expression using indirect immunofluorescence microscopy. Expression and localization of various constructs of c-myc, and GFP tagged LPP1 were evaluated, including mutants that result in catalytically inactive LPP1 and mutants that do not affect activity.

The expression systems above were primarily tested for total LPP activity in whole lysates or immunoprecipitates using a ^{3}H-labeled PA in Triton X-100 micelles.

The dephosphorylation of exogenous ^{32}P-labeled LPA was used to evaluate ecto-activity of LPP1. Western blot analysis using rabbit polyclonal antibodies raised against a C-terminal peptide from mouse LPP1, and antibodies against the c-myc, and GFP tags fused to LPP1 determined relative expression levels of LPP1. These methods established and characterized LPP1 for use in further studies on migration.

3.2 Lipid phosphate phosphatase-1 activity and expression in fibroblasts

3.2.1 *Stable over-expression of lipid phosphate phosphatase-1 in Rat2 fibroblasts* - RNA was collected from wild-type Rat2 fibroblasts and Rat2 fibroblasts stably over-expressing mouse LPP1. Real-time RT-PCR was performed to determine the levels of LPP1 mRNA in the fibroblasts. The LPP1 primers used for the real time RT-PCR were designed to recognize mouse, rat, and human orthologs of LPP1 cDNA, therefore, the sum of endogenous rat LPP1 and induced mouse LPP1 mRNA levels were measured. There was a 20-fold over-expression of total LPP1 mRNA (Fig. 3.1A).

To confirm that LPP1 was over-expressed in Rat2 fibroblasts, Western blot analysis was performed on membrane fractions. The proteins were loaded and resolved on a SDS-PAGE gel, and transferred to membranes that were blotted with polyclonal antibodies against a C-terminal sequence of mouse LPP1. Multiple protein bands between 34-36 kDa from cells over-expressing LPP1 were detected (Fig 3.1B). Western blot analysis using a monoclonal antibody against GFP detected LPP1 fused to a GFP tag (LPP1-GFP) that was stably transduced in Rat2 fibroblasts (Fig 3.1C). It also showed multiple bands, but with the fused GFP, which alone measures at 27 kDa, the LPP1 bands measured between 64 and 66 kDa.

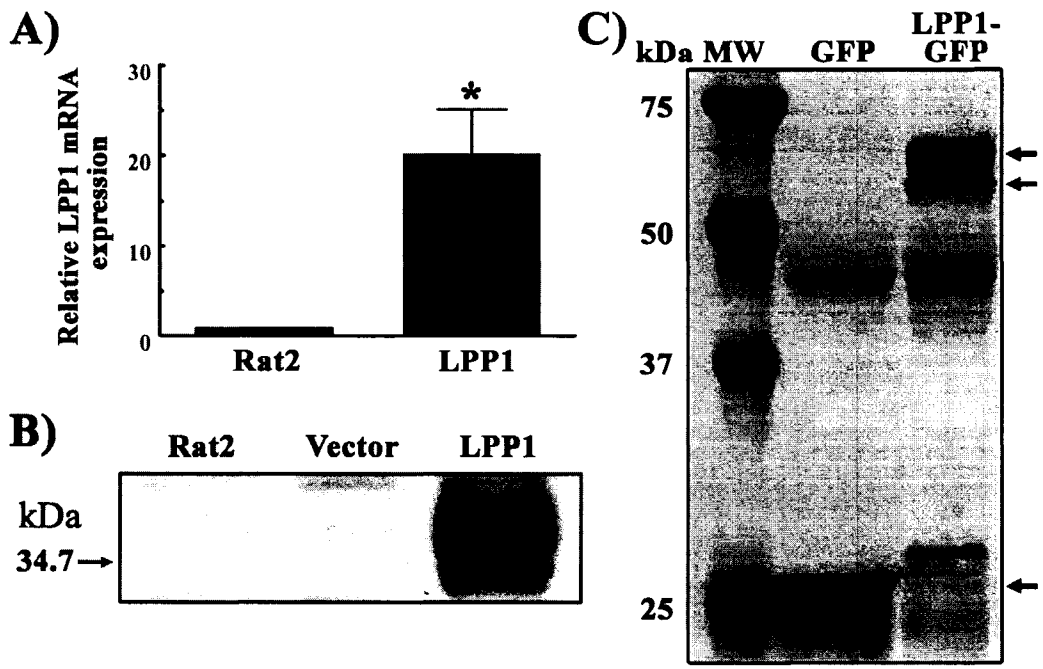

Figure 3.1 Stable over-expression of mouse LPP1 in Rat2 fibroblasts. *Panel A* shows relative LPP1 mRNA levels in Rat2 fibroblasts stably over-expressing *LPP1* compared to wild-type fibroblasts (*Rat2*). Results are mean ± SD from three independent experiments. Significant difference ($p<0.05$) between LPP1 over-expressing fibroblasts and wild-type fibroblasts is indicated by *. *Panel B* shows the Western blot of LPP1 using rabbit anti-mouse LPP1 as the primary antibody. 190 µg of membrane-protein was resolved on a 10% SDS-PAGE gel. The lane labeled *LPP1*, is from Rat2 fibroblasts stably transduced with mouse LPP1 cDNA, and are compared to the controls: *Rat2* are wild-type fibroblasts, and *Vector* are fibroblasts transduced with empty vector. The *arrow* is pointing at the position of a 34.7 kDa molecular weight marker. In *Panel C*, 500 µg of protein was immunoprecipitated using rabbit anti-GFP and subsequently resolved on a 4-16% gradient SDS-PAGE gel. Western blot of GFP alone and LPP1 tagged with GFP was performed using mouse anti-GFP as the primary antibody. The *arrows* point to the band representing GFP (27 kDa) in the lane labeled *GFP*, and to the multiple bands of LPP1-GFP (64 -66 kDa) in the lane labeled *LPP1-GFP*. *Panels B* and *C* are representatives of at least three separate experiments.

To measure the total LPP activity in Rat2 fibroblasts stably transduced with LPP1 and LPP1-GFP, the cells were solubilized in lysis buffer containing Triton X-100. The lysates were combined with ^{3}H-labeled phosphatidate (PA) dispersed in Triton X-100 micelles in the presence of N-ethylmaleimide. This assay measures the sum of all LPP activity. LPP1 over-expressing fibroblasts showed an approximately 4-fold increase in total LPP activity compared with wild-type, or vector control cells (Fig. 3.2A).

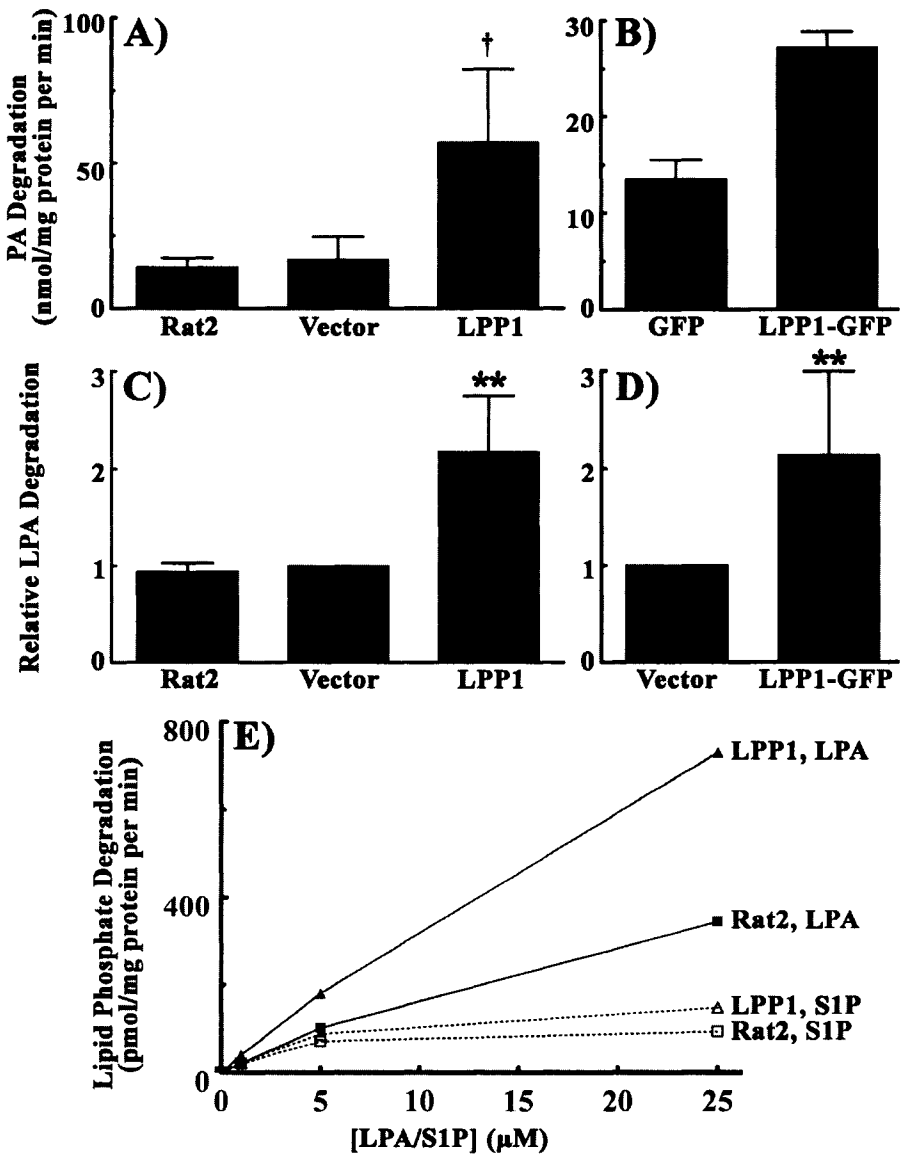

Figure 3.2 Catalytic activity of LPP1 stably over-expressed in Rat2 fibroblasts. *Panels A* and *B* show total LPP activity of PA degradation in Triton X-100 micelles by lysates from wild-type Rat2 fibroblasts (*Rat2*) or those stably transduced with the empty vector (*Vector*), *LPP1*, *GFP* alone or LPP1 tagged with GFP (*LPP1-GFP*). *Panel A* shows means ± S.D. from at least 9 independent experiments and *Panel B* shows means and ranges from two independent experiments. *Panels C*, and *D* shows the relative ecto-activity of LPP on a monolayer of intact fibroblasts in the presence of 0.4% BSA, 10 μM LPA, and 0.1% BSA, 50 μM LPA, respectively. The mean ecto-activities of the vector control cells were 155 and 200 pmol LPA dephosphorylated/min per mg of cell protein in *Panels C* and *D*, respectively. In *Panel C* results for Rat2 control cells are mean and range from 2 experiments and means ± S.D. for LPP1 over-expressing cells from at least 6 independent experiments. In *Panel D* results are means ± S.D. for LPP1-GFP over-expressing cells from at least 7 independent experiments. *Panel E* shows the dephosphorylation of exogenous LPA (*closed symbols*) and S1P (*opened symbols*) in the presence of 0.4% BSA by intact monolayers of wild-type Rat2 cells (*squares*) and cells over-expressing LPP1 (*triangles*). Results are from one representative of two experiments. Significant differences between LPP1 over-expressing fibroblasts and wild-type, or vector control fibroblasts are indicated by: †, $p<0.001$; **, $p<0.01$.

Over-expression of LPP1-GFP had a 2-fold increase over the GFP expressing control, demonstrating that the fusion protein retained catalytic activity (Fig. 3.2B).

The extracellular dephosphorylation of LPA was measured, and cells stably over-expressing LPP1 or LPP1-GFP, had a 2-fold increase of LPA dephosphorylation compared to controls (Fig. 3.2C and D).

3.2.2 *The dephosphorylation of external sphingosine-1-phosphate by fibroblasts over-expressing lipid phosphate phosphatase-1* – Since sphingosine-1-phosphate (S1P) can be found outside of cells, it could be a physiological substrate for the ecto-activity of LPP1. The extracellular hydrolysis of S1P was measured on an intact monolayer of fibroblasts that stably over-expressed LPP1. At all three concentration points there was not an increase of S1P dephosphorylation like there was for LPA (Fig. 3.2E), which had a 2-fold increase of dephosphorylation compared to controls. These results suggest that LPP1 ecto-activity has a specific preference for exogenous LPA over S1P, and that LPP1 could have a role for cell signaling by extracellular LPA, but less so for S1P.

3.2.3 *N-glycosylation of lipid phosphate phosphatase-1* – Figure 3.1B and C shows a Western blot of LPP1 as multiple bands. This suggests that LPP1 could be glycosylated. We tested this by incubating a membrane fraction from Rat2 fibroblasts stably over-expressing LPP1 with recombinant N-glycosidase F; an enzyme that cleaves asparagine bound N-glycans. The mixture was then analyzed by Western blot. In the presence of N-glycosidase F, the diffuse band of LPP1 shifted from about 35 kDa to 32 kDa, and became a more concentrated single band (Fig.3.3A above). The lower molecular weight of 32 kDa, was predicted from the cDNA sequence for mouse LPP1. Next, the putative glycosylation site was mutated by an amino acid substitution of

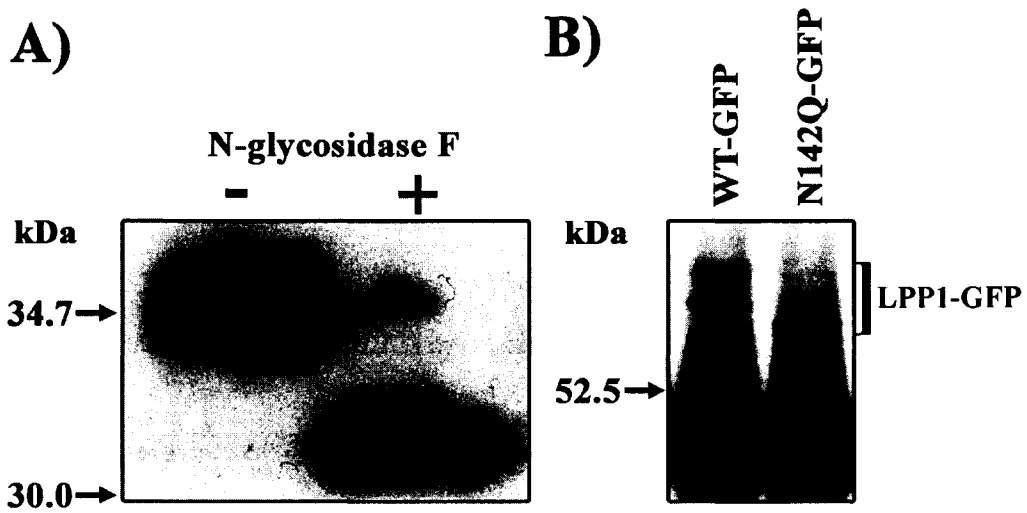

Figure 3.3 The N-glycosylation of LPP1. In *Panel A*, 500 μg of membrane-proteins from Rat2 fibroblasts stably producing mouse LPP1 were treated with *N-glycosidase F* as indicated and then analyzed by Western blotting using rabbit anti-mouse LPP1 as a primary antibody. In *Panel B* cell lysates of Rat2 fibroblasts stably producing wild-type LPP1 tagged with GFP (lane labeled *WT-GFP*) or LPP1-GFP with a point mutation at the putative site of glycosylation (lane labeled *N142Q-GFP*) were immunoprecipitated with rabbit anti-GFP and analyzed by Western blotting with the same antibody. The large over-exposed bands are from IgG. *Arrows* indicate the position of molecular weight markers that are labeled and are in units of kDa.

asparagine to glutamine at position 142 on mouse LPP1-GFP, and was analyzed by Western blot (Fig. 3.3B). This decreased the molecular weight of LPP1-GFP to about 62 kDa. Wild-type LPP1-GFP measured between 64 and 66 kDa. There was also one band present instead of the multiple bands of wild-type LPP1-GFP. Dr. Qiu-Xia Zhang from our group established that glycosylation is not required for catalytic activity [148].

3.2.4 *Biotinylation of cell surface lipid phosphate phosphatase-1 tagged with green fluorescent protein* - Increased exogenous hydrolysis of LPA by Rat2 fibroblasts over-expressing LPP1, and the N-glycosylation of LPP1 suggests that it is expressed at the cell surface. To determine if LPP1 is exposed at the cell surface EZ-Link Sulfo-N-hydroxysuccinimide (NHS)-LC-Biotin (Pierce) was used as a cell impermeable labeling agent to biotinylate exposed proteins on intact Rat2 fibroblasts over-expressing LPP1-GFP, or control cells transduced to express GFP alone. After biotin labeling, cell

membranes were collected, solubilized, and then immunoprecipitated using polyclonal anti-GFP. Proteins were resolved on SDS-PAGE, and then were transferred onto nitrocellulose membranes. They were probed with monoclonal anti-GFP followed by the secondary antibody, anti mouse-IgG conjugated to Alexa 680 to identify GFP. To identify biotin labeling the membrane was also incubated with streptavidin conjugated to IRDye 800. Analysis of the images scanned from the membranes using the Odyssey Infrared Imaging System, showed that LPP1-GFP was biotinylated and that cytosolic GFP was not (Fig. 3.4A). LPP1-GFP was exposed at the cell surface since the biotinylation reagent is cell impermeable, and labeling was performed on ice to stop any cycling of cellular membranes. It was also clear that the higher molecular weight band of LPP1-GFP of 66 kDa, was solely labeled with biotin (Fig. 3.4A and B). The lower molecular weight band of LPP1-GFP of 64 kDa, represents the population of LPP1-GFP that was not exposed to biotinylation. This LPP1-GFP population was probably not fully glycosylated and has not yet reached the cell surface, however, there is some post-translational modification as the molecular weight is larger than that of the non-glycosylated LPP1-GFP (Fig. 3.3B).

Rat2 fibroblasts stably expressing LPP1-GFP constructs with point mutations that inactivate LPP1-GFP were also evaluated for biotinylation. The catalytically inactive mouse LPP1-GFP constructs with Arg^{127} to Lys, and Arg^{217} to Lys amino acid substitution (R127K and R217K, respectively) were both biotinylated indicating cell surface exposure was not limited to active LPP1-GFP in Rat2 fibroblasts (Fig. 3.4C). Again, the higher molecular weight bands of the inactive LPP1-GFP are biotinylated, whereas the lower molecular weight bands are not (Fig. 3.4C).

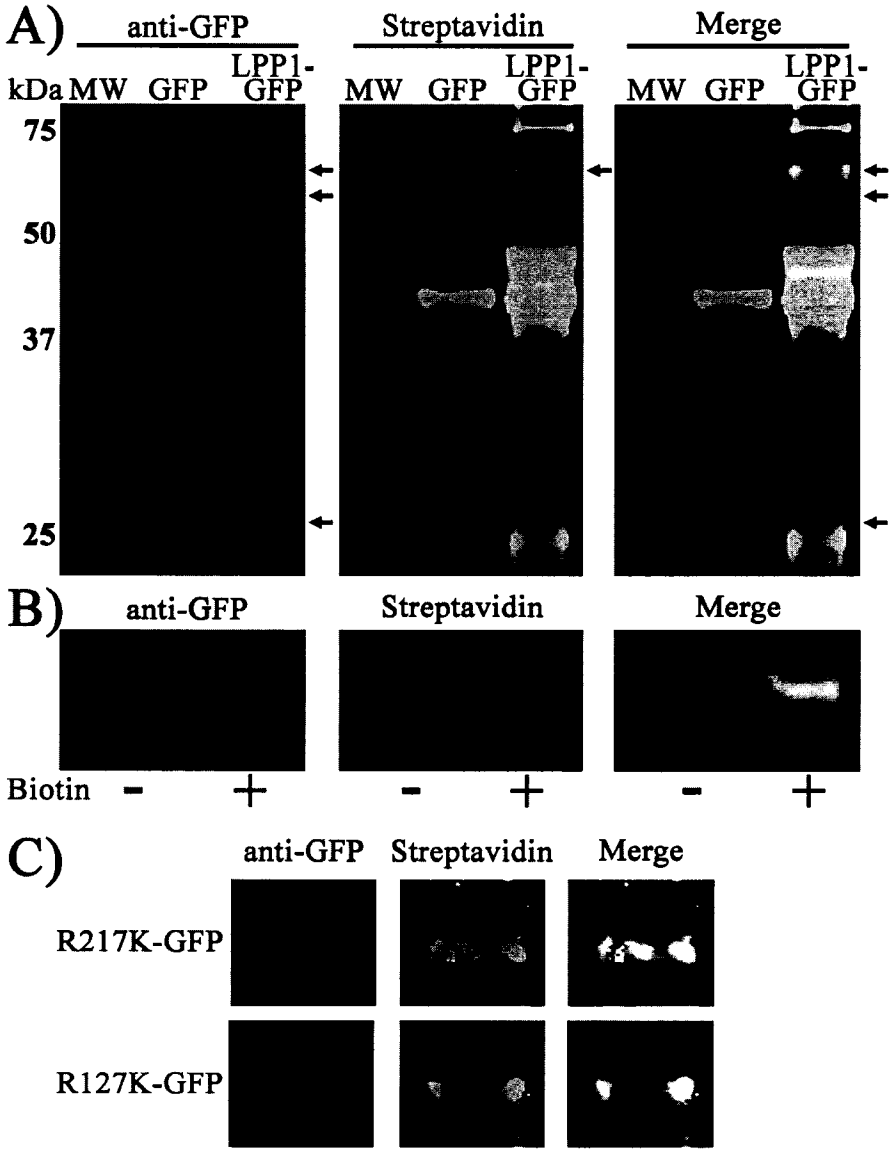

Figure 3.4 Biotinylation of cell surface LPP1 tagged with GFP. Intact monolayers of various stably transfected Rat2 cell lines were exposed to a cell impermeable biotinylation reagent, and their lysates were then immunoprecipitated with rabbit anti-GFP and analyzed by Western blotting with mouse anti-GFP and Alexa 680-labeled anti-mouse IgG secondary antibody. The membrane was also probed with streptadvidin conjugated to IRDye800. The membrane was scanned with the Odyssey Infared Imaging System to detect emission from the 700 nm (*anti-GFP - in red*) and 800 nm channel (*streptavidin - in green*). *Panel A* shows the biotinylation of wild-type LPP1 tagged with GFP (lane labeled *LPP1-GFP*), whereas, cytosolic GFP (lane labeled *GFP*) is not biotinylated. The *bottom arrow* indicates the position of the GFP band, and the *top two arrows* point to LPP1-GFP that *Panel B* shows more closely (from another experiment). *Panel B* also shows that the higher molecular weight band is predominately biotinylated and that streptavidin staining of wild-type LPP1-GFP is dependent on the addition of the cell impermeable biotinylation reagent. *Panels A* and *B* are representatives from three independent experiments. *Panel C* shows that catalytically inactive mutants of LPP1-GFP (*R217K-GFP* and *R127K-GFP*) stably produced in Rat2 fibroblasts are also expressed on the plasma membrane. This experiment was done once. The anti-GFP Western blot in *Panel A* also appears in *Figure 3.1C*.

3.2.5 *Rat2 fibroblasts infected with adenovirus to transiently over-express wild-type or a catalytically inactive mutant of lipid phosphate phosphatase-1* – Rat2 fibroblasts were infected with adenoviral vectors containing LPP1-myc, the inactive LPP1[R217K]-myc or an empty vector at 40 multiplicity of infection (MOI) for 24 h. Lysates from the fibroblasts infected with adenoviral vector containing wild-type LPP1 had a 4.8-fold increase of total LPP activity over the vector controls. There was no significant change in LPP activity of the cells expressing the inactive mutant of LPP1 (Fig. 3.5A).

Ecto-activity of the adenoviral-infected fibroblasts was also measured. Fibroblasts infected with adenoviral vectors containing LPP1-myc had an increase of external LPA dephosphorylation of 2.3-, and 3.8-fold over vector controls using 25 MOI and 40 MOI, respectively, and no change for cells expressing the inactive mutant of LPP1 (Fig. 3.5B). This demonstrates dose dependence of adenovirus transfection. The total LPP and LPP ecto-activity results confirm that the LPP1[R217K]-myc mutant was catalytically inactive, but that it did not have a dominant/negative effect. These results also demonstrate that the C-terminal c-myc tag on LPP1 does not abolish activity.

As a control, Western blotting confirmed that the inactive LPP1 mutant was expressed to similar levels compared to active LPP1 (Fig. 3.5C). Multiple bands were also apparent in both versions of the LPP1, indicating similar post-translational processing. Indirect immunofluorescence of adenovirus infected cells expressing c-myc-tagged wild-type LPP1 and the inactive mutant, showed that both versions of the LPP1

were expressed at the plasma membrane, and between the two, intracellular staining was similar (Fig. 3.5 D and E).

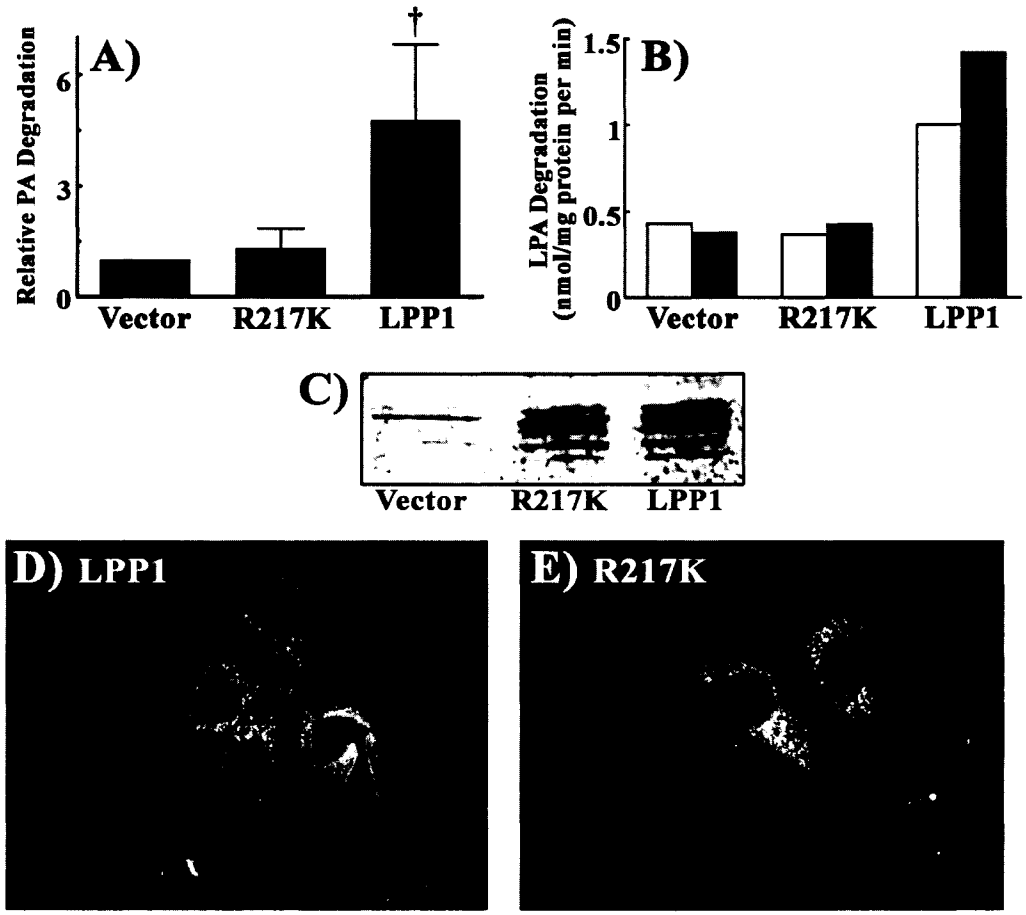

Figure 3.5 Infection of Rat2 fibroblasts with adenovirus. *Panel A* shows total LPP activities from lysates of Rat2 fibroblasts infected with adenovirus at 40 MOI, to express wild-type myc-tagged LPP1 (*LPP1*) and an inactive myc-tagged mutant form of LPP1 (*R217K*). The mean total LPP activity of vector control cells was 16.3 nmol of PA degraded/mg of protein per min. Results are means ± S.D. of five experiments. Significant differences ($p<0.001$) from vector controls are indicated by †. *Panel B* shows the dephosphorylation of exogenous LPA by ecto-LPP activity in the presence of 50 μM LPA and 0.4% BSA. Rat2 fibroblasts were infected with adenovirus with 25 MOI (*white bars*) or 40 MOI (*black bars*). This is a representative from two experiments. *Panel C* is a Western blot analysis of protein from Rat2 fibroblasts infected by adenovirus as in *Panel A*, using rabbit anti-mouse LPP1. This is a representative from three experiments. *Panels D* (wild-type LPP1 tagged with c-myc) and *E* (inactive LPP1 tagged with c-myc) show conventional indirect immunofluorescence of Rat2 fibroblasts infected with adenovirus as in *Panel A*. Myc-tagged LPP1s were detected using mouse monoclonal anti-myc, 9E10, and rhodamine-labeled donkey anti-mouse IgG. This experiment was performed once.

3.2.6 *Fibroblasts from transgenic mice over-expressing lipid phosphate phosphatase-1* – The expression and activity of LPP1 were also measured in immortalized fibroblasts from tails of wild-type and transgenic newborn pups described by Yue J. *et al.* [185]. Western blot analysis using polyclonal antibodies against mouse LPP1 shows multiple bands at about molecular weight of 36 kDa (Fig. 3.6A). There was also an increase in LPP1 protein expression (Fig. 3.6A), which correlated with the gene copy numbers, and mRNA levels determined by Yue J. *et al* [185].

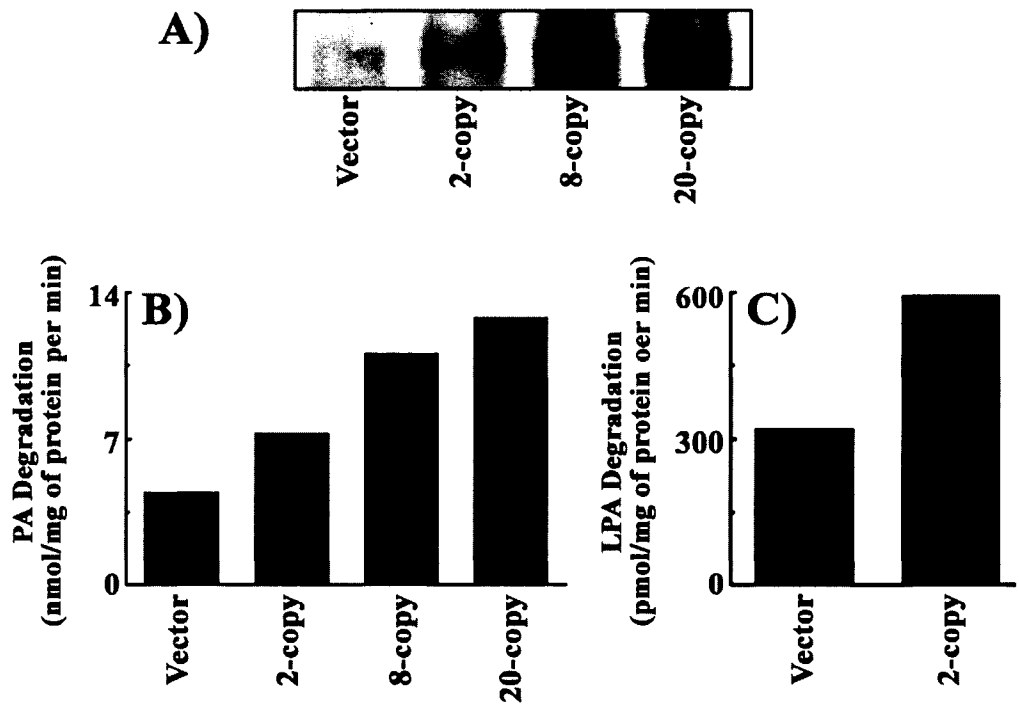

Figure 3.6 Expression of LPP1 in fibroblasts from transgenic mice. *Panel A* shows mouse LPP1 expression levels from membrane proteins of immortalized fibroblasts from vector control transgenic mice and transgenic mice with approximately 2-, 8-, and 20-gene-copies of mouse *Lpp1*. Mouse LPP1 protein was blotted using rabbit anti-mouse LPP1 antibodies. The Western blot is a representative of three experiments. *Panels B* and *C* show total LPP and ecto-LPP activities, respectively, of the fibroblasts of transgenic mice. Experiments were done once to confirm the results of Yue J. et al of which I am a co-author [185].

Total LPP activity in the lysates of fibroblasts derived from the transgenic mice were 1.6-, 2.5-, and 2.9-fold higher than the wild-type control in the cell lines with 2, 8, and 20 gene copies of mouse *Lpp1*, respectively (Fig. 3.6B).

Dephosphorylation of exogenous LPA in the cell line with 2 gene copies of LPP1 was 1.9-fold higher than the wild-type control (Fig. 3.6C). These experiments were done once to confirm the results of Yue J. *et al* of which I am a co-author [185].

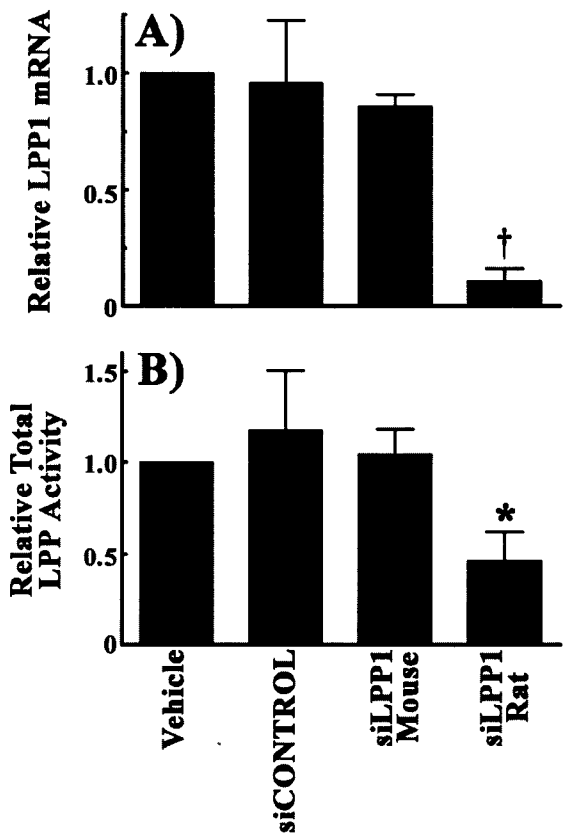

Figure 3.7 Knockdown of rat LPP1 using siRNA. Wild-type Rat2 fibroblasts were treated with transfection vehicle (*Vehicle*), non-targeting functional control siRNA (*siCONTROL*), siRNAs for mouse LPP1 (*siLPP1 Mouse*), and siRNAs for rat LPP1 (*siLPP1 Rat*). *Panel A* shows the mRNA levels of LPP1 normalized to housekeeping gene, cyclophilin A. For *Panel B* total LPP activity was measured using PA mixed in Triton X-100 micelles and lysates of the transfected fibroblasts. LPP activity in the vehicle control was 16.6 nmol of phosphatidate dephosphorylated/min per mg of protein. Results are means ± S.D. from at least three experiments and mean and range for siLPP1 mouse in two experiments. Significant differences between LPP1 knockdown and control fibroblasts in *Panels A* and *B* are indicated by: †, $p<0.001$; *, $p<0.05$.

3.2.7 *Knockdown of endogenous lipid phosphate phosphatase-1 in Rat2 fibroblasts using small interfering RNA* – Endogenous LPP1 in Rat2 fibroblasts was knocked down using a mixture of four siRNAs to rat LPP1. Messenger RNA levels for rat LPP1 was decreased by about 90% compared to a treatment with control siRNA, siRNA specific for mouse LPP1, or transfection vehicle alone (Fig. 3.7A above). This was accompanied by a 50% decrease in total LPP activity (Fig 3.7B above).

3.3 Lipid phosphate phosphatase-1 activity and expression in Cos7 cells

3.3.1 *Immunoprecipitation of various lipid phosphate phosphatase-1 constructs tagged with green fluorescent protein or c-myc from transiently transfected Cos7 cells* – Immunoprecipitation of recombinant and tagged LPP1 from a lysate is useful to measure expression and catalytic activity without the contribution from other isoforms of LPP including endogenous LPP1. Cos7 cells were transiently transfected with 20 μg of pCMV5 vectors containing cDNA for various LPP1 constructs using the calcium phosphate transfection method. The pCMV5 vector contains a cytomegalovirus (CMV) promoter that gives high-level expression of the desired transcript. The constructs used produced wild-type LPP1 and catalytically inactive LPP1[R217K] both fused to c-myc and GFP. Other constructs that produce LPP1-GFP fusion proteins with conservative amino acid substitutions were also used. To locate the relative position of each mutated amino acid reference the amino acid sequence, and topology of mouse LPP1 in Figure 1.9A and B, respectively. After transfection with these various constructs, lysates were collected and the proteins were immunoprecipitated with anti-GFP or anti-c-myc. Western blot analysis of the immunoprecipitates showed the expression of the various LPP1 fusion proteins (Fig. 3.8). Immunoprecipitates were also used to measure PA

hydrolysis in Triton X-100 micelles. LPP1-GFP with amino acid substitutions of Tyr^{168} to Phe (Y168F) and Thr^{122} to Ser (T122S) had intact lipid phosphatase activities (Table 3.1). Amino acid substitutions at Gly^{170} to Ala (G170A) and Tyr^{221} to Trp (Y221W) produced LPP1-GFP that had activities but were decreased by 50% and 44%, respectively (Table 3.1). His^{171} to Leu (H171L) and Ser^{169} to Thr (S169T) amino acid substitutions abolished PA hydrolysis by LPP1-GFP. These results confirmed the activities of the various LPP1 fusion proteins established by Zhang *et al.* of which I am a co-author [148]. Myc-tagged wild-type LPP1 protein was expressed, and had abundant catalytic activity. Myc-tagged catalytically inactive LPP1[R217K] protein was highly expressed, but did not have any PA hydrolysis activity above control (Fig. 3.8B and Table 3.1). It was also apparent that inactive LPP1 was expressed at much higher levels than the wild-type LPP1, and that there was a higher degree of molecular weight variability that was not shown by wild-type LPP1 protein.

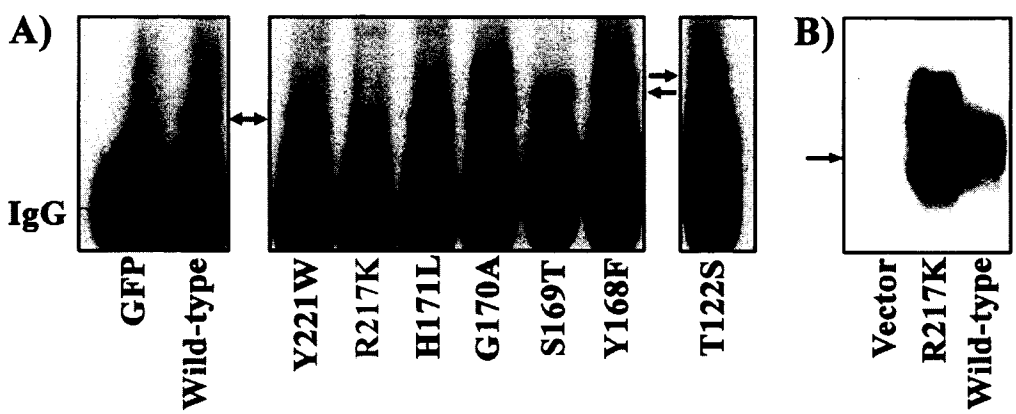

Figure 3.8 Western blot of various LPP1 constructs transiently expressed in Cos7 cells. Cos7 cells were transiently transfected with 20 μg of plasmid DNA to express GFP, wild-type or various mutants of LPP1 tagged with GFP (*Panel A*) or c-myc (*Panel B*). Lysates were collected and immunoprecipitated with rabbit polyclonal anti-GFP (*Panel A*) or mouse monoclonal anti-c-myc (*Panel B*) and analyzed by Western blotting using the same antibodies, respectively. *Panel A* shows selected lanes from the same Western blot. The *arrows* point to the bands representing LPP1-GFP at about 66 kDa. The large-lower band represents IgG. Only one experiment was performed. The *arrow* in *Panel B* shows the position of the 35 kDa molecular weight marker. *Panel B* is a representative of one experiment out of two. Each lane is labeled with what the cell was transfected with i.e. *wild-type* is LPP1-GFP of LPP1-myc, and the rest represent the amino acid substitutions of the LPP1 constructs.

Table 3.1 Relative PA hydrolysis by LPP1 mutants. Wild-type and various LPP1 mutants fused to either GFP or c-myc were transiently expressed in Cos7 cells and immunoprecipitated with anti-GFP, or anti-myc antibodies, respectively. The activities were then measured using ^{3}H-labeled PA in Triton X-100 micelles and the specific activities were normalized to the relative recovery of each immunoprecipitated LPP1-GFP, or LPP1-myc from the same lysate pool used for Western blot analysis (see *Figure 3.8*). Relative specific activities of the mutants are compared to wild-type LPP1, set at 100% with respect to tag type. Results are from one experiment. Dr. Qiu-Xia Zhang produced all of the GFP tagged LPP1 constructs and subcloned them into pCMV5 plasmids. Her work was originally published in the Biochemical Journal of which I am a co-author [148].

Mutation of amino acid and tag	Relative specific activity	Mutation of amino acid and tag	Relative specific activity
WT-GFP	100%	S169T-GFP	1%
Y221W-GFP	56%	Y168F-GFP	86%
R217K-GFP	0%	T122S-GFP	243%
H171L-GFP	4%	WT-myc	100%
G170A-GFP	50%	R217K-myc	4%

3.3.2 *Lipid phosphate phosphatase-1 is expressed in the plasma membrane of Cos7 cells* – To establish that LPP1 is expressed on the plasma membrane, pCMV5 vectors containing cDNA for myc-tagged wild-type LPP1 and a myc-tagged inactive mutant of LPP1 were transiently transfected in Cos7 cells plated on cover slips. They were then fixed, permeabilized, and probed for c-myc using a mouse monoclonal antibody, and epidermal growth factor receptor (EGFR) using sheep anti-EGFR. Fluorescein labeled anti-mouse IgG and rhodamine labeled anti-sheep IgG were used to show the expression of LPP1-myc and EGFR, respectively, by conventional indirect immunofluorescence microscopy. EGFR is a marker for plasma membrane localization, and the Cos7 cells had staining for EGFR on the perimeter, typical of plasma membrane staining (Fig. 3.9). Wild-type LPP1-myc was also expressed on the perimeter (Fig. 3.9A and B). Plasma membrane co-localization was confirmed by digitally superimposing the

two images of the same field. LPP1-myc also stained intracellular membrane compartments, as did EGFR, although it is difficult to confidently establish co-localization without using confocal fluorescence microscopy.

The catalytically inactive LPP1[R217]-myc on the other hand, had a decreased expression at the plasma membrane (Fig. 3.9C and D) relative to its intracellular staining. This suggests that the mutant LPP1-myc protein was mislocalized, and that it could be due to lack of activity, since the mutation is a very conservative amino acid substitution that should not significantly alter the tertiary structure of LPP1. To test this we expressed other LPP1-GFP mutants with conservative amino acid substitutions in Cos7 cells. Mutants that still maintained activity (Y168F and T122S) had similar staining patterns as wild-type LPP1-myc (Fig. 3.9A and B) and LPP1-GFP including staining of the perimeter (Fig. 3.10). Mutants that had a decrease in activity but still had some activity (G170A and Y221W) also had similar staining patterns as wild-type LPP1 (Fig. 3.10). However, Y221W (Fig. 3.10) showed some similar intracellular staining as the R217K in Figure 3.9C and D, although staining of the perimeter resembling plasma membrane was still detected. Mutations that abolished activity reduced LPP1-GFP expression in plasma membrane relative to intracellular expression and also showed similar reticulated staining as the R217K mutant (Figs. 3.10 and 3.9C and D). Although repeated experiments using plasma membrane markers must be performed, these results suggest that LPP1 activity is required to increase expression of LPP1 at the plasma membrane in Cos7 cells.

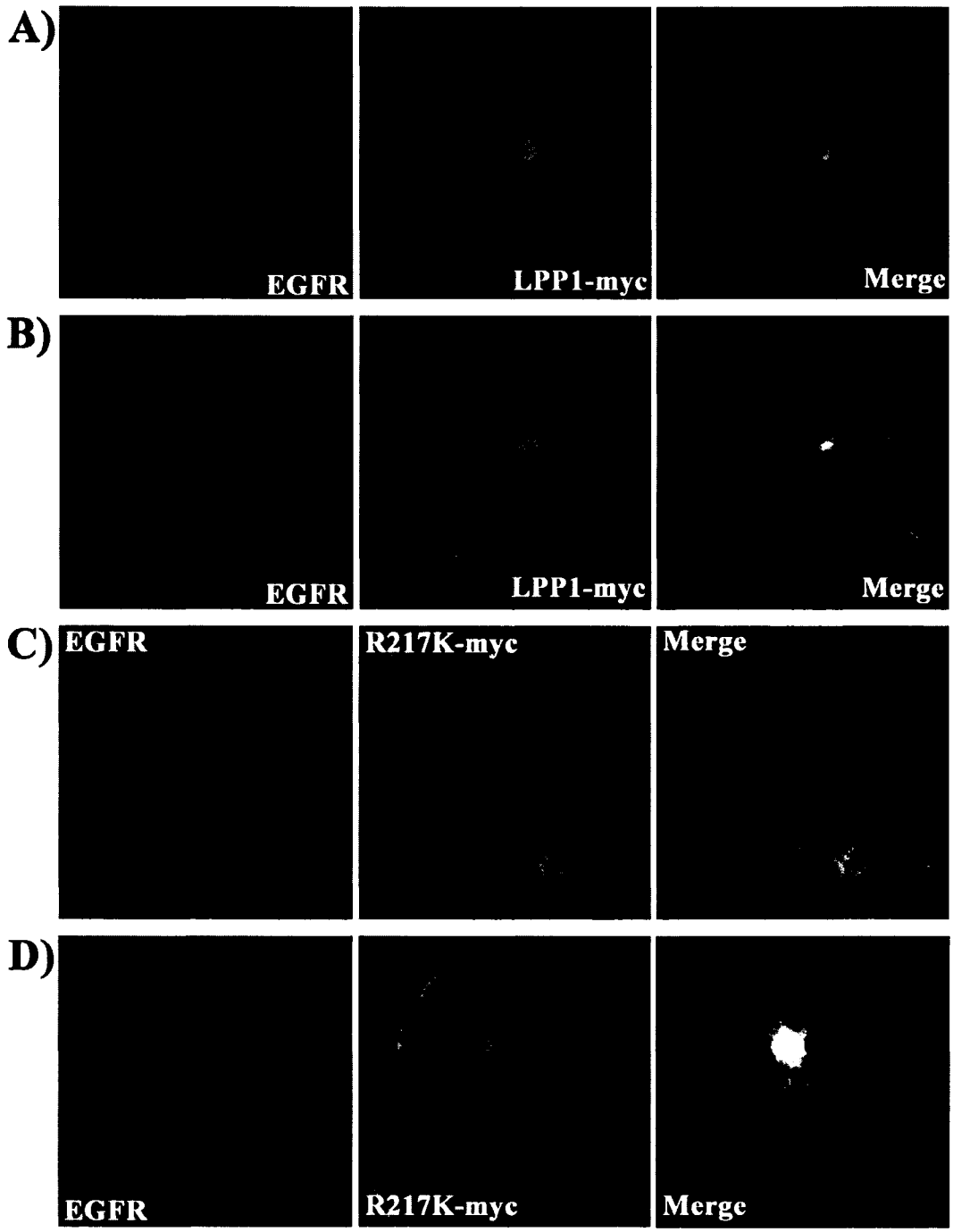

Figure 3.9 Transient transfection of Cos7 cells shows that active LPP1 is localized at the plasma membrane whereas inactive LPP1 is not detected at the plasma membrane. Cos7 cells that were transiently transfected with wild-type *LPP1-myc* (*Panels A* and *B*), or catalytically inactive LPP1-myc (*R217K-myc*, *Panels C* and *D*) were grown on cover slips and fixed. Myc was detected using mouse monoclonal anti-myc 9E10 and FITC-labeled donkey anti-mouse IgG (*green*). Plasma membrane marker EGFR was detected using sheep polyclonal anti-EGFR and rhodamine-labeled donkey anti-sheep IgG (*red*). Panels depict typical cells from one experiment with the help from Dr. Z. Wang using conventional indirect immunofluorescence microscopy.

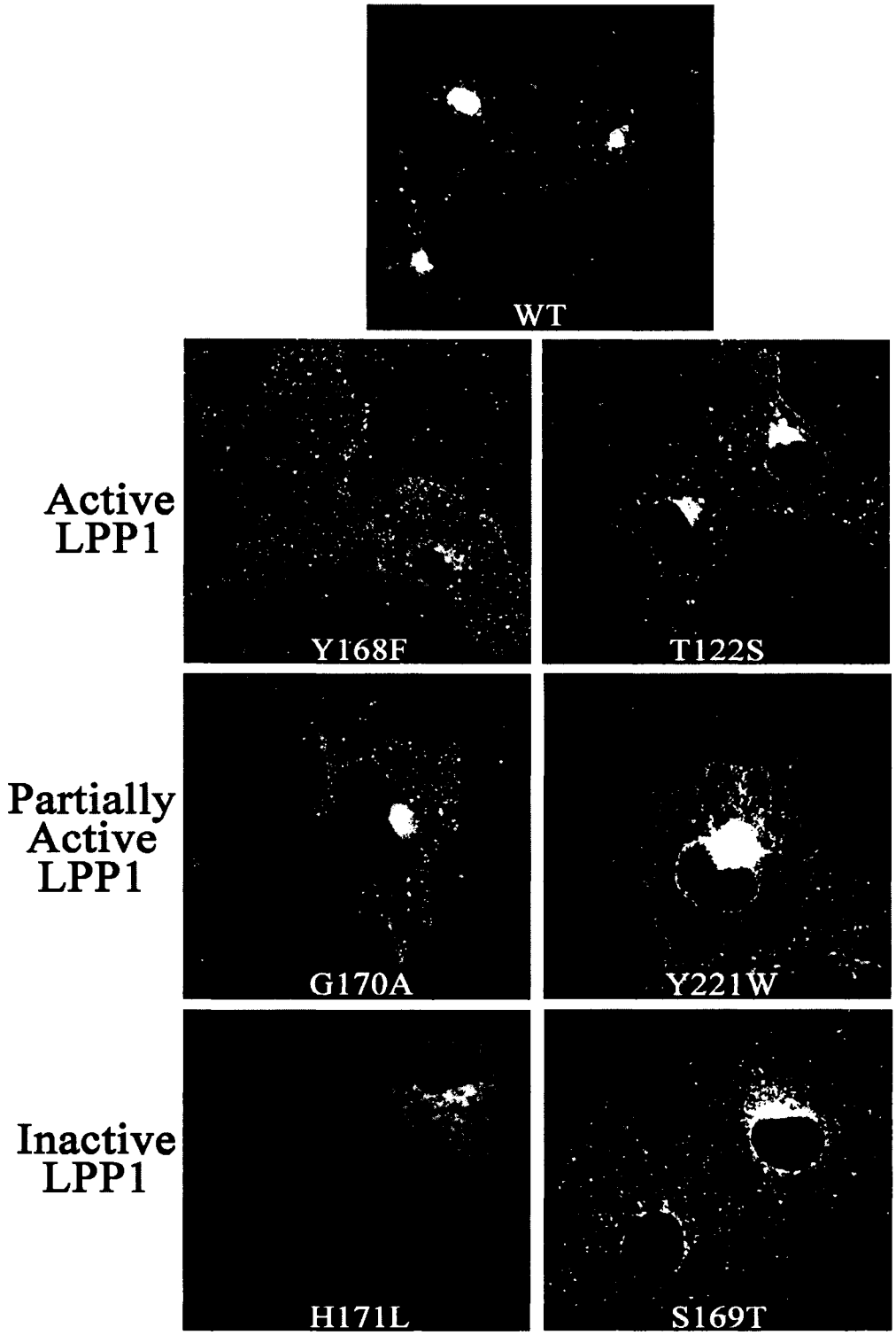

Figure 3.10 Catalytically inactive LPP1s have a decreased plasma membrane expression in Cos7 cells. Cos7 cells were transiently transfected to express LPP1-GFP fusion proteins with various conservative amino acid substitutions as indicated in the panels. LPP1-GFP fusion proteins were detected using rabbit polyclonal anti-GFP and FITC-labeled donkey anti-rabbit IgG. *Figure 3.8* and *Table 3.1* show relative expression and activity of each mutated LPP1-GFP fusion protein. *WT* stands for wild-type LPP1-GFP. Panels depict typical cells from one experiment using conventional indirect immunofluorescence microscopy.

To test whether expression of inactive LPP1 or wild-type LPP1 would affect the localization of either LPP1, Cos7 cells were transfected to co-express both active and inactive LPP1 fused to either a GFP or a c-myc tag, respectively. Wild-type LPP1-GFP was detected using rabbit anti-GFP, whereas LPP1(R217K)-myc was detected using a mouse anti-c-myc. Secondary antibodies were fluorescein-labeled anti-rabbit IgG and rhodamine-labeled anti-mouse IgG. Figure 3.11 shows that the co-expression of inactive LPP1 did not inhibit the expression of wild-type LPP1 to the plasma membrane, however intracellular staining of wild-type LPP1 matched that of the inactive LPP1. This is made clear in the second row of panels of Figure 3.11 in which the Cos7 cell expressing

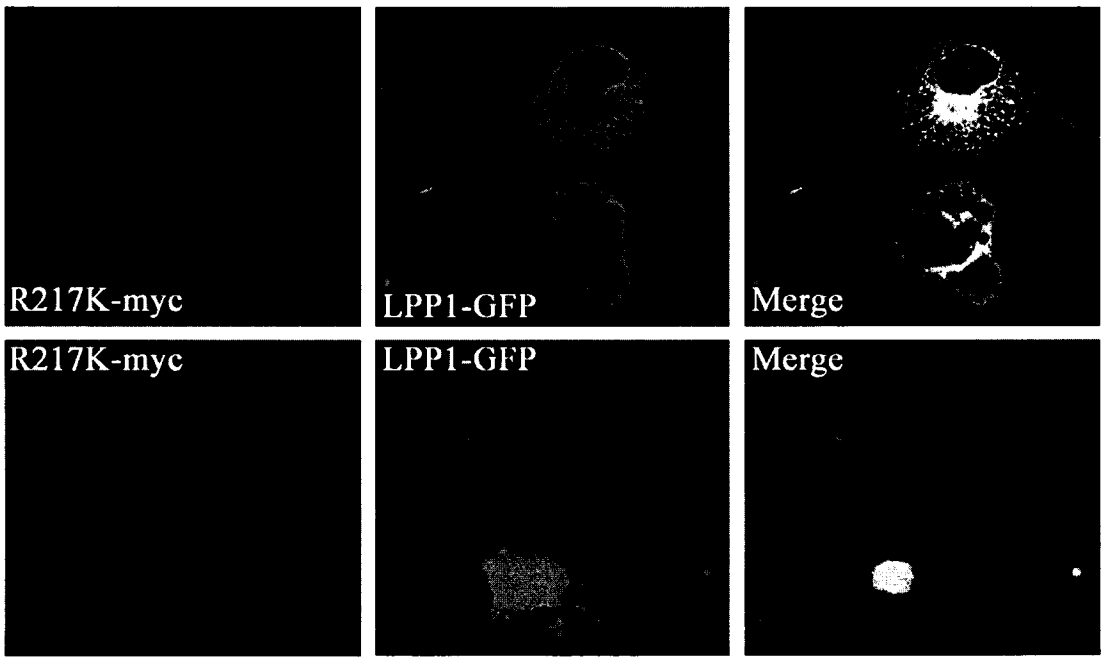

Figure 3.11 Wild-type LPP1-GFP is localized at the plasma membrane despite being co-expressed with the inactive LPP1[R217K]-GFP in Cos7 cells. Cos7 cells were transiently transfected to co-express both active and inactive LPP1 fused to GFP and c-myc tags, respectively. Wild-type LPP1-GFP was detected using rabbit polyclonal anti-GFP and FITC-labeled donkey anti-rabbit IgG (*green*). Inactive LPP1[R217K]-myc was detected using mouse monoclonal anti-myc 9E10 and rhodamine-labeled donkey anti-mouse IgG (*red*). Panels depict typical cells from two experiments using conventional indirect immunofluorescence microscopy.

predominantly active LPP1 had the same intracellular staining pattern as demonstrated by other active LPP1 (Figs 3.9A and B and 3.10). This is in contrast to the neighboring cell that expressed both active and inactive LPP1, and showed that the two versions of the LPP1 share the same reticulated compartment.

3.3.3 *Rat2 fibroblasts have higher endogenous lipid phosphate phosphatase activity than Cos7 cells* - The decrease of plasma membrane expression of the inactive LPP1 in Cos7 cells is in contrast to the plasma membrane expression of inactive LPP1 in Rat2 fibroblasts (Fig. 3.4C, shows cell surface biotinylation of inactive LPP1, and Fig. 3.5E shows indirect immunofluorescence of inactive LPP1 at the plasma membrane). This discrepancy could depend on the lower expression of endogenous LPP activity in Cos7 cells in comparison to Rat2 fibroblasts (Fig. 3.12), which had 7.4-fold more LPP activity. This result suggests that because there is higher endogenous LPP activity in Rat2 fibroblasts, these cells could have a more efficient folding or transport system to cope with LPP1 so that even inactive LPP1 is expressed at the plasma membrane.

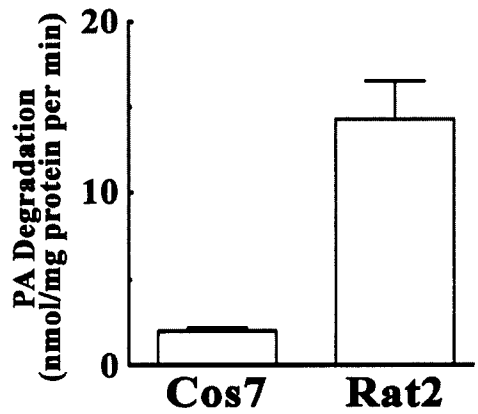

Figure 3.12 Endogenous LPP activity of Rat2 fibroblasts is 7.4-fold higher than that of Cos7 cells. Total LPP activity of lysates of Cos7 cells, and Rat2 fibroblasts was measured by the degradation of PA dispersed in Triton X-100 micelles. Results are means ± S.D. of triplicate samples from one experiment.

3.3.4 *Catalytically inactive lipid phosphate phosphatase-1 accumulates in the endoplasmic reticulum of Cos7 cells* - The expression of catalytically inactive mutant of LPP1 in Cos7 cells appeared to have a distinct expression pattern in contrast to wild-type LPP1. Co-transfection with both inactive and active LPP1 changed the intracellular expression pattern of the active LPP1 to match that of the inactive LPP1, however active LPP1 was still present in the plasma membrane (Fig. 3.10). These results suggest that the expression of inactive LPP1 accumulated in the ER, and its transport to the plasma membrane was reduced to an undetectable level. This was tested by staining Cos7 cells for calreticulin, a marker for the ER, in cells that were transfected to express wild-type LPP1-myc or inactive mutant LPP1[R217K]-myc. Cells that expressed the inactive LPP1 changed the staining pattern of calreticulin (Fig. 3.13C and D) compared to cells expressing wild-type LPP1-myc (Fig. 3.13A and B) and neighboring cells expressing neither. These results suggest that expressing high levels of inactive LPP1 can change the morphology of the ER, or change the localization of calreticulin within the ER.

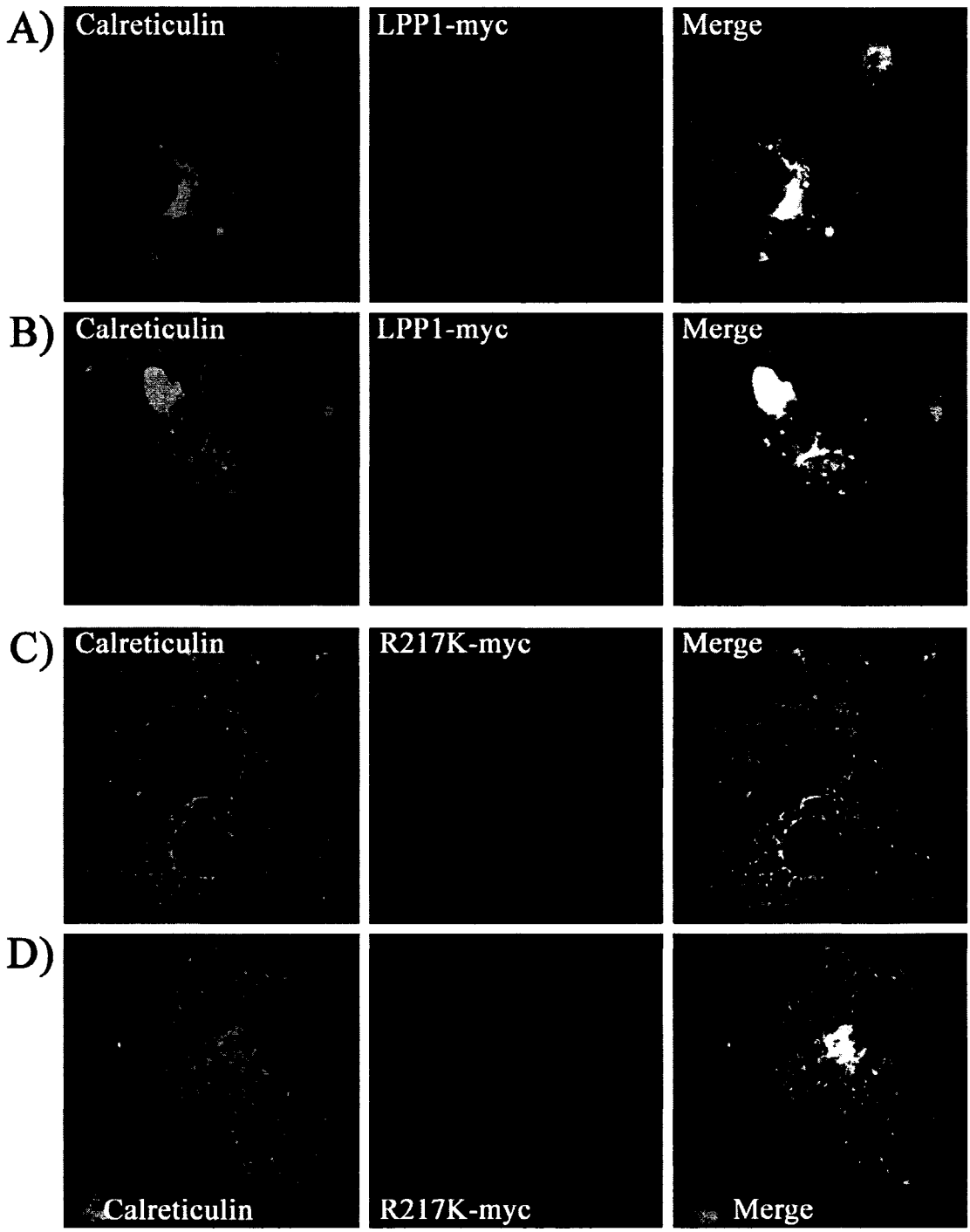

Figure 3.13 The staining pattern of endoplasmic reticulum marker, calreticulin, is changed upon the expression of inactive LPP1 in Cos7 cells. Cos7 cells were transiently transfected to express wild-type (*Panels A* and *B*) or catalytically inactive LPP1 (*Panels C* and *D*) tagged with myc. The endoplasmic reticulum was identified using goat anti-calreticulin and FITC-labeled donkey anti-goat IgG (*green*). LPP1 tagged with myc was identified using mouse monoclonal anti-myc 9E10 and rhodamine-labeled donkey anti-mouse IgG (*red*). Panels depict typical cells from two experiments using conventional indirect immunofluorescence microscopy.

3.3.5 *Expression of active or inactive lipid phosphate phosphatase-1 in Cos7 cells does not change the localization of giantin* - LPP1 is a transmembrane protein that must pass though the Golgi complex to be expressed at the plasma membrane. To test if the Golgi complex morphology is affected by the high-level expression of LPP1 we transduced Cos7 cells with both catalytically active and inactive LPP1-myc and analyzed the morphology of the Golgi complex by immunofluorescence using giantin antibody as a marker for the Golgi complex. There was no change in the pattern of giantin staining if either active or inactive LPP1-myc was expressed (Fig. 3.14) when comparing the staining patterns of giantin of neighboring cells that did not have LPP1-myc expressed.

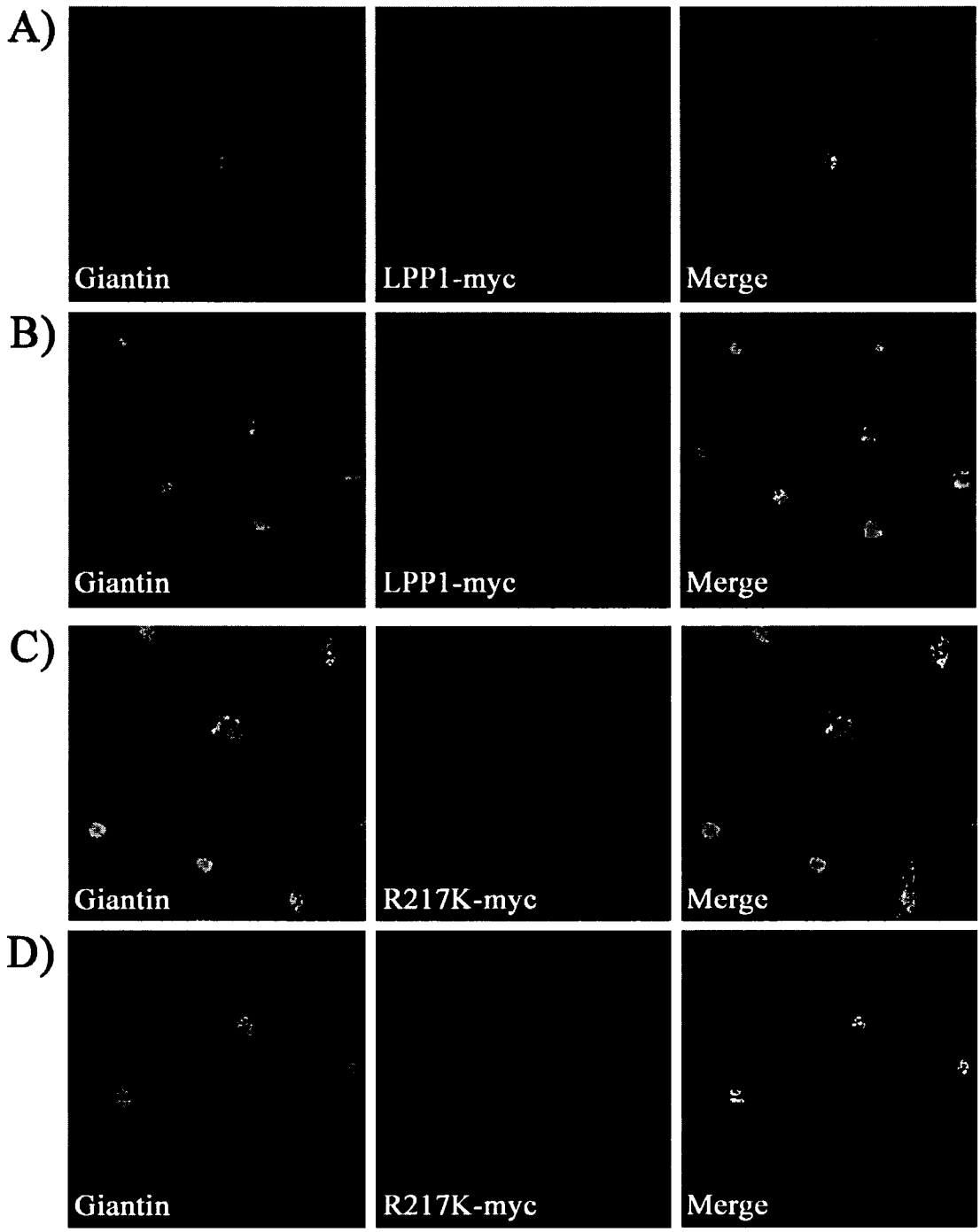

Figure 3.14 The expression of active or inactive LPP1-myc does not change the morphology of the Golgi complex of Cos7 cells. Cos7 cells were transiently transfected to express wild-type (*Panels A* and *B*) or catalytically inactive LPP1 (*Panels C* and *D*) tagged with myc. The Golgi complex was identified using rabbit polyclonal anti-giantin and FITC-labeled donkey anti-rabbit IgG (*green*). LPP1 tagged with myc was identified using mouse monoclonal anti-myc 9E10 and rhodamine-labeled donkey anti-mouse IgG (*red*). Panels depict typical cells from one experiment using conventional indirect immunofluorescence microscopy.

3.4 Discussion

To evaluate the function of LPP1, Rat2 fibroblasts and Cos7 cells were transfected by various methods to increase expression of mouse LPP1. In Rat2 fibroblasts stably transfected with mouse LPP1, there was a 20-fold increase of LPP1 mRNA levels, which confirms Morris *et al.* results of a 16-fold increase in mRNA levels [150]. This previous work also demonstrated that over-expression, or knockdown of LPP1 mRNA did not change mRNA expression for LPP2 and LPP3. Western blot analysis of these fibroblasts revealed multiple bands at about 34-36 kDa. The extent of LPP1 protein over-expression cannot be measured accurately by this method because the polyclonal antibodies used do not detect native rat LPP1 [158]. However, there was a 4-fold increase of total LPP activity over control cells measured by the dephosphorylation of PA in Triton X-100 micelles by lysates. Cells stably producing LPP1 fused with GFP at the C-terminus had a 2-fold increase of total LPP activity. This result demonstrates that the GFP tag does not abolish LPP activity. Western blot analysis of LPP1-GFP also showed multiple bands at about 64-66 kDa much like that found in untagged LPP1, which was about 30 kDa smaller.

It has been established that LPP1 is an integral membrane protein and found in the plasma membrane [138, 152]. Many of the experiments in this thesis show that LPP1 is expressed in the membrane fraction of the post-nucleus supernatant (Fig. 3.1B, 3.3A, and 3.7A). Additionally, the phosphatase active site is predicted to be arranged in a manner that is extracellular if expressed on the plasma membrane, or facing the lumen of intracellular membrane compartments. This is supported by the fact that intact Rat2 fibroblasts stably producing LPP1 had a 2-fold increase in the dephosphorylation of

exogenous LPA compared to control cells. LPP1 is also N-glycosylated on Asn^{142}. This residue is in the loop between two of the essential conserved phosphatase domains (C1 and C2 of Figures 1.8A, 1.9A and B) shared by the phosphatase super-family. This restricts the topology of LPP1 such that this loop should be extracellular or luminal. Exposure of LPP1 on the plasma membrane was demonstrated by labeling LPP1-GFP with biotin using a cell-impermeable biotinylation reagent that targets the deprotonated form of a primary amine, such as that found on lysine residues. Furthermore, indirect immunofluorescence studies on Rat2 cells and Cos7 cells show the plasma membrane localization of myc-, and GFP-tagged LPP1 (Figs. 3.5D and 3.9A and B) [158].

In stably transfected Rat2 fibroblasts, the increase of total LPP activity over control lysates was higher than the increase of LPP ecto-activity over control cells (4-fold vs. 2-fold, respectively). Confocal microscopy identified a population of LPP1 found in internal membrane compartments that could explain this disparity [158]. The biotin labeling experiments also showed that there was a small population of LPP1 that was not extracellularly exposed (Fig. 3.4B). This population of LPP1 was smaller in size by 2 kDa than the biotin-labeled LPP1; therefore this could represent LPP1 that is not fully processed with oligosaccharides. This result is compatible with the results found with non-glycosylated LPP1-GFP mutant (N142Q), which is smaller than the fully glycosylated wild-type LPP1-GFP by about 2 kDa (Fig. 3.3B) and is found as a single band not multiple bands like those of wild-type LPP1-GFP. These results suggest that LPP1 transport to the plasma membrane from an internal compartment is regulated.

LPP1 tagged with c-myc was transiently over-expressed in Rat2 fibroblasts by using adenovirus transfection. This allowed us to avoid any possible effects produced by

long-term LPP1 expression in stably transduced cells. We also used adenoviral vectors that produced a catalytically inactive form of myc-tagged LPP1 that had an arginine conservatively mutated to lysine at position 217 (R217K). Western blot analysis showed that both the wild-type and the catalytically inactive LPP1-myc were expressed at similar levels. Indirect immunofluorescence showed that both active and inactive LPP1-myc are partially localized at the plasma membrane of Rat2 fibroblasts, confirming the results of the cell surface biotinylation of both active and inactive forms of LPP1-GFP. Again, as with the fibroblasts that stably express LPP1-GFP, there is a population of myc-tagged LPP1 in internal compartments (Fig. 3.5D). Cells transiently producing wild-type LPP1-myc had about a 5-fold increase in total LPP activity, and a 3-fold increase of LPP ecto-activity compared to cells transfected with the inactive mutant of LPP1-myc or empty vectors. Since the expression of inactive LPP1 in Rat2 fibroblasts did not produce ectopic localization it will prove to be useful in differentiating catalytic and non-catalytic functions of LPP1.

To further complement the over-expression studies, immortalized fibroblasts were raised from wild-type and transgenic mice over-expressing LPP1 to various degrees [185]. Protein expression increased in cell lines concurrent with *Lpp1* gene-copy numbers as did both total LPP and ecto-activity.

Over-expression of enzymes can produce non-physiological results. Therefore, endogenous LPP1 was knocked down using siRNA specific for rat LPP1. Levels of LPP1 mRNA decreased by 90%, and this was accompanied by a 50% decrease in total LPP activity. The lower effect on LPP activities compared to mRNA levels is explained by the fact that the fibroblasts continue to express LPP2 and LPP3 [150]. Although, it

appears that LPP1 is a major contributor to LPP activity in the fibroblasts since increasing, or knocking down its expression significantly altered total LPP activity compared to changing LPP2 or LPP3 levels [150].

To investigate the localization of LPP1 in other mammalian cells, various constructs of LPP1 tagged with either GFP or c-myc were transiently transfected in Cos7 cells. Western blot analysis showed that all of the constructs were produced at various protein levels (Fig.3.8). To subtract the contribution of endogenous LPP activity, lysates were immunoprecipitated using the antibody specific for the tag fused to LPP1. The mutations S169T, H171L, and R217K from the second and third domains of the three conserved phosphatase domains, decreased LPP activity by more than 95% (Figures 1.8 and 1.9 show the sequences and arrangement of the LPPs and the three conserved phosphatase domains, C1, 2, and 3). G170A decreased activity by 50%. These residues are highly conserved in the phosphatase super-family [139] and confirmed the work by Dr. Zhang [148] in our group. The decreased LPP1 activity can be explained by comparison with other members of the phosphatase super-family such as chloroperoxidase, which has had its structure solved at atomic scale resolution [142], and its catalytic reaction mechanism thoroughly investigated [142-145]. The network of invariant lysine, arginine (i.e. Arg^{217} of mouse LPP1 in C3), serine (i.e. Ser^{169} of mouse LPP1 in C2) and glycine (i.e. Gly^{170} of mouse LPP1 in C2) residues donate hydrogen bonds to the phosphate oxygen molecules of the substrate and help stabilize the transition state of the reaction (see Fig. 1.8B for visual model of LPP reaction) [142, 146, 147]. His^{171} in the C2 of mouse LPP1 is believed to facilitate phosphate bond cleavage after the phosphohistidine intermediate is formed at His^{223} in C3. His^{171} is also believed to be

involved in freeing the active site for another round of catalysis by hydrolyzing the phosphohistidine intermediate. Residues within the conserved domains but not conserved within the phosphatase super-family were also mutated (T122S, and Y168F) but had relatively no effect on LPP1 activity. The mutant Y221W had a 44% decrease in LPP1 activity. Tyr^{221} is present in most mammalian LPPs, but not conserved in the phosphatase super-family [139, 148], thus it could be involved in substrate specificity, or protein stability.

Localization studies were performed on the various LPP1 constructs in Cos7 cells. Wild-type LPP1, and LPP1 mutants that retained full or partial activity showed partial localization to the plasma membrane and other unidentified intracellular compartments (Figs. 3.9 and 3.10). However, in Cos7 cells inactive LPP1 mutants had a distinct reticulated staining pattern and a decrease of expression in the plasma membrane. This is a hallmark of ER retention of misfolded or unstable proteins [228, 229]. There is an overlap of expression with inactive LPP1 and the resident ER marker, calreticulin, which appears to be redistributed within the ER (Fig. 3.13). This is not surprising since calreticulin is a chaperone for glycoproteins, such as LPP1, and is part of the ER quality control mechanism, which will retain glycoproteins in the ER if they are not stable or folded properly [228]. Additionally, those cells that expressed the inactive LPP1 appeared to be retracted. Retraction could be a sign that these cells are not healthy, and may be undergoing apoptosis, which could be a consequence of the ER retention response.

It is intriguing if the retention of LPP1 in the ER of Cos7 cells is solely dependent on abolished LPP1 catalytic activity. Point mutations on the LPP1 that did not abolish

catalytic activity did not inhibit transport to the plasma membrane (Fig. 3.10). Burnett *et al.* [202] demonstrated that LPP1 can form homodimers, but could not form heterodimers with LPP3 or wunen. Wunen is a LPP ortholog expressed in *Drosophila*, and it also forms homodimers, but the formation of dimers is dependent on catalytic activity. The authors of this study concluded that wunen dimerization was not essential for catalytic and biological activity, but perhaps conferred structural or functional stability [202]. This could explain why inactive LPP1 mutants were retained in the ER, and are partially co-localized with the ER chaperone, calreticulin. It was also intriguing to observe that wild-type LPP1 share the same intracellular compartments with inactive LPP1 when they were co-transfected (Fig. 3.11). In this experiment perhaps the journey of the wild-type LPP1 to the plasma membrane passed through the same compartment in the ER as the retained inactive LPP1. Alternatively, perhaps wild-type LPP1 could possibly still form an unstable dimer with inactive LPP1, and then be retained in the ER. In the same regard wild-type LPP1 was still present in the plasma membrane because random association in the ER dictates that it also dimerizes with another wild-type LPP1. If this is true, and taking into account that inactive LPP1 was not detected at the plasma membrane, it could take two active LPP1s to form a stable dimer and then transported to Cos7 plasma membrane.

This phenomenon appears true for Cos7 cells, but was not seen in Rat2 fibroblasts, where inactive LPP1 was expressed at the plasma membrane. Rat2 fibroblasts had 7.4-times higher endogenous LPP activity than Cos7 cells, and could be more equipped and efficient at stabilizing inactive LPP1 with chaperones that are not available in Cos7 cells. It was important to distinguish the expression patterns of LPP1 in other cell lines

since Rat2 fibroblasts were used to investigate the role LPP1 played in regulating fibroblast migration. The fact that inactive LPP1 appeared to have similar expression patterns as wild-type LPP1 in Rat2 fibroblasts increases its value as a model to elucidate catalytic and possible non-catalytic functions of LPP1.

LPP1 is widely expressed in human tissues (Table 1.1 and [113]), and is a major contributor to LPP activity in fibroblasts [150]. LPP1 is found in the ER and plasma membrane and possibly in other endomembrane compartments such as the Golgi complex and endosomes. Biochemical fractionation has found LPP1 and LPP3 in detergent-resistant membrane domains that could be the components of lipid rafts or caveolae [164, 165, 168]. This can be an important way to compartmentalize them with LPA and sphingosine-1-phosphate (S1P) receptors [170, 171] and other signaling enzymes such as phospholipase D 2 (PLD2), which are also found in detergent-resistant compartments [172, 173]. It is in the role of agonist induced cell signaling that LPP1 has been frequently studied. LPP1 can dephosphorylate numerous bioactive lipid phosphates such as PA, LPA, S1P, and ceramide-1-phosphate (C1P) presented in Triton X-100 micelles. These lipids can be found inside the cell and thus are potential targets for LPP1, and the byproducts themselves are bioactive. In this regard, LPP1 could be able to dephosphoryate PA generated from PLD, for example, thereby terminating PLD signaling and forming diacylglycerol (DAG), which could then activate DAG dependent protein kinase C isoforms.

Another potential role for LPP1 in cell signaling is at the cell surface. Since LPP1 at the plasma membrane has its phosphatase domain facing the outer surface, it is positioned to degrade exogenous LPA and S1P. These signaling lipid phosphates have

been found outside of cells and have numerous receptors, and thus invoke many kinds of biological activities including cell proliferation, cell survival, migration, metastasis, and angiogenesis. LPP1 readily dephosphorylates exogenous LPA compared to S1P (Fig. 3.2E) suggesting LPP1 could preferentially affect LPA signaling by degrading LPA before interacting with its receptor. In conclusion of this Chapter, the over-expression and knockdown of LPP1 in Rat2 fibroblasts has been established and will provide a system to examine its role in LPA-induced fibroblast migration.

CHAPTER 4

LIPID PHOSPHATE PHOSPHATASE-1 REGULATES LYSOPHOSPHATIDATE-INDUCED FIBROBLAST MIGRATION INDEPENDENTLY OF LIPID PHOSPHATE PHOSPHATASE ECTO-ACTIVITY

A version of this chapter has been published. Pilquil, C., Dewald, J., Cherney, A., Gorshkova, I., Tigyi, G., English, D., Natarajan, V., Brindley, D. N. 2006. J Biol. Chem. 281: 38418-29.

4.1 Introduction

LPA was first identified as a chemoattractant for the amoebae, *Dictyostelium discoideum* in 1993 [230]. Since then LPA has been established as a bona fide chemoattractant for various mammalian cell lines including fibroblasts. LPA is present in biological fluids and activates cells through families of G-protein coupled receptors [25, 26] that are coupled through G_i, $G_{12/13}$ or G_q. This leads to intracellular effects such as decreases in cAMP, stimulation of phospholipase D (PLD) and Rho effectors leading to stress fiber formation and activation of phospholipase C (PLC), protein kinase C (PKC) isoforms, extracellular signal-regulated kinase (ERK) and Ca^{2+}-transients. Extracellular LPA is produced in inflammatory conditions by secretory phospholipase A_2 acting on PA [31], and it is also produced from circulating lysophosphatidylcholine by the secreted lysophospholipase D, autotaxin [42, 231]. Autotaxin stimulates fibroblast migration and division for wound repair, and its expression shows a positive correlation with tumor progression, angiogenesis and metastasis [41, 42, 44, 231]. Importantly, LPA mimics many effects of autotaxin. These facts highlight our growing knowledge of the important physiological and pathological role that LPA plays as a signaling molecule.

Chapter 3 characterized LPP1 as an ecto-enzyme that readily dephosphorylates extracellular LPA. Consequently, LPP1 is positioned to control extracellular LPA concentrations, therefore, it could regulate LPA receptor activation. Intracellular LPP1 was also found, and could control lipid phosphate signaling within the cell when stimulated by LPA or other agonists from outside the cell. The previous Chapter also described methods to regulate the expression of LPP1, and these were employed to test its role in LPA-induced migration of Rat2 fibroblasts. Additionally, other agonists known

to stimulate fibroblast migration were used to examine the role of LPP1 in these processes. This would test if regulation of migration by LPP1 is specific for LPA. Finally, the crucial question of whether any effect by LPP1 on LPA signaling is dependent on the extracellular hydrolysis of LPA is answered by using the α-hydroxyphosphonate analogue of LPA. This molecule cannot be dephosphorylated by LPP1, and is proven to be an agonist of $LPA_{1/3}$ receptors [180, 232].

4.2 Lipid phosphate phosphatase-1 activity regulates the stimulation of fibroblast migration by lysophosphatidate, but not by platelet-derived growth factor or endothelin.

4.2.1 *In vitro wound healing assay* – An *in vitro* wound healing assay was employed to test if LPA can induce Rat2 fibroblast migration. This assay involves creating a "wound" by scratching a monolayer of fibroblasts with the pointed end of a 200 μl pipette tip. LPA at a concentration of 10 μM was incubated with the "wounded" monolayer for 36 h, after which the width of the scratch was measured relative to its initial width. LPA stimulated wild-type, and vector control fibroblasts to migrate into the "wound" (Fig. 4.1A). However, fibroblasts stably over-expressing LPP1 showed a severe inhibition of LPA-induced migration into the "wound" (Fig. 4.1A). There was a 2.9-fold stimulation of migration of wild-type fibroblasts by LPA, and this decreased by 75% upon over-expression of LPP1 (Fig.4.1B). To test if other known stimulators of migration would also have their effects attenuated by LPP1 over-expression, fibroblasts were incubated with platelet-derived growth factor (PDGF) or endothelin. LPP1-over-

expression did not significantly affect PDGF- or endothelin-induced fibroblast migration (Fig. 4.1B).

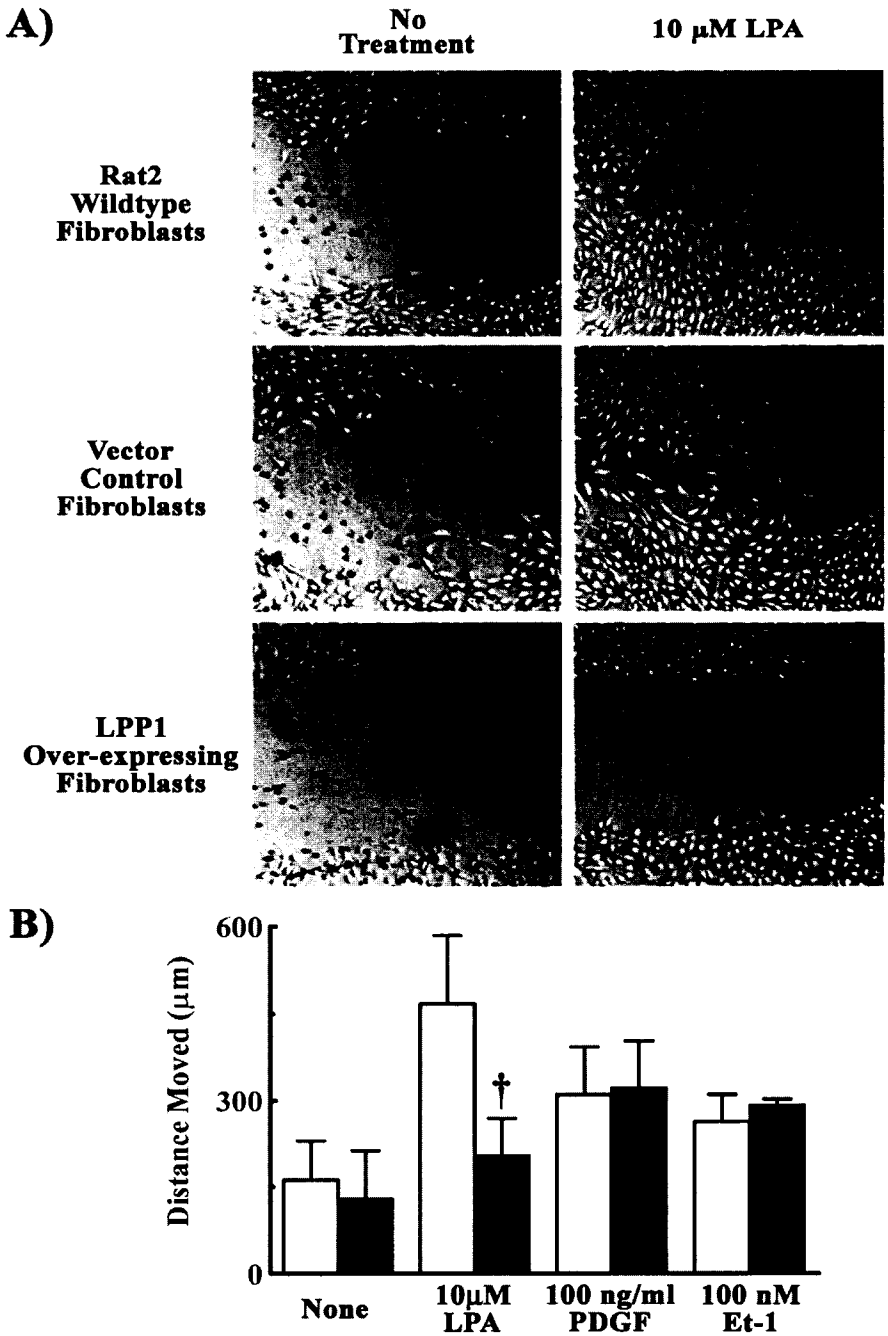

Figure 4.1 Increasing LPP1 activity attenuates LPA-induced fibroblast migration in an "*in vitro* wound healing" assay. *Panel A* shows the migration of wild-type, vector control and LPP-1-over-expressing Rat2 fibroblasts into a "wound" that was scratched 36 h previously. *Panel B* shows the average distance by which the gap between the fibroblasts closed over 24 h when the indicated concentrations of LPA, PDGF and endothelin-1 (Et-1) were added to the incubation medium. The results for wild-type and LPP1-over-expressing fibroblasts are shown in *white* and *black* columns, respectively. The values are means ± S.D. for 5 or 3 independent experiments for LPA and PDGF, respectively. Means and ranges for 2 experiments are shown for endothelin. Significant differences between LPP1 over-expressing fibroblasts and wild-type fibroblasts are indicated by †, $p<0.001$.

4.2.2 *Determination of chemotaxis and chemokinesis* - The wound healing assay measures mainly the non-directional, chemokinetic, movement of the fibroblasts since no diffusion gradient of the agonist is established. Therefore, we employed a Transwell chamber assay (Fig. 2.3) to distinguish between chemotaxis (migration towards a gradient of chemo-attractant) and chemokinesis. The mode of migration that was stimulated by the three agonists was determined by adding the same concentration of agonist to the top and bottom chambers and comparing the migration to when the agonist was present only in the bottom chamber. PDGF-induced migration was mainly through chemotaxis since adding 20 ng/ml PDGF to the top chamber inhibited migration to the bottom chamber by 74% (Table 4.1). By contrast, the migration to 0.5 μM LPA and 100 nM endothelin was mainly by chemokinesis. Adding the equivalent concentrations of LPA to the top chambers blocked migration by only 43%. For endothelin there was no significant decrease in migration. Our results concerning the mode of migration that is induced by LPA and PDGF agree with previous work with fibroblasts [233, 234].

Table 4.1 Determination of chemotaxis and chemokinesis in Transwell migration chambers. Wild-type Rat2 fibroblasts were plated in the top well of the Transwell chamber as in *Figure 2.3A*. Inhibition of migration (%) was calculated by dividing the number of migrated cells stimulated by the agonist present in both the top and bottom wells by the number of migrated cells stimulated by the agonist present in only the bottom well. This number was then converted to percent and subtracted from 100%. The concentrations of agonists were as follows: 0.5 μM LPA, 20 ng/ml PDGF, and 100 nM endothelin-1. Results are means ± S.D. of five experiments for LPA, and three experiments for PDGF. One-sample t-test using 0% inhibition as a theoretical mean value found significant differences between migration induced by agonist present in the lower chamber and migration induced by agonist present in both chambers ($p<0.05$ and $p<0.01$, are indicated by * and **, respectively). Two experiments were performed for endothelin-1 and there was no inhibition detected.

Treatment	LPA	PDGF	Endothelin-1
Inhibition of migration (%)	**43 ± 22 ***	**74 ± 7 ****	**0**

4.2.3 *Fibroblast migration in Transwell chambers* - The "wound healing assay" mainly measured chemokinesis, and gave significant migration after 24 h, which is the dividing time of Rat2 fibroblasts [150]. We used the Transwell migration chamber to enable us to expose the fibroblasts to a gradient of agonist. The Transwell migration assays also limited the impact of cell proliferation in the interpretation of the migration results since the fibroblasts migrated for only 6 h. The addition of LPA to the bottom chamber greatly enhanced the migration over non-treated cells up to 9-fold, compared to the wound healing assay which measured a 2.9-fold increase over non-treated cells (Fig. 4.1B and 4.2A). The results from the Transwell migration assay demonstrate that the migration of Rat2 fibroblasts in response to 0.1 to 10 μM LPA was severely inhibited by increased LPP1 expression. We also employed fibroblasts from mice that expressed two gene copies of LPP1 that showed about 2-fold increases in total and LPP ecto-activity compared to fibroblasts from control mice (Fig. 3.6B and C). These LPP-1 over-expressing fibroblasts also showed decreased migration to LPA (Fig. 4.2B) with the most striking effects at lower LPA concentrations.

To determine if the effects of LPP1 over-expression were specific for LPA-induced migration we measured the responses to PDGF and endothelin. First, within 6 h, wild-type fibroblasts robustly responded to PDGF in the Transwell chamber (up to a 20-fold increase over non-treated cells, Fig. 4.2C) compared to the "wound healing" assay (2-fold increase over non-treated cells, Fig. 4.1B). This was not a surprise since PDGF-induced migration was more effective in a PDGF-gradient (Table 4.1). There was a plateau of migration beginning at 20 ng/ml of PDGF (Fig. 4.2C). When compared to control cells, LPP1 over-expression did not significantly alter chemotaxis to PDGF, or

chemokinesis with endothelin (Fig. 4.2C and D) mimicking the results of the "wound healing" assay.

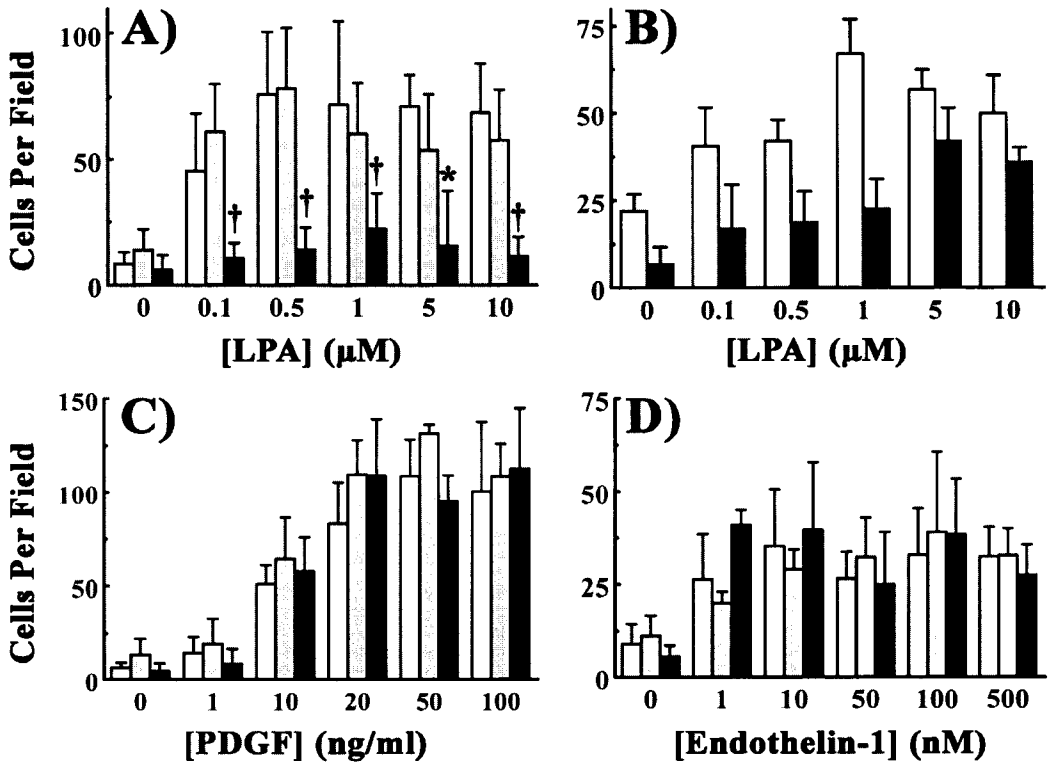

Figure 4.2 Over-expression of LPP1 decreases fibroblast migration in a Transwell assay in response to LPA, but not PDGF, or endothelin. *Panels A, C* and *D* shows the migration of Rat2 fibroblasts (*white bars*), and fibroblasts transduced stably with the empty vector (*grey bars*), or vector containing cDNA for LPP1 (*black bars*). Results are means ± S.D. for at least three independent experiments. Significant differences between LPP1 over-expressing fibroblasts and wild-type, or vector control fibroblasts in the same treatment groups are indicated by: †, $p<0.001$ and *, $p<0.05$. *Panel B* shows the migration of fibroblasts derived from control mice (*white bars*), or transgenic mice that over-expressed LPP1 (*black bars*). Results are from one experiment and show means ± S.D. of cells per field of at least five fields. Anton Cherney, a summer student, performed this experiment under my supervision.

4.2.4 *Attenuation of lysophosphatidate-induced migration requires an intact lipid phosphate phosphatase-1 active-site* - To investigate whether the effect of LPP1 on LPA-induced migration depends upon its catalytic activity, Rat2 fibroblasts were infected with adenoviral vectors containing mouse LPP1-myc, or the inactive mouse LPP1[R217K]-myc. Over-expression of the wild-type LPP1 increased total LPP activity by about

4.8-fold, whereas expression of the mutant did not change LPP activity significantly (Fig. 3.5A). As a control, Western blot analysis confirmed that the inactive LPP1 mutant was expressed to similar extents compared to active LPP1 (Fig. 3.5C). Transient expression of wild-type LPP1, but not LPP1[R217K], decreased LPA-induced migration by 60% compared to wild-type cells (Fig. 4.3). PDGF-induced migration was not affected by the over-expression of either the active or inactive versions of LPP1 (Fig. 4.3).

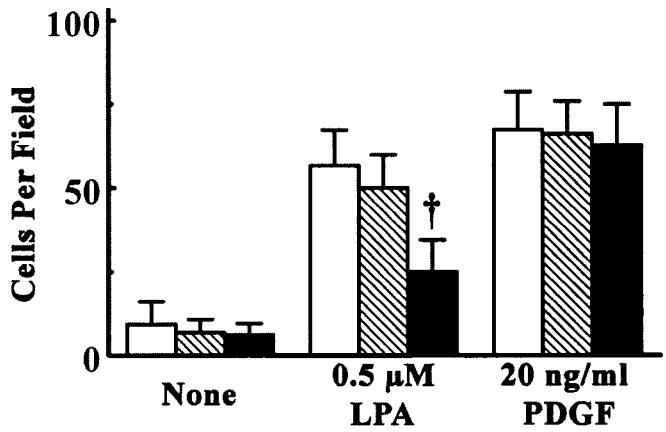

Figure 4.3 Attenuation of LPA-induced migration requires an intact LPP1 active-site. The histogram shows the migration of wild-type fibroblasts (*white bars*), or those that transiently over-expressed LPP-1-myc (*black bars*), or the inactive mutant, LPP1[R217K]-myc, (*hatched bars*). Results are means ± S.D. for at least three independent experiments. *Figure 3.5 Panel C*, shows a Western blot performed with rabbit anti-mLPP1 antibody and demonstrates that mutant LPP1 and wild-type LPP1 are over-expressed to similar levels. Significant differences ($p<0.001$) found between LPP1 over-expressing fibroblasts and wild-type fibroblasts, or fibroblasts over-expressing the inactive mutant, LPP1[R217K]-myc are indicated by †.

4.2.5 *Knockdown of lipid phosphate phosphatase-1 in Rat2 fibroblasts* - To provide further evidence that changing LPP1 activity controls LPA-induced migration, endogenous LPP1 expression was knocked down using a combination of four siRNAs to rat LPP1. Messenger RNA for rat LPP1 was decreased by about 90% compared to controls (Fig. 3.7A) and this was accompanied by about a 50% decrease in total LPP activity (Figs 3.7B). In all four experiments, the fibroblasts in which LPP1 activity was knocked down showed increased LPA-induced migration compared to control

transfections (Fig. 4.4). This was the opposite effect to increasing LPP1 expression. Overall, rat LPP1-knockdown did not show a significant effect on PDGF-induced migration compared to controls (Fig. 4.4). Knockdown of LPP1 also increased fibroblast migration in the absence of agonist (Fig. 4.4). This suggests that the basal fibroblast migration could result from LPA secreted from the cells.

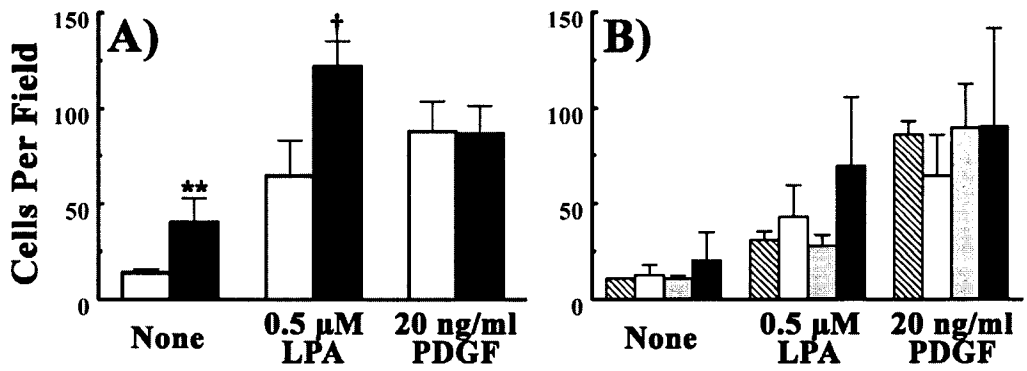

Figure 4.4 Knockdown of LPP1 activity increase Rat2 fibroblast migration in a Transwell migration assay in response to LPA, but not to PDGF. Wild-type Rat2 fibroblasts were transfected with vehicle (Lipofectamine 2000 in *hatched bars*), control siRNA (siCONTROL in *white bars*), siRNA for mouse LPP1 (*grey bars*), or siRNA for rat LPP1 (*black bars*). The results shown in *Panel A* are from one representative migration experiment showing means ± S.D. for cells per field from about 6 fields. *Panel B* shows means ± S.D. for cell numbers of four knockdown experiments performed including the results shown in *Panel A*. Means and ranges are shown for the transfections with vehicle control and transfections using siRNA for mouse LPP1. Significant differences between fibroblasts with LPP1 knockdown and the siRNA controls in *Panel A* are indicated by: †, $p<0.001$; and **, $p<0.01$.

4.2.6 *Lipid phosphate phosphatase-1 over-expressing fibroblasts readily detach from cell culture plates* – It was quickly observed that when Rat2 fibroblasts were detached from cell culture plates with a trypsin-EDTA solution, the cell lines over-expressing LPP1 would detach more readily than the control cell lines. Cell detachment of LPP1 over-expressing cells was measured since cell migration is a cycle of attachment-and-detachment of the single cell on the substratum. Treatment of a confluent monolayer of LPP1 over-expressing fibroblasts with trypsin-EDTA started to detach cells within the first minute, and plateau within 5 min. Fifty % of the LPP1 over-expressing

cells were detached at approximately 1.5 min, whereas wild-type, and empty vector control fibroblasts were 50% detached at approximately 6, and 3 min, respectively, and plateau at 10 min (Fig 4.5A). Confluent monolayers treated with 2 mM EDTA in HBS showed that 50% of the LPP1 over-expressing cells detached at approximately 7 min, on the other hand control cells did not detach within the time tested (Fig 4.5B). All cell-lines treated with only HBS as a control, remained on the plates within 60 min of observation (Fig. 4.5C).

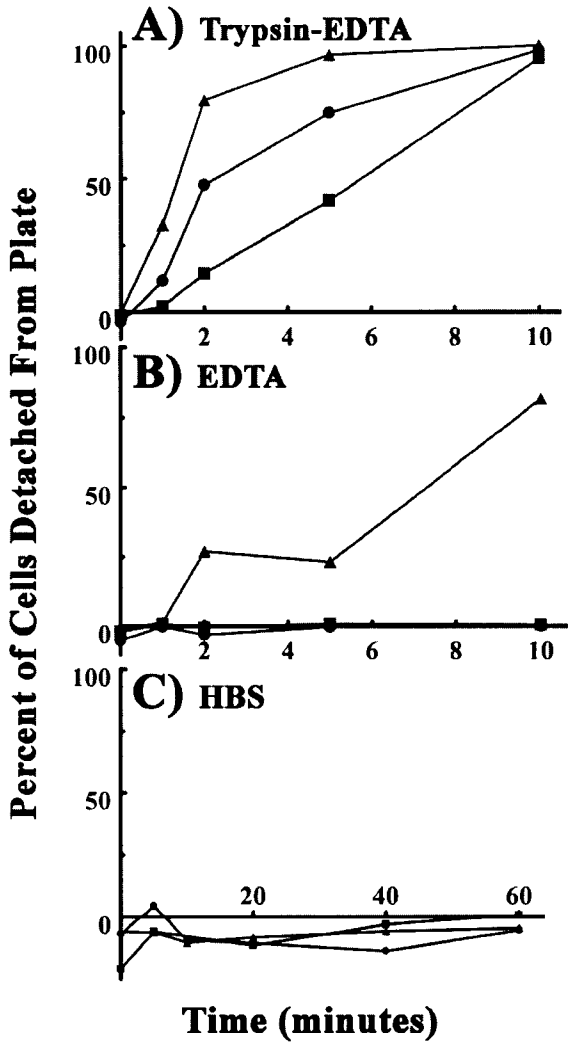

Figure 4.5 Fibroblasts over-expressing LPP1 readily detach from cell culture plates. To measure cell detachment from cell-culture plates, confluent monolayers of wild-type (■), vector (●), and stably over-expressing LPP1 (▲) Rat2 fibroblasts were treated with trypsin-EDTA (*Panel A*), 2mM EDTA (*Panel B*), and Hepes buffered saline (HBS in *Panel C*) as a control. At the indicated times supernatant from the plate was collected and centrifuged to concentrate the detached cells. Cells remaining on the plate were also collected. DNA from both fractions was measured using Hoechst 33258 to stain DNA and a fluorometer to detect fluorescence at 460 nm. The relative detachment of fibroblasts from the plates was calculated by dividing the amount of DNA in the supernatant by the total amount of DNA in the supernatant and remaining on the plate from attached cells. Results shown are a representative from two experiments that were performed in duplicate. Anton Cherney, a summer student, performed these experiments under my supervision.

4.3 The attenuation of lysophosphatidate-induced migration by lipid phosphate phosphatase-1 is not mediated through the degradation of extracellular lysophosphatidate.

4.3.1 *Degradation of extracellular lysophosphatidate during migration in Transwell chambers* – The dephosphorylation of LPA in the Transwell chamber was measured after 6 h of migration time. There was an average increase of LPA degradation of 1.6-fold in cells stably over-expressing LPP1 compared to control cells (Table 4.2). There was a 1.9-fold increase of LPA degradation in cells infected with 40 MOI of adenovirus to transiently express LPP1 over cells transfected with empty vector or inactive LPP1. Within this time an average of 22% of the exogenous LPA was degraded in cells over-expressing LPP1 both stably and transiently (Table 4.2). The percent of LPA degradation remained relatively constant for concentrations of LPA from 0.5 to 10 μM (Table 4.2).

In Transwell chambers the cells transfected with siRNA to knockdown LPP1 activity, had a 40% decrease of exogenous LPA degradation compared to controls (Table 4.2). These results confirm that over-expression and knockdown of LPP1 activity was efficacious in controlling LPP1 activity during the migration process.

Table 4.2 LPP1 ecto-activity in Transwell migration chambers. The dephosphorylation of exogenous ^{32}P-labeled LPA added to the bottom well of the Transwell migration chamber was measured by extracting $^{32}P_i$. Degradation of ^{32}P-labeled LPA was measured at concentrations of 10, 1, and 0.5 μM LPA in the presence of 0.4% BSA after 6 h of migration at 37°C and 5% CO_2 atmosphere. The first three rows of data (*Stable Transduction*) represent LPA degradation by wild-type Rat2 fibroblasts, and stably transduced Rat2 fibroblasts. The next three rows (*Adenoviral Infection*) represent Rat2 fibroblasts infected with 40 MOI of adenovirus that contain empty vector or vectors that express inactive LPP1[R217K] or active LPP1. The last three rows (*Knockdown by siRNA*) represent Rat2 fibroblasts transfected with Lipofectamine 2000 (Vehicle), or siCONTROL, or siLPP1 Rat siRNAs to knockdown rat LPP1. Results are means ± S.D. of at least three experiments, unless indicated by an (R), which indicates a range from two experiments. Significant differences between fibroblasts stably, or transiently producing LPP1 and wild-type, vector control fibroblasts, or transiently producing inactive LPP1 are indicated by: †, $p<0.001$; **, $p<0.01$ and *, $p<0.05$. Significant differences between fibroblasts with knockdown of rat LPP1 and controls are also labeled as above.

		Exogenous LPA Degradation								
		pmol LPA degraded			LPA degraded (%)			Relative LPA degradation		
	[LPA] (μM)	10	1	0.5	10	1	0.5	10	1	0.5
Stable Transduction	Rat2	314 ± 101	50 ± 12	13 ± 8	10.1 ± 3.6	14.6 ± 2.6	8.0 ± 4.7	1.00	1.00	1.00
	Vector	360 ± 51	38 ± 5	19 (R) 2	11.9 ± 1.8	11.1 ± 0.7	11.1 (R) 0	0.93 ± 0.18	0.78 ± 0.10	0.82 (R) 0.03
	LPP1	684* ± 327	82 **± 11	20 ± 15	22.7 * ± 11.0	24.3 † ± 3.2	19.3 * ± 7.8	1.68 **± 0.44	1.70 **± 0.37	1.52 **± 0.28
Adenoviral Infection	Vector	359 ± 115	52 ± 13	30 (R) 11	11.4 ± 3.8	14.0 ± 4.4	11.0 (R) 3.1	1.00	1.00	1.00
	R217K	357 ± 133	51 ± 19	27 (R) 10	11.3 ± 4.5	10.8 ± 5.7	10.3 (R) 4.4	1.04 ± 0.35	1.07 ± 0.56	1.14 (R) 0.73
	LPP1	543* ± 162	89 ± 20	66 (R) 14	19.1 ** ± 4.4	23.2 * ± 1.4	24.1 (R) 3.4	1.56 **± 0.37	1.78 ± 0.57	2.29 (R) 0.34
Knockdown by siRNA	Vehicle	303 ± 38	-	13.3	9.0 ± 0.8	-	9.0	1.00	-	1.00
	siCONTROL	328 ± 98	-	10.3	9.6 ± 2.1	-	7.0	1.07 ± 0.19	-	0.78
	siLPP1 Rat	200* ± 48	-	7.9	5.8* ± 0.6	-	5.3	0.66 * ± 0.08	-	0.59

4.3.2 *Mono-oleoylglycerol does not affect lysophosphatidate-induced migration of fibroblasts* – LPP ecto-activity could enable mono-oleoylglycerol formed from the dephosphorylation of exogenous oleoyl-LPA to enter the cell and thereby regulate cell signaling after re-phosphorylation [84, 85]. For example, intracellular LPA could signal through internal LPA receptors [106], or the peroxisome proliferator-activated receptor-γ (PPARγ) receptors [108, 109] and thereby affect migration. We excluded this ecto-LPP1 effect on LPA-induced migration by adding 10 nM to 5 μM exogenous

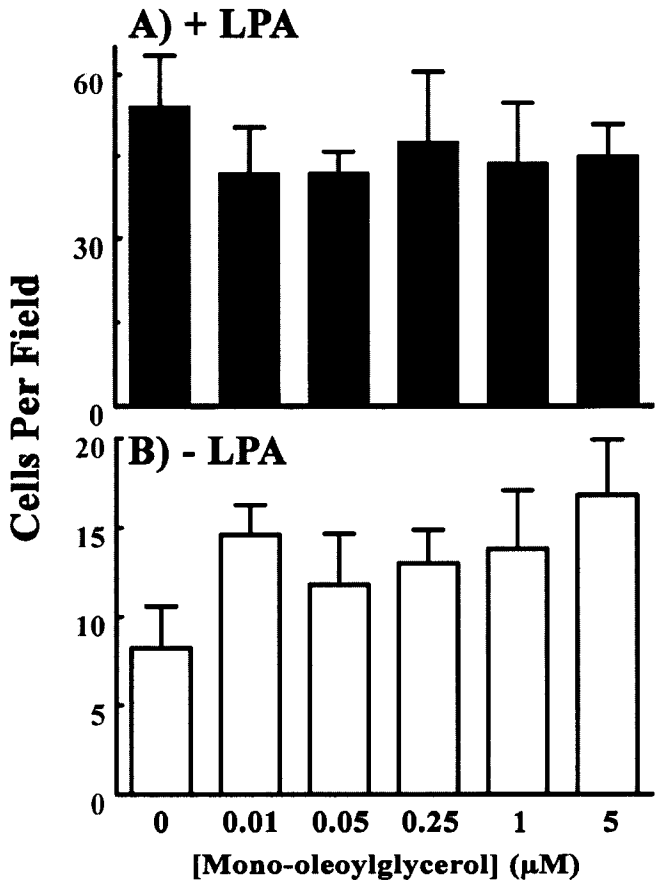

Figure 4.6 Mono-oleoylglycerol does not significantly affect LPA-induced migration of Rat2 fibroblasts. Various concentrations of mono-oleolyglycerol were added to the bottom well of the Transwell chamber in the presence (*black bars, Panel A*) or absence (*white bars, Panel B*) of 0.5 μM LPA. Results are means ± S.D. of migrated cells per field in about 6 fields that were counted. Results are from one experiment.

mono-oleoylglycerol to wild-type fibroblasts in the presence of 0.5 μM LPA. The large range of mono-oleoylglycerol mimics the amount of mono-oleoylglycerol that would be generated from the degradation of exogenous oleoyl-LPA by ecto-LPP activity, with the exception of 1 and 5 μM mono-oleoylglycerol as these concentrations are excessive. Additional mono-oleoylglycerol did not affect LPA-induced migration of wild-type Rat2 fibroblasts (Fig. 4.6A above). Mono-oleoylglycerol alone slightly increased migration (Fig. 4.6B above), however cell migration at this level (7-15 migrated cells per field counted) is small and repeated experiments are necessary to confirm whether a significant increase of migration exists.

4.3.3 *Peroxisome proliferator-activated receptor-γ is not required for lysophosphatidate-induced migration of fibroblasts* – It has been demonstrated that LPA is a ligand for the PPARγ receptor [108, 109]. Increased LPP activity could decrease levels of cellular LPA by dephosphorylation and decrease the activation of PPARγ. Alternatively, increased LPP activity could enable mono-oleoylglycerol formed from the dephosphorylation of exogenous oleoyl-LPA to enter the cell and thereby activate PPARγ after re-phosphorylation. To examine if PPARγ is involved in LPA-, and PDGF-induced migration of Rat2 fibroblasts we pre-incubated fibroblasts with 200 nM GW9662 to inhibit PPARγ activation during migration. This had no significant effect on LPA- or PDGF-induced migration (Fig. 4.7A). Furthermore, the concentration of PPARγ receptors, as determined by Western blotting, was not significantly different among the wild-type, vector control and LPP1 expressing fibroblast after 10 min or 6 h of stimulation by LPA or PDGF (Fig. 4.7B). These combined results suggests that changes

in PPARγ receptor activation do not explain the actions of LPP1 in decreasing fibroblast migration under the 6 h of the present migration assay.

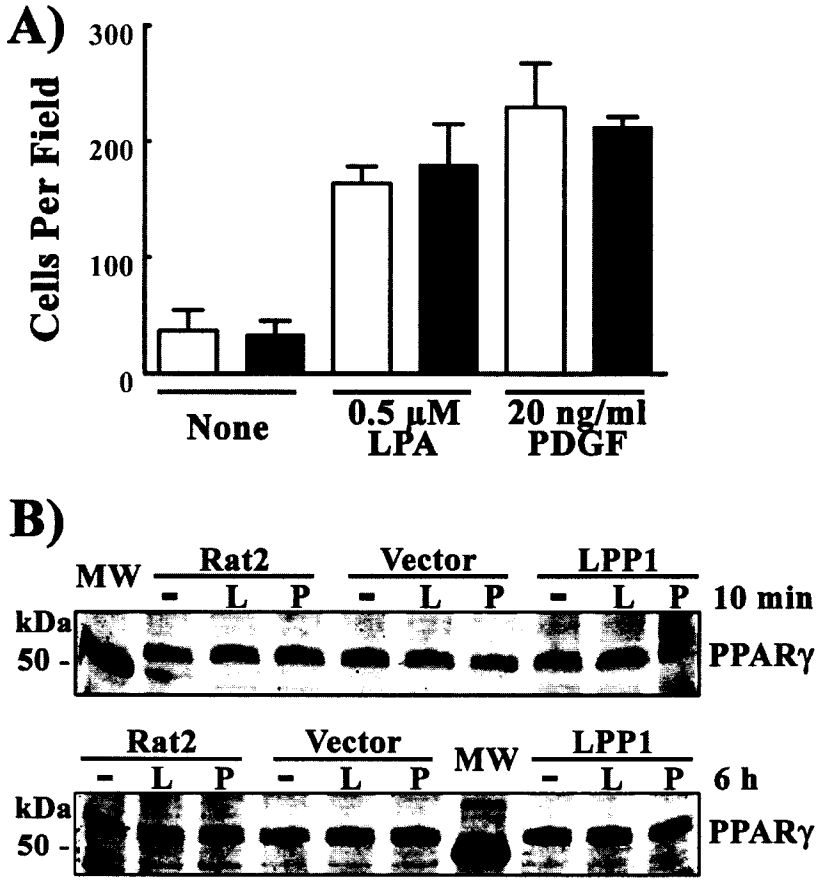

Figure 4.7 PPARγ receptor is not required for LPA-induced migration of fibroblasts. *Panel A* shows migration of wild-type Rat2 fibroblasts in Transwell chambers induced by LPA and PDGF in the presence of 0.1% DMSO (vehicle control in *white bars*), or 200 nM of PPARγ–inhibitor, GW9662 (*black bars*). Results are means ± S.D. for three independent experiments. *Panel B* shows Western blots performed with mouse monoclonal anti-PPARγ antibody. One hundred μg of protein from cells treated for 10 min or 6 h with 0.5 μM LPA (*L*), 20 ng/ml PDGF (*P*), or no treatment (-), were resolved on 7.5%-SDS-PAGE gels. Wild-type (*Rat2*), *vector*, and *LPP1*-over-expressing fibroblasts were analyzed for PPARγ protein levels. The molecular weight standard (*MW*) is 50 kDa. These are representative Western blots from two independent experiments

4.3.4 *Migration induced by lysophosphatidate and the α-hydroxyphosphonate analogue of lysophosphatidate is dependent on $G\alpha_i$* - To investigate the role of the LPP ecto-activity more directly we used the α-hydroxyphosphonate analogue (wls-31) of LPA to promote cell migration (Fig. 4.8A). On the α-position of the hydroxyphosphonate there

is a carbon with a hydroxyl group instead of a phosphodiester as found on LPA (Fig. 4.8A). Therefore, this LPA-analogue cannot be dephosphorylated by the LPPs. However, it is an agonist for $LPA_{1,3}$ receptors [180, 232]. RT-PCR analysis demonstrated that Rat2 fibroblasts express LPA_1, but not LPA_2 or LPA_3, and that vector controls and fibroblasts over-expressing LPP1 have similar LPA_1 mRNA levels (Fig.4.8B). Therefore, it is predicted that any receptor activity induced by wls-31 in Rat2 fibroblasts would be through LPA_1. Indeed, wls-31 stimulated migration of Rat2 fibroblasts (Fig. 4.8C). After pre-incubation of the cells with pertussis toxin, fibroblast migration to LPA, or wls-31 was inhibited by 90 and 85%, respectively, indicating the coupling of LPA_1 to $G\alpha_i$ (Fig. 4.8C). Pertussis toxin, as expected, did not alter PDGF-induced migration.

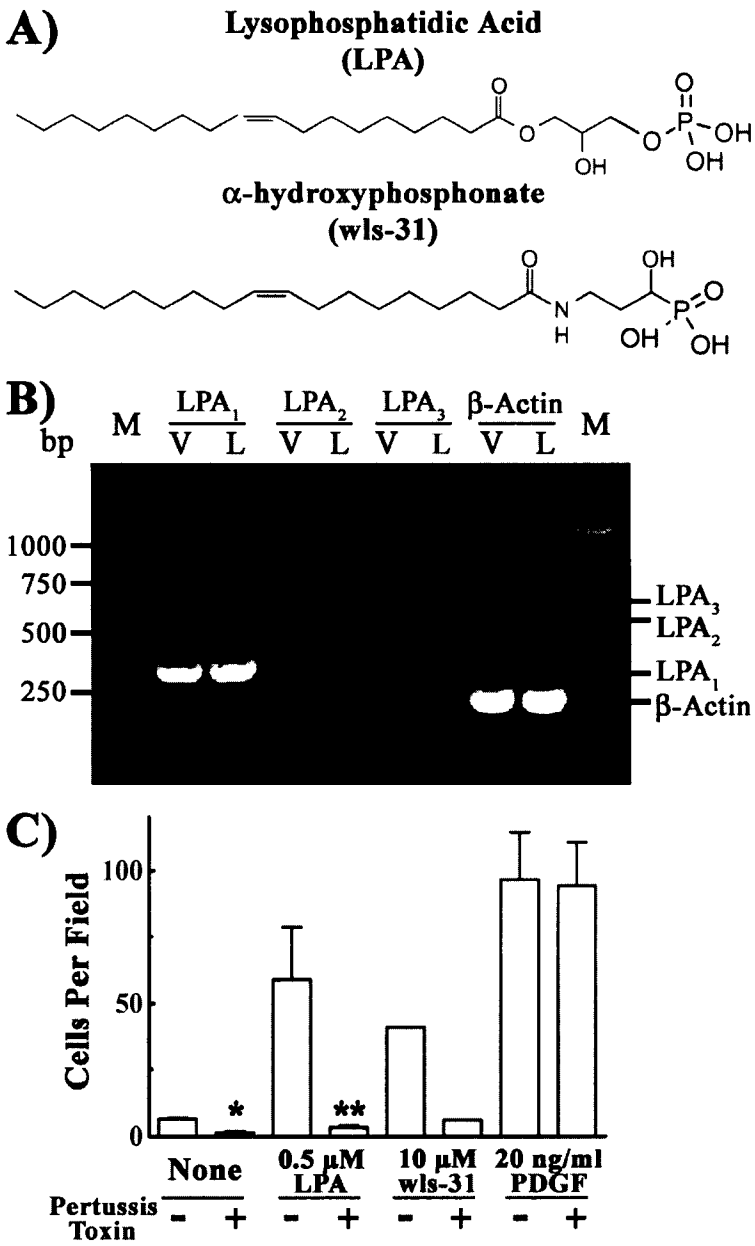

Figure 4.8 LPA, and the non-hydrolysable LPA-analogue stimulated pertussis toxin-sensitive migration. *Panel A* shows the structures of LPA (1-oleoyl, 2-hydroxyl-*sn*-glycerol-3-phosphate) and the non-hydrolysable LPA analogue, wls-31/α-hydroxyphosphonate (*N*-oleoyl-hydroxy propanolamide phosphonic acid). Structures are from Hooks, S.B. *et al* [177]. *Panel B* shows the results of RT-PCR analysis for mRNA for LPA_{1-3} in Rat2 fibroblasts that were transduced with empty vector (*V*) or cDNA for mLPP1 (*L*). The positions of the size marker (base pairs, *bp*) are shown in the lanes labeled "*M*". These results were reproduced in two additional experiments and were performed by De-An Wang, David J. Fischer, and Gabor Tigyi from the University of Tennessee. In *Panel C* wild-type Rat2 fibroblasts were pre-incubated for 18 h with 100 nM pertussis toxin as indicated, before being stimulated with migration agonists. Results are means ± S.D. for three independent experiments. Values for wls-31 in *Panel C* are means from at least five fields of migrated cells in one experiment. Significant differences of the pertussis toxin effect on None-, or LPA-treated fibroblasts (*Panel C*) are indicated by: **, $p<0.01$ and *, $p<0.05$.

4.3.5 *Over-expression of lipid phosphate phosphatase-1 decreases the effects of the α-hydroxyphosphonate analogue of lysophosphatidate in inducing migration of fibroblasts* – The most direct explanation for the specific effects of LPP1 on LPA-induced cell migration is that the ecto-activity of LPP1 decreases the ability of exogenous LPA to stimulate its receptors. Wls-31 is a non-hydrolysable analogue of LPA, capable of inducing Rat2 fibroblast migration through LPA_1 receptor coupled to $G\alpha_i$ (Fig. 4.8C). To test whether the LPP ecto-activity of LPP1 over-expressing cells is responsible for the decrease of LPA-induced migration, we stimulated these cells with wls-31 and measured migration in the Transwell chamber. Increased expression of LPP1 decreased the stimulation of migration by wls-31 (Fig. 4.9). These results suggest that the hydrolysis of extracellular LPA is not required for the LPP1 induced regulation of LPA-induced migration.

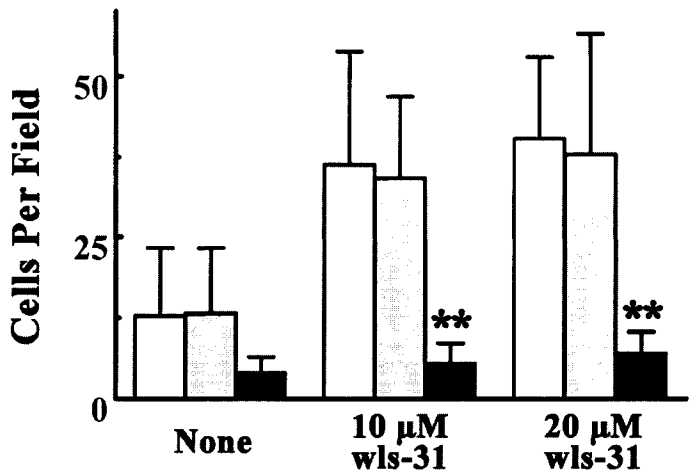

Figure 4.9 The inhibitory effects of LPP1 do not result from the dephosphorylation of extracellular LPA. Wild-type Rat2 fibroblasts (*white bars*), fibroblasts transduced with empty vector (*grey bars*) and fibroblasts that stably over-expressed LPP1 (*black bars*) were stimulated with the non-hydrolysable LPA-analogue, wls-31, to induce migration in Transwell chambers. Results are means ± S.D. for three independent experiments. Significant differences ($p<0.01$) between LPP1 over-expressing fibroblasts and wild-type, or vector control fibroblasts in the same treatment groups are indicated by **.

4.4 Discussion

This Chapter presented work on fibroblast migration that employed both a wound healing assay that detects mainly chemokinesis and a Transwell chamber assay that can detect both chemotaxis and chemokinesis. We used a variety of approaches to establish that the catalytic activity of LPP1 regulates LPA-induced chemokinesis in fibroblasts. The inhibition of LPA-induced migration was observed in Rat2 fibroblasts that stably over-expressed LPP1 by retroviral transduction, in fibroblasts that transiently over-expressed LPP1 after adenoviral infection and in fibroblasts derived from transgenic mice that over-expressed LPP1. Over-expression of enzymes can produce ectopic expression and non-physiological results. Therefore, further evidence was provided by knocking down endogenous LPP1 activity and showing that this increased LPA-induced migration.

Our next objective was to determine the mechanism by which LPP1 controls LPA-induced fibroblast migration. First, LPPs have non-catalytic effects on migration. Human LPP3 possesses an extracellular RGD cell adhesion sequence that promotes cell/cell interactions by binding to integrins (Fig. 1.9A) [187]. Human LPP3 bound to a subset of integrins, and anti-$\alpha_v\beta_3$ and anti-$\alpha_5\beta_1$ antibodies blocked this binding. In platelets, LPP3 co-localized with $\alpha_{IIb}\beta_3$ [179]. Human LPP1 has RGN instead of RGD in hLPP3 (Fig. 1.9A) [141]. This sequence could be involved in regulating migration since peptides with RGD and RGN sequences antagonize the binding of T-lymphocytes to fibronectin [235]. The equivalent sequence in the mouse and rat LPP1 used in the present work is QGN (Fig. 1.9A and B) [141], which probably do not affect cell-cell interactions. The fact that expressing the inactive R217K mutant [148] of mouse LPP1 did not decrease LPA-induced fibroblast migration eliminates a non-catalytic effect of

LPP1 in the present work. However, LPP1 over-expressing fibroblasts readily detach from the plate upon the addition of EDTA, whereas control cells do not. EDTA is a chelator of the divalent cations, particularly Ca^{2+}, that integrins require for their stable interaction with the extracellular matrix (ECM). This evidence suggests that LPP1 could regulate the way integrins interact with the ECM, and that LPP1 over-expression could result in an unstable interaction with the substratum. Since migration is a coordinated cycle of cell detachment-and-re-attachment involving integrins, it is conceivable to hypothesize that the enzymatic activity of LPP1 can regulate integrin function. Chapters 5 and 6 explore possible mechanisms for this phenomenon that is worth further investigation.

The effect of LPP1 on fibroblast migration was specific for LPA since there was no significant effect of LPP1 expression on the stimulation of migration of Rat2 fibroblasts by endothelin, which also stimulates G-protein coupled receptors, or to PDGF that signals through a receptor tyrosine kinase. This lack of effect of LPP1 activity on PDGF-induced migration differs from that reported by Long *et al.* who used a wound healing assay with mouse fibroblasts that expressed 20 gene copies of *Lpp1* [186]. This level of LPP1 expression resulted in decreased ERK activation in response to LPA, PDGF and S1P [186]. We used the equivalent fibroblasts that expressed 2 gene copies of *Lpp1* and therefore had lower LPP1 activity [185, 186]. In these mouse fibroblasts there was no significant LPP1-induced decrease in ERK activation by LPA, or PDGF [185, 186]. However, LPA-induced migration was attenuated in the mouse fibroblasts that expressed 2-gene copies of *Lpp1* (Fig. 4.2B). Therefore, ERK activation in the latter

fibroblasts does not appear to be the target for LPP1 in controlling LPA-induced migration.

Another major difference in our studies and those of Long *et al.* [186] is that we used Transwell chambers that for PDGF determined its predominant effects on chemotaxis rather than chemokinesis, which is determined by the "wound healing" assays. Again, LPP1 expression failed to decrease PDGF-induced fibroblast migration (Figs. 4.2C and 4.3). The effects of LPP1 on LPA-induced migration do not simply relate to a specific blocking of chemokinesis in general since there was no significant action of LPP1 activity on the chemokinetic effects of endothelin (Figs. 4.1B and 4.2D).

Although, the selection of migration stimulants was limited, it appears that LPP1 specifically regulates LPA-induced migration. If this is true the observed decrease of basal migration of fibroblasts over-expressing LPP1, and the enhanced basal migration in fibroblasts with LPP1 knocked down, suggests that fibroblasts generate LPA to induce the majority of the chemokinetic basal migration in a autocrine/paracrine mode. This is supported by the observation that pertussis toxin, which inhibits the function of $G\alpha_i$ coupled to the LPA_1 receptor, almost eliminates basal migration (Fig. 4.8C). Additionally, if the slight increase of migration of fibroblasts by the addition of exogenous mono-oleoylglycerol alone (Fig. 4.6B) can be reproduced in further experiments there is a possibility that LPA can be generated by the phosphorylation of mono-oleoylglycerol by the cell. A role for LPA in an autocrine/paracrine stimulation of cell migration is of interest to investigate in terms of its involvement in the initiation and progression of cancer.

The next question was whether LPP1 modified fibroblast migration specifically to LPA by dephosphorylating exogenous LPA and therefore its ability to activate LPA receptors. Indeed, compared to control cells, over-expression of LPP1 resulted in an increase of exogenous LPA degradation that was maintained during the migration process (Table 4.2). The total breakdown of LPA in the Transwell assay by LPP1 over-expressing fibroblasts never exceeded 22% of the exogenous LPA. We also added excess LPA (up to 10 μM) to stimulate migration, but this did not reverse the LPP1-induced inhibition. Also, mice with transgenic over-expression of the LPP1 show several abnormalities, but their plasma LPA levels remain unchanged compared to wild-type mice [185]. Therefore, these results support the possibility that LPP activity on the bulk concentrations of exogenous LPA cannot account for the observed changes in LPA-induced migration. It is possible that a small pool of added LPA has access to LPA receptors and that this is the pool specifically metabolized by LPP1 to control migration. Alternatively, the ecto-activity could enable mono-oleoylglycerol formed from exogenous oleoyl-LPA to enter the cell and thereby regulate LPA-induced migration after re-phosphorylation [84, 113] and stimulation of internal LPA_1 [106], or PPARγ receptors [108, 109]. We excluded this possibility by adding mono-oleoylglycerol to the outside of wild-type fibroblasts in the presence of oleoyl-LPA and demonstrated that there was no effect on LPA-induced migration. We also showed that using an inhibitor of PPARγ receptor activity did not alter migration and that PPARγ receptor expression was not altered significantly by increasing LPP1 activity. It would be necessary to determine if the inhibitor did actually inhibit PPARγ by using a reporter assay that measures its transcription activity.

However, the most compelling result that excludes an effect of ecto-LPP1 activity on migration is that over-expressing LPP1 also decreased migration to the α-hydroxyphosphonate analogue of LPA, wls-31. Wls-31 cannot be hydrolyzed by LPP1. This compound has agonist activity for LPA_1 receptors [180, 232] that are expressed in Rat2 fibroblasts. In our work the effects of LPA and wls-31 on migration was inhibited by pertussis toxin, indicating receptor coupling to $G\alpha_i$. Since the LPP1 effect is depended on catalytic activity, it could be mediated by changing the metabolism of a lipid phosphate formed downstream of LPA_1 activation. LPP1 potentially hydrolyzes a variety of intracellular lipid phosphates including LPA, PA, ceramide 1-phosphate and S1P provided that these substrates have access to the enzyme [84, 113]. Evidence to support an intracellular role for LPP1 has been growing and will be discussed in the next Chapter.

CHAPTER 5

LIPID PHOSPHATE PHOSPHATASE-1 REGULATES CELL SIGNALING

A version of this chapter has been published. Pilquil, C., Dewald, J., Cherney, A., Gorshkova, I., Tigyi, G., English, D., Natarajan, V., Brindley, D. N. 2006. J Biol. Chem. 281: 38418-29.

5.1 Introduction

Chapter 4 established that the catalytic activity of lipid phosphate phosphatase 1 (LPP1) was responsible for the decrease of lysophosphatidate (LPA)-induced migration. However, pertussis toxin-sensitive migration stimulated by LPA was not attenuated by LPP1-mediated extracellular dephosphorylation of LPA. It was demonstrated that fibroblast migration induced by an LPA analogue that could not be dephosphorylated by LPP activity, was still attenuated when LPP1 was over-expressed. This suggests that the LPP1 target is downstream of the LPA receptor. Evidence of a role for LPP1 in regulating signaling within the cell has been accumulating (read Section 1.4.6 for examples).

This Chapter will focus on the effect that LPP1 activity has on intracellular signaling events that follow the stimulation by LPA or PDGF. LPP1 expression changed the activation of important signaling effectors for LPA and PDGF such as phospholipase D (PLD), extracellular signal-regulated kinase (ERK), and the Rho family of GTPases. We determined that PLD2 plays a role in LPA-, but not PDGF-induced migration although they both can stimulate PLD2 activity. We also examined how LPP1 affects phosphorylation patterns of proteins in whole lysates from cells stimulated by various agonists other than LPA.

5.2 Lipid phosphate phosphatase-1 expression decreases phosphatidate accumulation and phospholipase D activity after stimulation with either lysophosphatidate or platelet-derived growth factor

5.2.1 *Phosphatidate accumulation in agonist-stimulated fibroblasts* – Since the decrease of LPA-induced migration by LPP1 is not dependent on the external breakdown of exogenous LPA, and is dependent on LPP1 catalytic activity, we hypothesized that an intracellular signaling lipid phosphate is the target of dephosphorylation that results in the decrease of LPA-induced migration. We chose to investigate phosphatidate (PA) as the internal target. We measured the mass of cellular PA by collecting total phospholipids from fibroblasts and then separated and resolved PA from the other lipids using thin layer chromatography (TLC, see Section 2.8.1). The TLC plate was then stained with Coomassie brilliant blue and the PA was identified and quantitated by comparison to a PA standard. PA was quantified by scanning with the Odyssey Infrared Imaging System using the 700 nm channel where Coomassie stained lipids can be detected with high-sensitivity (Fig. 5.1A and B). Under basal conditions, the levels of PA are about 0.3% of total phospholipids in wild-type Rat2 fibroblasts and fibroblasts stably transduced with empty vector (Fig. 5.1C). Fibroblasts stably expressing LPP1 have 3-fold less basal PA. Upon stimulation with LPA or platelet-derived growth factor (PDGF) there was a 58 and 74% inhibition, respectively, of PA generation in LPP1 over-expressing fibroblasts compared to control fibroblasts (Fig. 5.1C).

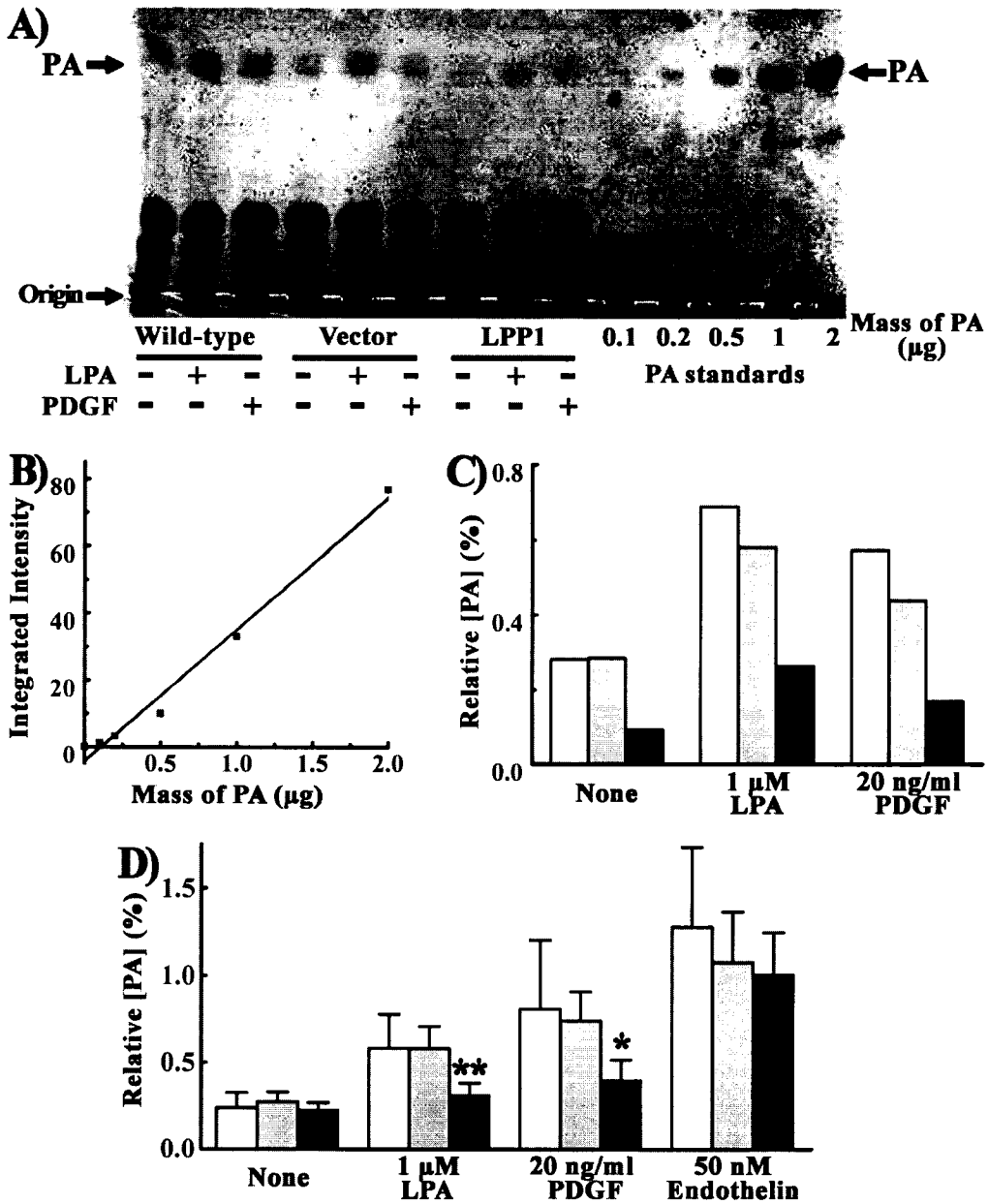

Figure 5.1 Increased LPP1 activity decreases LPA- and PDGF-, but not endothelin-1 induced PA accumulation. *Panel A* shows the Coomassie stained thin layer chromatograph of PA standards and PA from LPA- and PDGF-treated *wild-type* Rat2 fibroblasts, fibroblasts transduced with empty *vector* or cDNA for mouse *LPP1*. Cells were treated with agonists for 30 min before collection of total phospholipids. *Panel B* shows the PA standard curve (r^2= 0.9869) that was used to calculate the mass of total PA relative to the total amount of phospholipid applied to the thin layer chromatography plate (*Panel C*). One experiment was performed. *Panel D* shows the steady-state accumulation of ^{3}H-labeled PA relative to ^{3}H-labeled phosphatidylcholine. The cells are as indicated: wild-type Rat2 fibroblasts (*white bars*), fibroblasts transduced stably with the empty vector (*grey bars*) or cDNA for mouse LPP1 (*black bars*). Results are means ± S.D. for at least four independent experiments. Significant differences between LPP1 over-expressing fibroblasts and wild-type, or vector control fibroblasts in the same treatment groups are indicated by: **, $p<0.01$ and *, $p<0.05$.

It was difficult to stain the silica-based TLC plate with Coomassie, as the silica often separated from the plastic-support in the staining solution. To alleviate this problem we incubated fibroblasts overnight in the presence of [^{3}H]palmitate. The [^{3}H]palmitate readily incorporated into the pool of phospholipids that were separated and resolved in the same methods explained above, so that the labeling of PA could be determined. Basal PA concentrations were not significantly different among the three cell lines (Fig. 5.1D) in contrast to what was observed for PA levels in LPP1 over-expressing cells when stained with Coomassie blue (Fig. 5.1C). Coomassie blue stains total PA, whereas the labeled PA under basal conditions could represent a pool of newly synthesized PA not accessible to LPP1 mediated regulation. Over-expression of LPP1 decreased the LPA- and PDGF-induced increases in the steady-state accumulation of [^{3}H]PA by 70 and 80%, respectively (Fig. 5.1D). Endothelin-1 stimulated PA generation, however LPP1 over-expression did not decrease this accumulation, therefore the cells ability to generate PA was not universally compromised by LPP1 over-expression.

5.2.2 *The measurement of diacylglycerol* – LPP1 dephosphorylates PA to diacylglycerol (DAG), therefore we determined the effects of LPP1 expression on steady state DAG concentrations. LPA, PDGF, and endothelin increased the relative mass of DAG in LPP1 over-expressing fibroblasts, but there was no significant effect of increasing LPP1 activity on DAG accumulation (Figure 5.2).

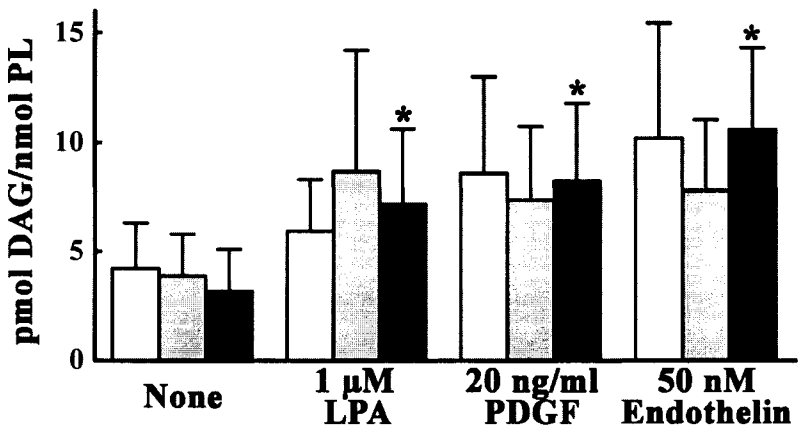

Figure 5.2 Steady-state DAG accumulation is not effected by increased LPP1 activity. Steady-state mass of DAG relative to total phospholipid (PL) assayed was determined by converting DAG to PA in the presence of [γ-^{32}P]ATP and DAG kinase. The cells were treated with the agonists for 30 minutes before total phospholipids were collected. The cells are as indicated: wild-type Rat2 fibroblasts (*white bars*), fibroblasts transduced stably with the empty vector (*grey bars*) or cDNA for mouse LPP1 (*black bars*). Results are means ± S.D. for at least five independent experiments. T-tests between treated and non-treated LPP1 over-expressing cells showed significant differences (p<0.05) indicated by *.

5.2.3 *Phospholipase D activation in fibroblasts* – To determine the site of the LPP1 effect on PA accumulation we measured the effect on phospholipase D (PLD) activation. PLD generates PA by the degradation of the membrane phospholipid, phosphatidylcholine (PC). Over-expression of LPP1 decreased PLD activation after stimulation with both PDGF and LPA (Figure 5.3). Thus the decreased accumulation of PA can result from both decreased formation from PC and by the action of LPP1 on the PA. However, LPP1 did not affect endothelin-induced PLD activity significantly suggesting that LPP1 does not decrease the activation of PLD activities universally (Figure 5.3).

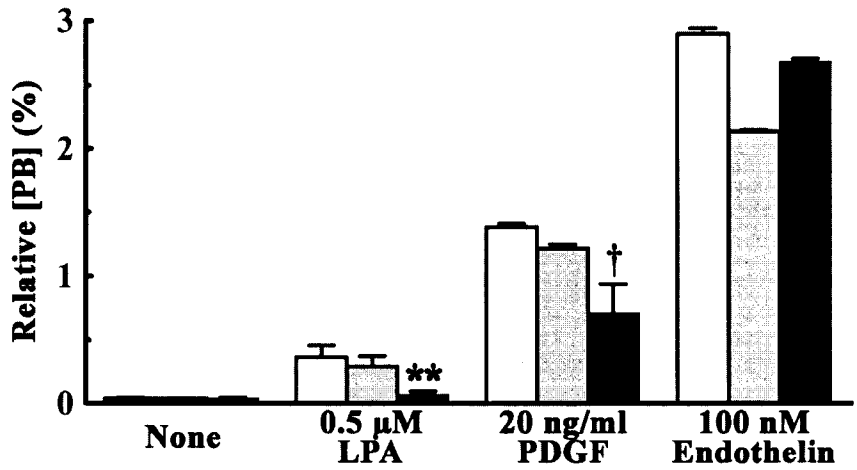

Figure 5.3 Increased LPP1 activity decreases LPA- and PDGF-, but not endothelin-induced PLD activity. Cells were preincubated with 30 mM butan-1-ol for 15 min and then treated with agonists for 6 min before total lipids were collected. PLD activity was measured via the production of ^{3}H-labeled phophatidylbutanol (PB) relative to phosphatidylcholine. The cells are as indicated: wild-type Rat2 fibroblasts (*white bars*), fibroblasts transduced stably with the empty vector (*grey bars*) or cDNA for mouse LPP1 (*black bars*). Results are means ± S.D. for at least three independent experiments for LPA and PDGF, and means and ranges for two independent experiments with endothelin treatment. Significant differences between LPP1 over-expressing fibroblasts and wild-type, or vector control fibroblasts in the same treatment groups are indicated by: †, $p<0.001$ and **, $p<0.01$.

5.3 Phospholipase D2-dependent phosphatidate formation is required for lysophosphatidate-induced migration

5.3.1 *The generation of phosphatidate from phospholipase D activity is required for lysophosphatidate-, but not platelet-derived growth factor- or endothelin-induced migration* – The fact that LPP1 decreased PA accumulation and the activity of PLD did not explain the differential effect of LPP1 in only attenuating LPA-, but not PDGF-induced migration. We, therefore, postulated that PLD activation and PA formation was required for fibroblast migration to LPA, whereas it was not necessary for PDGF-induced migration. This was tested by adding butan-1-ol to the migration assays to block PA formation by PLD. This treatment inhibited the stimulation of migration by LPA, but not to PDGF (Figure 5.4). As a negative control we used butan-2-ol, which does not participate in the transphosphatidylation reaction of PLD. Butan-2-ol did not alter LPA-,

or PDGF-induced migration significantly (Figure 5.4). Endothelin-induced migration of fibroblasts also did not require PA generated from PLD activity (Figure 5.4).

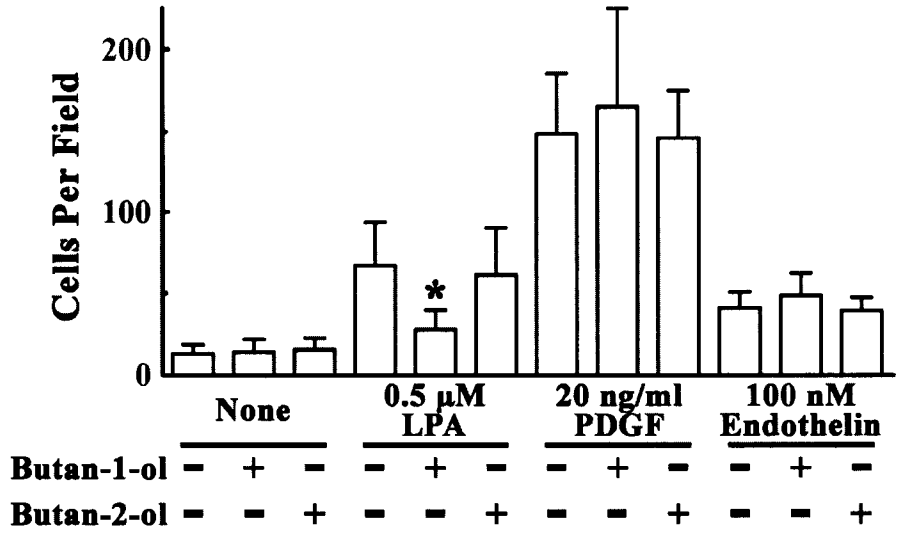

Figure 5.4 PLD activity is required for LPA-, but not PDGF- and endothelin-induced fibroblast migration. Wild-type Rat2 fibroblasts were preincubated with butan-1-ol or butan-2-ol for 15 min before the indicated agonists were added to induce migration in Transwell chambers. Butan-2-ol was used as a negative control because, unlike butan-1-ol, it does not prevent the formation of PA by PLD. Results are means ± S.D. for at least three independent experiments. Significant differences between control and treated fibroblasts are indicated by: *, $p<0.05$.

5.3.2 *Phospholipase D1 and phospholipase D2 activations were induced by lysophosphatidate, platelet-derived growth factor, and endothelin-1* - There are two isoforms of PLD that can contribute to the generation of PA required for LPA-induced migration. To determine if the PLDs are activated by treatment with LPA, PDGF, or endothelin-1 we transfected the fibroblasts with adenoviral vectors that encoded wild-type PLD1 or wild-type PLD2. Adenoviral mediated expression of wild-type PLD1 or PLD2 enhanced the activity of total PLD when Rat2 fibroblasts were treated with the agonists (Fig. 5.5). Therefore, both PLD isoforms were capable of being induced by these agonists including LPA. Although Western blots were not produced to determine the levels of relative PLD expression, the basal PLD activity of fibroblasts with PLD2 over-

expression was 20- and 6-fold higher than vector controls and PLD1 over-expressing fibroblasts, respectively (Fig. 5.5). This observation is consistent with the literature that states PLD2 is constitutively active, whereas PLD1 is not [74].

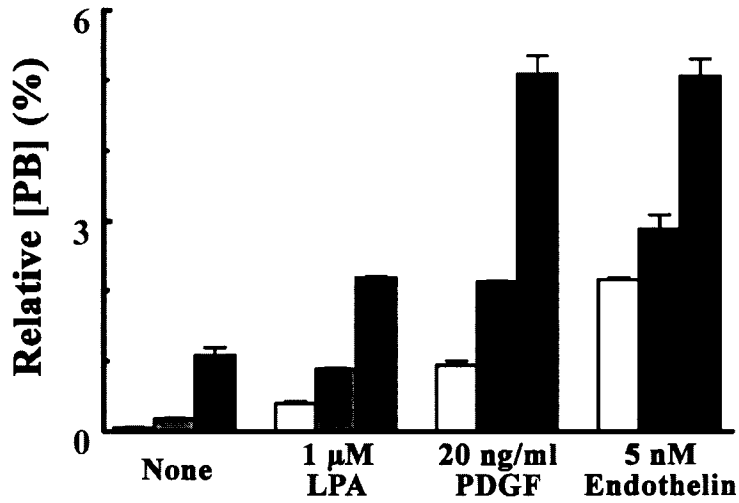

Figure 5.5 Activation of over-expressed wild-type PLD1 or wild-type PLD2 were induced by LPA, PDGF and endothelin-1 in Rat2 fibroblasts. Cells were preincubated with 30 mM butan-1-ol for 15 min and then treated with agonists for 6 min before total lipids were collected. Phospholipase D activity was measured via the production of ^{3}H-labeled phosphatidylbutanol (PB) relative to phosphatidylcholine. Cells were infected with 50 MOI of adenovirus to transiently express wild-type PLD1 (*grey columns*), wild-type PLD2 (*black columns*), or empty vector (*white columns*). Results are means and ranges of duplicate samples from one experiment.

5.3.3 *Phospholipase D2, but not phospholipase D1 is necessary for lysophosphatidate-induced migration* – To determine if there is a specific PLD-isoform responsible for LPA-induced migration, we transfected the fibroblasts with adenoviral vectors that encoded dominant/negative mutants of PLD1 and PLD2. Expression of both mutant PLDs was confirmed by Western blotting (Fig. 5.6A and B). We also showed that expressing dominant/negative PLD1 and PLD2 under these conditions decreased LPA-induced PLD activity by an average of 38 and 46%, respectively (Fig.5.6C). Thus, the combined inhibition of total PLD activity was about 84%. These results are compatible with previous work on the efficacy of the mutants in blocking LPA-induced PLD activity

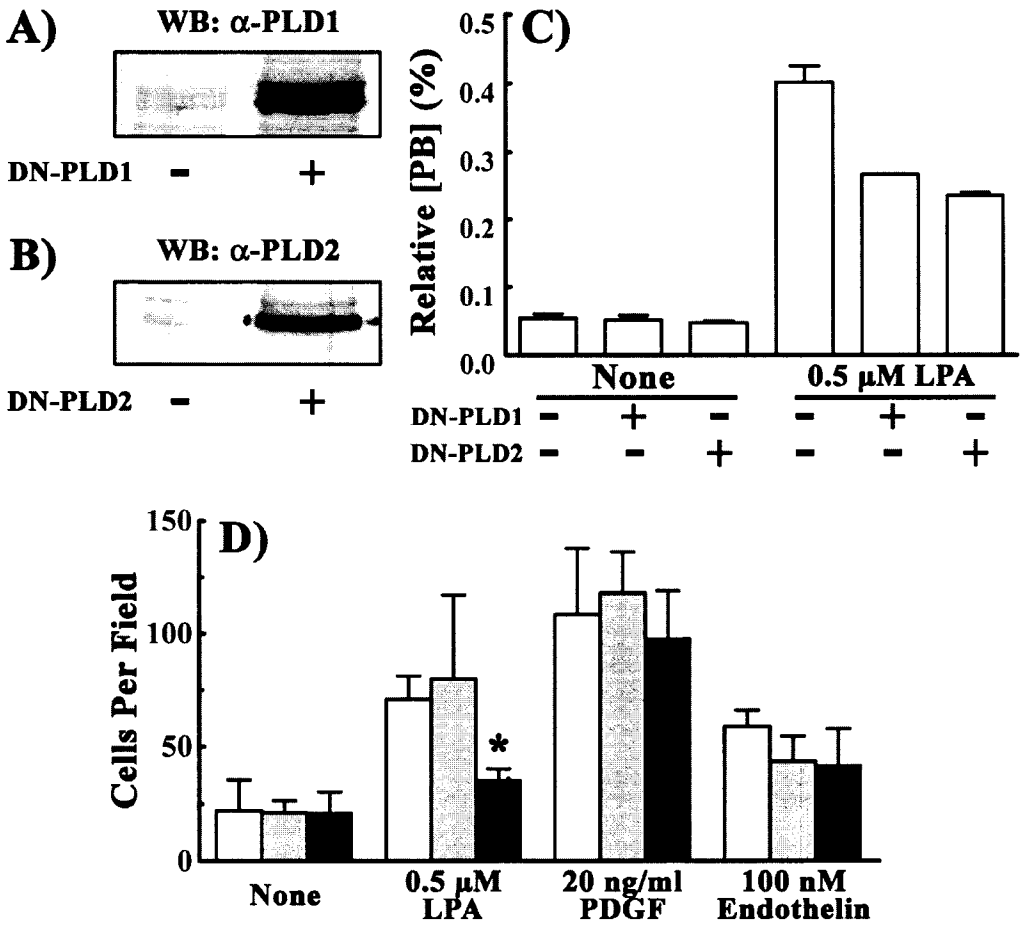

Figure 5.6 PLD2 is required for LPA-, but not PDGF- and endothelin-induced fibroblast migration. *Panels A* and *B* show Western blots that demonstrate the over-expression of dominant/negative (DN) PLD1 and PLD2, respectively, by adenoviral infection of Rat2 fibroblasts. These Western blots are representatives of six independent experiments. *Panel C* shows total LPA-stimulated PLD activities of adenovirus-infected fibroblasts that express empty vector or DN-PLD1 or DN-PLD2. Results are means and ranges of duplicate samples from one experiment. *Panel D* shows the effects of expressing DN mutants of PLD1 (*gray bars*) and PLD2 (*black bars*) compared with vector controls (*white bars*) on LPA-, PDGF-, and endothelin-induced migration of wild-type Rat2 fibroblasts. Results are means ± S.D. for four independent experiments. Significant differences between control and treated fibroblasts are indicated by: *, $p<0.05$.

[80]. The expression of dominant/negative PLD2 decreased LPA-induced migration by about 75%, whereas expression of dominant/negative PLD1 had no significant effect (Fig 5.6D). By contrast, there was no significant effect of either PLD mutant on PDGF-, and endothelin-induced migration.

5.3.4 *Lysophosphatidate does not stimulate phosphorylation of the platelet-derived growth factor receptor-β* – It has been reported that PLD2 activity is required for LPA-induced transactivation and tyrosine phosphorylation of the PDGF receptor (PDGFR) in human bronchial epithelial cells [80]. Using an antibody specific for phosphorylated Tyr^{751} of the PDGFRβ, Western blot analysis showed that 1 μM LPA does not induce any detectable PDGFRβ phosphorylation in Rat2 fibroblasts (Fig. 5.7A). Additionally, Western blot analysis using an antibody to probe for general phosphotyrosine confirmed that LPA does not induce phosphorylation of the PDGFRβ (Fig. 5.7B).

However, pretreatment with the tyrphostin, AG1296, a potent and selective inhibitor of the PDGF receptor tyrosine kinase, inhibited LPA-induced fibroblast migration by about 50%, while PDGF-induced migration was inhibited by 89% (Fig. 5.7C). Epidermal growth factor (EGF)-induced migration was not significantly affected by AG1296 (Fig. 5.7C). This experiment suggested that LPA-induced migration partially requires the tyrosine kinase activity of the PDGF receptors, although LPA-induced tyrosine phosphorylation of the receptor itself was not detected.

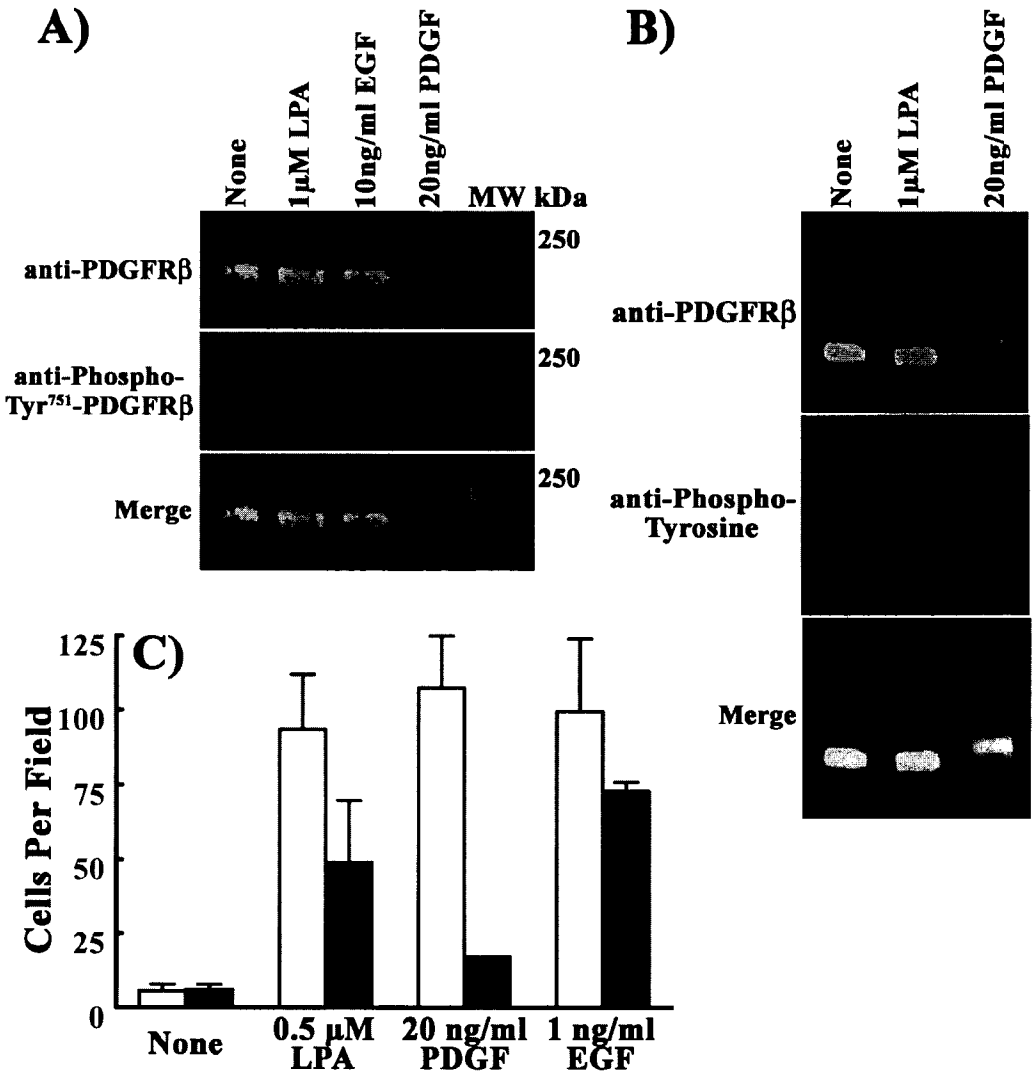

Figure 5.7 LPA does not increase tyrosine phosphorylation on PDGFRβ in Rat2 fibroblasts. *Panels A* and *B* show Western blots of the PDGFRβ (*green*), and phosphorylated Tyr^{751} (*Panel A, in red*), or total tyrosine phosphorylation (*Panel B, in red*) after stimulation with agonists as indicated for 10 min. Primary antibodies used: rabbit polyclonal anti-PDGFRβ (Santa Cruz), mouse monoclonal anti-phospho-Tyr^{751}-PDGFRβ (Cell Signaling), and mouse monoclonal anti-phospho-tyrosine (PY20, Santa Cruz). Nitrocellulose membranes were scanned with the Odyssey Infrared Imaging System to detect emission from the 700 nm (*red*), and 800 nm (*green*) channels, which were then digitally merged to show that the PDGFRβ was tyrosine phosphorylated. *Panel A* is from one experiment whereas *Panel B* is a representative from at least six independent experiments performed by Anton Cherney, a summer student under my supervision. *Panel C* shows agonist-induced migration of wild-type Rat2 fibroblasts that were preincubated for 30 min with 0.1% DMSO (*white bars*) or 10 μM AG1296 dissolved in DMSO (*black bars*). AG1296 is a drug that inhibits the tyrosine kinase activity of PDGFR. Results are means and ranges from two independent experiments.

5.4 Lipid phosphate phosphatase-1 regulates the activation of Rho family GTPases

5.4.1 *Measuring steady-state levels of GTP-bound Rho, Rac, and Cdc42 in fibroblasts under basal conditions and in response to lysophosphatidate and platelet-derived growth factor* - We determined the effects of LPP1 expression on the activation of the small G-proteins Rho, Rac, and Cdc42 which are well known to be involved in cell migration [73]. Total Rho, and Rac concentrations were not changed significantly by LPP1 expression (Fig. 5.8A and D). Activation was measured by affinity precipitation with the domains of proteins that specifically bind the GTP-bound form of the small G-proteins (see Section 2.5). Basal Rho-GTP concentrations in wild-type, vector control and LPP1 over-expressing fibroblasts were not significantly different (Fig. 5.8B and C). However, the LPA-induced increase in Rho-GTP concentration was significantly attenuated in fibroblasts that over-expressed LPP1. Stimulation of the fibroblasts with PDGF under these experimental conditions produced no significant increase in Rho-GTP in any of the cell lines (Fig. 5.8B and C).

The concentration of Rac-GTP under basal conditions was decreased in the LPP1 over-expressing fibroblasts compared to wild-type fibroblasts and the vector controls (Fig. 5.8E and F). Treatment with LPA did not change Rac-GTP concentrations significantly in any of the cell lines under these conditions. Stimulation of the LPP1 over-expressing fibroblasts with PDGF appeared to increase Rac-GTP concentrations in the LPP1 over-expressing fibroblast such that its concentration was not significantly different from the wild-type or vector control fibroblasts (Fig. 5.8E and F). Similarly, Cdc42-GTP concentrations under basal conditions were significantly decreased by an average of 44% in LPP1 over-expressing fibroblasts compared to wild-type fibroblasts

and the vector controls (Fig. 5.7G and H). However, there was no increase of Cdc42-GTP concentrations upon activation with LPA or PDGF in any of the cell lines under these conditions (Fig. 5.8G and H).

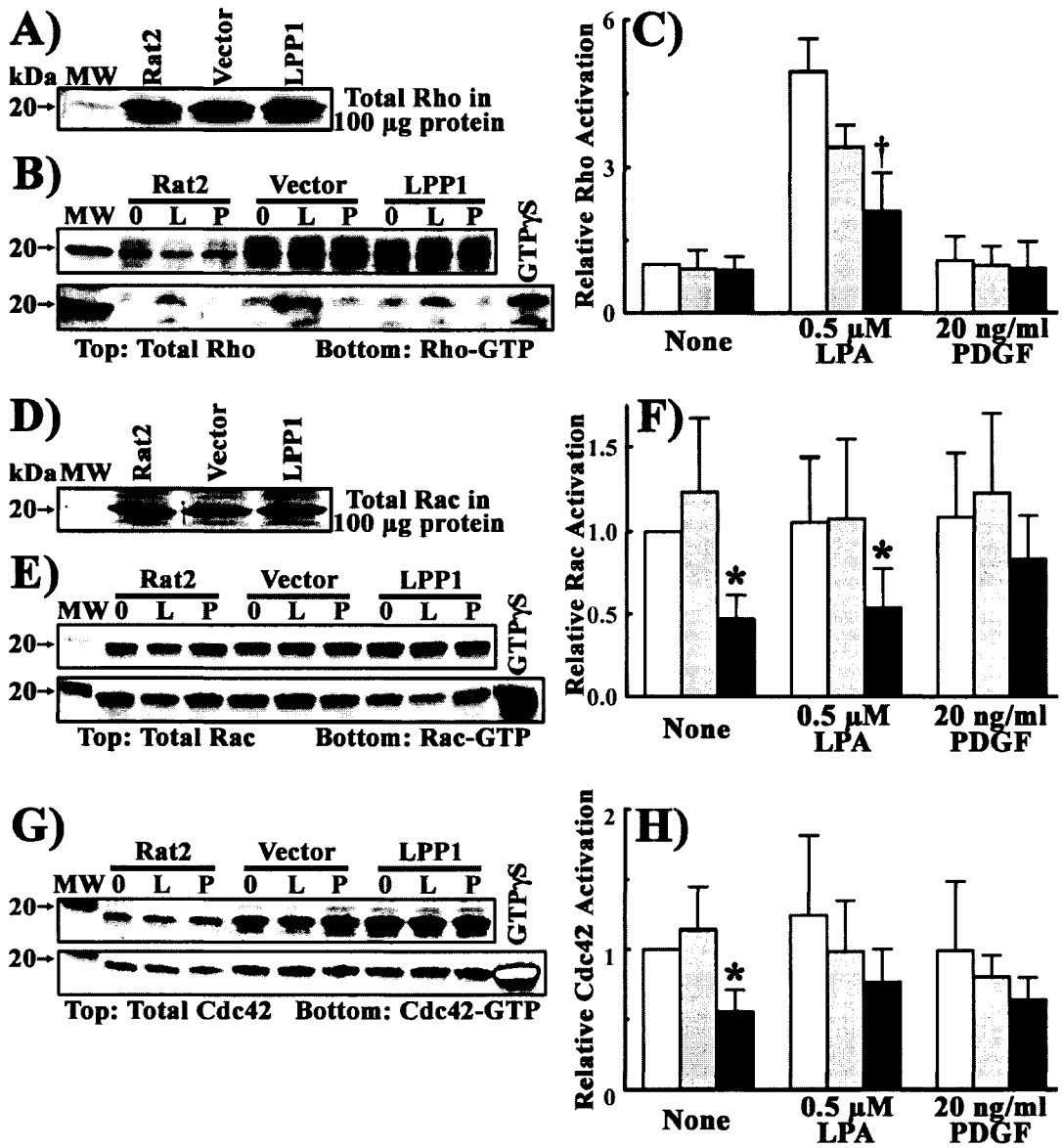

Figure 5.8 Increased LPP1 activity decreases LPA-induced activation of Rho, and the basal activities of Rac and Cdc42. *Panels A*, and *D* show Western blots of total Rho and Rac, respectively, in 100 µg protein from lysates of wild-type *Rat2*, *vector* control, and *LPP1* over-expressing fibroblasts. These are representatives from two independent experiments. *Panels B, E,* and *G* show Western blots of Rho, Rac, and Cdc42, respectively. Fibroblasts were treated with 0.5 µM LPA (*L*), 20 ng/ml PDGF (*P*), or with nothing (*0*) for 10 minutes before their lysates were collected. The top windows show total Rho, Rac, and Cdc42, respectively. There are different amounts of total small G-proteins between the cell lines because the protein assay was bypassed to avoid GTP-hydrolysis in the lysates. The bottom windows show Rho, Rac, and Cdc42, respectively, that were bound to immobilized peptides that specifically recognize, and pull-down their GTP-bound forms. The lane labeled GTPγS is where the G-proteins of wild-type Rat2 fibroblasts were pulled down in the presence of non-hydrolysable GTPγS. *Panels C, F,* and *H* show the relative effects of treating wild-type (*white columns*), vector control (*grey columns*), and LPP1 over-expressing fibroblasts (*black columns*) with the indicated agonists. See Section 2.5 for calculation details. Results are means ± S.D. for at least six independent experiments. Significant differences between LPP1 over-expressing cells and wild-type, or vector control cells in the same treatment groups are indicated by: *, $p<0.05$.

5.4.2 *Phospholipase D does not regulate Rho activity* – Since there was a decrease in steady-state levels of GTP-bound Rho upon stimulation with LPA in fibroblasts over-expressing LPP1, we investigated whether the activation of Rho was dependent on phospholipase D activity, which was also attenuated by LPP1. Pre-treatment of wild-type fibroblasts with butan-1-ol did not inhibit LPA stimulation of Rho, nor did the expression of dominant/negative PLD1 or PLD2 (Figure 5.9). Therefore, the activation of Rho induced by LPA was not dependent on PLD activity.

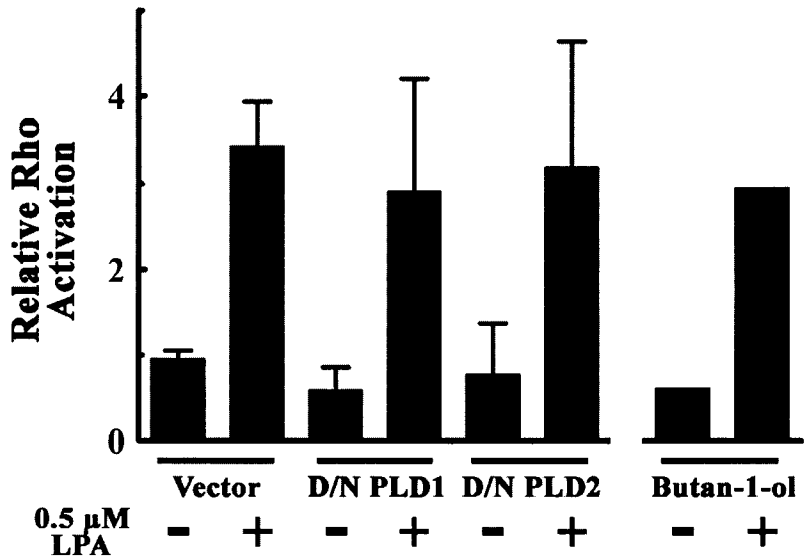

Figure 5.9 Inhibition of PLD does not affect Rho activation by LPA. Wild-type Rat2 fibroblasts were infected with an empty adenoviral vector, or vectors containing cDNA for dominant/negative PLD1, or PLD2. Wild-type Rat2 fibroblasts were also pretreated with 30 mM butan-1-ol for 15 min, before treatment with 0.5 μM LPA for 10 min. Results are means ± S.D. for at least three independent experiments using adenoviral infected cells and one experiment was performed with butan-1-ol pretreatment.

5.5 Lipid phosphate phosphatase-1 regulates intracellular signaling in Rat2 fibroblasts

5.5.1 *Lipid phosphate phosphatase-1 decreased ERK1/2 activation induced by lysophosphatidate* – Our work showing that LPP1 decreased PLD activity induced by both LPA and PDGF supports our findings that LPP1 affects intracellular signaling

downstream receptor activation. To investigate if other signaling proteins were affected we measured agonist-induced phosphorylation of ERK1, and 2, which is marker for ERK activation. Under the present experimental conditions, LPA-induced ERK phosphorylation was decreased by an average of 62% by stable over-expression of LPP1 (Fig. 5.10A and B). However, there was no significant effect of LPP1 over-expression on PDGF-induced ERK activation.

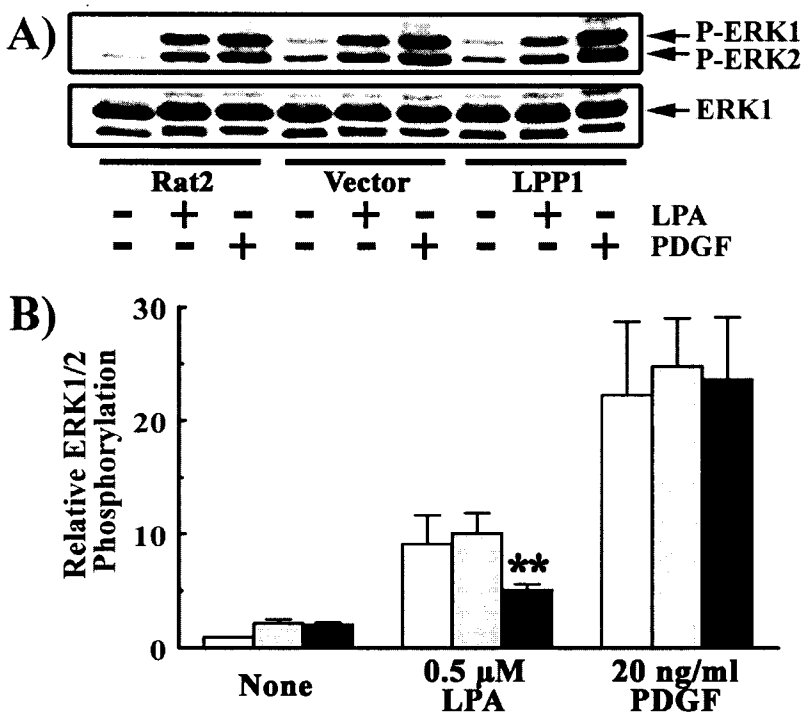

Figure 5.10 Increased LPP1 activity decreases ERK1 and 2 stimulation by LPA, but not PDGF. *Panel A* shows a representative Western blot for phospho-ERK1/2, and total ERK1 that were measured simultaneously on the same membrane. *Panel B* shows the quantitation of the Western blots at 10 min after stimulation of wild-type fibroblasts (*white columns*), vector control cells (*grey columns*) and LPP1 over-expressing cells (*black columns*) with LPA, or PDGF. Results are means ± S.D. for three independent experiments. Significant differences between LPP1 over-expressing fibroblasts and wild-type, or vector control fibroblasts in the same treatment groups are indicated by: **, $p<0.01$.

5.5.2 *ERK1/2 activation are partially required for lysophosphatidate- and platelet-derived growth factor-induced migration of fibroblasts* – We also investigated whether the decreased activation of ERK could contribute to the effect of LPP1 expression on LPA-induced migration by treating wild-type fibroblasts with 40 μM PD98059 to block ERK activation. This treatment inhibited LPA- and PDGF-induced ERK phosphorylation by about 93 and 77%, respectively (Figs. 5.11A and B). LPA- and PDGF-induced migrations were decreased by about 57 and 37%, respectively, in the presence of 40 μM PD98059 (Figs. 5.11C). These results confirm that ERK activation is partially required for fibroblasts migration. The lack of effect of LPP1 on PDGF-induced migration is compatible with a failure to decrease ERK activation significantly by this agonist in our experimental system.

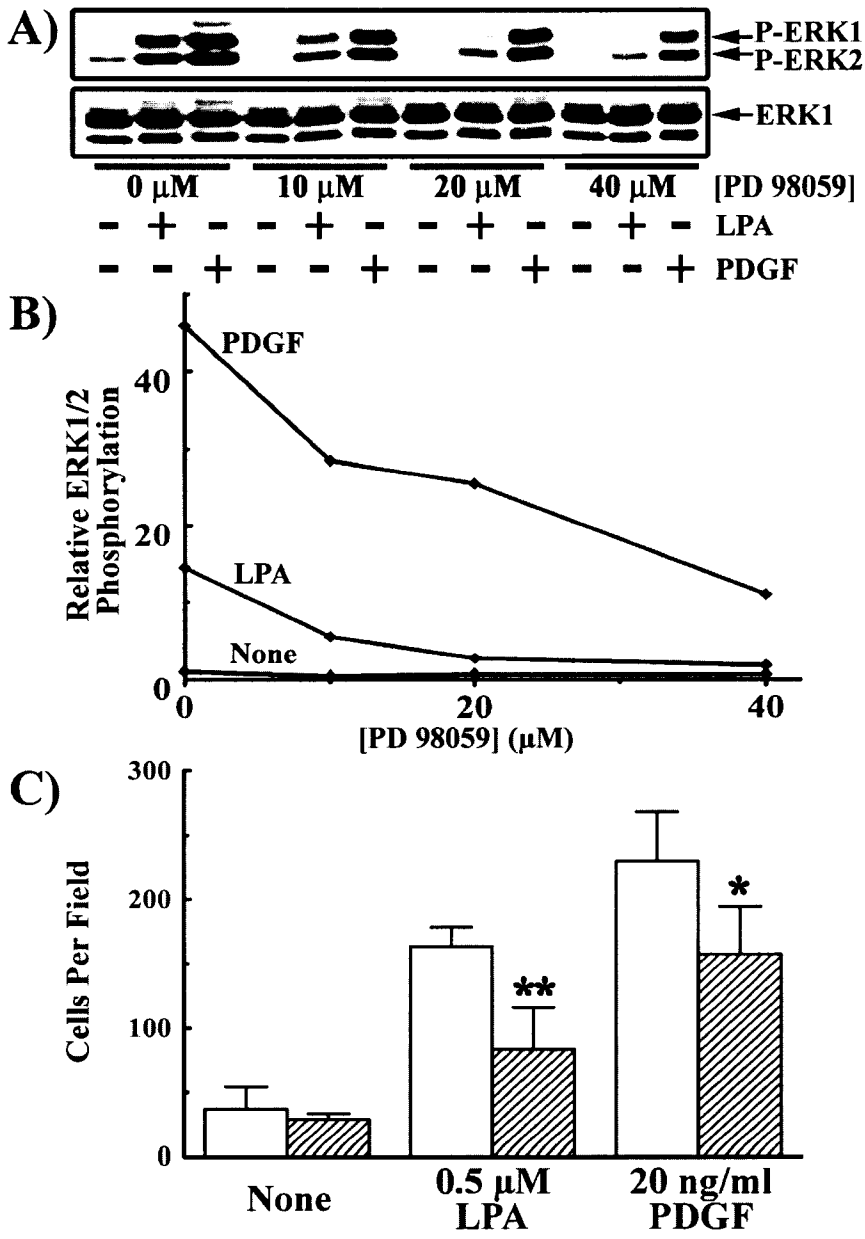

Figure 5.11 Inhibition of ERK1 and 2 decreases LPA- and PDGF-induced migration of Rat2 fibroblasts. *Panel A* shows a Western blot for phospho-ERK1/2, and total ERK1 that were measured simultaneously on the same membrane. Wild-type Rat2 fibroblasts were preincubated with the indicated amounts of PD98059 for 30 min to block ERK1/2 activation induced by either LPA or PDGF as indicated. *Panel B* shows a representative quantitation of *Panel A*. The results in *Panel C* show the effects of 40 μM PD98059 (*hatched columns*) on LPA- and PDGF-induced fibroblast migration compared to vehicle (0.1% DMSO) treated fibroblasts (*white columns*). Results are means ± S.D. for three independent experiments. Significant differences between the PD98059 treatment vehicle control in *Panel C* are indicated by: **, $p<0.01$ and *, $p<0.05$.

5.5.3 *Total phospholipase D activity is required for lysophosphatidate-ERK1/2 activation* – Since ERK is important for LPA-induced migration of fibroblasts, we investigated the role of PLD on the activation of ERK. Pre-treatment of fibroblasts with butan-1-ol to block the formation of PA by PLD1 and 2 inhibited LPA-induced ERK activation (Figure 5.12). This decrease of ERK activation by attenuated PLD activity could explain the decrease of LPA-induced migration by LPP1. However, this experiment was not performed with the required negative control, butan-2-ol, therefore specificity of the butan-1-ol effect is in question.

Infection of the fibroblasts with adenovirus to transiently produce dominant/negative PLD1 or PLD2 did not decease ERK activation by LPA (Figure 5.12). Taken together it appeared the activation of ERK by LPA involves PA that can be generated by either PLD1 or PLD2 activities, however inhibition of PLD1 or PLD2 separately did not alter LPA-induced ERK activation.

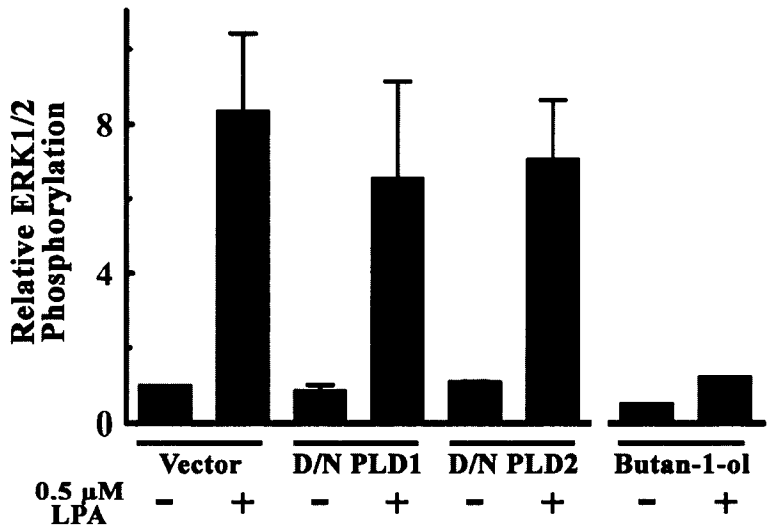

Figure 5.12 Inhibition of PA-generation by total PLD activity inhibits the activation of ERK1 and 2. Wild-type Rat2 fibroblasts were infected with an empty adenoviral vector, or vectors containing cDNA for dominant/negative PLD1, or PLD2. Wild-type Rat2 fibroblasts were also pretreated with 30 mM butan-1-ol for 15 min, before treatment with 0.5 μM LPA for 10 min. Results are means ± S.D. for at least three independent experiments using adenoviral infected cells and one experiment was performed with butan-1-ol pretreatment.

5.5.4 *Calcium ion release is essential for Rat2 fibroblast migration* – Our laboratory previously determined the effects of LPP1 expression on LPA- and PDGF-induced Ca^{2+}-transients. Dr. Indrapal Singh found that increasing LPP1 inhibited Ca^{2+}-release in response to LPA, but not to PDGF (Fig. 5.13A) [174]. This could also explain the different effects of LPP1 in inhibiting LPA-, but not PDGF-induced migration

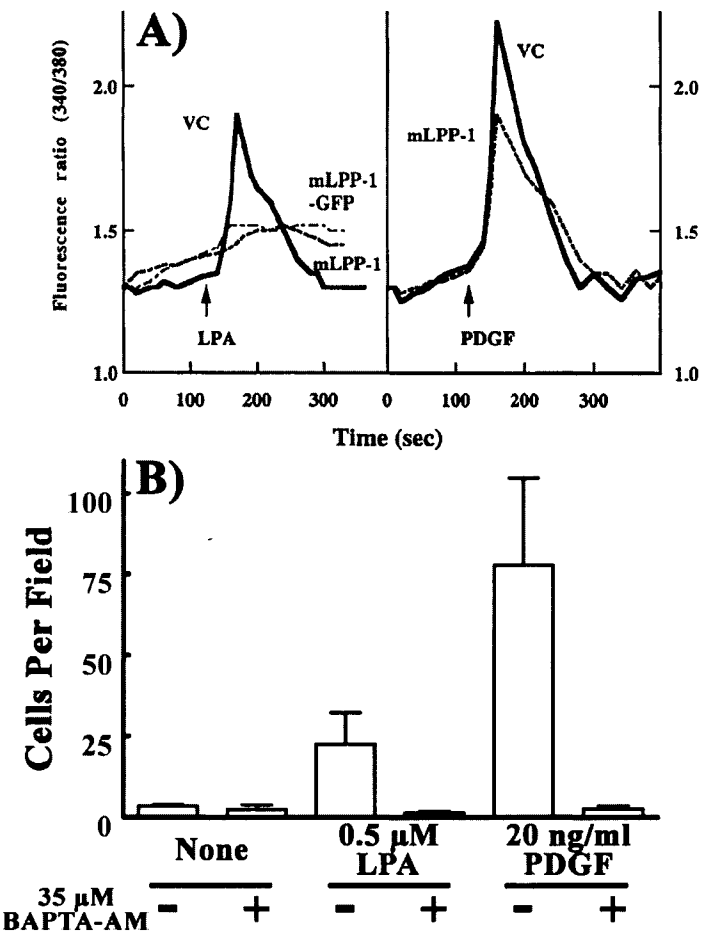

Figure 5.13 Ca^{2+} release is essential for LPA-, and PDGF-induced migration of Rat2 fibroblasts. *Panel A* is a figure prepared by Dr. Indrapal Singh from a paper published in *Prostaglandins* by authors Pilquil, C. *et al* [174]. It shows the increases of intracellular Ca^{2+} as changes in Fura-2-AM fluorescence ratio ($R_{340/380}$). Vector control fibroblasts and fibroblasts expressing mouse LPP1 and mouse LPP1-GFP fusion protein were simulated with 10 μM LPA, or 50 ng/ml PDGF at 120 s. *Panel B* shows the migration of wild-type Rat2 fibroblasts in Transwell chambers induced by LPA or PDGF in the presence of BAPTA-AM. Results are means ± S.D. of cells counted in at least five fields in one experiment. Alistair Ilich, a summer student under my supervision, performed this experiment.

since the stimulation of fibroblast migration by both of these agonists depends upon the Ca^{2+}-transient. This conclusion is illustrated by our observation that adding BAPTA-AM to specifically bind intracellular Ca^{2+} transients blocked LPA- and PDGF-induced migration by 83 and 97%, respectively (Fig. 5.13B).

5.5.5 *Lipid phosphate phosphatase 1 expression changes phosphorylation patterns of proteins from fibroblasts stimulated by various agonists* – LPP1 decreased LPA-, and PDGF-induced PLD activity. LPP1 decreased LPA-induced Rho, and ERK activation. LPP1 also decreased the basal activities of Rac and Cdc42 in fibroblasts. It is apparent that LPP1 can affect important signaling proteins that regulate a broad range of cell functions. To appreciate the broader role LPP1 has on cell signaling we treated fibroblasts stably over-expressing LPP1, and control cell lines, with various agonists. Because a significant aspect of cell signaling depends on the level of protein phosphorylation, we performed Western blot analysis on the proteins of these stimulated cells using various antibodies that detect phosphorylated serine and threonines. An increase of intensity of a band representing a protein from stimulated cells indicates an increase of phosphorylation of that protein, and vice versa. Cells were stimulated with platelet-derived growth factor (PDGF), and epidermal growth factor (EGF) that activate receptor tyrosine kinases. We also employed LPA, sphingosine-1-phosphate (S1P), bradykinin, and thrombin, which are ligands for G-protein coupled receptors.

Western blot analysis using an antibody that detected phosphorylated threonine only when followed by proline revealed some differences under basal conditions between control cells and LPP1-over-expressing cells. For example the intensity of a band around 55 kDa was higher in vector control cells (Fig. 5.14A). In control cells the intensity of

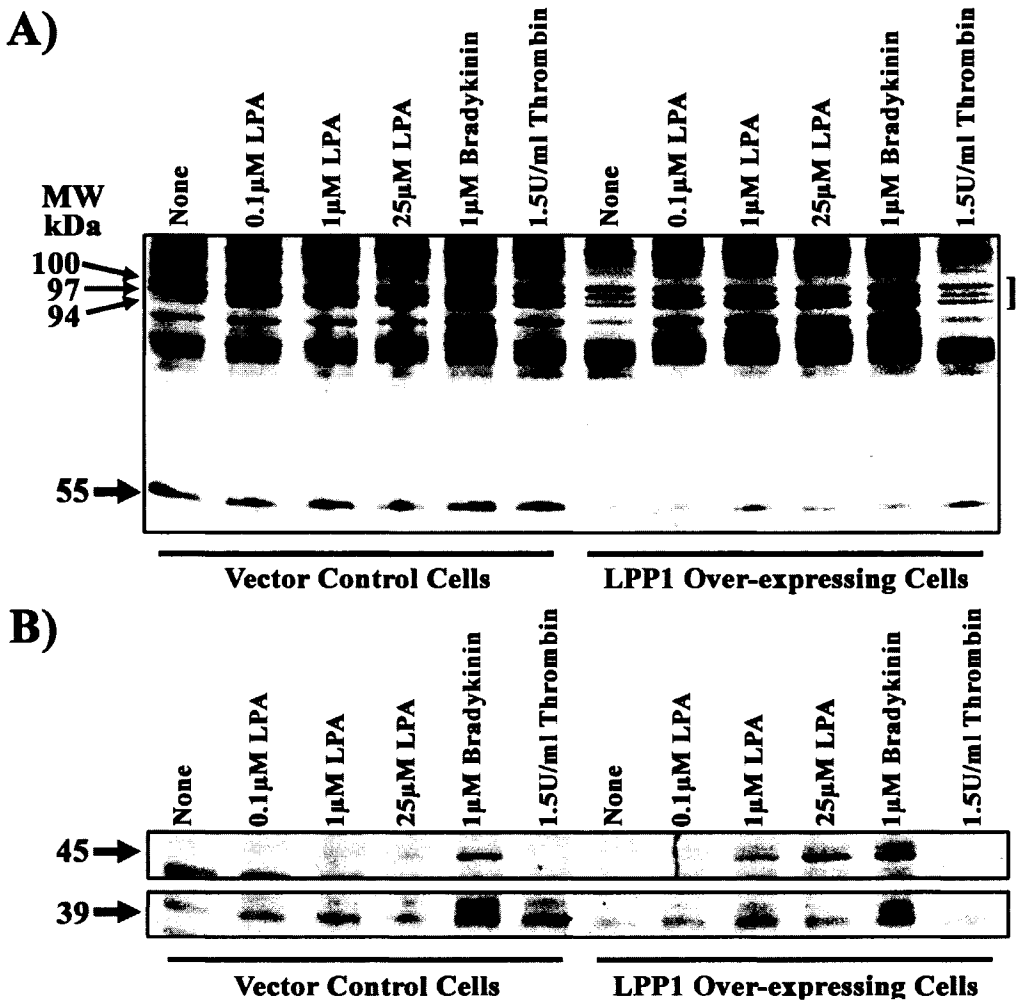

Figure 5.14 Western blot analysis using a primary antibody that detects phospho-threonine if only followed by a proline. Rat2 fibroblasts stably transduced with an empty vector or cDNA for mouse LPP1 were treated with the indicated agonists for 10 minutes. Lysates were collected and 100 μg of protein was resolved on a 10% SDS-PAGE gel. Proteins were transferred to nitrocellulose membrane, which was probed with a monoclonal antibody that detects phospho-threonine if only followed by a proline. Detection of phoshphorylated proteins was achieved with an anti-mouse IgG conjugated to horseradish peroxidase, ECL and Kodak BioMax film. *Panel A* shows the Western blot spanning the molecular weight markers of 120 to 52.2 kDa, which are not shown. The left half of the blot shows the samples from fibroblasts transduced with empty vector in comparison to the right half, which shows the samples from fibroblasts transduced to stably express LPP1. *Panel B* shows parts of the same Western blot in *Panel A*, but at regions of smaller molecular weights and with longer exposure of the film to the ECL-treated membrane. Bands of interest are indicated with *arrows*, *square brackets* and *apparent molecular weight*. This experiment was performed once.

this band did not change upon stimulation, however in LPP1 over-expressing cells there was an increase of intensity upon stimulation by LPA, bradykinin and thrombin, which showed 5-fold stimulation (Fig. 5.14A). There was a set of three bands at about 94, 97,

and 100 kDa. Under basal conditions the intensity of the 94 kDa band in vector control cells was lower than that of LPP1-over-expressing cells (Fig. 5.14A). Upon stimulation with LPA and bradykinin the intensity of this band increased in both cell lines. Although intensity of the band was higher in LPP1-over-expressing cells, the stimulation by LPA was similar in both of the cell lines (Fig. 5.14A). However, stimulation by thrombin was attenuated by up to 100% in LPP1 over-expressing cells compared to control cells (Fig. 5.14A). Stimulation of LPP1 over-expressing cells with LPA or bradykinin revealed a band at 45 kDa that was not present in LPA-stimulated control cells (Fig. 5.14B). Stimulation with thrombin increased the intensity of a 39 kDa band in control cells, but not in LPP1 over-expressing cells (Fig. 5.14B).

Western blot analysis using an antibody that detected phospho-serine or -threonine in the context of tyrosine, tryptophan or phenylalanine at the -1 position or phenylalanine at the +1 position showed that vector control cells stimulated with bradykinin and thrombin increased phosphorylation of a protein at about 78 kDa, whereas it did not increase phosphorylation in LPP1-over-expressing cells (Fig. 5.15). Intensity of a 59 kDa protein was higher in control cells, but stimulation of phosphorylation with LPA was similar in both cell lines (Fig. 5.15). However, stimulation of phosphorylation of the 59 kDa protein by bradykinin was attenuated by more than half in LPP1 over-expressing cells.

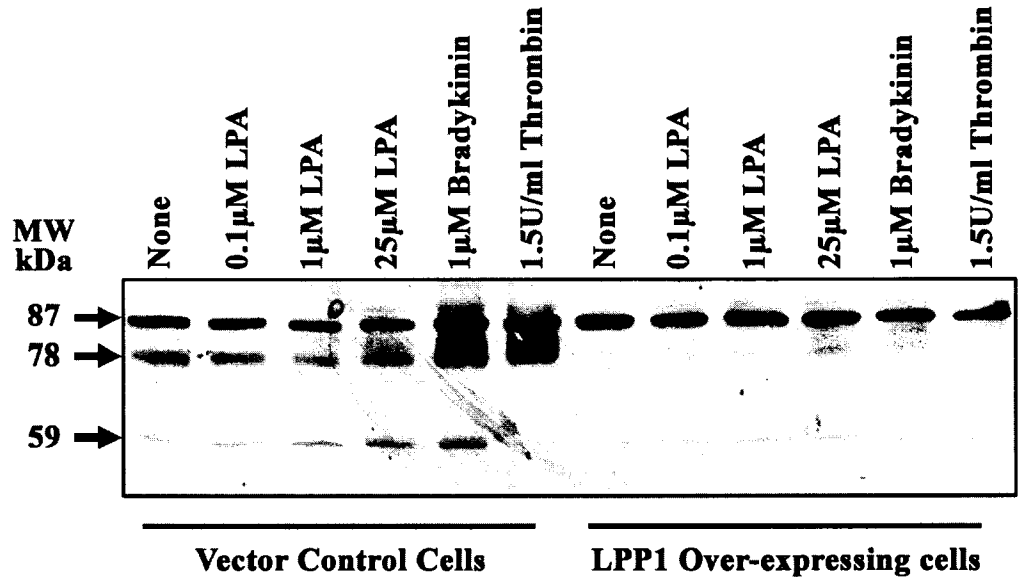

Figure 5.15 Western blot analysis using primary antibodies that detect phospho-threonine or phospho-serine when tyrosine, tryptophan or phenylalanine is at the -1 position or when phenylalanine is at the +1 position. Rat2 fibroblasts stably transduced with an empty vector or cDNA for mouse LPP1 were treated with the indicated agonists for 10 minutes. Lysates were collected and 100 μg of protein was resolved on a 10% SDS-PAGE gel. Proteins were transferred to nitrocellulose membrane, which was probed with polyclonal antibodies that detect phospho-threonine or phospho-serine when tyrosine, tryptophan or phenylalanine is at the -1 position or when phenylalanine is at the +1 position. Detection of phoshphorylated proteins was achieved with an anti-rabbit IgG conjugated to horseradish peroxidase, ECL and Kodak BioMax film. The left half of the blot shows the samples from fibroblasts transduced with empty vector in comparison to the right half, which shows the samples from fibroblasts transduced to stably express LPP1. Bands of interest are indicated with arrows, and apparent molecular weight. This experiment was performed once.

A phospho-threonine antibody that detected proteins phosphorylated at threonine residues in a manner largely independent of the surrounding amino acid sequence showed that upon PDGF stimulation of vector control cells there was a decrease of phosphorylation of a protein at about 105 kDa. However, in LPP1-over-expressing cells there was no decrease of phosphorylation (Fig. 5.16). This was specific for PDGF, because EGF, LPA, bradykinin, and thrombin treatment decreased the phosphorylation of this protein in both cell lines (Fig. 5.16). Proteins of 45 and 39 kDa showed an enhanced phosphorylation upon treatment with PDGF, and EGF in LPP1 over-expressing cells, but

showed an attenuated stimulation of phosphorylation when treated with bradykinin and thrombin compared to vector controls (Fig. 5.16).

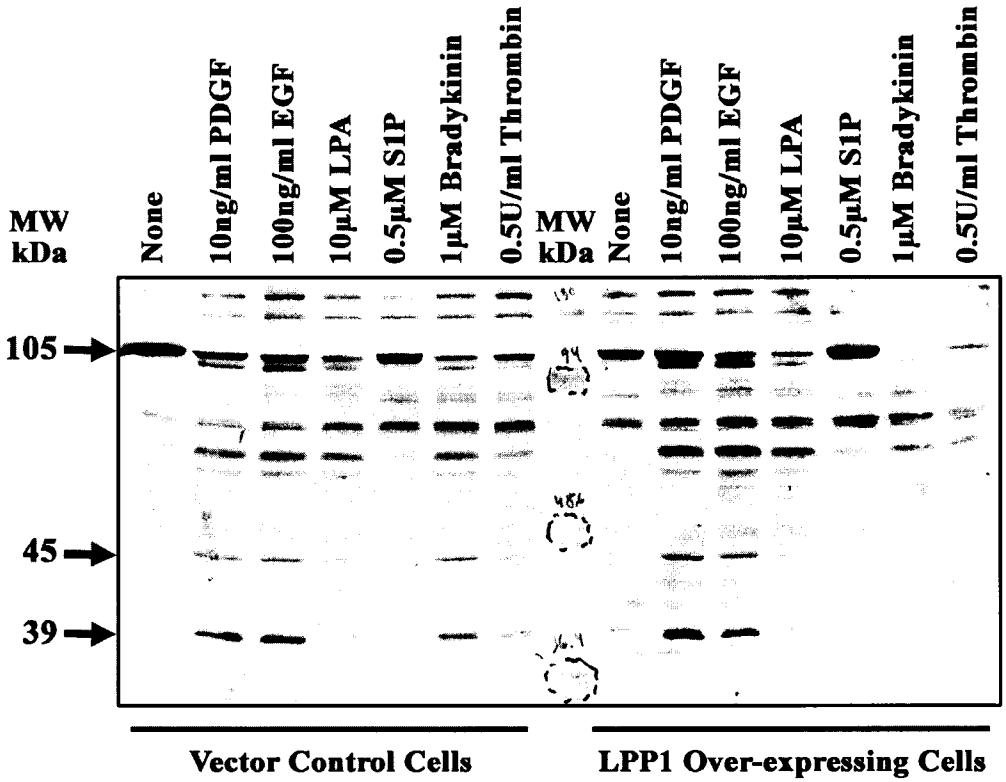

Figure 5.16 Western blot analysis using primary antibodies that detect phospho-threonine. Rat2 fibroblasts stably transduced with an empty vector or cDNA for mouse LPP1 were treated with the indicated agonists for 10 minutes. Lysates were collected and 100 μg of protein was resolved on a 10% SDS-PAGE gel. Proteins were transferred to nitrocellulose membrane, which was probed with polyclonal antibodies that detect phospho-threonine regardless of surrounding amino acid sequence. Detection of phoshphorylated proteins was achieved with an anti-rabbit IgG conjugated to horseradish peroxidase, ECL and Kodak BioMax film. The left half of the blot shows the samples from fibroblasts transduced with empty vector in comparison to the right half, which shows the samples from fibroblasts transduced to stably express LPP1. Bands of interest are indicated with *arrows*, and *apparent molecular weight*. This experiment was performed once.

We also employed an antibody that was specific for phosphorylated threonine or serine phosphorylated by Akt (also known as protein kinase B). Among differences in phosphorylation between the two cell lines the most dramatic was the enhancement of phosphorylation of proteins at about 45 kDa in LPP1-over-expressing cells stimulated

with PDGF, EGF and LPA (Fig. 5.17). This enhancement of phosphorylation was not seen after stimulation with bradykinin or thrombin, in fact there was an attenuation of bradykinin- and thrombin-stimulated phosphorylation of these proteins in LPP1 over-expressing cells (Fig 5.17).

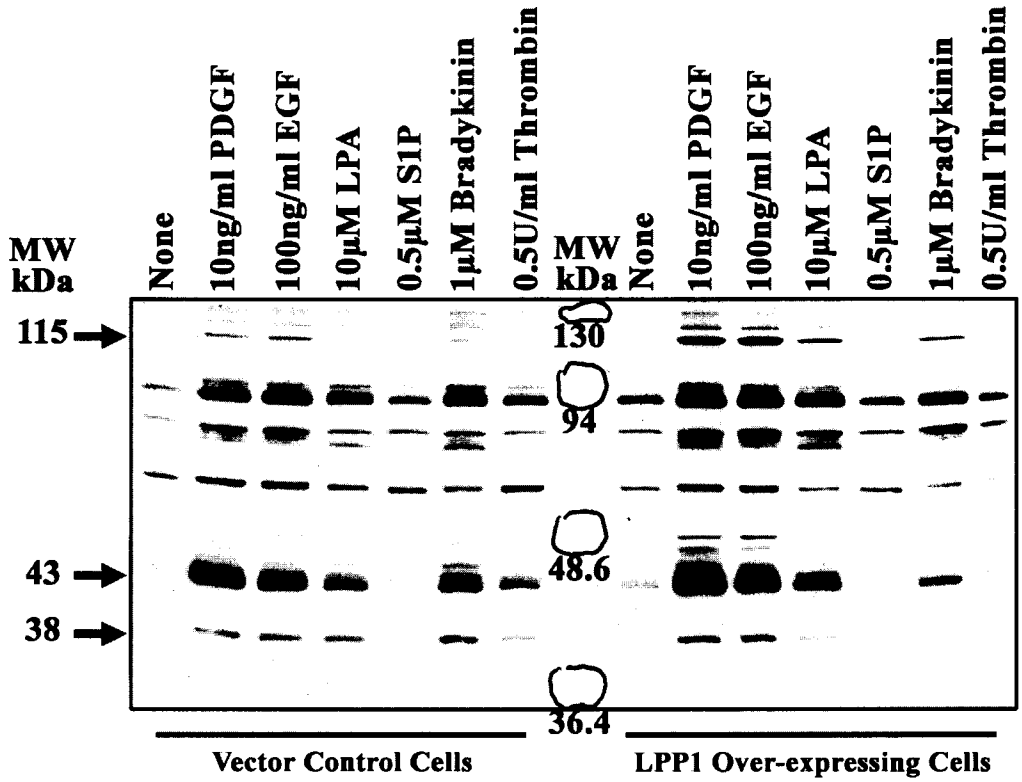

Figure 5.17 Western blot analysis using primary antibodies that detect threonine or serine phosphorylated by Akt. Rat2 fibroblasts stably transduced with an empty vector or cDNA for mouse LPP1 were treated with the indicated agonists for 10 minutes. Lysates were collected and 100 μg of protein was resolved on a 10% SDS-PAGE gel. Proteins were transferred to nitrocellulose membrane, which was probed with polyclonal antibodies that detect serine or threonine phosphorylated by Akt. Detection of phosphorylated proteins was achieved with an anti-rabbit IgG conjugated to horseradish peroxidase, ECL and Kodak BioMax film. The left half of the blot shows the samples from fibroblasts transduced with empty vector in comparison to the right half, which shows the samples from fibroblasts transduced to stably express LPP1. Bands of interest are indicated with *arrows*, and *apparent molecular weight*. This experiment was performed once.

Akt is a kinase that is activated by phosphoinositides produced by phosphoinositol 3-kinase (PI3-kinase). Pre-treatment of LPP1 over-expressing cells with the PI3-kinase inhibitor, LY294002 (EMD Biosciences), inhibited LPA induced phosphorylation of the proteins, confirming that they are phosphorylated in a PI3-kinase dependent manner (Fig. 5.18A). A time course of EGF-treatment showed that phosphorylation peaked at 5 minutes and continued for at least 1 h after stimulation in both control and LPP1 over-expressing cells (Fig. 5.18B and C).

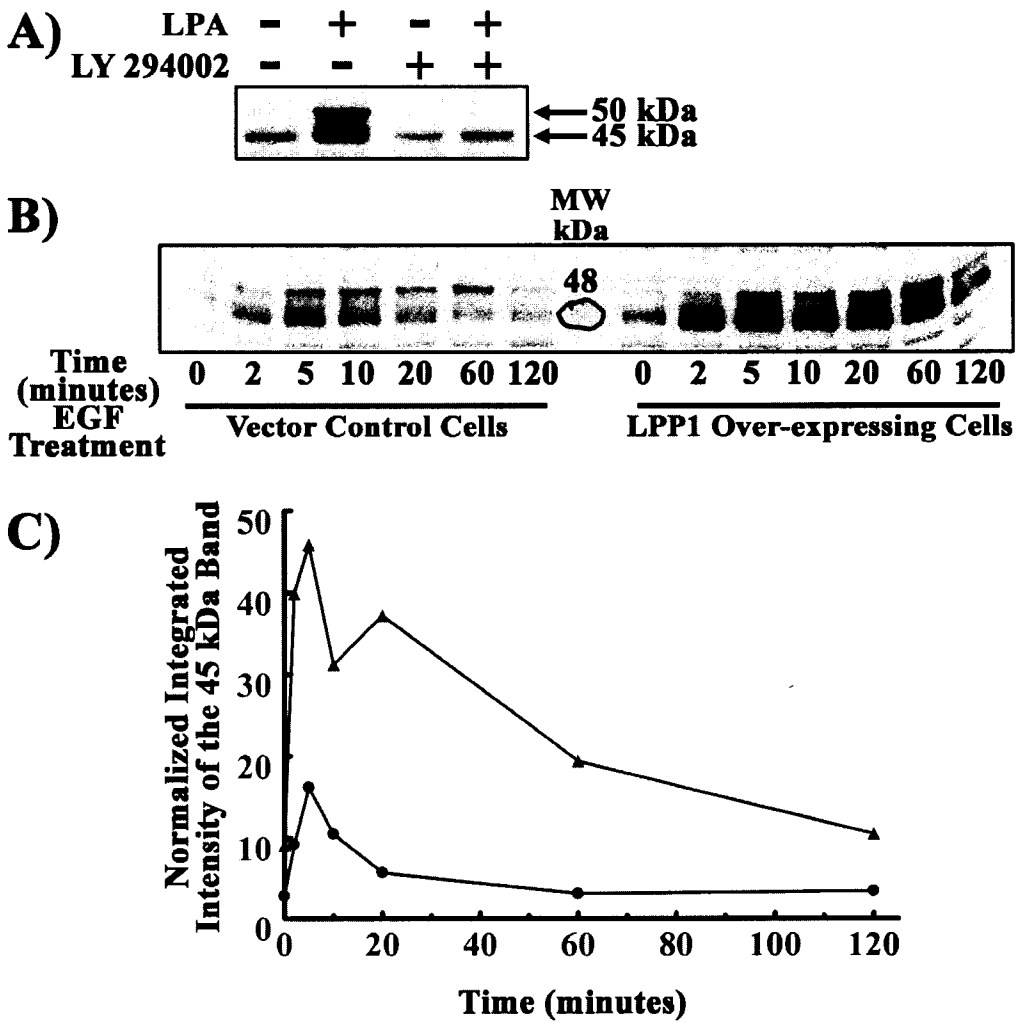

Figure 5.18 Phosphorylation of the 45 and 50 kDa Akt-subtrates peak after 5 min of agonist treatment, and is blocked by a PI3-kinase inhibitor. *Panel A* shows the 45 and 50 kDa proteins of the Western blot that was probed with primary antibodies that detect threonine or serine phosphorylated by Akt. Fibroblasts transduced to stably produce LPP1 were pre-incubated with 0.1% DMSO as a vehicle control, or 20 μM LY294002 (PI3-kinase inhibitor) for 1 h before treatment with or without 5 μM LPA for 5 minutes. *Panel B* shows the Western blot analysis of the 45 and 50 kDa Akt-substrates from vector control cells (*left-half*) or cells over-expressing LPP1 (*right-half*) treated with 100 ng/ml EGF for the indicated times. *Panel C* shows the quantitation of the 45 kDa band in *Panel B*. Samples from vector control cells and LPP1 over-expressing cells are represented as ● and ▲, respectively. Integrated intensity (I.I) of the bands was normalized to the I.I. of a background lane. I.I. was calculated using ImageMaster TotalLab version 2.01 software (GE). The above experiments are representatives of two independent experiments.

Two-dimensional electrophoresis showed a series of spots at about 45-50 kDa that were hyper-phosphorylated in LPP1 over-expressing cells stimulated with EGF (Fig. 5.19). These proteins were similar in molecular weight. They also had different isoelectric points that were found in the center of an immobilized pH gradient isoelectric focusing strip with a pH range of 3 to 10. These spots could represent the same protein with various degrees of phosphorylation. Unfortunately, identification of one of these spots was not possible because a large and intense Coomassie positive spot covered the entire area of interest (Fig. 5.19).

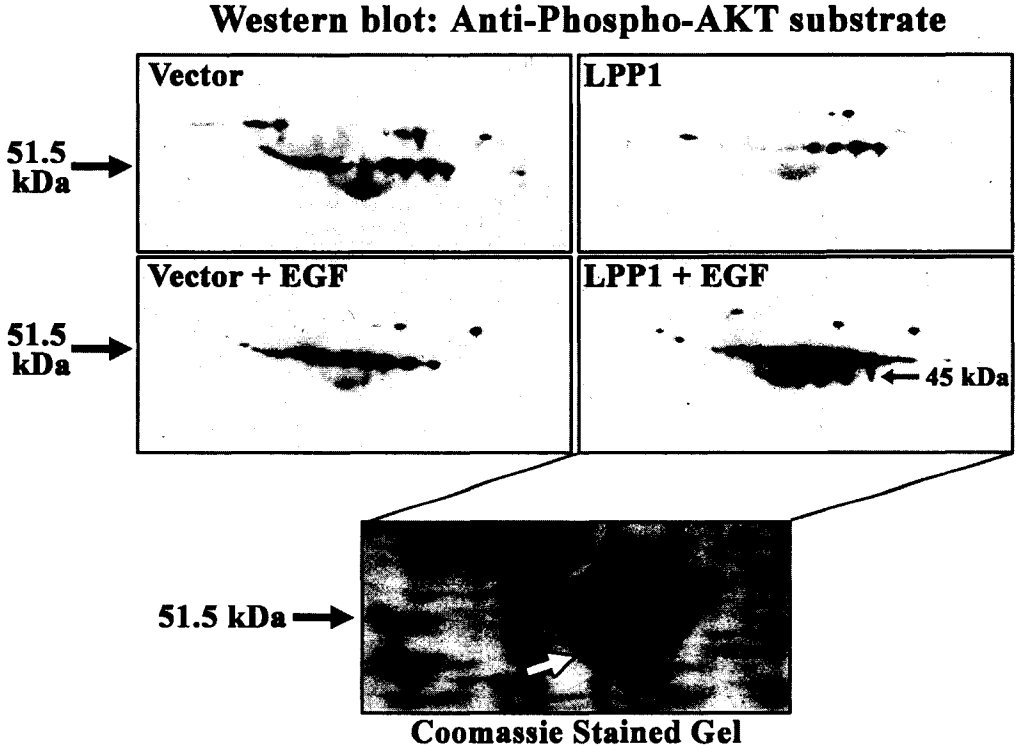

Figure 5.19 Two-dimensional electrophoresis analysis of the phosphorylated 45 kDa Akt-substrate shown in Fig.5.17 and 5.18. Fibroblasts transduced with empty vector or cDNA for mouse LPP1 were treated for 5 minutes with 100 ng/ml EGF. One mg of protein from each sample was used to re-hydrate immobilized pH gradient strips for isoelectric focusing. A gradient of pH 3-10 was used for this experiment. The proteins were then separated according to molecular weight by a 4-16% SDS-PAGE gradient gel. The proteins were transferred to nitrocellulose membranes and probed with the polyclonal antibodies that detect phospho-serine or phospho-threonine phosphorylated by Akt. The Figure shows the cropped Western blots of the phosphorylated 45 kDa Akt-substrates. The bottom panel shows the cropped Coomassie blue-stained gel of proteins from LPP1 over-expressing cells treated with EGF. The region shown is from the middle of the immobilized pH gradient strips that had a pH range of 3-10. The *closed arrows* indicate the position of the molecular weight marker, and the *open arrow* points to the protein spot that covers the area where the Akt-substrates were identified by Western blot. This experiment was performed once.

5.6 Discussion

The topology of LPP1 positions its active-site extracellular when expressed at the cell surface. Indeed, as described in Chapter 3, LPP1 acts partly in the plasma membrane as an ecto-enzyme. It was originally proposed that this ecto-activity explained how LPP1 over-expression attenuated the effects of exogenous LPA in activating cell division,

ERK, phospholipase D and Ca^{2+} transients [158, 174]. Although, partly true, other mechanisms of action have been demonstrated downstream of the activated LPA receptors. Our most compelling result that excludes an effect of ecto-LPP1 activity on migration in our model is that over-expressing LPP1 also decreased migration to the α-ketophosphonate analogue (wls-31) of LPA, which cannot be hydrolyzed.

The decrease of migration induced by LPA by LPP1 was dependent on its catalytic activity. Therefore, if LPP1 affects signaling downstream of the activated receptor, it would be mediated by the metabolism of an intracellular signaling lipid phosphate. LPP1 can hydrolyze a variety of intracellular signaling lipid phosphates including LPA, PA, ceramide 1-phosphate and S1P, provided they have access to the enzyme [84, 113]. We concentrated our attention on the generation of PA through PLD. The LPPs can dephosphorylate PA to DAG following PLD activation [84, 113] and the over-expression of different LPPs can decrease intracellular PA accumulation [153, 161, 167, 183, 185]. In the present work, over-expressing LPP1 severely decreased PA accumulation after stimulating the fibroblasts with both LPA and PDGF. Long *et al.* [186] postulated that the long-term effects of increased LPP1 activity in increasing DAG concentrations decreased the expression of DAG-responsive PKCs and that this could account for decreased ERK activation. Equally, DAG-dependent PKCs activate PLD2 as well as PLD1 [236, 237]. A decrease in these PKC activities could, therefore, explain the attenuation of PLD1 and PLD2 activation in cells that have increased LPP1 activity. This could represent a negative feed-back loop to prevent further DAG formation through the PLD pathways. However, in our studies there were no significant effects of LPP1 activity on the accumulation of bulk cell DAG. The fact that DAG accumulation was maintained

in the LPP1 over-expressing cells despite a severely decreased PA accumulation (Fig. 5.2) is therefore remarkable. This maintenance of DAG concentrations in the LPP1 over-expressing fibroblasts is compatible with the hypothesis that LPP1 is involved in the conversion of PA to DAG. In addition, DAG could be derived by the stimulation of phospholipase C activities by LPA and PDGF.

We hypothesized that LPP1 would degrade the PA generated by PLD activation to DAG. It was surprising not to see an enhancement of DAG concentrations in LPP1 over-expressing cells compared to control cell lines. To determine at what point is PA accumulation affected by LPP1, we looked at the activation of PLD in LPP1 over-expressing cells. We demonstrated that LPP1 attenuated both LPA- and PDGF-induced activation of PLD. This is in addition to the role of LPP1 in converting PA to DAG. Our work therefore extends the studies of Long *et al.* [186] who showed that LPP1 over-expression regulated signaling by PDGF as well as by LPA.

It was interesting to observe that PA accumulation induced by endothelin was not affected by LPP1. Equally, the endothelin activation of PLD itself was not affected. Endothelin is a ligand for the G-protein coupled receptors, endothelin-A (ET_A), which is known to be coupled to G_q and G_s, and endothelin-B (ET_B), which is coupled to G_q and G_i [238, 239]. The activation of PLD by endothelin was much more robust than it was for PDGF and more so compared to LPA (Fig. 5.3). A study by Van Der Bend *et al.* [240] on Rat1 fibroblasts confirmed that LPA was less efficient than endothelin in the activation of PLD, and that LPA stimulation of PLD was short-lived, leveling off after 2 min, whereas endothelin-stimulated PLD activity persisted for at least 1 h. In mouse embryonic fibroblasts endothelin and PDGF required PLCγ1 to activate PLD, whereas LPA-

activation of PLD does not [241, 242]. Another important difference is that unlike LPA and PDGF, endothelin is a poor stimulator of ERK activation in Rat1 fibroblasts [243].

It is clear that all three PLD stimulators have different downstream effectors that are able to affect PLD, which result in differences in the rate and intensities of PLD activation. In addition, LPP1 over-expression does not affect PLD activation by all of the agonists tested. However, the decrease of PDGF-induced PLD activity and PA accumulation by LPP1 does not explain the reason why PDGF-induced fibroblast migration is not affected. These results could be explained if increased PA formation were essential for LPA-induced migration, but not PDGF-induced migration. We verified this prediction by showing that blocking PLD-induced PA formation with butan-1-ol attenuated migration to LPA, but not to PDGF.

To further examine the role of PLD in fibroblast migration we expressed dominant/negative forms of both the PLD isoforms and found that PLD2, and not PLD1, is required for LPA-induced migration. Neither PLD isoform was required for PDGF- or endothelin- induced fibroblast migration. However, LPP1 could still be an important regulator of other aspects of PDGF-induced cell activation, or in the internalization and cycling of the PDGF receptor.

PLD2 activation was required for LPA-induced transactivation and tyrosine phosphorylation of the PDGFR in human bronchial epithelial cells [80]. However, no significant tyrosine phosphorylation of the PDGFR was observed with 0.5 μM LPA which supported optimum migration. Sakai *et al.* [234] reached the same conclusion concerning the relatively low LPA concentrations that stimulate fibroblast migration compared to the higher concentrations needed for PDGFR transactivation. Furthermore,

if LPA-induced migration required activation of the PDGFR it should stimulate mainly chemotaxis, whereas LPA controls mainly chemokinesis. However, the use of the tyrphostin, AG1296, a potent inhibitor of the PDGFR tyrosine kinase showed that there was a 50% inhibition of LPA-induced migration of Rat2 fibroblasts. This result suggests that LPA could use the PDGFR signaling apparatus for migration, which was not detectable by measuring tyrosine phosphorylation of the PDGFR. This is compatible with the work from Dr. Nigel Pyne's laboratory. They suggest that the G protein coupled receptors (GPCR) for LPA and S1P are tethered to receptor tyrosine kinases (RTK). This close association allows for integrated signaling in response to growth factor and/or S1P/LPA, and provides a mechanism for more efficient activation (due to integrated close-proximity signaling from both receptor classes) of the ERK pathway [78]. For example, pertussis toxin pre-treatment decreases PDGF-induced ERK activation. Since pertussis toxin acts to uncouple GPCRs from $G\alpha_i$, this result suggests that the PDGFR uses GPCR-mediated signaling pathways to stimulate ERK. Over-expression of PDGFRβ enhances the activation of ERK by S1P, and over-expression of $S1P_1$ enhances the activation of ERK by PDGF. Importantly, they found that $S1P_1$ receptor is tethered to the PDGFRβ [244], which could create a platform to integrate and share signaling molecules. Perhaps the LPA_1 receptor in Rat2 fibroblasts is coupled to PDGFR such that this association enhances LPA-induced migration without inducing tyrosine phosphorylation of the PDGFR. Similarly, S1P did not induce tyrosine phosphorylation of PDGFRβ [78]. Equally, PDGF-induced stimulation can use components of the LPA_1 receptor for efficient signaling. This proposed integrative signaling by close-proximity could explain why LPP1 decreased the PLD activation by both LPA and PDGF. Perhaps they share the

same molecular machinery for PLD activation that can be regulated by LPP1. In this regard the GPCRs for endothelin are not expected to couple with the PDGFR, and endothelin-induced PLD activation is not affected by LPP1.

PLD2-induced PA formation is also required for the stimulation of phosphatidylinositol 4-phosphate 5-kinase Iγβ and the synthesis of phosphatidylinositol 4,5-bisphosphate [245]. These effects are required for the activation of the cell surface integrins that mediate cell adhesion and migration [245]. Significantly, β_1A integrin is required for LPA-induced fibroblast migration [234]. The action of LPP1 in decreasing PLD2 activation by LPA could, therefore, result in decreased engagement of integrins with the extracellular matrix resulting in decreased migration. This is supported by our work demonstrating that the LPP1 over-expressing cells had a weak interaction with the substratum, and that EDTA alone readily detached these cells from cell tissue plates (Fig. 4.5).

We also investigated the effects of LPP1 expression on the activation of the small G-proteins, Rho, Rac and Cdc42 known to be important in migration [73, 246]. LPP1 expression significantly decreased Rac-GTP and Cdc42-GTP concentrations in unstimulated fibroblasts and decreased Rac-GTP in those activated with LPA, but not PDGF. Increased LPP1 expression also decreased LPA-induced increases in Rho-GTP concentrations. There was no significant effect of PDGF on Rho activation under these conditions. In recent work, there is high Rho activation in protrusions from mouse embryonic fibroblasts that were migrating non-directionally (as produced with LPA in our work) compared to cells stimulated with PDGF [247], which induces chemotaxis. Our results with LPP1 and the differences in signaling between LPA and PDGF are

compatible with those of Kam and Exton [96]. They found that inhibition of the activation of Rho family GTPases has a greater effect on the activation of PLD by LPA compared to PDGF. This resembles the effects of LPP1 shown in Fig. 5.3, which showed that the inhibition of PLD activity by LPP1 over-expression was greater for LPA (92% inhibition) than it was for PDGF (50% inhibition). Our observation that expression of dominant/negative PLD1, or PLD2, or the inhibition of total PLD by butan-1-ol did not alter the LPA-induced activation of Rho is compatible with Rho activation being upstream and not downstream of PLD. Significantly, Rho activation and PA formation are necessary for actin polymerization [97, 98] that is required for cell migration.

Another important LPA, and PDGF effector that was investigated was ERK. In the discussion of Chapter 4 the involvement of ERK in fibroblasts migration was touched upon when comparing our work with that of Long *et al* [186]. They used mouse embryonic fibroblasts from transgenic mice that expressed 20 gene copies of *Lpp1* and found that in an *in vitro* wound healing assay, PDGF-induced chemokinesis was attenuated. They attributed this to the attenuation of PDGF-induced ERK activity [186]. We used the same mouse embryonic fibroblasts, however, they were from the transgenic mice that expressed 2 gene copies of *Lpp1,* and therefore had lower LPP activity [185, 186]. These fibroblasts did not show a decreased ERK activation when treated with LPA or PDGF [185, 186], yet in our Transwell assays there was an attenuation of LPA-induced migration (Fig. 4.2B). Therefore, ERK activation in the latter fibroblasts does not appear to be the target for LPP1 in controlling LPA-induced migration. In Rat2 fibroblasts, over-expression of LPP1 did attenuate ERK activation by LPA, but not by PDGF. This decrease in LPA-induced ERK activation was not explained by inhibition of

PLD1 or PLD2 specifically. However, inhibition of PA generation from total PLD activity by butan-1-ol (Fig. 5.12) attenuated LPA-induced ERK activation. Although this experiment was performed once and does not have the proper control (pre-incubation of cells with non-reactive butan-2-ol) this experiment confirmed studies that demonstrated LPA-induced ERK activation was inhibited by butan-1-ol, but not butan-2-ol [248, 249]. Therefore, either PLD isoform is sufficient to activate ERK induced by LPA.

The attenuation of LPA-induced PA accumulation and total PLD activity in LPP1 over-expressing fibroblasts could account for this decrease in LPA-induced ERK activation. It has been shown in fibroblasts that PDGF-induced activation of ERK does not depend on PLD activity [242, 250], but rather a phosphatidylcholine-specific phospholipase C activity [250]. This explains why PDGF-induced activation of ERK in LPP1 over-expressing cells is not affected despite having an attenuated PDGF-induced PA accumulation and PLD activation. In addition, our work showed that when ERK activation was inhibited with PD98059, this resulted in an inhibition of LPA- and PDGF-induced migration of Rat2 fibroblasts. Since LPA-, but not PDGF-induced activation of ERK is attenuated in LPP1 over-expressing fibroblasts, this result could also explain why LPA-, and not PDGF-induced migration was affected by LPP1 over-expression. Additionally, ERK activation by LPA in NIH 3T3 fibroblasts is dependent on Rho [251]. Since we found that LPP1 over-expressing cells have a decreased LPA-induced Rho activation, this could account for the observed attenuation of LPA-induced ERK activation.

The release of Ca^{2+} transients is also important in fibroblast migration as shown in Fig. 5.13B, which demonstrated that the binding of intracellular Ca^{2+} by BAPTA-AM

inhibited migration induced by both LPA and PDGF. Increasing LPP1 inhibited Ca^{2+} release by LPA, but not PDGF; therefore, the requirement of Ca^{2+} release for migration could also explain why LPA- and not PDGF-induced migration is decreased by LPP1.

An interesting outcome of this work was the observation that not only is LPA signaling affected by LPP1, but that PDGF signaling can also be affected. The decrease of PDGF-induced PLD activity by LPP1 was not important for regulating migration. The activation of ERK by PDGF was also not affected by decreased PLD activity, in contrast to LPA-stimulated ERK, which was dependent on PLD. Various PDGF endpoints dependent on PLD activity in the context of LPP1 over-expression were not explored in this work. For example, sphingosine kinase-1 activity [90], cell mitogenesis, and cell survival involving mTOR [94-96], protein kinase D activation [252], various PKCs that are activated by PLD-generated PA such as PKC-ζ [87], or PKCs activated by DAG, a by-product of LPP activity after PA production by PLD [165].

There could be more signaling proteins and pathways that are affected by LPP1. This is emphasized by our work using various antibodies that recognize phosphorylated residues. We found that the phosphorylation patterns of many proteins were changed by LPP1 over-expression in fibroblasts treated with various agonists in addition to PDGF and LPA, including EGF, S1P, bradykinin, and thrombin. Changes included deceases or increases of agonist-induced phosphorylation, and there were differences in phosphorylation between agonists. There were also differences in the amount of stimulation between vector controls and LPP1 over-expressing cells. There was potential over-lap of phosphorylation of proteins at about 39 and 45 kDa between antibodies that recognize phospho-threonine residues. This over-lap matched in both molecular weight

and in amount of stimulation, or lack-thereof by LPA, bradykinin and thrombin. They could represent the same protein, therefore according to the specificity of the antibodies, they would be phosphorylated by Akt on a threonine residue that is followed by a proline residue. We tried to identify the 45 kDa protein by resolving the proteins in lysates by two-dimensional electrophoresis, and found that there was a very large protein spot that spanned the area of interest (Fig. 4.19). This problem could be solved by immunoprecipitating the phosphorylated proteins with the various phospho-specific antibodies immobilized on agarose beads. This method would help clear the lysates of any proteins not phosphorylated that can interfere with identification of target proteins resolved on Coomassie blue-stained gels. Furthermore, technologies that were not available at the time of this work are now available. Qiagen offers a kit to purify all phosphorylated proteins using a patented affinity chromatography column. We did not pursue our work any further because we decided to concentrate our efforts on investigating the effects of LPP1 on migration. However, the work on phosphorylation forms the basis for future work taking a proteomic approach in identifying phosphorylated proteins that could be regulated by LPP1. Most of these analyses were preliminary results and need to be repeated and expanded on, but they give us a sense that LPP1 can regulate a broad range of cellular function.

CHAPTER 6

REGULATION OF MIGRATION BY CONDITIONED MEDIA FROM LIPID PHOSPHATE PHOSPHATASE-1 OVER-EXPRESSING FIBROBLASTS

6.1 Introduction

Cellular migration is a complex process that involves a coordinated response from the migrating cell. Not only are there intracellular events that the induced cell must orchestrate for migration, but there is also the immediate extracellular environment that the migrating cell must navigate through. Increased activity of LPP1 leads to an attenuation of LPA-induced migration. We have found that the activation of important intracellular signaling molecules involved in fibroblast migration, such as PLD, ERK and Rho family GTPases are regulated by LPP1 activity. These findings could be extended to a possible role of LPP1 in regulating cancer, metastasis, fibrosis and wound healing. These physiological and pathophysiological processes involve the interaction of many cell types, with fibroblasts being only one of them. In this Chapter we investigated whether LPP1 expressed in one population of cells can affect LPA-induced migration of another population of cells that do not over-express LPP1. Since LPP1 has ecto-activity it is possible to hypothesize that the cells expressing a higher level of LPP1 would reduce extracellular LPA-levels so that LPA signaling of cells with less LPP1 expression would also be attenuated [178, 179, 181]. In the previous Chapters we amassed evidence to suggest that attenuation of LPA-induced migration by LPP1 activity occurred downstream of the LPA receptor in addition to an effect on the extracellular degradation of LPA. Therefore, in our experimental conditions any effect by cells expressing higher levels of LPP1 could be a result of secreting a factor that inhibits migration not only of themselves, but migration of neighboring cells with lower LPP1 production.

We found that there was an inhibitory neighbor effect, and a heat-labile inhibitory factor existed in conditioned media from LPP1 over-expressing fibroblasts. Possible

candidates for the regulation of migration could be microvesicle associated LPP1, or the matrix metalloproteinases (MMP). MMPs are secreted zinc-dependent endoproteinases that degrade components of the extracellular matrix (ECM), which then facilitates the detachment and migration of cells in many processes including wound healing, angiogenesis, tumor invasion and metastasis (reviewed in [206, 208]). We examined the activities of the gelatinases, MMP-2 and MMP-9 in Rat2 fibroblasts that over-express LPP1. We also analyzed the conditioned media by two-dimensional electrophoresis and found changes in the levels of proteins that regulate MMP activity. Our findings broaden the impact LPP1 has on the regulation of LPA signaling from within the cell, to its effects on LPA-induced migration outside of the cell.

6.2 Paracrine effects by cells over-expressing lipid phosphate phosphatase-1

6.2.1 *Fibroblasts over-expressing lipid phosphate phosphatase-1 can affect the migration of neighboring fibroblasts not over-expressing lipid phosphate phosphatase-1* – Since the dephosphorylation of exogenous LPA was 2-fold higher in fibroblasts over-expressing LPP1 compared to control cells, we investigated if the over-expression of LPP1 can affect migration of neighboring cells that do not over-express LPP1. To explore if there was a neighbor effect, we differentially labeled wild-type Rat2 fibroblasts and LPP1-over-expressing fibroblasts with PKH fluorescent cell linkers. These fluorescent dyes have long aliphatic tails that embed into the lipid bilayer with very low cell-to-cell transfer, and are known not to modify normal functions of the cell. Migration of labeled-fibroblasts was induced by LPA, and PDGF in Transwell chambers (Fig. 6.1). The migration of labeled fibroblasts was compatible with previous Transwell migration assays

with unlabeled fibroblasts, therefore the effect of the dyes on migration was not apparent in this experiment. To test if there was an affect on vector control cells by LPP1-over-expressing cells the differentially labeled fibroblast were mixed 1:1, while keeping the

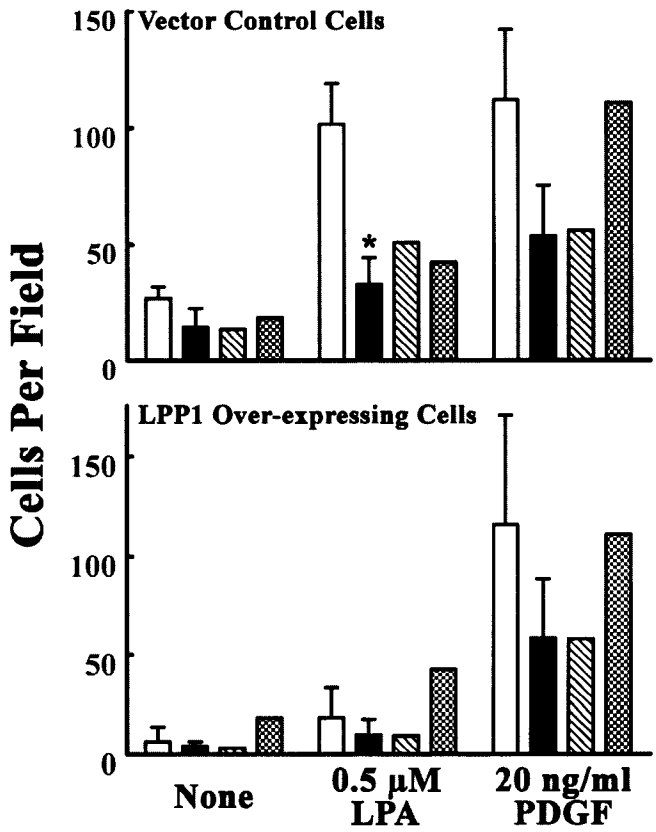

Figure 6.1 Fibroblasts over-expressing LPP1 decreased LPA-induced migration of neighboring fibroblasts that do not over-express LPP1. Fibroblasts stably transduced with empty vector or cDNA for mouse LPP1 were differentially labeled with fluorescent dyes so that they could be counted separately on the same microporous Transwell membrane using a fluorescent microscope. The *top histogram* shows the number of vector control cells that have migrated in the presence of agonists. The *bottom histogram* shows the number of migrated LPP1 over-expressing cells in the same experiments. The mean number of labeled cells migrated when they were not mixed with the other labeled cell line are represented by the *white columns*. *Black columns* represent the mean number of migrated cells when the two differentially labeled cell lines were mixed 1:1, but had a constant total amount of cells plated in the upper chamber of the Transwell. The *hatched columns* represent the predicted amount of migration if there was no effect of migration by the neighboring cell line. These were calculated by dividing the number of cells migrated alone (*white columns*) by two. The *checkered columns* represent the mean sum of migration of the cell lines when they were mixed. Results are means ± S.D. of at least four independent experiments. One sample T-tests were performed using the predicted amount of migration as a hypothetical value against the amount of migration of cells when mixed with the other cell line (i.e. *hatched columns* versus *black columns*, respectively). There was significant difference ($p<0.05$ indicated by *) between the predicted value and the mean migration of vector control cells when stimulated by LPA in the presence of LPP1 over-expressing cells.

total number of cells constant. The mixed populations of fibroblasts were then induced by LPA or PDGF to migrate in Transwell chambers. It was predicted that if there were not a neighbor effect, the number of vector control cells that would migrate would be half that of the number of vector control cells migrated if they were not mixed with LPP1 over-expressing cells. In the Transwell assay with the mixed population of cells the decrease of migration of vector control cells was about 70%. The decrease of migration was not 50% like it was for PDGF. This result suggests that fibroblasts over-expressing LPP1 can affect the LPA-induced migration of neighboring cells that do not have LPP1 over-expression.

6.2.2 *Conditioned media from fibroblasts over-expressing lipid phosphate phosphatase-1 decreases lysophosphatidate-induced migration of wild-type fibroblasts* – We next investigated if this neighbor effect by LPP1-over-expressing fibroblasts was cell-associated or if there was a factor released in the medium that could attenuate LPA-induced migration of wild-type fibroblasts. To do this conditioned media was collected from control fibroblasts, and LPP1 over-expressing fibroblasts over 18 h. The conditioned media was then added to the bottom chamber of the Transwell and used as the medium for migration of wild-type Rat2 fibroblasts induced by LPA or PDGF. When conditioned media from LPP1 over-expressing cells was used, the migration of wild-type fibroblast induced by LPA was inhibited by 60% (Fig. 6.2). The conditioned media from LPP1 over-expressing cells did not affect PDGF-induced migration of wild-type fibroblasts. When the media was heated to 80°C for 10 minutes inhibition was abolished (Fig. 6.2), suggesting that fibroblasts over-expressing LPP1 releases a heat-labile factor to the medium that inhibits fibroblast migration induced by LPA but not by PDGF.

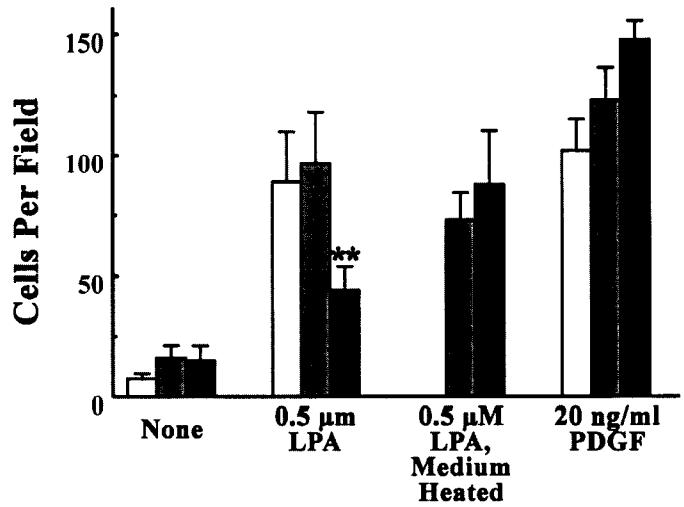

Figure 6.2 Medium conditioned by LPP1 over-expressing fibroblasts decreased the LPA-induced migration of wild-type fibroblasts. Conditioned media was prepared by incubating fibroblasts stably transduced with empty vector or cDNA of mouse LPP1 with DMEM containing 0.4% BSA, and 0.1% charcoal-treated FBS for 18 h. This media was placed in the bottom chamber of the Transwell as the migration medium for wild-type fibroblasts. The *grey columns* represent wild-type fibroblast migration in the presence of medium conditioned by vector control cells, and the *black columns* represent wild-type fibroblast migration in the presence of medium conditioned by LPP1 over-expressing cells. The *white columns* represent wild-type fibroblast migration in the presence of freshly prepared migration medium. Media was heated for 10 min at 80°C. Results are means ± S.D. of at least four independent experiments, and means and ranges of two independent migration experiments in the presence of heated conditioned media. Significant differences between migration in the presence of the conditioned media within the same treatment group are indicated by: **, $p<0.01$.

6.2.3 *Conditioned media from lipid phosphate phosphatase-1 over-expressing fibroblasts have increased total lipid phosphate phosphatase activities* - LPP1 over-expressing fibroblasts released a heat-labile factor into the media that attenuated LPA-, but not PDGF-induced migration of vector control fibroblasts. We explored the possibility that LPP1 was the factor. Indeed, there was 8-fold more total LPP activity in the conditioned media from LPP1 over-expressing cells (Table 6.1) compared to control conditioned media. Most cellular debris in the conditioned media was removed by an initial centrifugation at 2500 rpm for 20 min. Therefore it is unlikely that the LPP activity was from detached cells. LPP1 is a transmembrane enzyme, and to be functional it must be in a membranous compartment such as a microvesicle. Ultra-centrifugation of the

conditioned media removed most of the LPP activity (Table 6.1). This experiment suggests that LPP1 was released in microvesicles, and could possibly degrade exogenous LPA to modify fibroblast migration in an autocrine and paracrine manner.

Table 6.1 Total LPP activity in conditioned media from Rat2 fibroblasts. Conditioned media from vector control fibroblasts or LPP1-over-expressing fibroblasts was collected over 18 h. The volume of conditioned media was normalized and fixed relative to the number of cells on the plates. Total LPP activity in conditioned media was measured by the PA degradation in Triton X-100 micelles. Total LPP activity was measured before and after an ultra-centrifugation (99 000 rpm for 1 h). Results are relative to LPP activity in conditioned media from vector control cells. One experiment was performed for conditioned media that was ultra-centrifuged. Three experiments were performed on conditioned media that were not ultra-centrifuged. The mean total LPP activity in non-centrifuged conditioned media from vector control fibroblasts was 1.19 pmol of PA degraded/μl of conditioned media in 2 h.

Conditioned Media from ...	Relative PA degradation before Ultra-spin	Relative PA degradation after Ultra-spin
Vector control cells	1	0.77
LPP1 over-expressing cells	8.0 ± 4.7	1.47

6.3 The stable over-expression of lipid phosphate phosphatase-1 regulates matrix metalloproteinases

6.3.1 *Matrix metalloproteinase inhibitors decreased the migration of Rat2 fibroblasts* – Although LPP activity was measured in the conditioned media from LPP1 over-expressing fibroblasts, we explored the possibility that there could be other factors that regulate migration. Matrix metalloproteinases (MMP) are zinc-dependent endoproteinases that are involved in extracellular matrix (ECM) remodeling [206, 208] and play a role in a vast range of physiological and pathophysiological conditions. For example, by remodeling the ECM, they allow cells to detach and migrate to sites of tissue injury for repair. They are also known to solubilize membrane-bound growth factors such as heparin-bound epidermal growth factor [253], and various other latent growth factors and cytokines involved in regulating cell growth and migration (reviewed in [206]). We

investigated if MMPs were important in the migration of fibroblasts induced by LPA or PDGF by using various MMP inhibitors in the Transwell assay. 1,10-phenanthroline is a tricyclic aromatic hydrocarbon with three fused benzene rings. It can bind and remove zinc ions from metalloproteinases, thus inhibiting them. Doxycycline is a tetracycline class antibiotic that can effectively inhibit a broad range of MMPs by chelating the zinc atoms at the enzyme-binding site [209]. Batimastat, marimastat, and TNF-α processing inhibitor (TAPI-1) are hydroxamate derivatives that have been synthesized to mimic the structure of collagen at the site where MMP binds to cleave it. The inhibitors then chelate the zinc atom [212]. All of the MMP inhibitors decreased migration of the fibroblasts induced by both LPA and PDGF (Table 6.2), therefore migration of Rat2 fibroblasts in Transwells was dependent on the actions of MMPs.

Table 6.2 The inhibition of LPA- and PDGF- induced migration by various matrix metalloproteinase inhibitors. LPA- and PDGF-induced migration of wild-type fibroblasts was measured in Transwell chambers. Fibroblasts were pretreated with various matrix metalloproteinase inhibitors at the indicated concentrations for 30 min before the migration began with the addition of the agonists. Inhibition (%) of agonist-stimulated migration was calculated from one experiment or unless indicated by a (R), which is the range from two independent experiments.

	Phenanthroline 0.4 mM	Doxycycline 100 μM	Batimastat 20 μM	Marimastat 20 μM	TAPI-1 100 μM
0.5 μM LPA	100%	100%	89 (R) 21%	65%	82 (R) 5%
20ng/ml PDGF	100%	89%	98 (R) 5%	-	-

6.3.2 *Stable over-expression of lipid phosphate phosphatase-1 decreased matrix metalloproteinase-2 activity, and increased matrix metalloproteinase-9 activity in conditioned media* – Migration induced by LPA and PDGF was dependent on the actions of MMPs, therefore we investigated if there was change in MMP activities in fibroblasts that over-express LPP1 compared to control fibroblasts. We employed a sensitive

zymography assay to determine the activities of the gelatinase A and B, which are also known as MMP-2 and -9, respectively. This assay involves resolving a sample of the conditioned media in a non-denaturing SDS-PAGE gel impregnated with gelatin. After electrophoresis the SDS was washed away and the gel was incubated such that the gelatinase was allowed to degrade the gelatin embedded in the gel, which was subsequently stained with Coomassie blue. It was found that 72 kDa-MMP-2 activity in the conditioned medium from LPP1 over-expressing fibroblasts was decreased 97% (Fig. 6.3A and C), whereas 92 kDa-MMP-9 activity was increased 14-fold (Fig. 6.3A and E), compared to medium conditioned by control fibroblasts. As a control for zinc-dependent gelatinase activity the MMP inhibitor, phenanthroline, was shown to abolish any detectable gelatinase activity (Fig. 6.3B).

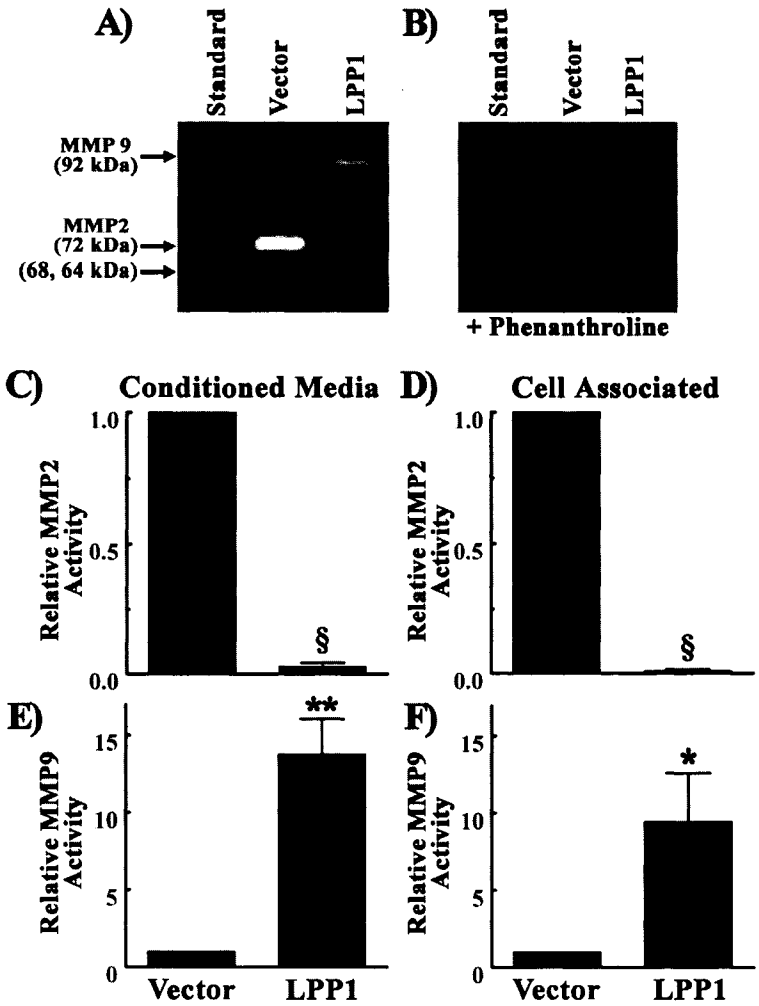

Figure 6.3 Increased LPP1 activity in stably transduced fibroblasts decreased MMP-2 activity, and increased MMP-9 activity. *Panel A* shows a gelatin-zymograph of samples from media conditioned by Rat2 fibroblasts stably transduced with empty vector (*Vector*) or cDNA of mouse LPP1 (*LPP1*). The standard is medium conditioned by HT1080 human fibrosarcoma cells. *Panel B* shows the same samples, however during the incubation period, when the MMPs degrade the gelatin in the gel, 20μM phenanthroline was present. *Panels C-F* show the quantitation of gelatin degradation normalized to MMP activities from vector control cells. *Panels C* and *E* show relative MMP-2 and -9 activities, respectively, in conditioned media. *Panels D* and *F* show relative MMP-2 and -9 activities, respectively, in cell lysates. Results are means ± S.D. from four independent experiments. Significant differences of MMP activity between cell lines are indicated by: §, $p<0.0001$; **, $p<0.01$ and *, $p<0.05$.

6.3.3 *Stable over-expression of lipid phosphate phosphatase-1 decreased matrix metalloproteinase-2 mRNA levels, and increased matrix metalloproteinase-9 mRNA levels* – The differences in the secreted matrix metalloproteinase (MMP) activities in conditioned media from LPP1 over-expressing fibroblasts could result from changes in

the expression of the *Mmp* genes, or changes in the levels of steady state MMP protein concentration. There can also be a change in the regulation of secretion or activation of the MMPs. MMP-2 and -9 activities from cell lysates of wild-type fibroblasts and LPP1 over-expressing fibroblasts were measured using the same zymography assay employed for the conditioned media. Similar to the conditioned media, cell-associated 72 kDa-MMP-2 activity decreased 99% (Fig. 6.3D), and 92 kDa-MMP-9 activity increased 9.4-fold (Fig, 6.3F). These results suggest that changes in the MMP-2 and MMP-9 activities are caused by a change in the expression of the *Mmp2* and *9* genes and not due to changes in the secretion of MMPs. Dr. Katherine Morris performed real time RT-PCR and showed that in LPP1 over-expressing fibroblasts MMP-2 mRNA levels are decreased 91% and MMP-9 mRNA levels are increased 54-fold [149]. This result confirms that stable LPP1 over-expression could regulate *Mmp2* and *9* gene expression in serum-starved Rat2 fibroblasts, which could affect LPA-induced migration of cells in an autocrine and paracrine fashion.

6.3.4 *Treatment of fibroblasts with lysophosphatidate, platelet-derived growth factor, and phorbol myristate acetate increased the gelatinase activity of matrix metalloproteinase-9, but did not change the activities of matrix metalloproteinase-2* – Agonists, such as LPA and PDGF can increase the expression and activation of MMPs [206, 254, 255]. To investigate if stimulation of fibroblasts can increase or decrease MMP-2 or MMP-9 activity, and if LPP1 can regulate this, we treated vector control and LPP1 over-expressing fibroblasts with LPA, PDGF and phorbol myristate acetate (PMA) 6 h before the conditioned media was collected. Conditioned media and lysates of the fibroblasts were collected for zymography analysis of MMP-2- and MMP-9-gelatinase

activity. Treatment with any of the cell stimulants did not change the MMP-2-gelatinase activity in either vector control cells or LPP1 over-expressing cells (Fig. 6.4A). However, there was about a 2-fold increase of MMP-9-gelatinase activity in the conditioned media and lysates from vector control cells that were treated with the agonists, significantly in the conditioned media of cells treated with LPA or PDGF (Fig. 6.4B). There was no increase of MMP-9-gelatinase activity in conditioned media or cell lysates from fibroblasts with stable LPP1 over-expression. These cells already produced higher

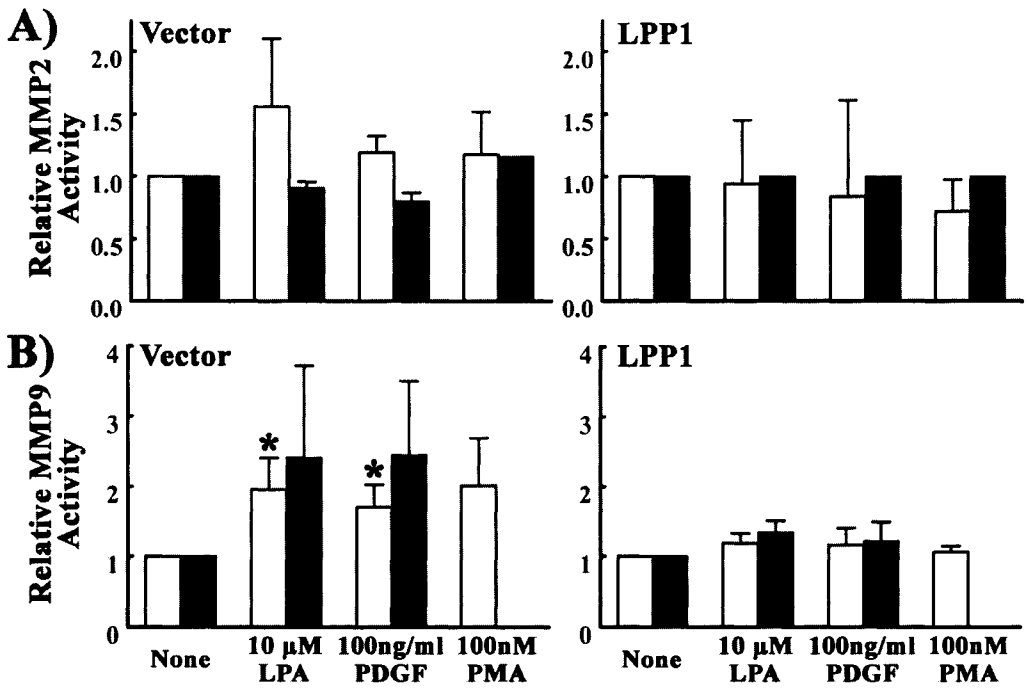

Figure 6.4 MMP-2 and -9 activities after treatment of fibroblasts with various agonists. Fibroblasts were treated with the indicated agonists for 6 h before the conditioned media and the cell lysates were collected. *Panels A* and *B* show the relative activities of MMP-2 and -9, respectively in conditioned media (*white columns*) and cell lysates (*black columns*) from fibroblasts that were stably transduced with empty vector (*Vector*) or cDNA for mouse LPP1 (*LPP1*). Due to high variability between experiments results are shown as relative MMP activity within cell lines. Basal MMP-2 activity in LPP1 over-expressing fibroblasts was decreased by an average of 97% compared to MMP-2 activity in vector control samples. Basal MMP-9 activity in LPP1 over-expressing fibroblasts increased by a range of 3- to 14-fold over MMP-9 activity in vector control samples. Results are means ± S.D. for at least three independent experiments with conditioned media, and means and ranges for two independent experiments with cell lysates. Significant differences between non-treated and treated cells are indicated by: *, $p<0.05$.

amounts of basal MMP-9 activity compared to the vector control cells (Fig. 6.3A, E and F) and perhaps could not be induced to produce more.

6.3.5 *Two-dimensional electrophoresis analysis detects the increased expression of tissue inhibitor of metalloproteinase-2 and procollagen C-proteinase enhancer in conditioned media from Rat2 fibroblasts stably over-expressing lipid phosphate phosphatase-1* – To determine which secreted protein from LPP1 over-expressing fibroblasts could be involved in attenuating LPA-induced migration of wild-type fibroblasts we took a broader approach by employing two-dimensional electrophoresis. We concentrated conditioned media 10-times using a filter that allowed molecules smaller than 10 kDa to pass through to the filtrate. The proteins in the concentrated conditioned media were then separated by two-dimensional electrophoresis (Fig. 6.5). Image Master 2D software identified protein-spots on the gels that were different in intensity between secreted proteins from wild-type and LPP1 over-expressing fibroblasts. Three spots were identified that were higher in intensity in LPP1 over-expressing fibroblasts (Fig. 6.5). One was identified as tissue inhibitor of metalloproteinase-2 (TIMP-2) and two were identified as procollagen C-proteinase enhancer (PCPE) (Fig. 6.5). TIMP-2 and PCPE are involved in the remodeling of the ECM. TIMP-2 is an MMP-2 inhibitor and is known to regulate the migration of fibroblasts [256]. However, TIMP-2 at low concentrations can activate MMP-2 by mediating the formation of mature MMP-2 from pro-MMP-2 [221]. At high concentrations, TIMP-2 inhibits MMP-2 activity and activation [221, 256, 257]. MMP-2 activity is important in the migration of cells [220, 256, 258, 259], and the increase of concentration of the MMP-2 inhibitor, TIMP2, in the conditioned medium from LPP1 over-expressing fibroblasts could be

enough to inhibit MMP2 activity or its activation in neighboring wild-type fibroblasts, thereby decreasing migration induced by LPA.

PCPE is a glycoprotein that can bind C-propeptides of procollagens and enhances the cleavage of procollagen by procollagen C-proteinases, which is a crucial step for collagen deposition [260]. It is interesting to note that PCPE has a C-terminal netrin-like domain that shows homology to TIMPs [261] and that it can act as a weak inhibitor of MMP-2 [262].

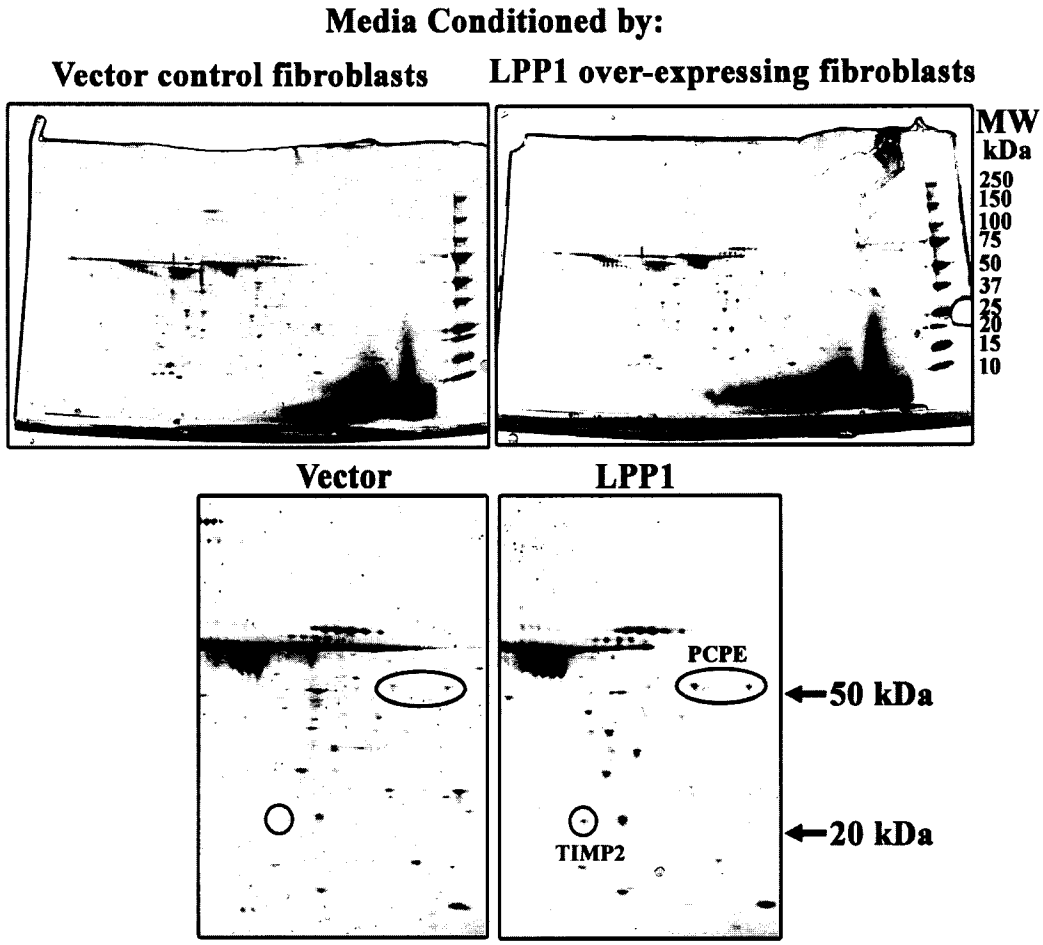

Tissue inhibitor of metalloproteinase-2 (TIMP-2); *Rattus norvegicus*

```
  1 mgaaarslrl alglllatl lrpadacscs pvhpqqafcn advviraka sekevdsgnd
 61 iygnpikriq yeikqikmfk gpdkdiefiy tapssavcgv sldvggkkey liagkaegdg
121 kmhitlcdfi vpwdtlsitq kkslnhryqm gceckitrcp mipcyisspd eclwmdwvte
181 ksinghqakf facikrsdgs cawyrgaapp kqefldiedp
```

Procollagen C-proteinase enhancer (PCPE); *Rattus norvegicus*

```
  1 mlpaaltsll gpfllawvlp largqtpnyt rpvflcggdv tgesgyvase gfpnlyppnk
 61 kciwtitvpe gqtvslsfrv fdmelhpscr ydalevfags qtsqqrlgrf cgtfrpapvv
121 apgnqvtlrm ttdegtggrg fllwysgrat sgtehqfcgg rmekaqgtlt tpnwpesdyp
181 pgiscswhii apsnqvimlt fqkfdvepdt ycrydsvsvf ngavsddskr lgkfcgdkap
241 spissegnel lvqfvsdlsv tadgfsasyr tlprdaveke sapspqedaq hqpqsrsdpk
301 tgtgpkvkpp skpkvqpvek pegspatqat pvapdapsit cpkqykrsgt lqsnfcsssl
361 vvtgtvkamv rgpgegltvt vsllgvykte dldlpspasq tslkfyvpck qmppmkkgas
421 yllmgqveen rgpilppesf vvlyrpnqdq ilsnlskrkc psqprpda
```

Figure 6.5 Two-dimensional electrophoresis analysis of conditioned media. Conditioned medium from fibroblasts that were stably transduced with empty vector (*Vector*) or cDNA for mouse LPP1 (*LPP1*) were concentrated 10-times with 10,000 Dalton cut-off, Millipore filters. The proteins were resolved by isoelectric focusing on immobilized pH gradient strips (pH 3-10), and then separated based on molecular weight on an SDS-PAGE gel with a 4-16% cross-linking gradient. Chosen spots are indicated and labeled. A MALDI-Tof mass spectrometer identified two spots as procollagen C-proteinase enhancer (PCPE), and the spot with the molecular weight of about 20 kDa as tissue inhibitor of metalloproteinase 2 (TIMP-2). Their amino acid sequences are shown. Identified peptides are underlined and are in bold. Highlighted peptides in the PCPE sequence were from the PCPE spot found in the more acidic isoelectric point (the left PCPE spot).

6.4 Discussion

In the previous Chapters, it was demonstrated over-expression of LPP1 decreased LPA-induced fibroblast migration. It was hypothesized that the LPP1 ecto-activity would decrease the concentrations of extracellular LPA, and decrease the activation of LPA receptors on the cells themselves. Regulation of the activation of LPA receptors by this mechanism could then be extended to neighboring cells that do not over-express LPP1. In our experimental conditions the inhibition of LPA-induced migration by LPP1 over-expression was not dependent on exogenous LPA degradation by LPP1, but rather an attenuation of activation of important intracellular signaling molecules downstream of the LPA receptor including Ca^{2+} transients, PLD, ERK, and Rho. This model would then translate to a decreased migration of the cells that expressed high levels of LPP1, and one would not expect a decrease of LPA-induced migration of neighboring cells that do not have high levels of LPP1 expression. This prediction was dismissed when we mixed control fibroblasts and fibroblasts over-expressing LPP1 in a Transwell migration assay and differentially labeled them. We found that LPP1 over-expressing cells decreased the LPA-induced migration of control cells. Since the decrease of LPA-induced migration was not dependent on LPA degradation by the ecto-activity of LPP1, we hypothesized that these cells secrete a soluble factor that can decrease LPA-, but not PDGF-induced migration in an autocrine and paracrine manner. We confirmed this hypothesis by attenuating LPA-induced migration of control fibroblasts using conditioned media from LPP1 over-expressing fibroblasts. As predicted, this conditioned media did not affect PDGF-induced migration. In addition, heating the conditioned media abolished the attenuation of migration.

These experiments did not eliminate the possibility that active LPP1 was present in microvesicles that were shed from the cells. These microvesicles could represent the heat-labile factor in conditioned media that attenuated LPA-induced migration of control cells. Indeed, we found there was 8-fold more LPP activity in conditioned media from LPP1 over-expressing cells compared to conditioned media from vector control cells. Most of this LPP activity was removed after ultra-centrifugation of the conditioned media, but not after low speed centrifugation. This suggests that LPP1 is present in microvesicles (exosomes) that were shed from the cell. This also suggests that the degradation of exogenous LPA by microvesicle-associated LPP1 could decrease LPA-induced migration. We surmised that this would be unlikely since the amount of LPA degradation during migration of the differentially labeled cell lines in the Transwell chamber would be even less than that measured when solely LPP1 over-expressing fibroblasts were migrating (i.e. 19% LPA degradation from Table 4.2), yet control cells still showed an attenuation of LPA-induced migration by neighboring LPP1 over-expressing cells. A migration experiment using conditioned media after ultracentrifugation that reduces LPP activity, or using the non-hydrolysable LPA analogue would determine whether the attenuation of migration by the conditioned media was partly dependent on exogenous LPA degradation by LPP1.

We also explored the possibility that the extracellular matrix remodeling endoproteinases, matrix metalloproteinases (MMP) in the conditioned media could be responsible for the decreased LPA-induced migration of control cells. Indeed, a broad range of MMP-inhibitors abolished LPA- and PDGF-induced migrations. We found that in fibroblasts that stably produced LPP1 there was a decreased expression of MMP-2, and

an enhanced expression of MMP-9. We also confirmed that MMP-2 expression was not inducible [206, 208], whereas MMP-9 expression was induced by LPA, PDGF, and PMA in control Rat2 fibroblasts. It was unlikely that MMP-9 activity would be induced any further in LPP1 over-expressing cells because MMP-9 activity was already induced about 9-fold over control fibroblasts.

Transcriptional regulation of the *Mmp2* gene is mediated by various regulatory elements, such as the activating protein-2 (AP-2), and two selective promoter factor-1 (Sp-1) binding sites in the proximal region of the promoter [263, 264], a profile associated with housekeeping genes. An inducible AP-1 site was also found far upstream of the transcriptional initiation start site [264], however MMP-2 has been widely considered to be an AP-1-unresponsive gene, primarily based on the absence of gene induction following exposure to PMA ([265] and our results, Fig. 6.4). However, signaling proteins, such as ERK, PLD, and Rho family GTPases can influence expression and activation of MMP-2 [266-269]. There is also the possibility that MMP-2 mRNA stability is decreased when LPP1 is over-expressed. In contrast to MMP-2, expression of MMP-9 is readily inducible by many cytokines, growth factors and PMA [263]. The MMP-9 promoter region contains multiple AP-1 sites, a polyoma enhancer A binding protein-3 (PEA3) site that cooperates with AP-1 protein to enhance gene expression, and an NF-κB binding site that mediates MMP-9 expression by growth factors [270]. Equally, ERK, PLD, and Rho family GTPases also influence MMP-9 expression [271-274]. An evaluation of these signaling proteins and their influence on MMP gene expression in serum-starved Rat2 fibroblasts could offer some clues as to how LPP1 over-expression sharply suppresses MMP-2 expression and enhances MMP-9 expression.

Equally, the altered expression of these MMPs could affect the activation of the signaling proteins listed above. MMPs are not only involved in ECM remodeling, but are known to affect receptor and integrin signaling. They solubilize membrane-bound growth factors, and activate latent cytokines to induce receptor signaling (reviewed in [206]). They also inhibit receptor signaling, for example MMP-2 cleaves fibroblast growth factor receptor-1 [214]. Therefore the change of basal MMP activities could have long-term, and short-term effects on intracellular signaling proteins.

PDGF-induced migration also requires the activities of MMPs (Table 6.1). In contrast to possibly affecting LPA-induced migration the observed gelatinase profile does not affect PDGF-induced migration of Rat2 fibroblasts. PDGF has been reported to induce other MMPs such as MMP-1, MMP-3, MMP-11, in addition to MMP-9 [275-278]. These MMPs in combination or alone could mediate PDGF-induced migration, and we do not currently know if their expression or activities are affected by LPP1. We suggest that LPP1 over-expression does not alter the MMP profile necessary for PDGF-induced migration of fibroblasts.

The decrease of MMP-2 expression can be the mechanism to inhibit the LPA-induced migration of LPP1 over-expressing fibroblasts themselves, but it is unlikely that the decreased MMP-2 levels in LPP1 over-expressing cells would affect neighboring wild-type cells, since these cells express higher basal-levels of MMP-2. In addition to released LPP in the media, the paracrine effect by LPP1 over-expressing cells could also be attributed to the increased levels of the secreted MMP-2 inhibitor, TIMP-2. The TIMP-2 promoter fits the profile of a housekeeping gene consistent with its absence of gene induction following exposure of fibroblasts to PMA, PDGF, interleukin-1, and

tumor necrosis factor-α [279, 280]. Although TIMP-2 is not inducible, perhaps LPP1 somehow stabilizes TIMP-2 mRNA so that more TIMP-2 is produced. LPP1 could also possibly enhance secretion of TIMP-2.

TIMP-2 is a natural specific inhibitor of MMP-2. However, regulation of MMP-2 by TIMP-2 *in vivo* is complicated, in that high concentrations of TIMP-2 inhibits activation of the latent form, pro-MMP-2, but in low concentrations, plasma membrane-associated TIMP-2 increases the processing and activation of pro-MMP-2. Activation of pro-MMP-2 is dependent on the binding of the N-terminus of TIMP-2 to the catalytic domain of membrane type-1 (MT1)-MMP (Fig. 1.11B). This association inhibits MT1-MMP endoproteinase activity. Pro-MMP-2 is recruited to the TIMP-2/MT1-MMP complex by binding to the C-terminus of TIMP-2 (Fig. 1.11B). Another MT1-MMP, not bound to TIMP-2, is required to cleave the propeptide domain of pro-MMP-2 and partially activates MMP-2 (Fig. 1.11B). MMP-2 is then fully activated by another fully active MMP-2 not bound to TIMP-2, which finalizes MMP-2 processing (Fig. 1.11B) [219-222]. This mechanism of MMP-2 activation ensures high ECM remodeling proximal to the migrating cell. This mechanism also makes the MMP-2 and MT1-MMP to TIMP-2 concentration ratio an important determinant in the activation of MMP-2. High TIMP-2 concentrations would bind, occupy, and inhibit all pro-MMP-2, fully activated MMP2, and all of the membrane-bound MT1-MMP enzymes necessary for MMP-2 activation. MMP-2 activity is known to be crucial in the random cell migration induced by collagen [220, 256, 258, 259], whereas MMP-9 is dispensable [259]. Therefore, it is conceivable that the increased secretion of TIMP-2 from LPP1 over-expressing fibroblasts can be enough to inhibit pro-MMP-2 processing at the cell-surface

necessary for LPA-induced migration. This effect is exasperated by the decrease of MMP-2 expression by over 95% in LPP1 over-expressing fibroblasts. Therefore even more TIMP-2 is available to bind and inhibit secreted-MMP-2 and membrane-associated MT1-MMP from neighboring cells with wild-type MMP-2 and MT1-MMP levels. The excess TIMP-2 could inhibit pro-MMP-2 processing and therefore inhibit migration of neighboring cells in a paracrine fashion. The increased expression of PCPE can also contribute to a decrease of MMP-2 activation since it can act as a weak inhibitor of MMP-2 and MT1-MMP [262].

TIMP-2 has additional functions independent of direct MMP inhibition. It was found that TIMP-2 specifically binds to the $\alpha_3\beta_1$ integrin. In endothelial cells, TIMP-2 binding on the $\alpha_3\beta_1$ integrin causes dissociation of the protein tyrosine phosphatase, Shp-1, from the β_1-integrin subunit, and increases its association with vascular endothelial growth factor receptor and fibroblast growth factor receptor that are involved in endothelial proliferation and angiogenesis. This association decreases receptor tyrosine phosphorylation and thus decreases endothelial cell growth and angiogenesis (reviewed in [257]). TIMP-2 binding to $\alpha_3\beta_1$ also increases Rap1 activity, which is responsible for decreasing Rac1 activation, and increasing expression of the membrane-bound MMP inhibitor, reversion-inducing–cysteine-rich protein with Kazal motifs (RECK). Increased RECK expression inhibits basal cell migration. Embryonic fibroblasts from RECK-null mice failed to demonstrate a TIMP-2–mediated decrease in cell migration despite activation of Rap1 [281, 282]. Fibroblasts also express $\alpha_3\beta_1$ integrins. In Chapters 4 and 5 we showed that Rat2 fibroblasts readily detached from the plate, and that basal Rac activation was decreased. An increased TIMP-2 expression in LPP1 over-expressing

fibroblasts would increase the binding of TIMP-2 to fibroblast $\alpha_3\beta_1$ integrins. This binding could explain the decreased basal activation of Rac, and the decreased basal and LPA-induced migration of fibroblasts. Significantly, β_1A integrin is required for LPA-induced fibroblast migration [234]. TIMP-2 binding could decrease availability of functional β_1A integrin for migration. Additionally, mouse keratinocytes plated on laminin V, a ligand for the $\alpha_3\beta_1$ integrin, are dependent on the $\alpha_3\beta_1$ integrin for enhanced MMP-9 mRNA stability and increased MMP-9 expression [283]. MMP-9 mRNA stability and MMP-9 expression are decreased in α_3–null keratinocytes [283]. Engagement of the $\alpha_3\beta_1$ integrin with TIMP-2 could increase the stability of MMP-9 mRNA in our fibroblasts, which could explain the higher concentrations of MMP-9 mRNA and increased MMP-9 activity in LPP1 over-expressing cells.

Preliminary work to determine if TIMP-2 regulates fibroblast migration was performed by Dr. Meltem Sariahmetoglu. She identified TIMP-2 as the inhibitory factor of LPA-induced migration of fibroblasts in sub-fractionated conditioned media (unpublished work). She also performed a knockdown of TIMP-2 in LPP1 over-expressing fibroblasts using specific siRNA and found that conditioned medium from these cells no longer inhibited LPA-induced migration of wild-type fibroblasts in the Transwell assay (unpublished work). Moreover, the knockdown of TIMP-2 by siRNA in LPP1 over-expressing fibroblasts increased LPA-induced migration of these cells. Therefore, TIMP-2 expression in LPP1 over-expressing fibroblasts decreased their migration induced by LPA and was a migration inhibitory factor in the conditioned media.

This Chapter provided some insight as to how LPP1 could possibly alter the

migration of cells in an autocrine and paracrine manner. We found that LPP activity could be secreted into the medium, and that this could possibly regulate LPA-induced migration of neighboring cells. We also found that LPP1 can regulate the expression levels of proteins responsible for the remodeling of the ECM. This is important in migration, since it requires cycles of detachment and reattachment of the cell through the ECM. Preliminary work by Dr. Meltem Sariahmetoglu demonstrated that one of these proteins, TIMP-2, could be the factor that decreases LPA-induced migration in the conditioned media of LPP1 over-expressing fibroblasts. More work has to be done to establish the mechanism for this regulation by TIMP-2. We also have to determine the cause-and-effect relationship between intracellular signaling molecules such as ERK, PLD, the Rho family GTPases, and the ECM remodeling proteins, which can also control cellular signaling in their own right. These questions should be approached in the context of LPP1 function. Particularly, what lipid phosphate or lipid phosphates are desphosphorylated by LPP1 that could mediate all these intriguing signaling changes?

CHAPTER 7

GENERAL DISSCUSSION AND FUTURE DIRECTIONS

There has been a concentrated effort to study the role of lipid phosphate phosphatase-1 (LPP1) in cellular signaling. LPP1 exerts its signaling effects by its lipid phosphatase activity, which has been demonstrated to dephosphorylate lysophosphatidate (LPA), phosphatidate (PA), sphingosine-1-phosphate (S1P), and ceramide-1-phosphate (C1P) *in vitro*. The corresponding dephosphorylated forms are monoacylglycerol (MAG), diacylglycerol (DAG), sphingosine, and ceramide, respectively. With the exception of MAG, these by-products are signaling molecules in their own right. However, LPA with an arachidonoyl acyl chain could be dephosphorylated by ecto-LPP activity to produce the *sn*-2 arachidonylglycerol (2-AG), a natural ligand for cannabinoid receptors. In our experiments we used oleoyl-LPA that when dephosphorylated produces mono-oleoylglycerol, which is not known to have any biological activity. It is not known which lipid phosphate is regulated by LPP1 *in vivo*, although studies have mainly centered on PA and LPA. LPP1 expression at the plasma membrane and the topology that positions the active site to the extracellular face of the cell surface led to the hypothesis that LPP1 could regulate the concentrations of important extracellular lipid phosphates, most notably LPA and S1P. This would then decrease the availability of the lipid phosphates to bind and activate their specific receptors on the cell surface. In some reports this was proven to be true, particularly for LPA-induced signaling [175, 178-181]. However, there is a growing body of evidence that show LPP1 also affects signaling from within the cell induced by agonists ranging from LPA to thrombin to platelet-derived growth factor (PDGF) [161, 184, 186]. This thesis demonstrates that LPP1 over-expression attenuates the random migration of Rat2 fibroblasts induced by exogenous LPA. However, inhibition of LPA-induced fibroblast migration was not dependent on the

dephosphorylation of exogenous LPA. We found that LPP1 over-expression decreased various important intracellular signaling effectors downstream of LPA receptor activation, including Ca^{2+} mobilization, phospholipase D (PLD), extracellular signal-regulated kinase 1 and 2 (ERK1/2), and Rho. Although PDGF-induced chemotaxis was not affected by LPP1 over-expression, there was an attenuation of PDGF-induced PLD activity.

In addition to LPP1's role in regulating LPA-induced migration of the cells over-expressing LPP1, we found that the conditioned medium from these cells also decreased the migration of wild-type cells. Examination of the conditioned media showed that increased LPP activity was present, and that expression of matrix metalloproteinases (MMP) and the natural inhibitor of MMP-2, TIMP-2, was changed by LPP1 over-expression. This thesis provides a characterization of fibroblasts that were affected by increased LPP1 expression and describes a general shift in the behavior of the cells to lean toward a decrease of migration induced by LPA.

We stably over-expressed LPP1 in Rat2 fibroblasts, and showed that there was a 20-fold increase of LPP1 mRNA levels, a 4-fold increase of total LPP activity, and a 2-fold increase of exogenous LPA dephosphorylation. Over-expression of LPP1 did not affect the expression of the other LPP isoforms [150]. Western blot analysis confirmed the presence of multiple bands corresponding to a glycosylated-membrane bound LPP1 with apparent molecular weight between 34- and 36-kDa. Removal of the asparagine bound N-glycan by amino acid substitution or enzymatically by a N-glycosidase, shifted the molecular weight of LPP1 to a value predicted from the cDNA sequence.

Biotinylation of cell surface proteins confirmed that GFP-tagged LPP1 and catalytically inactive LPP1[R217K]-GFP were expressed at the plasma membrane.

Adenoviruses packaged with cDNA coding for myc-tagged mouse LPP1 or inactive LPP1[R217K]-myc were used to efficiently and transiently over-express the recombinant LPP. These experiments showed that the fusion of GFP- or myc-tags on the C-termini of LPP1 did not abolish activity, nor did it affect plasma membrane expression in Rat2 fibroblasts. This system also allowed us to express similar levels of catalytically inactive LPP1. Indirect immunofluorescence showed that both active and inactive LPP1 were expressed at the plasma membrane and in similar intracellular locations. Therefore, experiments elucidating whether a LPP1 effect depends on catalytic activity can be performed in Rat2 fibroblasts without concern for ectopic expression of the mutant LPP1. This became a concern when it was observed that inactive LPP1 had decreased plasma membrane expression in transiently transfected Cos7 cells. Inactive LPP1 appeared to be retained and concentrated in a reticular compartment that partially over-lapped with calreticulin, the endoplasmic reticulum (ER) marker and the glycoprotein-chaperone. Protein retention is a hallmark of ER retention of misfolded or unstable proteins [228, 229]. Although the reason for this discrepancy between Rat2 fibroblasts and Cos7 cells was not resolved, we found that Rat2 fibroblasts had 7.4-fold more endogenous LPP activity, and perhaps were more able to deal with the proper expression and localization of catalytically inactive LPP1 than were Cos7 cells. This observation also assured us that Rat2 fibroblasts were the appropriate model for exploring how LPP1 activity regulates migration. This aspect of proper folding and transport of LPP1 in Cos7 cells would be of interest for future study, but it was not considered to be a priority for my work.

Over-expression of enzymes can produce non-physiological results. Therefore, LPP1 production was knocked down by the use of siRNA specific for endogenous rat LPP1. This resulted in a 90% decrease of rat LPP1 mRNA, and a 50% decrease in total LPP activity. The lower effect on LPP activities compared to mRNA levels is explained by the fact that the fibroblasts continue to express LPP2 and LPP3 at their basal levels [150]. It appears that LPP1 is a major contributor to LPP activity in the fibroblasts since increasing, or knocking down its expression significantly altered total LPP activity compared to changing LPP2 or LPP3 levels [150].

After it was established that LPP1 had ecto-activity in our model, we set out to determine if it would regulate LPA-induced migration. LPP1 decreased the stimulation of fibroblast migration by LPA determined by wound healing and Transwell chamber migration assays. The LPA receptor most likely involved is LPA_1, since LPA_2, and LPA_3 mRNAs were not detected in Rat2 fibroblasts by semi-quantitative RT-PCR. The expressions of LPA_4 and the putative LPA_5 were not measured, however it is unlikely that they would be the receptors mediating LPA-induced migration in Rat2 fibroblasts [70, 284]. LPA_4 and LPA_5 mediate the accumulation of cAMP by activating adenylyl cyclase. This is significant in our experiments because LPA-induced migration was completely inhibited by pertussis toxin. Pertussis toxin uncouples $G\alpha_i$ from the G protein coupled receptor (GPCR). Activated $G\alpha_i$ is responsible for inhibition of adenylyl cyclase, and is necessary for LPA-induced migration. Additionally, $G\alpha_i$ is associated with LPA_1 [285]. LPA-induced migration of embryonic fibroblasts and glioma cells also requires LPA_1, and it is inhibited by pertussis toxin treatment [46, 286]. Similarly, migration induced by a non-hydrolysable LPA-analogue was also pertussis toxin sensitive (Fig 4.8C). The

LPA-analogue, an α-hydroxyphosphonate, was previously shown to be an agonist for $LPA_{1/3}$ [166, 232].

Similar to LPA, migration of LPP1 over-expressing fibroblasts induced by the non-hydrolysable LPA-analogue was also attenuated. Therefore, the attenuation of LPA-induced migration is not dependent on the dephosphorylation of exogenous LPA by increased LPP1 expression. The attenuation of LPA-induced migration by LPP1 was repeated in fibroblasts from transgenic mice expressing 2-gene copies of *Lpp1*, and in fibroblasts infected by adenovirus to transiently express active myc-tagged LPP1. Catalytically inactive myc-tagged LPP1 was similarly expressed, but did not show attenuation of LPA-induced migration. We hypothesized that the decrease of migration is mediated by the dephosphorylation of a lipid phosphate downstream of LPA_1 receptor activation provided there is access to the LPP1 active site. This hypothesis is compatible with the observations that the attenuation of LPA-induced migration is dependent on catalytically intact LPP1, but not dependent on LPP1 mediated dephosphorylation of external LPA. Measuring the levels of internal LPA, PA, S1P, and C1P accumulation and their dephosphorylated by-products upon agonist treatment of control cells and LPP1 over-expressing cells could give us an answer to which lipid phosphate LPP1 regulates concentrations. By controlling internal lipid phosphate concentrations, LPP1 could regulate signaling in the cell. For example, LPA-induced Ca^{2+} mobilization in human SH-SY5Y neuroblastoma cells is dependent on S1P produced by sphingosine kinase (SK) [287]. The degradation of this S1P by LPP1 could therefore account for the decreased Ca^{2+}-mobilization induced by S1P, and not the PDGF-induced Ca^{2+}release, which is

dependent on PLCγ-mediated production of inositol phosphate [242]. Intracellular S1P is also known to regulate ERK1/2, PLD, and the Rho family GTPases [288, 289].

Among the lipid phosphates mentioned, this thesis demonstrated that LPA-, and PDGF- induced PLD activation and accumulation of PA was attenuated by LPP1. PA can be generated by PLD, therefore we predicted that LPP1 would act downstream of PLD activation to decrease PA levels by converting it to DAG. Alderton *et al.* [161] found that LPP1 over-expression in HEK 293 cells double the basal DAG to PA ratio. LPP3 was also found to be downstream of PLD2 activation after stimulation by PMA [165]. Unlike the examples mentioned above we found the formation of DAG in LPP1 over-expressing fibroblasts was not changed. This finding is compatible with that of Sciorra *et al* [165] who showed that LPP1 over-expression did not increase DAG concentrations after PMA stimulation. However, we did not prove that LPP1 was not downstream of PLD activity, since we only measured steady state levels of DAG. In fact we found that DAG levels significantly increased in the activated LPP1 over-expressing cells whereas they did not in the control cells (Fig 5.2). This is compatible with the role of LPP1 in the conversion of PA to DAG upon cell stimulation. In this regard, it is remarkable that DAG levels were maintained in LPP1 over-expressing fibroblasts despite a severely decreased PLD activity and PA accumulation. In addition, DAG could be derived from LPA- and PDGF-stimulation of phospholipase C (PLC) activities.

Unlike the attenuated activity of PLD induced by LPA and PDGF in LPP1 over-expressing fibroblasts, endothelin-induced PLD activation was not affected. Therefore the endothelin-signaling pathway bypasses the mechanism that LPA and PDGF utilize for PLD activation. It was also apparent that the activation of PLD by endothelin was much

more robust than it was for PDGF and more so compared to LPA (Fig. 5.3). A study by Van Der Bend *et al.* [240] on Rat1 fibroblasts confirms that LPA is less efficient than endothelin in the activation of PLD, and that LPA stimulation of PLD is short-lived, leveling off after 2 min, whereas endothelin-stimulated PLD activity persists for at least 1 h. An investigation for the activation of PLD by these three agonists would be of interest for future study to elucidate how LPP1 regulates LPA- and PDGF-induced PLD activation. Factors that regulate PLD activity include ADP-ribosylation factors (ARF), tyrosine kinases, PKCs, PLCs, phosphoinositides and Rho family GTPases (reviewed in [74]).

We found that increasing LPP1 expression decreased Rho activation by LPA, however we found that PDGF did not activate Rho. This is consistent with the work by the Exton laboratory showing that PDGF induced the translocation of Rac1, but not RhoA to a membrane fraction in Swiss 3T3 fibroblasts [290]. PDGF-induced membrane protrusions have low RhoA activity [247]. However, LPA translocated RhoA to the membrane fraction [290]. We also found that inhibiting PLD activity did not affect Rho activity, consistent with a role for Rho upstream of PLD activation. It is apparent that the molecular mechanisms controlling the stimulation of fibroblast migration by LPA, PDGF and endothelin are different. This explains the observation in Chapter 4 that showed the mode of migration of Rat2 fibroblasts induced by LPA and endothelin was mainly chemokinentic (random motility) and that PDGF induced mainly chemotaxis (Figure 7.1 shows a schematic diagram of agonist stimulation of fibroblasts, and the effect of LPP1 over-expression on the activation of signaling molecules).

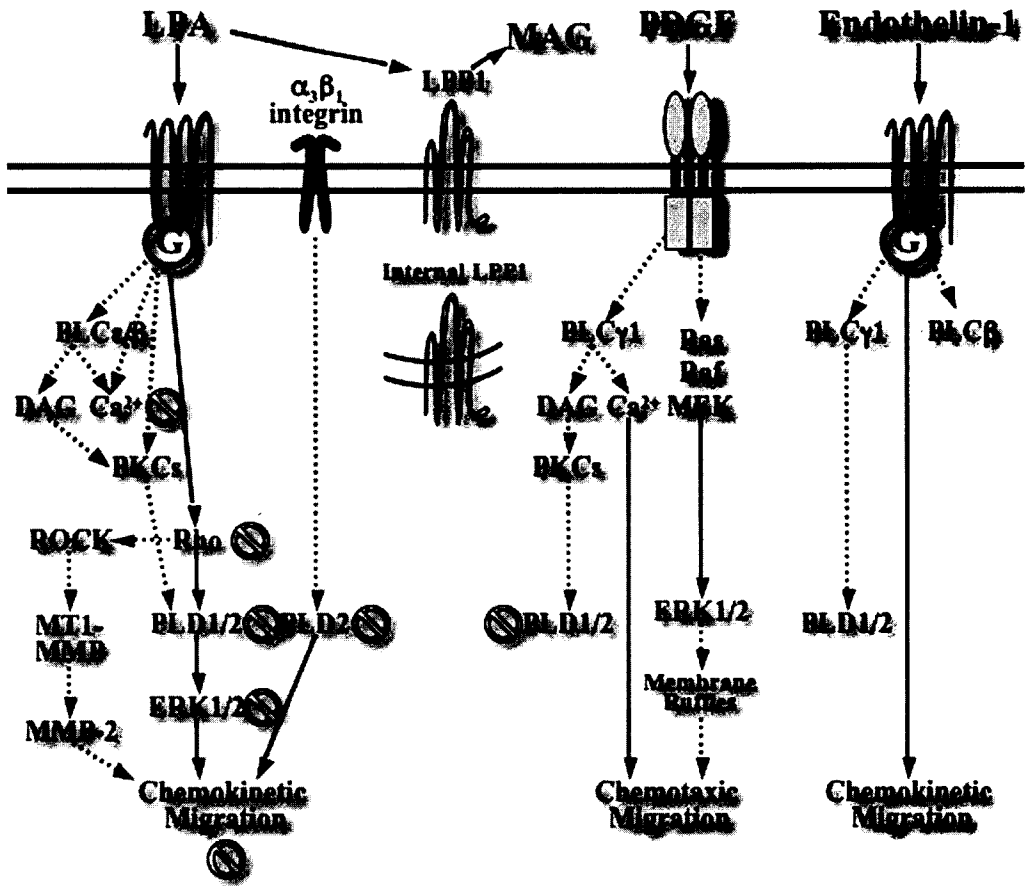

Figure 7.1 Migration signaling pathways induced by LPA, PDGF, and endothelin-1 in fibroblasts. This model shows the effects LPP1 has on signaling pathways induced by extracellular LPA, PDGF, and endothelin. The *circles with through-lines* indicate observed attenuations by LPP1 over-expression. *Dotted arrows* represent pathways not confirmed in this thesis, but supported by literature. *Solid arrows* represent the pathways that were demonstrated in Rat2 fibroblasts, and discussed in the thesis. *Arrows* do not necessarily implicate direct activations. Although it is not shown in the model we demonstrated that Ca^{2+} release is required for LPA-induced migration. Activation of MMP-2 by MT1-MMP occurs on the cell surface. PDGF-induced membrane ruffles are generally associated with Rac1 activation.

Other intriguing lipid phosphate candidates are pyrophosphorylated isoprenoids. Yeast LPP1, and diacylglycerol-pyrophospate phosphatase 1 (DPP1) have 49% similarity at the amino acid level to mouse LPP1, the same putative topology as mouse LPP1, and belong to the phosphatase super-family that share a strictly conserved domain required for phosphatase activity [141]. Yeast LPP1 and DPP1 were shown to account for most of the isoprenoid pyrophosphate phosphatase activities in *Saccharomyces cerevisiae* [291].

Recombinant human LPP1 efficiently degraded farnesylpyrophosphate *in vitro* [292], and it was shown that farnesol enhances apoptosis by its inhibition of PLD signaling [293]. Therefore, the inhibition of PLD by LPP1 could be through the degradation of farnesylpyrophosphate, and/or farnesylphosphate to farnesol. Equally, LPP1 could affect the isoprenylation of signaling proteins. Pyrophosphorylated isoprenoids; farnesylpyrophosphate and geranylgeranylpyrosphosphate, are covalently added to proteins with a C-terminal CaaX sequence where 'C' is a cysteine residue that is prenylated, 'a' is an aliphatic amino acid, and 'X' can be serine, methionine, glutamine, alanine, or threonine, and determines which prenyl group is added by farnesyl transferase, or geranyl transferases [294]. Prenylation is an important mechanism in post-translational attachment of proteins to membranes, and together with other factors can facilitate the targeting of proteins to specific cellular compartments. Ras proteins are farnesylated and Rho family GTPases are geranylated. Activation of PLD by Cdc42, and RhoA requires isoprenylation of these G proteins [295, 296]. Our work showed that LPP1 over-expression decreased LPA-induced Rho activation, and the basal activities of Rac, and Cdc42, which are all geranylated. Furthermore, LPA-induced ERK1/2 activation is mediated by the Ras-Raf-MEK pathway. A decrease of farnesylated Ras by LPP1 could account for the decreased LPA-induced ERK1/2 activation, but does not account for intact PDGF-induced ERK1/2 activation. In some cases unprenylated forms of Ras and other G proteins can maintain partial function or interfere with the actions of other prenylated proteins [294]. It would be of interest to examine if LPP1 could regulate the concentrations of the isoprenoid pyrophosphates, and thus regulate prenylation levels of these G proteins.

LPP1 over-expresssion decreased the activation of each signaling molecule that was tested and known to be downstream of LPA receptor activation. It would be a good idea to look at the expression of the LPA receptor, LPA_1, in Rat2 fibroblasts. Perhaps over-expression of LPP1 decreased the expression of the *Lpa1* gene as it influenced expression of the *Mmp* and *Timp2* genes. This could be measured by real time RT-PCR, although semi-quantitative RT-PCR failed to show a decrease of LPA_1 mRNA levels in LPP1 over-expressing fibroblasts. Another level of control for LPA signaling is the expression of LPA_1 at the plasma membrane. LPA_1 undergoes rapid ligand-induced internalization from the plasma membrane via β-arrestin- and clatherin-dependent pathways [170, 297]. Upon removal of LPA, LPA_1 recycles back to the plasma membrane [297]. The relative concentrations of LPA and PA in membranes control their curvature and vesicle budding [101, 102] and the control of their concentrations by LPP1 could effect the expression of cell surface LPA_1 receptors in serum-starved fibroblasts. In a recent study, it was found that PLD2 and not PLD1 is required for the recycling of transferrin receptors to the plasma membranes of HeLa cells, whereas the internalization rate is unaffected by depletion of either PLD [298]. Cells with reduced PLD2 accumulate a greater fraction of transferrin receptors in a perinuclear compartment containing markers for endosomes involved in receptor recycling [298]. In another study depletion of PLD2, not PLD1, and expression of a dominant/negative PLD2 inhibits ligand binding-induced angiotensin II receptor endocytosis, and subsequent accumulation in recycling endosomes [299]. In this case PLD2 affects the endocytosis process, and could inhibit signaling dependent on receptor internalization. Therefore, it would be of interest to study the observed PLD2 inhibition by LPP1 over-expression in relation to LPA_1

endocytosis and recycling. We could also study other receptors that are internalized, although we predict that there would be no effect by LPP1 of endothelin and PDGFR-β receptor localization since migration mediated by their activation was not affected.

Observing that LPP1 attenuated PDGF-induced PLD activation indicated to us that LPP1 can have a broader influence on cell signaling, other than on just LPA-induced signaling. Indeed, we found that the phosphorylation patterns of proteins from lysates of fibroblasts over-expressing LPP1 treated with various agonists were altered compared to control fibroblasts. For example, a set of proteins with molecular weight around 45 kDa was hyperphosphorylated by Akt in response to EGF, PDGF, and LPA in LPP1 over-expressing fibroblasts. Therefore, LPP1 also has the potential to regulate signaling by the PI3-kinase/Akt pathway. Identification of these phosphorylated proteins would not only expand our knowledge of other signaling pathways that could be affected by LPP1, but could also help us decipher how LPP1 exerts its effects on signaling. We found many candidate phosphorylated proteins of interest, however, confidently picking the phosphorylated proteins identified by Western blot from the corresponding Coomassie blue-stained gel of resolved protein from total lysate was difficult. This problem could be solved by immunoprecipitating the phosphorylated proteins with the various phospho-specific antibodies immobilized on agarose beads. This method would help clear the lysates of any proteins not phosphorylated that can interfere with identification of target proteins resolved on Coomassie blue-stained gels. If this is ineffective, it is possible to purify all phosphorylated proteins using a patented affinity chromatography column from Qiagen.

After an extracellular stimulation instructs the cell to migrate, a coordinated response within the cell induces the detachment and reattachment of the cell on the sub-stratum. Migration through the extracellular matrix (ECM) requires that contacts between the cell and ECM are constantly changing. A significant part of this process is mediated by proteins that are secreted, or associated with the cell surface that are involved in the remodeling of the ECM, and additional external cell signaling. These proteins include matrix metalloproteinases (MMP) and their regulators, tissue inhibitor of metalloproteinases (TIMP). We found a decreased MMP-2 production, and enhanced MMP-9 and TIMP-2 production in serum-starved fibroblasts over-expressing LPP1. The reasons for these changes have not been explored. PLD, Rho, and especially ERK1/2 have been found to play roles in the expression and activation of these proteins [206, 208, 266-269, 271-274]. For example, laminin induced activation of PLD increased MMP-2 expression in a metastatic cell model [266]. Activation of ERK 1/2, Rac1, and Rho, and Rho-associated coiled-coil forming protein kinase (ROCK) mediate the upregulation of membrane-type 1 (MT1)-MMP (Fig. 7.1) [268, 300, 301]. MT1-MMP increases the activation of MMP-2. This is significant because LPA-induced migration of cancer cells depends on the expression of MT1-MMP [302]. Future work on the affects of LPP1 on gene expression should focus on these signaling molecules and their effects on transcription factors on their promoters [263, 279]. Additionally, the expression of MMP-2, MMP-9 and TIMP-2 could be regulated by the stability of their mRNA transcripts. Activation of the $\alpha_3\beta_1$ integrin increases the expression of MMP-9 [283]. This was not mediated by an increased activation of the MMP-9 promoter, but by increasing the stability of MMP-9 mRNA. Since MMP-2 and TIMP-2 are not inducible in

non-transformed cells [206, 266] perhaps LPP1 over-expression can regulate their transcript stabilities.

Decreased MMP-2 and increased TIMP-2 indicate that there is an overall decrease of MMP-2 activity in LPP1 over-expressing cells (Figure 7.2). Membrane type-1 (MT1)-MMP activation of pro-MMP-2 at the cell surface is mediated by low concentrations of TIMP-2 [219-222]. Cell surface activation of MMP-2 is required for efficient migration [220, 256, 258, 259], however high concentrations of TIMP-2 will inhibit pro-MMP-2 processing and MMP-2 activity, thus inhibiting migration. Enhanced TIMP-2 levels in conditioned medium from LPP1 over-expressing fibroblasts could explain the inhibitory effect on LPA-induced migration of wild-type fibroblasts. Unpublished work by Dr. Meltem Sariahmetoglu identified the inhibitory factor from the conditioned medium as TIMP-2. Also, knockdown of TIMP-2 using siRNA in LPP1 over-expressing fibroblasts relieved the inhibitory effect of the conditioned media on LPA-induced migration of wild-type fibroblasts. Furthermore, LPA-induced migration of fibroblasts over-expressing LPP1 increased when TIMP-2 was knocked down (unpublished work). The evidence suggests that increasing LPP1 levels increased TIMP-2 secreted into the conditioned media, which is then responsible for the attenuation of LPA-induced migration in an autocrine and paracrine manner.

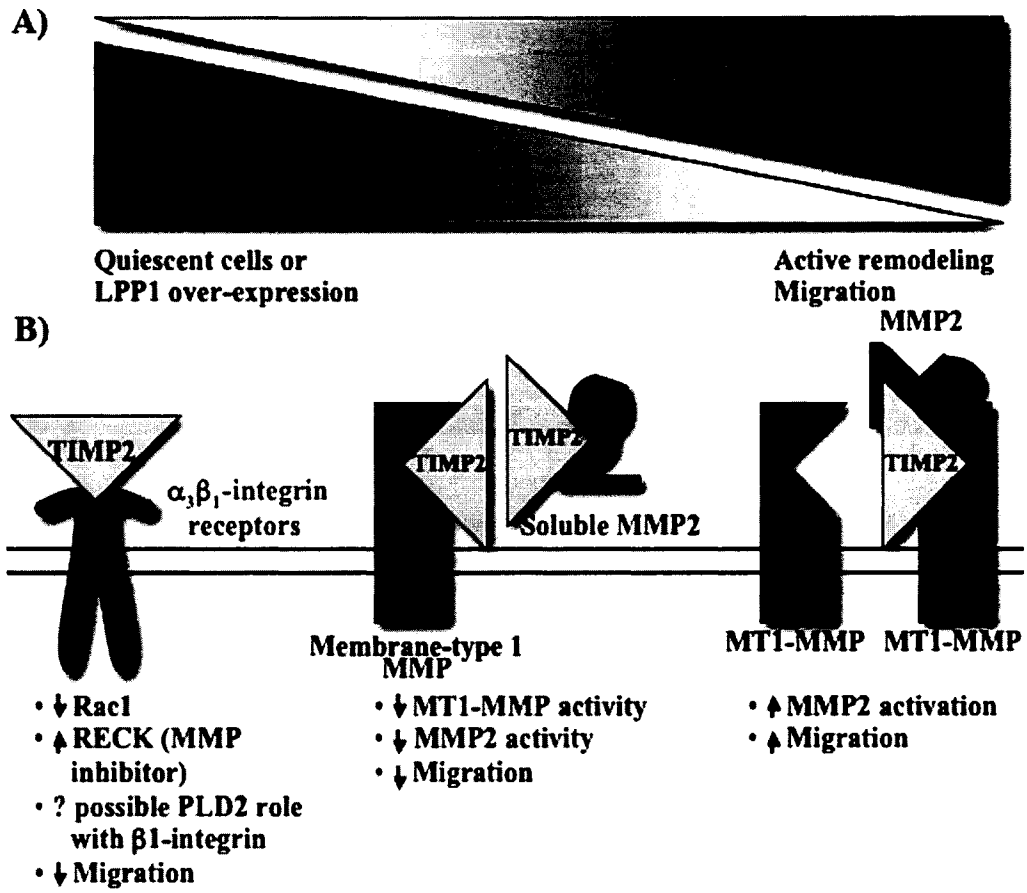

Figure 7.2 Model for TIMP-2 regulation of migration through its binding of $\alpha_3\beta_1$-intergrin receptors and indirectly by modulating the activities of MT1-MMP and MMP-2. *Panel A* shows that quiescent cells or fibroblasts over-expressing LPP1 with high TIMP-2 and low MMP2 levels. Excess free-TIMP-2 binds to $\alpha_3\beta_1$-intergrin receptors (*Panel B*) to increase RECK expression and therefore decrease migration. This occurs independently of direct TIMP-2 inhibitory action on MMP. When cells start to increase active MMP and limit TIMP-2 expression, the MMPs act as a sink and decrease free-TIMP-2 concentrations. At low concentrations, TIMP-2 is insufficient to inhibit MMP activity and leads to an enhanced MMP-2 activation mediated by MT1-MMP. This results in extracellular remodeling, and increased migration (*Panels A* and *B*). This model was adapted from Stetler-Stevenson *et al* [257].

In the discussion section of Chapter 6, it was mentioned that TIMP-2 bound and activated the $\alpha_3\beta_1$ integrin (reviewed in [257]). In fibroblasts, binding of TIMP-2 to the $\alpha_3\beta_1$ integrin [281, 282] decreases Rac activity, and increases the expression of the MMP inhibitor, RECK. RECK inhibits basal cell migration (Figure 7.2B). Embryonic fibroblasts from RECK-null mice failed to demonstrate TIMP-2–mediated decrease in

cell migration [281]. It would be of interest to study the involvement of PLD2 in this process, since it was reported that PLD2 activity strengthened the interaction of β_1 integrin with the substratum [245]. In Rat2 fibroblasts, we found that PLD2 was required for LPA-induced migration, and that LPP1 over-expression in these cells, which decreased PLD activity, weakened interaction of the fibroblasts with the tissue culture plates. Furthermore, LPA-induced migration requires β_1A integrin [234]. Therefore, the enhanced basal secretion of TIMP-2 in LPP1 over-expressing fibroblasts could constantly bind $\alpha_3\beta_1$ integrins. This could occupy functional β_1 integrin required for LPA-induced migration on the sub-stratum, decrease basal Rac activity, and perhaps decrease PLD2 activity, which could then weaken the interaction of the fibroblasts to the ECM. A result of this could be an attenuation of LPA-induced migration. The involvement of the other signaling molecules described in this thesis, including ERK1/2, and Rho would also be targets of interest in verifying this hypothesis.

In the context of wound healing it appears that increased LPP1 expression in fibroblasts is related to a decrease of fibroblast migration induced by LPA. Therefore, it is conceivable that LPP1 expression in fibroblasts would be low or decreased during the fibroblast migration stage that culminates in the immigration of fibroblasts to the granulation tissue starting at day 3 of healing (Fig 1.1 B-D). PDGF-induced fibroblast migration is also significant in wound healing [5]. There are studies that demonstrate LPA synergistically enhances PDGF-induced fibroblast migration [303-305]. Although we did not perform an experiment to show this, it is hypothesized that decreased LPP1 expression would enhance LPA synergism with PDGF-induced fibroblast migration. Conversely, LPP1 over-expression would attenuate LPA enhancement of PDGF-induced

fibroblast migration. In physiological terms, both LPA and PDGF could work in concert to maximize fibroblast migration to the granulation tissue. LPP1 would only affect LPA-signaling in this process. Once the fibroblasts arrive to the site of the wound, migration decreases. It is postulated that LPP1 activity is increased so that LPA-induced migration in the wound site is decreased.

At the wound site TGF-β1 induces fibroblasts to quickly lay down a collagen-rich matrix, and replace the provisional matrix with granulation tissue [4, 5]. In dermal fibroblasts, LPA-induced activation of ERK antagonizes TGF-β1 induced collagen deposition [306]. Therefore, inhibiting LPA-signaling by increased LPP1 expression would not only decrease fibroblast migration, but also aid in the formation of the granulation tissue. It would be useful to investigate whether TGF-β1 can also increase LPP1 expression to facilitate collagen deposition. Additionally, LPP1 over-expression increased the accumulation of procollagen C-proteinase enhancer (PCPE) in conditioned media. PCPE enhances the activity of procollagen C-proteinase (PCP) that cleaves soluble procollagens at their C-terminus to facilitate the production of insoluble fibrillar collagens for the ECM [260]. PCPE enhances PCP activity 20-fold [307]. It appears by increasing LPP1 production, the fibroblasts also increase their capacity to deposit and remodel collagen to produce ECM, indicated by the increase of PCPE secretion in the conditioned media. It would be interesting to investigate if fibroblasts that over-express LPP1 have increased collagen-fibril production. Additionally, the increased expression of PCPE could also contribute to a decrease of MMP-2/MT1-MMP activation that would reduce ECM degradation. PCPE C-terminal netrin-like domain shows homology to that of the TIMPs [261], and acts as a weak inhibitor of MMP-2 and MT1-MMP [262].

Together with an increase of secreted TIMP-2 and PCPE in the conditioned media, and a decrease of MMP-2 production, LPP1 over-expressing fibroblasts appear poised to attenuate response to LPA-induced migration, and increase collagen deposition. However, the decrease of MMP-2 activity and increase of TIMP-2 regulation in our LPP1 over-expressing fibroblasts does not correspond to what happens in normal cutaneous wound healing. During normal wound healing MMP-2, MMP-9, MT1-MMP, and TIMP-2 expression are all increased in granulation tissue [216-218]. The ratio of pro-MMP-2 to mature MMP-2, which is mediated by TIMP-2 and MT1-MMP, is constant during normal healing and scar formation, and is similar to unwounded skin [216]. The healing of fetal wounds result in the absence of a scar, and are associated with high MMP activities and a decrease of MMP regulation by TIMPs [308]. In the other extreme, the decrease of MMP-2 activity and increase of its regulator TIMP-2 suggests that our fibroblasts over-expressing LPP1 are more similar to those in fibrotic diseases [309]. Fibrotic diseases are characterized by an excess accumulation of collagen, and decreased ECM degradation and remodeling associated with decreased MMP activities and increased TIMP levels [309-312]. In fact biopsies from fibrotic livers have increased PAP-2 activities [313]. It would be interesting to investigate whether this PAP-2 activity is attributed to increased LPP1 expression.

Most of the affects of LPP1 described in this thesis involved the use of the stably transduced fibroblasts. We were successful in knocking down LPP1 by transiently transfecting siRNA specific for the endogenous gene. Knockdown of LPP1 enhanced migration of fibroblasts induced by LPA, therefore it would be of interest to determine which of the signaling molecules are affected. This includes the expression of the

TIMP-2, MMP-2 and MMP-9, and the activation of PLD1 and PLD2, ERK, and the Rho family GTPases. We should complement these studies using the knockdown technology and the efficient transient transfection by adenovirus infection, and then determine which of these effects are due to long-term or short-term expression of LPP1. This would be important in ovarian cancers where the expression of LPP1 mRNA is down-regulated and is attributed to the increased LPA concentrations in malignant ascites fluid, which stimulates cell proliferation, cell survival, and resistance to cancer treatment [178]. Long-term knockdown of LPP1 could be achieved by creating fibroblasts that stably express short-hairpin RNA to silence endogenous LPP1 expression.

In conclusion, the results in this thesis demonstrate that LPP1 can regulate various pathways of cell signaling. We focused on the endpoint of fibroblast migration, which is important in wound healing. Also, excessive fibroblast activation is involved in scarring and fibrosis that occurs in a variety of inflammatory conditions. It is also important to study the role of LPP1 in other aspects of cellular function including cell proliferation, and survival. These are important questions particularly in tumor growth, protection from apoptosis, and metastasis. The possible function of LPP1 in regulating ECM remodeling broadens the role that LPP1 could play in these physiological and pathophysiological conditions.

BIBILOGRAPHY

1. Alberts, B., et al., *Molecular Biology of the Cell.* 3rd ed. 1994, New York: Garland Publishing. 1294.

2. Brakebusch, C., *Keratinocyte Migration in Wound Healing*, in *Cell Migration in Development and Disease*, D. Wedlich, Editor. 2005, Wiley-VCH: Weinheim. p. 275-293.

3. Bosman, F.T. and I. Stamenkovic, *Functional structure and composition of the extracellular matrix.* J Pathol, 2003. **200**(4): p. 423-8.

4. Martin, P., *Wound healing--aiming for perfect skin regeneration.* Science, 1997. **276**(5309): p. 75-81.

5. Singer, A.J. and R.A. Clark, *Cutaneous wound healing.* N Engl J Med, 1999. **341**(10): p. 738-46.

6. Aoki, J., *Mechanisms of lysophosphatidic acid production.* Semin Cell Dev Biol, 2004. **15**(5): p. 477-89.

7. English, D., J.G. Garcia, and D.N. Brindley, *Platelet-released phospholipids link haemostasis and angiogenesis.* Cardiovasc Res, 2001. **49**(3): p. 588-99.

8. Tani, M., M. Ito, and Y. Igarashi, *Ceramide/sphingosine/sphingosine 1-phosphate metabolism on the cell surface and in the extracellular space.* Cell Signal, 2007. **19**(2): p. 229-37.

9. Bonner, J.C., *Regulation of PDGF and its receptors in fibrotic diseases.* Cytokine Growth Factor Rev, 2004. **15**(4): p. 255-73.

10. Kraft, M., et al., *IL-4, IL-13, and dexamethasone augment fibroblast proliferation in asthma.* J Allergy Clin Immunol, 2001. **107**(4): p. 602-6.

11. Levitzki, A., *PDGF receptor kinase inhibitors for the treatment of PDGF driven diseases.* Cytokine Growth Factor Rev, 2004. **15**(4): p. 229-35.

12. Fredriksson, L., H. Li, and U. Eriksson, *The PDGF family: four gene products form five dimeric isoforms.* Cytokine Growth Factor Rev, 2004. **15**(4): p. 197-204.

13. Bergsten, E., et al., *PDGF-D is a specific, protease-activated ligand for the PDGF beta-receptor.* Nat Cell Biol, 2001. **3**(5): p. 512-6.

14. Li, X., et al., *PDGF-C is a new protease-activated ligand for the PDGF alpha-receptor.* Nat Cell Biol, 2000. **2**(5): p. 302-9.

15. Gilbertson, D.G., et al., *Platelet-derived growth factor C (PDGF-C), a novel growth factor that binds to PDGF alpha and beta receptor.* J Biol Chem, 2001. **276**(29): p. 27406-14.

16. Fredriksson, L., et al., *Tissue plasminogen activator is a potent activator of PDGF-CC.* Embo J, 2004. **23**(19): p. 3793-802.

17. Ronnstrand, L. and C.H. Heldin, *Mechanisms of platelet-derived growth factor-induced chemotaxis.* Int J Cancer, 2001. **91**(6): p. 757-62.

18. Kazlauskas, A. and J.A. Cooper, *Autophosphorylation of the PDGF receptor in the kinase insert region regulates interactions with cell proteins.* Cell, 1989. **58**(6): p. 1121-33.

19. Wang, Y., et al., *Platelet-derived growth factor receptor-mediated signal transduction from endosomes.* J Biol Chem, 2004. **279**(9): p. 8038-46.

20. Martinet, Y., et al., *Exaggerated spontaneous release of platelet-derived growth factor by alveolar macrophages from patients with idiopathic pulmonary fibrosis.* N Engl J Med, 1987. **317**(4): p. 202-9.

21. Bonner, J.C., et al., *Induction of PDGF receptor-alpha in rat myofibroblasts during pulmonary fibrogenesis in vivo.* Am J Physiol, 1998. **274**(1 Pt 1): p. L72-80.

22. Betsholtz, C., *Insight into the physiological functions of PDGF through genetic studies in mice.* Cytokine Growth Factor Rev, 2004. **15**(4): p. 215-28.

23. Hellstrom, M., et al., *Role of PDGF-B and PDGFR-beta in recruitment of vascular smooth muscle cells and pericytes during embryonic blood vessel formation in the mouse.* Development, 1999. **126**(14): p. 3047-55.

24. Ostman, A., *PDGF receptors-mediators of autocrine tumor growth and regulators of tumor vasculature and stroma.* Cytokine Growth Factor Rev, 2004. **15**(4): p. 275-86.

25. Moolenaar, W.H., L.A. van Meeteren, and B.N. Giepmans, *The ins and outs of lysophosphatidic acid signaling.* Bioessays, 2004. **26**(8): p. 870-81.

26. Tigyi, G. and A.L. Parrill, *Molecular mechanisms of lysophosphatidic acid action.* Prog Lipid Res, 2003. **42**(6): p. 498-526.

27. Balazs, L., et al., *Topical Application of the Phospholipid Growth Factor Lysophosphatidic Acid Promotes Wound Healing In Vivo.* Am. J. Physiol., 2000: p. in press.

28. Parizi, M., E.W. Howard, and J.J. Tomasek, *Regulation of LPA-promoted myofibroblast contraction: role of Rho, myosin light chain kinase, and myosin light chain phosphatase.* Exp Cell Res, 2000. **254**(2): p. 210-20.

29. Umezu-Goto, M., et al., *Lysophosphatidic acid production and action: validated targets in cancer?* J Cell Biochem, 2004. **92**(6): p. 1115-40.

30. Sano, T., et al., *Multiple mechanisms linked to platelet activation result in lysophosphatidic acid and sphingosine 1-phosphate generation in blood.* J Biol Chem, 2002. **277**(24): p. 21197-206.

31. Fourcade, O., et al., *Secretory phospholipase A2 generates the novel lipid mediator lysophosphatidic acid in membrane microvesicles shed from activated cells.* Cell, 1995. **80**(6): p. 919-27.

32. Sonoda, H., et al., *A novel phosphatidic acid-selective phospholipase A1 that produces lysophosphatidic acid.* J Biol Chem, 2002. **277**(37): p. 34254-63.

33. Eder, A.M., et al., *Constitutive and lysophosphatidic acid (LPA)-induced LPA production: role of phospholipase D and phospholipase A2.* Clin Cancer Res, 2000. **6**(6): p. 2482-91.

34. Luquain, C., et al., *Role of phospholipase D in agonist-stimulated lysophosphatidic acid synthesis by ovarian cancer cells.* J Lipid Res, 2003. **44**(10): p. 1963-75.

35. Shen, Z., et al., *Phorbol 12-myristate 13-acetate stimulates lysophosphatidic acid secretion from ovarian and cervical cells but not from breast or leukemia cells.* Gynecol. Oncol., 1998. **71**: p. 364-368.

36. Xie, Y., et al., *Role for 18:1 lysophosphatidic acid as an autocrine mediator in prostate cancer cells.* J Biol Chem, 2002. **277**(36): p. 32516-26.

37. Bektas, M., et al., *A novel acylglycerol kinase that produces lysophosphatidic acid modulates cross talk with EGFR in prostate cancer cells.* J Cell Biol, 2005. **169**(5): p. 801-11.

38. Brindley, D.N., *Hepatic secretion of lysphosphatidylcholine: a novel transport system for polyunsaturated fatty acids and choline.* J. Nutr. Biochem., 1993. **4**: p. 442-449.

39. Aoki, J., et al., *Serum lysophosphatidic acid is produced through diverse phospholipase pathways.* J Biol Chem, 2002. **277**(50): p. 48737-44.

40. Jonas, A., *Lecithin cholesterol acyltransferase.* Biochim Biophys Acta, 2000. **1529**(1-3): p. 245-56.

41. Mills, G.B. and W.H. Moolenaar, *The emerging role of lysophosphatidic acid in cancer.* Nat Rev Cancer, 2003. **3**(8): p. 582-91.

42. Umezu-Goto, M., et al., *Autotaxin has lysophospholipase D activity leading to tumor cell growth and motility by lysophosphatidic acid production.* J Cell Biol, 2002. **158**(2): p. 227-33.

43. Tokumura, A., et al., *Identification of human plasma lysophospholipase D, a lysophosphatidic acid-producing enzyme, as autotaxin, a multifunctional phosphodiesterase.* J Biol Chem, 2002. **277**(42): p. 39436-42.

44. Moolenaar, W.H., *Lysophospholipids in the limelight: autotaxin takes center stage.* J Cell Biol, 2002. **158**(2): p. 197-9.

45. Sato, K., et al., *Identification of autotaxin as a neurite retraction-inducing factor of PC12 cells in cerebrospinal fluid and its possible sources.* J Neurochem, 2005. **92**(4): p. 904-14.

46. Hama, K., et al., *Lysophosphatidic acid and autotaxin stimulate cell motility of neoplastic and non-neoplastic cells through LPA1.* J Biol Chem, 2004. **279**(17): p. 17634-9.

47. Tanaka, M., et al., *Autotaxin stabilizes blood vessels and is required for embryonic vasculature by producing lysophosphatidic acid.* J Biol Chem, 2006. **281**(35): p. 25822-30.

48. van Meeteren, L.A., et al., *Autotaxin, a secreted lysophospholipase D, is essential for blood vessel formation during development.* Mol Cell Biol, 2006. **26**(13): p. 5015-22.

49. Mazereeuw-Hautier, J., et al., *Production of lysophosphatidic acid in blister fluid: involvement of a lysophospholipase D activity.* J Invest Dermatol, 2005. **125**(3): p. 421-7.

50. Valet, P., et al., *Alpha2-adrenergic receptor-mediated release of lysophosphatidic acid by adipocytes. A paracrine signal for preadipocyte growth.* J Clin Invest, 1998. **101**(7): p. 1431-8.

51. Ferry, G., et al., *Autotaxin is released from adipocytes, catalyzes lysophosphatidic acid synthesis, and activates preadipocyte proliferation. Up-regulated expression with adipocyte differentiation and obesity.* J Biol Chem, 2003. **278**(20): p. 18162-9.

52. English, D., et al., *Lipid mediators of angiogenesis and the signalling pathways they initiate.* Biochim Biophys Acta, 2002. **1582**(1-3): p. 228-39.

53. Liu, Y., et al., *Edg-1, the G protein-coupled receptor for sphingosine 1-phosphate, is essential for vascular maturation.* J. Clin. Invest., 2000. **106**(8): p. 951-961.

54. English, D., et al., *Sphingosine 1-phosphate released from platelets during clotting accounts for the potent endothelial cell chemotactic activity of blood serum and provides a novel link between hemostasis and angiogenesis.* Faseb J, 2000. **14**(14): p. 2255-65.

55. Matloubian, M., et al., *Lymphocyte egress from thymus and peripheral lymphoid organs is dependent on S1P receptor 1.* Nature, 2004. **427**(6972): p. 355-60.

56. Visentin, B., et al., *Validation of an anti-sphingosine-1-phosphate antibody as a potential therapeutic in reducing growth, invasion, and angiogenesis in multiple tumor lineages.* Cancer Cell, 2006. **9**(3): p. 225-38.

57. Yatomi, Y., et al., *Sphingosine 1-phosphate, a bioactive sphingolipid abundantly stored in platelets, is a normal constituent of human plasma and serum.* J Biochem (Tokyo), 1997. **121**(5): p. 969-73.

58. Clair, T., et al., *Autotaxin hydrolyzes sphingosylphosphorylcholine to produce the regulator of migration, sphingosine-1-phosphate.* Cancer Res, 2003. **63**(17): p. 5446-53.

59. Ancellin, N., et al., *Extracellular export of sphingosine kinase-1 enzyme. Sphingosine 1-phosphate generation and the induction of angiogenic vascular maturation.* J Biol Chem, 2002. **277**(8): p. 6667-75.

60. Dubyak, G.R. and C. el-Moatassim, *Signal transduction via P2-purinergic receptors for extracellular ATP and other nucleotides.* Am J Physiol, 1993. **265**(3 Pt 1): p. C577-606.

61. Arakaki, N., et al., *Possible role of cell surface H+ -ATP synthase in the extracellular ATP synthesis and proliferation of human umbilical vein endothelial cells.* Mol Cancer Res, 2003. **1**(13): p. 931-9.

62. Spiegel, S. and S. Milstien, *Exogenous and intracellularly generated sphingosine 1-phosphate can regulate cellular processes by divergent pathways.* Biochem Soc Trans, 2003. **31**(Pt 6): p. 1216-9.

63. Hanel, P., P. Andreani, and M.H. Graler, *Erythrocytes store and release sphingosine 1-phosphate in blood.* Faseb J, 2007.

64. Mitra, P., et al., *Role of ABCC1 in export of sphingosine-1-phosphate from mast cells.* Proc Natl Acad Sci U S A, 2006. **103**(44): p. 16394-9.

65. Zhao, Y., et al., *Intracellular Generation of Sphingosine 1-Phosphate in Human Lung Endothelial Cells: ROLE OF LIPID PHOSPHATE PHOSPHATASE-1 AND SPHINGOSINE KINASE 1.* J Biol Chem, 2007. **282**(19): p. 14165-77.

66. Mizugishi, K., et al., *Essential role for sphingosine kinases in neural and vascular development.* Mol Cell Biol, 2005. **25**(24): p. 11113-21.

67. An, S., et al., *Molecular cloning of the human Edg2 protein and its identification as a functional cellular receptor for lysophosphatidic acid.* Biochem. Biophys. Res. Commun., 1997. **231**: p. 619-622.

68. Hecht, J.H., et al., *Ventricular zone gene-1 (vzg-1) encodes a lysophosphatidic acid receptor expressed in neurogenic regions of the developing cerebral cortex.* J Cell Biol, 1996. **135**(4): p. 1071-83.

69. Gardell, S.E., A.E. Dubin, and J. Chun, *Emerging medicinal roles for lysophospholipid signaling.* Trends Mol Med, 2006. **12**(2): p. 65-75.

70. Lee, C.W., et al., *GPR92 as a new G12/13- and Gq-coupled lysophosphatidic acid receptor that increases cAMP, LPA5.* J Biol Chem, 2006. **281**(33): p. 23589-97.

71. Radeff-Huang, J., et al., *G protein mediated signaling pathways in lysophospholipid induced cell proliferation and survival.* J Cell Biochem, 2004. **92**(5): p. 949-66.

72. Yamada, T., et al., *Physical and functional interactions of the lysophosphatidic acid receptors with PDZ domain-containing Rho guanine nucleotide exchange factors (RhoGEFs).* J Biol Chem, 2005. **280**(19): p. 19358-63.

73. Raftopoulou, M. and A. Hall, *Cell migration: Rho GTPases lead the way.* Dev Biol, 2004. **265**(1): p. 23-32.

74. McDermott, M., M.J. Wakelam, and A.J. Morris, *Phospholipase D.* Biochem Cell Biol, 2004. **82**(1): p. 225-53.

75. Ishii, I., et al., *Marked perinatal lethality and cellular signaling deficits in mice null for the two sphingosine 1-phosphate (S1P) receptors, S1P(2)/LP(B2)/EDG-5 and S1P(3)/LP(B3)/EDG-3.* J Biol Chem, 2002. **277**(28): p. 25152-9.

76. Li, C., et al., *Lysophosphatidic acid inhibits cholera toxin-induced secretory diarrhea through CFTR-dependent protein interactions.* J Exp Med, 2005. **202**(7): p. 975-86.

77. Piiper, A. and S. Zeuzem, *Receptor tyrosine kinases are signaling intermediates of G protein-coupled receptors.* Curr Pharm Des, 2004. **10**(28): p. 3539-45.

78. Pyne, N.J., et al., *Receptor tyrosine kinase-GPCR signal complexes.* Biochem Soc Trans, 2003. **31**(Pt 6): p. 1220-5.

79. Luttrell, L.M., et al., *Gbetagamma subunits mediate Src-dependent phosphorylation of the epidermal growth factor receptor. A scaffold for G protein-coupled receptor-mediated Ras activation.* J Biol Chem, 1997. **272**(7): p. 4637-44.

80. Wang, L., et al., *Involvement of phospholipase D2 in lysophosphatidate-induced transactivation of platelet-derived growth factor receptor-beta in human bronchial epithelial cells.* J Biol Chem, 2003. **278**(41): p. 39931-40.

81. Fischer, O.M., et al., *EGFR signal transactivation in cancer cells.* Biochem Soc Trans, 2003. **31**(Pt 6): p. 1203-8.

82. Donkor, J., et al., *Three mammalian lipins act as phosphatidate phosphatases with distinct tissue expression patterns.* J Biol Chem, 2006.

83. Boujaoude, L.C., et al., *Cystic fibrosis transmembrane regulator regulates uptake of sphingoid base phosphates and lysophosphatidic acid: modulation of cellular activity of sphingosine 1-phosphate.* J Biol Chem, 2001. **276**(38): p. 35258-64.

84. Brindley, D.N., *Lipid phosphate phosphatases and related proteins: signaling functions in development, cell division, and cancer.* J Cell Biochem, 2004. **92**(5): p. 900-12.

85. Roberts, R.Z. and A.J. Morris, *Role of phosphatidic acid phosphatase 2a in uptake of extracellular lipid phosphate mediators.* Biochim Biophys Acta, 2000. **1487**(1): p. 33-49.

86. Rossi, F., et al., *Phosphatidic acid and not diacylglycerol generated by phospholipase D is functionally linked to the activation of the NADPH oxidase by*

fMLP in human neutrophils. Biochem. Biophys. Res. Commun., 1990. **168**: p. 320-327.

87. Limatola, C., et al., *Phosphatidic acid activation of protein kinase C-zeta overexpressed in COS cells: comparison with other protein kinase C isotypes and other acidic lipids.* Biochem J, 1994. **304 (Pt 3)**: p. 1001-8.

88. Jones, G.A. and G. Carpenter, *The regulation of phospholipase C-gamma 1 by phosphatidic acid. Assessment of kinetic parameters.* J Biol Chem, 1993. **268**(28): p. 20845-50.

89. Tsai, M.H., et al., *The effect of GTPase activating protein upon ras is inhibited by mitogenically responsive lipids.* Science, 1989. **243**(4890): p. 522-6.

90. Delon, C., et al., *Sphingosine kinase 1 is an intracellular effector of phosphatidic acid.* J Biol Chem, 2004. **279**(43): p. 44763-74.

91. Jones, J.A. and Y.A. Hannun, *Tight binding inhibition of protein phosphatase-1 by phosphatidic acid. Specificity of inhibition by the phospholipid.* J Biol Chem, 2002. **277**(18): p. 15530-8.

92. Ghosh, S., et al., *Raf-1 kinase possesses distinct binding domains for phosphatidylserine and phosphatidic acid. Phosphatidic acid regulates the translocation of Raf-1 in 12-O-tetradecanoylphorbol-13-acetate-stimulated Madin-Darby canine kidney cells.* J Biol Chem, 1996. **271**(14): p. 8472-80.

93. Rizzo, M.A., et al., *Phospholipase D and its product, phosphatidic acid, mediate agonist-dependent raf-1 translocation to the plasma membrane and the activation of the mitogen-activated protein kinase pathway.* J Biol Chem, 1999. **274**(2): p. 1131-9.

94. Avila-Flores, A., et al., *Modulation of the mammalian target of rapamycin pathway by diacylglycerol kinase-produced phosphatidic acid.* J Biol Chem, 2005. **280**(11): p. 10091-9.

95. Fang, Y., et al., *Phosphatidic acid-mediated mitogenic activation of mTOR signaling.* Science, 2001. **294**(5548): p. 1942-5.

96. Kam, Y. and J.H. Exton, *Role of phospholipase D1 in the regulation of mTOR activity by lysophosphatidic acid.* Faseb J, 2004. **18**(2): p. 311-9.

97. Cross, M.J., et al., *Stimulation of actin stress fibre formation mediated by activation of phospholipase D.* Curr Biol, 1996. **6**(5): p. 588-97.

98. Ha, K.S. and J.H. Exton, *Activation of actin polymerization by phosphatidic acid derived from phosphatidylcholine in IIC9 fibroblasts.* J Cell Biol, 1993. **123**(6 Pt 2): p. 1789-96.

99. Moritz, A., et al., *Phosphatidic acid is a specific activator of phosphatidylinositol-4-phosphate kinase.* J Biol Chem, 1992. **267**(11): p. 7207-10.

100. Jenkins, G.H., P.L. Fisette, and R.A. Anderson, *Type I phosphatidylinositol 4-phosphate 5-kinase isoforms are specifically stimulated by phosphatidic acid.* J. Biol. Chem., 1994. **269**: p. 11547-11554.

101. Huijbregts, R.P., L. Topalof, and V.A. Bankaitis, *Lipid metabolism and regulation of membrane trafficking.* Traffic, 2000. **1**(3): p. 195-202.

102. Zimmerberg, J., *Are the curves in all the right places?* Traffic, 2000. **1**(4): p. 366-8.

103. Jones, G.A. and G. Carpenter, *The regulation of phospholipase-Cγ by phosphatidic acid. Assessment of kinetic parameters.* J. Biol. Chem., 1993. **268**: p. 20845-20850.

104. Ktistakis, N.T., et al., *Evidence that phospholipase D mediates ADP ribosylation factor-dependent formation of Golgi coated vesicles.* J. Cell Biol., 1996. **134**: p. 295-306.

105. Pettitt, T.R., et al., *Diacylglycerol and phosphatidate generated by phospholipases C and D, respectively, have distinct fatty acid compositions and functions. Phospholipase D-derived diacylglycerol does not activate protein kinase C in porcine aortic endothelial cells.* J Biol Chem, 1997. **272**(28): p. 17354-9.

106. Gobeil, F., Jr., et al., *Modulation of pro-inflammatory gene expression by nuclear lysophosphatidic acid receptor type-1.* J Biol Chem, 2003. **278**(40): p. 38875-83.

107. Moughal, N.A., et al., *Nerve growth factor signaling involves interaction between the Trk A receptor and lysophosphatidate receptor 1 systems: nuclear translocation of the lysophosphatidate receptor 1 and Trk A receptors in pheochromocytoma 12 cells.* Cell Signal, 2004. **16**(1): p. 127-36.

108. McIntyre, T.M., et al., *Identification of an intracellular receptor for lysophosphatidic acid (LPA): LPA is a transcellular PPARgamma agonist.* Proc Natl Acad Sci U S A, 2003. **100**(1): p. 131-6.

109. Zhang, C., et al., *Lysophosphatidic acid induces neointima formation through PPARgamma activation.* J Exp Med, 2004. **199**(6): p. 763-74.

110. Simon, M.F., et al., *Lysophosphatidic acid inhibits adipocyte differentiation via lysophosphatidic acid 1 receptor-dependent down-regulation of peroxisome proliferator-activated receptor gamma2.* J Biol Chem, 2005. **280**(15): p. 14656-62.

111. Chalfant, C.E. and S. Spiegel, *Sphingosine 1-phosphate and ceramide 1-phosphate: expanding roles in cell signaling.* J Cell Sci, 2005. **118**(Pt 20): p. 4605-12.

112. Futerman, A.H. and Y.A. Hannun, *The complex life of simple sphingolipids.* EMBO Rep, 2004. **5**(8): p. 777-82.

113. Sigal, Y.J., M.I. McDermott, and A.J. Morris, *Integral membrane lipid phosphatases/phosphotransferases: common structure and diverse functions.* Biochem J, 2005. **387**(Pt 2): p. 281-93.

114. Spiegel, S. and S. Milstien, *Sphingosine-1-phosphate: an enigmatic signalling lipid.* Nat Rev Mol Cell Biol, 2003. **4**(5): p. 397-407.

115. Shu, X., et al., *Sphingosine kinase mediates vascular endothelial growth factor-induced activation of ras and mitogen-activated protein kinases.* Mol Cell Biol, 2002. **22**(22): p. 7758-68.

116. Suomalainen, L., V. Pentikainen, and L. Dunkel, *Sphingosine-1-phosphate inhibits nuclear factor kappaB activation and germ cell apoptosis in the human testis independently of its receptors.* Am J Pathol, 2005. **166**(3): p. 773-81.

117. Meyer zu Heringdorf, D., et al., *Photolysis of intracellular caged sphingosine-1-phosphate causes Ca2+ mobilization independently of G-protein-coupled receptors.* FEBS Lett, 2003. **554**(3): p. 443-9.

118. Choi, O.H., J.H. Kim, and J.P. Kinet, *Calcium mobilization via sphingosine kinase in signalling by the Fc epsilon RI antigen receptor.* Nature, 1996. **380**(6575): p. 634-6.

119. Maceyka, M., et al., *SphK1 and SphK2, sphingosine kinase isoenzymes with opposing functions in sphingolipid metabolism.* J Biol Chem, 2005. **280**(44): p. 37118-29.

120. Gómez-Muñoz, A., et al., *Role of sphingolipids in regulating the phospholipase D pathway and cell division.* Sphingolipid-mediated Signal Transduction, ed. Y.A.e. Hannun. 1997, Austin, TX: Landes Co. 104-120.

121. Gomez-Munoz, A., et al., *Short-chain ceramide-1-phosphates are novel stimulators of DNA synthesis and cell division: antagonism by cell-permeable ceramides.* Mol Pharmacol, 1995. **47**(5): p. 833-9.

122. Brindley, D.N., et al., *Lipid phosphate phosphatases regulate signal transduction through glycerolipids and sphingolipids.* Biochim Biophys Acta, 2002. **1582**(1-3): p. 33-44.

123. Dougherty, M.K., et al., *Regulation of Raf-1 by direct feedback phosphorylation.* Mol Cell, 2005. **17**(2): p. 215-24.

124. Hancock, C.N., S. Dangi, and P. Shapiro, *Protein phosphatase 2A activity associated with Golgi membranes during the G2/M phase may regulate phosphorylation of ERK2.* J Biol Chem, 2005. **280**(12): p. 11590-8.

125. Chalfant, C.E., et al., *De novo ceramide regulates the alternative splicing of caspase 9 and Bcl-x in A549 lung adenocarcinoma cells. Dependence on protein phosphatase-1.* J Biol Chem, 2002. **277**(15): p. 12587-95.

126. Pettus, B.J., et al., *Ceramide 1-phosphate is a direct activator of cytosolic phospholipase A2.* J Biol Chem, 2004. **279**(12): p. 11320-6.

127. Mitsutake, S., et al., *Ceramide kinase is a mediator of calcium-dependent degranulation in mast cells.* J Biol Chem, 2004. **279**(17): p. 17570-7.

128. Hinkovska-Galcheva, V.T., et al., *The formation of ceramide-1-phosphate during neutrophil phagocytosis and its role in liposome fusion.* J Biol Chem, 1998. **273**(50): p. 33203-9.

129. Brindley, D.N., *Phosphatidate phosphohydrolase: its role in glycerolipid synthesis.* Brindley, D.N. ed. ed. In Phosphatidate Phosphohydrolase, ed. C.S.o.E. Biology. Vol. 1. 1988, Boca Raton: CRC Press Inc. 21-77.

130. Jamal, Z., et al., *Plasma membrane fractions from rat liver contain a phosphatidate phosphohydrolase distinct from that in the endoplasmic reticulum and cytosol.* J Biol Chem, 1991. **266**(5): p. 2988-96.

131. Brindley, D.N. and D.W. Waggoner, *Phosphatidate phosphohydrolase and signal transduction.* Chem. and Phys. of Lipids, 1996. **80**: p. 45-57.

132. Han, G.S., W.I. Wu, and G.M. Carman, *The Saccharomyces cerevisiae lipin homolog is a Mg2+-dependent phosphatidate phosphatase enzyme.* J Biol Chem, 2006.

133. Johnson, C.A., et al., *Regulation of cyclooxygenase-2 expression by phosphatidate phosphohydrolase in human amnionic WISH cells.* J Biol Chem, 1999. **274**(39): p. 27689-93.

134. Grkovich, A., et al., *Lipopolysaccharide-induced cyclooxygenase-2 expression in human U937 macrophages is phosphatidic acid phosphohydrolase-1-dependent.* J Biol Chem, 2006. **281**(44): p. 32978-87.

135. Jiang, Y., et al., *Regulation of phosphatidic acid phosphohydrolase by epidermal growth factor. Reduced association with the EGF receptor followed by increased association with protein kinase Cepsilon.* J Biol Chem, 1996. **271**(47): p. 29529-32.

136. Dillon, D.A., et al., *Mammalian Mg2+-independent phosphatidate phosphatase (PAP2) displays diacylglycerol pyrophosphate phosphatase activity.* J Biol Chem, 1997. **272**(16): p. 10361-6.

137. Waggoner, D.W., et al., *Phosphatidate phosphohydrolase catalyzes the hydrolysis of ceramide 1-phosphate, lysophosphatidate, and sphingosine 1-phosphate.* J Biol Chem, 1996. **271**(28): p. 16506-9.

138. Kai, M., et al., *Identification and cDNA cloning of 35-kDa phosphatidic acid phosphatase (type 2) bound to plasma membranes. Polymerase chain reaction amplification of mouse H2O2-inducible hic53 clone yielded the cDNA encoding phosphatidic acid phosphatase.* J Biol Chem, 1996. **271**(31): p. 18931-8.

139. Brindley, D.N. and D.W. Waggoner, *Mammalian lipid phosphate phosphohydrolases.* J Biol Chem, 1998. **273**(38): p. 24281-4.

140. Roberts, R., V.A. Sciorra, and A.J. Morris, *Human type 2 phosphatidic acid phosphohydrolases. Substrate specificity of the type 2a, 2b, and 2c enzymes and cell surface activity of the 2a isoform.* J Biol Chem, 1998. **273**(34): p. 22059-67.

141. Waggoner, D.W., et al., *Structural organization of mammalian lipid phosphate phosphatases: implications for signal transduction.* Biochim Biophys Acta, 1999. **1439**(2): p. 299-316.

142. Hemricka, W., et al., *From phosphatases to vanadium peroxidases: a similar architecture of the active site.* Proc. Natl. Acad. Sci. USA, 1997. **94**: p. 2145-2149.

143. Macedo-Ribeiro, S., et al., *X-ray crystal structures of active site mutants of the vanadium-containing chloroperoxidase from the fungus Curvularia inaequalis.* J Biol Inorg Chem, 1999. **4**(2): p. 209-19.

144. Renirie, R., et al., *Cofactor and substrate binding to vanadium chloroperoxidase determined by UV-VIS spectroscopy and evidence for high affinity for pervanadate.* Biochemistry, 2000. **39**(5): p. 1133-41.

145. Renirie, R., W. Hemrika, and R. Wever, *Peroxidase and phosphatase activity of active-site mutants of vanadium chloroperoxidase from the fungus Curvularia inaequalis. Implications for the catalytic mechanisms.* J Biol Chem, 2000. **275**(16): p. 11650-7.

146. Messerschmidt, A. and R. Wever, *X-ray structure of a vanadium-containing enzyme: chloroperoxidase from the fungus Curvularia inaequalis.* Proc. Natl. Acad. Sci., 1996. **93**: p. 392-396.

147. Messerschmidt, A., L. Prade, and R. Wever, *Implications for the catalytic mechanism of the vanadium-containing enzyme chloroperoxidase from the fungus Curvularia inaequalis by X-ray structures of the native and peroxide form.* Biol. Chem. Hoppe-Seyler, 1997. **378**: p. 309-315.

148. Zhang, Q.X., et al., *Identification of structurally important domains of lipid phosphate phosphatase-1: implications for its sites of action.* Biochem J, 2000. **345 Pt 2**: p. 181-4.

149. Morris, K.E., *The Function of Lipid Phosphate Phosphatase-2 in Fibroblasts*, in *Department of Biochemistry*. 2006, University of Alberta: Edmonton. p. 231.

150. Morris, K.E., L.M. Schang, and D.N. Brindley, *Lipid phosphate phosphatase-2 activity regulates S-phase entry of the cell cycle in Rat2 fibroblasts.* J Biol Chem, 2006. **281**(14): p. 9297-306.

151. Escalante-Alcalde, D., et al., *The lipid phosphatase LPP3 regulates extra-embryonic vasculogenesis and axis patterning.* Development, 2003. **130**(19): p. 4623-37.

152. Kai, M., et al., *Cloning and characterization of two human isozymes of Mg^{2+}-independent phosphatidic acid phosphatase.* J. Biol. Chem., 1997. **272**(39): p. 24572-24578.

153. Leung, D.W., C.K. Tompkins, and T. White, *Molecular cloning of two alternatively spliced forms of human phosphatidic acid phosphatase cDNAs that are differentially expressed in normal and tumor cells.* DNA Cell Biol, 1998. **17**(4): p. 377-85.

154. Nanjundan, M. and F. Possmayer, *Molecular cloning and expression of pulmonary lipid phosphate phosphohydrolases.* J. Physiol., 2001. ***in press***.

155. Brauer, A.U., et al., *A new phospholipid phosphatase, PRG-1, is involved in axon growth and regenerative sprouting.* Nat Neurosci, 2003. **6**(6): p. 572-8.

156. Savaskan, N.E., A.U. Brauer, and R. Nitsch, *Molecular cloning and expression regulation of PRG-3, a new member of the plasticity-related gene family.* Eur J Neurosci, 2004. **19**(1): p. 212-20.

157. Sigal, Y.J., et al., *Cdc42 and ARP2/3-independent regulation of filopodia by an integral membrane lipid-phosphatase-related protein.* J Cell Sci, 2007. **120**(Pt 2): p. 340-52.

158. Jasinska, R., et al., *Lipid phosphate phosphohydrolase-1 degrades exogenous glycerolipid and sphingolipid phosphate esters.* Biochem J, 1999. **340 (Pt 3)**: p. 677-86.

159. Barila, D., et al., *The Dri 42 gene, whose expression is up-regulated during epithelial differentiation, encodes a novel endoplasmic reticulum resident transmembrane protein.* J. Biol. Chem., 1996. **271**(47): p. 29928-29936.

160. Kihara, A., et al., *Transmembrane topology of sphingoid long-chain base-1-phosphate phosphatase, Lcb3p.* Genes Cells, 2003. **8**(6): p. 525-35.

161. Alderton, F., et al., *G-protein-coupled receptor stimulation of the p42/p44 mitogen-activated protein kinase pathway is attenuated by lipid phosphate phosphatases 1, 1a, and 2 in human embryonic kidney 293 cells.* J Biol Chem, 2001. **276**(16): p. 13452-60.

162. Ishikawa, T., et al., *Cell surface activities of the human type 2b phosphatidic acid phosphatase.* J Biochem (Tokyo), 2000. **127**(4): p. 645-51.

163. Jia, Y.J., et al., *Differential localization of lipid phosphate phosphatases 1 and 3 to cell surface subdomains in polarized MDCK cells.* FEBS Lett, 2003. **552**(2-3): p. 240-6.

164. Nanjundan, M. and F. Possmayer, *Pulmonary lipid phosphate phosphohydrolase in plasma membrane signalling platforms.* Biochem. J., 2001. **358**: p. 637-646.

165. Sciorra, V.A. and A.J. Morris, *Sequential actions of phospholipase D and phosphatidic acid phosphohydrolase 2b generate diglyceride in mammalian cells.* Mol. Biol. Cell, 1999. **10**: p. 3863-3876.

166. Hooks, S.B., S.P. Ragan, and K.R. Lynch, *Identification of a novel human phosphatidic acid phosphatase type 2 isoform.* FEBS Lett., 1998. **427**: p. 188-192.

167. Long, J., et al., *Regulation of cell survival by lipid phosphate phosphatases involves the modulation of intracellular phosphatidic acid and sphingosine 1-phosphate pools.* Biochem J, 2005. **391**(Pt 1): p. 25-32.

168. Kai, M., et al., *Lipid phosphate phosphatases 1 and 3 are localized in distinct lipid rafts.* J Biochem (Tokyo), 2006. **140**(5): p. 677-86.

169. Nanjundan, M. and F. Possmayer, *Pulmonary phosphatidic acid phosphatase and lipid phosphate phosphohydrolase.* Am J Physiol Lung Cell Mol Physiol, 2003. **284**(1): p. L1-23.

170. Urs, N.M., et al., *A requirement for membrane cholesterol in the beta-arrestin- and clathrin-dependent endocytosis of LPA1 lysophosphatidic acid receptors.* J Cell Sci, 2005. **118**(Pt 22): p. 5291-304.

171. Igarashi, J. and T. Michel, *Agonist-modulated targeting of the EDG-1 receptor to plasmalemmal caveolae. eNOS activation by sphingosine 1-phosphate and the role of caveolin-1 in sphingolipid signal transduction.* J Biol Chem, 2000. **275**(41): p. 32363-70.

172. Czarny, M., et al., *Localization of phospholipase D in detergent-insoluble, caveolin-rich membrane domains. Modulation by caveolin-1 expression and caveolin-182-101.* J Biol Chem, 1999. **274**(5): p. 2717-24.

173. Czarny, M., et al., *Phospholipase D2: functional interaction with caveolin in low-density membrane microdomains.* FEBS Lett, 2000. **467**(2-3): p. 326-32.

174. Pilquil, C., et al., *Lipid phosphate phosphatase-1 dephosphorylates exogenous lysophosphatidate and thereby attenuates its effects on cell signalling.* Prostaglandins, 2001. **64**(1-4): p. 83-92.

175. Imai, A., et al., *A gonadotropin-releasing hormone-responsive phosphatase hydrolyses lysophosphatidic acid within the plasma membrane of ovarian cancer cells.* J Clin Endocrinol Metab, 2000. **85**(9): p. 3370-5.

176. Sun, W.S., et al., *Translocation of lysophosphatidic acid phosphatase in response to gonadotropin-releasing hormone to the plasma membrane in ovarian cancer cell.* Am J Obstet Gynecol, 2004. **191**(1): p. 143-9.

177. Tanyi, J.L., et al., *The human lipid phosphate phosphatase-3 decreases the growth, survival, and tumorigenesis of ovarian cancer cells: validation of the lysophosphatidic acid signaling cascade as a target for therapy in ovarian cancer.* Cancer Res, 2003. **63**(5): p. 1073-82.

178. Tanyi, J.L., et al., *Role of decreased levels of lipid phosphate phosphatase-1 in accumulation of lysophosphatidic acid in ovarian cancer.* Clin Cancer Res, 2003. **9**(10 Pt 1): p. 3534-45.

179. Smyth, S.S., et al., *Lipid phosphate phosphatases regulate lysophosphatidic acid production and signaling in platelets: studies using chemical inhibitors of lipid phosphate phosphatase activity.* J Biol Chem, 2003. **278**(44): p. 43214-23.

180. Hooks, S.B., et al., *Lysophosphatidic acid-induced mitogenesis is regulated by lipid phosphate phosphatases and is Edg-receptor independent.* J Biol Chem, 2001. **276**(7): p. 4611-21.

181. Simon, M.F., et al., *Expression of ectolipid phosphate phosphohydrolases in 3T3F442A preadipocytes and adipocytes. Involvement in the control of lysophosphatidic acid production.* J Biol Chem, 2002. **277**(26): p. 23131-6.

182. Pagano, R.E. and K.J. Longmuir, *Phosphorylation, transbilayer movement and facilitated intracellular transport of diacylglycerol are involved in the uptake of a fluorescent analog of phosphatidic acid by cultured fibroblasts.* J. Biol. Chem., 1985. **260**(3): p. 1909-1916.

183. Garcia-Murillas, I., et al., *lazaro encodes a lipid phosphate phosphohydrolase that regulates phosphatidylinositol turnover during Drosophila phototransduction.* Neuron, 2006. **49**(4): p. 533-46.

184. Zhao, Y., et al., *Lipid phosphate phosphatase-1 regulates lysophosphatidic acid-induced calcium release, NF-kappaB activation and interleukin-8 secretion in human bronchial epithelial cells.* Biochem J, 2005. **385**(Pt 2): p. 493-502.

185. Yue, J., et al., *Mice with transgenic overexpression of lipid phosphate phosphatase-1 display multiple organotypic deficits without alteration in circulating lysophosphatidate level.* Cell Signal, 2004. **16**(3): p. 385-99.

186. Long JS, Y.K., Tigyi G, Pyne NJ, Pyne S., *Lipid phosphate phosphatase-1 regulates lysophosphatidic acid- and platelet-derived-growth-factor-induced cell migration.* Biochem. J. , 2006. **394**: p. 495-500.

187. Humtsoe, J.O., et al., *Regulation of cell-cell interactions by phosphatidic acid phosphatase 2b/VCIP.* Embo J, 2003. **22**(7): p. 1539-54.

188. Wary, K.K. and J.O. Humtsoe, *Anti-lipid phosphate phosphohydrolase-3 (LPP3) antibody inhibits bFGF- and VEGF-induced capillary morphogenesis of endothelial cells.* Cell Commun Signal, 2005. **3**: p. 9.

189. Humtsoe, J.O., et al., *Murine lipid phosphate phosphohydrolase-3 acts as a cell-associated integrin ligand.* Biochem Biophys Res Commun, 2005. **335**(3): p. 906-19.

190. Park, J.I., et al., *Kaiso/p120-catenin and TCF/beta-catenin complexes coordinately regulate canonical Wnt gene targets.* Dev Cell, 2005. **8**(6): p. 843-54.

191. Spring, C.M., et al., *The catenin p120ctn inhibits Kaiso-mediated transcriptional repression of the beta-catenin/TCF target gene matrilysin.* Exp Cell Res, 2005. **305**(2): p. 253-65.

192. Zhang, N., J.P. Sundberg, and T. Gridley, *Mice mutant for Ppap2c, a homolog of the germ cell migration regulator wunen, are viable and fertile.* Genesis, 2000. **27**(4): p. 137-40.

193. Sherr, C.J. and J.M. Roberts, *Living with or without cyclins and cyclin-dependent kinases.* Genes Dev, 2004. **18**(22): p. 2699-711.

194. Starz-Gaiano, M., et al., *Spatially restricted activity of a Drosophila lipid phosphatase guides migrating germ cells.* Development, 2001. **128**(6): p. 983-91.

195. Zhang, N., et al., *The Drosophila protein Wunen repels migrating germ cells.* Nature, 1997. **385**(6611): p. 64-7.

196. Burnett, C. and K. Howard, *Fly and mammalian lipid phosphate phosphatase isoforms differ in activity both in vitro and in vivo.* EMBO Rep, 2003. **4**(8): p. 793-9.

197. Renault, A.D., et al., *Soma-germ line competition for lipid phosphate uptake regulates germ cell migration and survival.* Science, 2004. **305**(5692): p. 1963-6.

198. Ulrix, W., et al., *Identification of the phosphatidic acid phosphatase type 2a isozyme as an androgen-regulated gene in the human prostatic adenocarcinoma cell line LNCaP.* J. Biol. Chem., 1998. **273**: p. 4660-4665.

199. Wang, D.A., et al., *Injury-elicited differential transcriptional regulation of phospholipid growth factor receptors in the cornea.* Am J Physiol Cell Physiol, 2002. **283**(6): p. C1646-54.

200. Ishida, T., et al., *The expression of phosphatidic acid phosphatase 2a, which hydrolyzes lipids to generate diacylglycerol, is regulated by p73, a member of the p53 family.* Biochem Biophys Res Commun, 2007. **353**(1): p. 74-9.

201. Pyne, S., et al., *Lipid phosphate phosphatases and lipid phosphate signalling.* Biochem Soc Trans, 2005. **33**(Pt 6): p. 1370-4.

202. Burnett, C., et al., *Lipid phosphate phosphatases dimerise, but this interaction is not required for in vivo activity.* BMC Biochem, 2004. **5**: p. 2.

203. Fleming, I.N. and S.J. Yeaman, *Purification and characterization of N-ethylmaleimide-insensitive phosphatidic acid phosphohydrolase (PAP2) from rat liver.* Biochem. J., 1995. **308**: p. 983-989.

204. Kanoh, H., et al., *Purification and properties of phosphatidic acid phosphatase from porcine thymus membranes.* J. Biol. Chem., 1992. **267**: p. 25309-25314.

205. Pyne, S., K.C. Kong, and P.I. Darroch, *Lysophosphatidic acid and sphingosine 1-phosphate biology: the role of lipid phosphate phosphatases.* Semin Cell Dev Biol, 2004. **15**(5): p. 491-501.

206. Stamenkovic, I., *Extracellular matrix remodelling: the role of matrix metalloproteinases.* J Pathol, 2003. **200**(4): p. 448-64.

207. McCawley, L.J. and L.M. Matrisian, *Matrix metalloproteinases: they're not just for matrix anymore!* Curr Opin Cell Biol, 2001. **13**(5): p. 534-40.

208. Stamenkovic, I., *Matrix metalloproteinases in tumor invasion and metastasis.* Semin Cancer Biol, 2000. **10**(6): p. 415-33.

209. Viappiani, S., M. Sariahmetoglu, and R. Schulz, *The role of matrix metalloproteinase inhibitors in ischemia-reperfusion injury in the liver.* Curr Pharm Des, 2006. **12**(23): p. 2923-34.

210. Sottrup-Jensen, L. and H. Birkedal-Hansen, *Human fibroblast collagenase-alpha-macroglobulin interactions. Localization of cleavage sites in the bait regions of five mammalian alpha-macroglobulins.* J Biol Chem, 1989. **264**(1): p. 393-401.

211. Oh, J., et al., *The membrane-anchored MMP inhibitor RECK is a key regulator of extracellular matrix integrity and angiogenesis.* Cell, 2001. **107**(6): p. 789-800.

212. Hidalgo, M. and S.G. Eckhardt, *Development of matrix metalloproteinase inhibitors in cancer therapy.* J Natl Cancer Inst, 2001. **93**(3): p. 178-93.

213. Kopfstein, L. and G. Christofori, *Metastasis: cell-autonomous mechanisms versus contributions by the tumor microenvironment.* Cell Mol Life Sci, 2006. **63**(4): p. 449-68.

214. Levi, E., et al., *Matrix metalloproteinase 2 releases active soluble ectodomain of fibroblast growth factor receptor 1.* Proc Natl Acad Sci U S A, 1996. **93**(14): p. 7069-74.

215. Knauper, V., et al., *Activation of progelatinase B (proMMP-9) by active collagenase-3 (MMP-13).* Eur J Biochem, 1997. **248**(2): p. 369-73.

216. Okada, A., et al., *Expression of matrix metalloproteinases during rat skin wound healing: evidence that membrane type-1 matrix metalloproteinase is a stromal activator of pro-gelatinase A.* J Cell Biol, 1997. **137**(1): p. 67-77.

217. Salo, T., et al., *Expression of matrix metalloproteinase-2 and -9 during early human wound healing.* Lab Invest, 1994. **70**(2): p. 176-82.

218. Soo, C., et al., *Differential expression of matrix metalloproteinases and their tissue-derived inhibitors in cutaneous wound repair.* Plast Reconstr Surg, 2000. **105**(2): p. 638-47.

219. Deryugina, E.I., et al., *MT1-MMP initiates activation of pro-MMP-2 and integrin alphavbeta3 promotes maturation of MMP-2 in breast carcinoma cells.* Exp Cell Res, 2001. **263**(2): p. 209-23.

220. Itoh, T., et al., *The role of matrix metalloproteinase-2 and matrix metalloproteinase-9 in antibody-induced arthritis.* J Immunol, 2002. **169**(5): p. 2643-7.

221. Itoh, Y., et al., *Homophilic complex formation of MT1-MMP facilitates proMMP-2 activation on the cell surface and promotes tumor cell invasion.* Embo J, 2001. **20**(17): p. 4782-93.

222. Strongin, A.Y., et al., *Mechanism of cell surface activation of 72-kDa type IV collagenase. Isolation of the activated form of the membrane metalloprotease.* J Biol Chem, 1995. **270**(10): p. 5331-8.

223. Brooks, P.C., et al., *Localization of matrix metalloproteinase MMP-2 to the surface of invasive cells by interaction with integrin alpha v beta 3.* Cell, 1996. **85**(5): p. 683-93.

224. Gottardi, C.J., L.A. Dunbar, and M.J. Caplan, *Biotinylation and assessment of membrane polarity: caveats and methodological concerns.* Am J Physiol, 1995. **268**(2 Pt 2): p. F285-95.

225. Benard, V., B.P. Bohl, and G.M. Bokoch, *Characterization of rac and cdc42 activation in chemoattractant-stimulated human neutrophils using a novel assay for active GTPases.* J Biol Chem, 1999. **274**(19): p. 13198-204.

226. Anderson, N.G., et al., *Requirement for integration of signals from two distinct phosphorylation pathways for activation of MAP kinase.* Nature, 1990. **343**(6259): p. 651-3.

227. Payne, D.M., et al., *Identification of the regulatory phosphorylation sites in pp42/mitogen-activated protein kinase (MAP kinase).* Embo J, 1991. **10**(4): p. 885-92.

228. Ellgaard, L. and A. Helenius, *Quality control in the endoplasmic reticulum.* Nat Rev Mol Cell Biol, 2003. **4**(3): p. 181-91.

229. Swanton, E., S. High, and P. Woodman, *Role of calnexin in the glycan-independent quality control of proteolipid protein.* Embo J, 2003. **22**(12): p. 2948-58.

230. Jalink, K., W.H. Moolenaar, and B. Van Duijn, *Lysophosphatidic acid is a chemoattractant for Dictyostelium discoideum amoebae.* Proc Natl Acad Sci U S A, 1993. **90**(5): p. 1857-61.

231. Tokumura, A., *Physiological and pathophysiological roles of lysophosphatidic acids produced by secretory lysophospholipase D in body fluids.* Biochim Biophys Acta, 2002. **1582**(1-3): p. 18-25.

232. Heise, C.E., et al., *Activity of 2-substituted lysophosphatidic acid (LPA) analogs at LPA receptors: discovery of a LPA1/LPA3 receptor antagonist.* Mol Pharmacol, 2001. **60**(6): p. 1173-80.

233. Anand-Apte, B., et al., *Platelet-derived growth factor and fibronectin-stimulated migration are differentially regulated by the Rac and extracellular signal-regulated kinase pathways.* J Biol Chem, 1997. **272**(49): p. 30688-92.

234. Sakai, T., et al., *Restoration of beta1A integrins is required for lysophosphatidic acid-induced migration of beta1-null mouse fibroblastic cells.* J Biol Chem, 1998. **273**(31): p. 19378-82.

235. Preciado-Patt, L., et al., *Inhibition of cell adhesion to glycoproteins of the extracellular matrix by peptides corresponding to serum amyloid A. Toward understanding the physiological role of an enigmatic protein.* Eur J Biochem, 1994. **223**(1): p. 35-42.

236. Chen, J.S. and J.H. Exton, *Regulation of phospholipase D2 activity by protein kinase C alpha.* J Biol Chem, 2004. **279**(21): p. 22076-83.

237. Meacci, E., et al., *Activation of phospholipase D by bradykinin and sphingosine 1-phosphate in A549 human lung adenocarcinoma cells via different GTP-binding proteins and protein kinase C delta signaling pathways.* Biochemistry, 2003. **42**(2): p. 284-92.

238. Aramori, I. and S. Nakanishi, *Coupling of two endothelin receptor subtypes to differing signal transduction in transfected Chinese hamster ovary cells.* J Biol Chem, 1992. **267**(18): p. 12468-74.

239. Takagi, Y., et al., *Structural basis of G protein specificity of human endothelin receptors. A study with endothelinA/B chimeras.* J Biol Chem, 1995. **270**(17): p. 10072-8.

240. van der Bend, R.L., et al., *The biologically active phospholipid, lysophosphatidic acid, induces phosphatidylcholine breakdown in fibroblasts via activation of phospholipase D. Comparison with the response to endothelin.* Biochem J, 1992. **285 (Pt 1)**: p. 235-40.

241. Hess, J.A., et al., *Altered activation of phospholipase D by lysophosphatidic acid and endothelin-1 in mouse embryo fibroblasts lacking phospholipase C-gamma1.* Cell Signal, 2000. **12**(1): p. 37-45.

242. Hess, J.A., et al., *Analysis of platelet-derived growth factor-induced phospholipase D activation in mouse embryo fibroblasts lacking phospholipase C-gamma1.* J Biol Chem, 1998. **273**(32): p. 20517-24.

243. Hordijk, P.L., et al., *Protein tyrosine phosphorylation induced by lysophosphatidic acid in Rat-1 fibroblasts. Evidence that phosphorylation of map kinase is mediated by the Gi-p21ras pathway.* J Biol Chem, 1994. **269**(1): p. 645-51.

244. Alderton, F., et al., *Tethering of the platelet-derived growth factor beta receptor to G-protein-coupled receptors. A novel platform for integrative signaling by these receptor classes in mammalian cells.* J Biol Chem, 2001. **276**(30): p. 28578-85.

245. Powner, D.J., et al., *Phospholipase D2 stimulates integrin-mediated adhesion via phosphatidylinositol 4-phosphate 5-kinase Igamma b.* J Cell Sci, 2005. **118**(Pt 13): p. 2975-86.

246. Webb, D.J., J.T. Parsons, and A.F. Horwitz, *Adhesion assembly, disassembly and turnover in migrating cells -- over and over and over again.* Nat Cell Biol, 2002. **4**(4): p. E97-100.

247. Pertz, O., et al., *Spatiotemporal dynamics of RhoA activity in migrating cells.* Nature, 2006. **440**(7087): p. 1069-72.

248. Hong, J.H., et al., *Enhancement of lysophosphatidic acid-induced ERK phosphorylation by phospholipase D1 via the formation of phosphatidic acid.* Biochem Biophys Res Commun, 2001. **281**(5): p. 1337-42.

249. Kim, J.I., et al., *Stimulation of early gene induction and cell proliferation by lysophosphatidic acid in human amnion-derived WISH cells: role of phospholipase D-mediated pathway.* Biochem Pharmacol, 2004. **68**(2): p. 333-40.

250. van Dijk, M.C., et al., *Involvement of phosphatidylcholine-specific phospholipase C in platelet-derived growth factor-induced activation of the mitogen-activated protein kinase pathway in Rat-1 fibroblasts.* J Biol Chem, 1997. **272**(17): p. 11011-6.

251. Hill, C.S., J. Wynne, and R. Treisman, *The Rho family GTPases RhoA, Rac1, and CDC42Hs regulate transcriptional activation by SRF.* Cell, 1995. **81**(7): p. 1159-70.

252. Kam, Y. and J.H. Exton, *Role of phospholipase D in the activation of protein kinase D by lysophosphatidic acid.* Biochem Biophys Res Commun, 2004. **315**(1): p. 139-43.

253. Suzuki, M., et al., *Matrix metalloproteinase-3 releases active heparin-binding EGF-like growth factor by cleavage at a specific juxtamembrane site.* J Biol Chem, 1997. **272**(50): p. 31730-7.

254. Fishman, D.A., et al., *Lysophosphatidic acid promotes matrix metalloproteinase (MMP) activation and MMP-dependent invasion in ovarian cancer cells.* Cancer Res, 2001. **61**(7): p. 3194-9.

255. Wu, W.T., et al., *Lysophospholipids enhance matrix metalloproteinase-2 expression in human endothelial cells.* Endocrinology, 2005. **146**(8): p. 3387-400.

256. Itoh, Y., et al., *Plasma membrane-bound tissue inhibitor of metalloproteinases (TIMP)-2 specifically inhibits matrix metalloproteinase 2 (gelatinase A) activated on the cell surface.* J Biol Chem, 1998. **273**(38): p. 24360-7.

257. Stetler-Stevenson, W.G. and D.W. Seo, *TIMP-2: an endogenous inhibitor of angiogenesis.* Trends Mol Med, 2005. **11**(3): p. 97-103.

258. Kajita, M., et al., *Membrane-type 1 matrix metalloproteinase cleaves CD44 and promotes cell migration.* J Cell Biol, 2001. **153**(5): p. 893-904.

259. Makela, M., et al., *Matrix metalloproteinase 2 (gelatinase A) is related to migration of keratinocytes.* Exp Cell Res, 1999. **251**(1): p. 67-78.

260. Prockop, D.J. and K.I. Kivirikko, *Collagens: molecular biology, diseases, and potentials for therapy.* Annu Rev Biochem, 1995. **64**: p. 403-34.

261. Banyai, L. and L. Patthy, *The NTR module: domains of netrins, secreted frizzled related proteins, and type I procollagen C-proteinase enhancer protein are homologous with tissue inhibitors of metalloproteases.* Protein Sci, 1999. **8**(8): p. 1636-42.

262. Mott, J.D., et al., *Post-translational proteolytic processing of procollagen C-terminal proteinase enhancer releases a metalloproteinase inhibitor.* J Biol Chem, 2000. **275**(2): p. 1384-90.

263. Westermarck, J. and V.M. Kahari, *Regulation of matrix metalloproteinase expression in tumor invasion.* Faseb J, 1999. **13**(8): p. 781-92.

264. Qin, H., Y. Sun, and E.N. Benveniste, *The transcription factors Sp1, Sp3, and AP-2 are required for constitutive matrix metalloproteinase-2 gene expression in astroglioma cells.* J Biol Chem, 1999. **274**(41): p. 29130-7.

265. Tryggvason, K., et al., *Structure and expression of type IV collagenase genes.* Cell Differ Dev, 1990. **32**(3): p. 307-12.

266. Reich, R., M. Blumenthal, and M. Liscovitch, *Role of phospholipase D in laminin-induced production of gelatinase A (MMP-2) in metastatic cells.* Clin Exp Metastasis, 1995. **13**(2): p. 134-40.

267. Ara, T., et al., *Membrane type 1-matrix metalloproteinase expression is regulated by E-cadherin through the suppression of mitogen-activated protein kinase cascade.* Cancer Lett, 2000. **157**(2): p. 115-21.

268. Zhuge, Y. and J. Xu, *Rac1 mediates type I collagen-dependent MMP-2 activation. role in cell invasion across collagen barrier.* J Biol Chem, 2001. **276**(19): p. 16248-56.

269. Guccione, M., et al., *Estradiol upregulates mesangial cell MMP-2 activity via the transcription factor AP-2.* Am J Physiol Renal Physiol, 2002. **282**(1): p. F164-9.

270. Bond, M., et al., *Synergistic upregulation of metalloproteinase-9 by growth factors and inflammatory cytokines: an absolute requirement for transcription factor NF-kappa B.* FEBS Lett, 1998. **435**(1): p. 29-34.

271. Wakelam, M.J., et al., *Role and regulation of phospholipase D activity in normal and cancer cells.* Adv Enzyme Regul, 1997. **37**: p. 29-34.

272. Williger, B.T., W.T. Ho, and J.H. Exton, *Phospholipase D mediates matrix metalloproteinase-9 secretion in phorbol ester-stimulated human fibrosarcoma cells.* J Biol Chem, 1999. **274**(2): p. 735-8.

273. Eberhardt, W., et al., *Amplification of IL-1 beta-induced matrix metalloproteinase-9 expression by superoxide in rat glomerular mesangial cells is mediated by increased activities of NF-kappa B and activating protein-1 and involves activation of the mitogen-activated protein kinase pathways.* J Immunol, 2000. **165**(10): p. 5788-97.

274. Turner, N.A., et al., *Simvastatin inhibits MMP-9 secretion from human saphenous vein smooth muscle cells by inhibiting the RhoA/ROCK pathway and reducing MMP-9 mRNA levels.* Faseb J, 2005. **19**(7): p. 804-6.

275. Singer, C.F., et al., *Local cytokines induce differential expression of matrix metalloproteinases but not their tissue inhibitors in human endometrial fibroblasts.* Eur J Biochem, 1999. **259**(1-2): p. 40-5.

276. Alvares, O., et al., *Growth factor effects on the expression of collagenase and TIMP-1 in periodontal ligament cells.* J Periodontol, 1995. **66**(7): p. 552-8.

277. Bond, M., A.H. Baker, and A.C. Newby, *Nuclear factor kappaB activity is essential for matrix metalloproteinase-1 and -3 upregulation in rabbit dermal fibroblasts.* Biochem Biophys Res Commun, 1999. **264**(2): p. 561-7.

278. Kanaki, T., et al., *Functional analysis of aortic endothelial cells expressing mutant PDGF receptors with respect to expression of matrix metalloproteinase-3.* Biochem Biophys Res Commun, 2002. **294**(2): p. 231-7.

279. De Clerck, Y.A., et al., *Characterization of the promoter of the gene encoding human tissue inhibitor of metalloproteinases-2 (TIMP-2).* Gene, 1994. **139**(2): p. 185-91.

280. Shapiro, S.D., D.K. Kobayashi, and H.G. Welgus, *Identification of TIMP-2 in human alveolar macrophages. Regulation of biosynthesis is opposite to that of metalloproteinases and TIMP-1.* J Biol Chem, 1992. **267**(20): p. 13890-4.

281. Oh, J., et al., *Tissue inhibitors of metalloproteinase 2 inhibits endothelial cell migration through increased expression of RECK.* Cancer Res, 2004. **64**(24): p. 9062-9.

282. Oh, J., et al., *TIMP-2 upregulates RECK expression via dephosphorylation of paxillin tyrosine residues 31 and 118.* Oncogene, 2006. **25**(30): p. 4230-4.

283. Iyer, V., K. Pumiglia, and C.M. DiPersio, *Alpha3beta1 integrin regulates MMP-9 mRNA stability in immortalized keratinocytes: a novel mechanism of integrin-mediated MMP gene expression.* J Cell Sci, 2005. **118**(Pt 6): p. 1185-95.

284. Noguchi, K., S. Ishii, and T. Shimizu, *Identification of p2y9/GPR23 as a novel G protein-coupled receptor for lysophosphatidic acid, structurally distant from the Edg family.* J Biol Chem, 2003. **278**(28): p. 25600-6.

285. Contos, J.J., I. Ishii, and J. Chun, *Lysophosphatidic acid receptors.* Mol Pharmacol, 2000. **58**(6): p. 1188-96.

286. Malchinkhuu, E., et al., *Role of p38 mitogen-activated kinase and c-Jun terminal kinase in migration response to lysophosphatidic acid and sphingosine-1-phosphate in glioma cells.* Oncogene, 2005. **24**(44): p. 6676-88.

287. Young, K.W., et al., *Lysophosphatidic acid-induced Ca2+ mobilization requires intracellular sphingosine 1-phosphate production. Potential involvement of endogenous EDG-4 receptors.* J Biol Chem, 2000. **275**(49): p. 38532-9.

288. Pyne, S. and N.J. Pyne, *Sphingosine 1-phosphate signalling in mammalian cells.* Biochem J, 2000. **349**(Pt 2): p. 385-402.

289. Hanna, A., et al., *Tumor necrosis factor-alpha induces stress fiber formation through ceramide production: Role of sphingosine kinase.* Mol. Biol. Cell, 2001. **12**: p. 3618-3630.

290. Fleming, I.N., C.M. Elliott, and J.H. Exton, *Differential translocation of rho family GTPases by lysophosphatidic acid, endothelin-1, and platelet-derived growth factor.* J Biol Chem, 1996. **271**(51): p. 33067-73.

291. Faulkner, A., et al., *The LPP1 and DPP1 gene products account for most of the isoprenoid phosphate phosphatase activities in Saccharomyces cerevisiae.* J Biol Chem, 1999. **274**(21): p. 14831-7.

292. Fukunaga, K., et al., *Identification and functional characterization of a presqualene diphosphate phosphatase.* J Biol Chem, 2006. **281**(14): p. 9490-7.

293. Taylor, M.M., et al., *Enhanced apoptosis through farnesol inhibition of phospholipase D signal transduction.* Febs J, 2005. **272**(19): p. 5056-63.

294. McTaggart, S.J., *Isoprenylated proteins.* Cell Mol Life Sci, 2006. **63**(3): p. 255-67.

295. Bae, C.D., et al., *Determination of interaction sites on the small G protein RhoA for phospholipase D.* J Biol Chem, 1998. **273**(19): p. 11596-604.

296. Walker, S.J., et al., *Activation of phospholipase D1 by Cdc42 requires the Rho insert region.* J Biol Chem, 2000. **275**(21): p. 15665-8.

297. Murph, M.M., et al., *Agonist-induced endocytosis of lysophosphatidic acid-coupled LPA1/EDG-2 receptors via a dynamin2- and Rab5-dependent pathway.* J Cell Sci, 2003. **116**(Pt 10): p. 1969-80.

298. Padron, D., R.D. Tall, and M.G. Roth, *Phospholipase D2 is required for efficient endocytic recycling of transferrin receptors.* Mol Biol Cell, 2006. **17**(2): p. 598-606.

299. Du, G., et al., *Phospholipase D2 localizes to the plasma membrane and regulates angiotensin II receptor endocytosis.* Mol Biol Cell, 2004. **15**(3): p. 1024-30.

300. Matsumoto, Y., et al., *Small GTP-binding protein, Rho, both increased and decreased cellular motility, activation of matrix metalloproteinase 2 and invasion of human osteosarcoma cells.* Jpn J Cancer Res, 2001. **92**(4): p. 429-38.

301. Takino, T., et al., *Membrane type 1 matrix metalloproteinase regulates collagen-dependent mitogen-activated protein/extracellular signal-related kinase activation and cell migration.* Cancer Res, 2004. **64**(3): p. 1044-9.

302. Fisher, K.E., et al., *Tumor cell invasion of collagen matrices requires coordinate lipid agonist-induced G-protein and membrane-type matrix metalloproteinase-1-dependent signaling.* Mol Cancer, 2006. **5**: p. 69.

303. Cerutis, D.R., et al., *Lysophosphatidic acid modulates the regenerative responses of human gingival fibroblasts and enhances the actions of platelet-derived growth factor.* J Periodontol, 2004. **75**(2): p. 297-305.

304. Sakai, T., J.M. de la Pena, and D.F. Mosher, *Synergism among lysophosphatidic acid, beta1A integrins, and epidermal growth factor or platelet-derived growth factor in mediation of cell migration.* J Biol Chem, 1999. **274**(22): p. 15480-6.

305. Tangkijvanich, P., et al., *Platelet-derived growth factor-BB and lysophosphatidic acid distinctly regulate hepatic myofibroblast migration through focal adhesion kinase.* Exp Cell Res, 2002. **281**(1): p. 140-7.

306. Sato, M., et al., *Lysophosphatidic acid inhibits TGF-beta-mediated stimulation of type I collagen mRNA stability via an ERK-dependent pathway in dermal fibroblasts.* Matrix Biol, 2004. **23**(6): p. 353-61.

307. Kessler, E. and R. Adar, *Type I procollagen C-proteinase from mouse fibroblasts. Purification and demonstration of a 55-kDa enhancer glycoprotein.* Eur J Biochem, 1989. **186**(1-2): p. 115-21.

308. Dang, C.M., et al., *Scarless fetal wounds are associated with an increased matrix metalloproteinase-to-tissue-derived inhibitor of metalloproteinase ratio.* Plast Reconstr Surg, 2003. **111**(7): p. 2273-85.

309. Murawaki, Y., et al., *The proMMP-2 activation rate in patients with chronic viral liver disease.* Clin Chim Acta, 2002. **324**(1-2): p. 99-103.

310. Peters, C.A., et al., *Dysregulated proteolytic balance as the basis of excess extracellular matrix in fibrotic disease.* Am J Physiol, 1997. **272**(6 Pt 2): p. R1960-5.

311. Yazawa, N., et al., *Serum levels of tissue inhibitor of metalloproteinases 2 in patients with systemic sclerosis.* J Am Acad Dermatol, 2000. **42**(1 Pt 1): p. 70-5.

312. Knittel, T., et al., *Expression patterns of matrix metalloproteinases and their inhibitors in parenchymal and non-parenchymal cells of rat liver: regulation by TNF-alpha and TGF-beta1.* J Hepatol, 1999. **30**(1): p. 48-60.

313. Day, C.P., et al., *Plasma membrane form of phosphatidate phosphohydrolase: a possible role in signal transduction during liver fibrogenesis.* Clin Sci (Lond), 1993. **85**(3): p. 281-7.

PUBLICATIONS

Pilquil, C., Dewald, J., Cherney, A., Gorshkova, I., Tigyi, G., English, D., Natarajan, V., Brindley, D. N. *Lipid phosphate phosphatase-1 regulates lysophosphatidate-induced fibroblast migration by controlling phospholipase D2-dependent phosphatidate generation.* J Biol Chem. 2006 Dec 15;281(50):38418-29.

Yue, J., Yokoyama, K., Balazs, L., Baker, D. L., Smalley, D., **Pilquil, C.**, Brindley, D. N., Tigyi, G. *Mice with transgenic overexpression of lipid phosphate phosphatase-1 display multiple organotypic deficits without alteration in circulating lysophosphatidate level.* Cell Signal. 2004 Mar;16(3):385-99.

Brindley, D. N., English, D., **Pilquil, C.**, Buri, K., Ling, Z. C. *Lipid phosphate phosphatases regulate signal transduction through glycerolipids and sphingolipids.* Biochim Biophys Acta. 2002 May 23;1582(1-3):33-44. Review.

Pilquil, C., Ling, Z. C., Singh, I., Buri, K., Zhang, Q. X., Brindley, D. N. *Co-ordinate regulation of growth factor receptors and lipid phosphate phosphatase-1 controls cell activation by exogenous lysophosphatidate.* Biochem Soc Trans. 2001 Nov;29(Pt 6):825-30. Review.

Pilquil, C., Singh, I., Zhang, Q., Ling, Z., Buri, K., Stromberg, L. M., Dewald, J., Brindley, D. N. *Lipid phosphate phosphatase-1 dephosphorylates exogenous lysophosphatidate and thereby attenuates its effects on cell signaling.* Prostaglandins. 2001 Apr;64(1-4):83-92.

Xu, J., Zhang, Q. X., **Pilquil, C.**, Berthiaume, L. G., Waggoner, D. W., Brindley, D. N. *Lipid phosphate phosphatase-1 in the regulation of lysophosphatidate signaling.* Ann N Y Acad Sci. 2000 Apr;905:81-90.

Zhang, Q. X., **Pilquil, C**. S., Dewald, J., Berthiaume, L. G., Brindley, D. N. *Identification of structurally important domains of lipid phosphate phosphatase-1: implications for its sites of action.* Biochem J. 2000 Jan 15;345 Pt 2:181-4.

Jasinska, R., Zhang, Q. X., **Pilquil, C**., Singh, I., Xu, J., Dewald, J., Dillon, D. A., Berthiaume, L. G., Carman, G. M., Waggoner, D. W., Brindley, D. N. *Lipid phosphate phosphohydrolase-1 degrades exogenous glycerolipid and sphingolipid phosphate esters.* Biochem J. 1999 Jun 15;340 (Pt 3):677-86.